DOT/FAA/TC-12/18

Federal Aviation Administration
William J. Hughes Technical Center
Aviation Research Division
Atlantic City International Airport
New Jersey 08405

Advanced Guidance and Control—Task 2: Operational and Safety Benefits

October 2012

Final Report

This document is available to the U.S. public through the National Technical Information Services (NTIS), Springfield, Virginia 22161.

This document is also available from the Federal Aviation Administration William J. Hughes Technical Center at actlibrary.tc.faa.gov.

U.S. Department of Transportation
Federal Aviation Administration

NOTICE

This document is disseminated under the sponsorship of the U.S. Department of Transportation in the interest of information exchange. The U.S. Government assumes no liability for the contents or use thereof. The U.S. Government does not endorse products or manufacturers. Trade or manufacturer's names appear herein solely because they are considered essential to the objective of this report. The findings and conclusions in this report are those of the author(s) and do not necessarily represent the views of the funding agency. This document does not constitute FAA policy. Consult the FAA sponsoring organization listed on the Technical Documentation page as to its use.

This report is available at the Federal Aviation Administration William J. Hughes Technical Center's Full-Text Technical Reports page: actlibrary.tc.faa.gov in Adobe Acrobat portable document format (PDF).

Technical Report Documentation Page

1. Report No.	2. Government Accession No.	3. Recipient's Catalog No.
DOT/FAA/TC-12/18		

4. Title and Subtitle	5. Report Date
ADVANCED GUIDANCE AND CONTROL—TASK 2: OPERATIONAL AND SAFETY BENEFITS	October 2012
	6. Performing Organization Code
7. Author(s)	8. Performing Organization Report No.
Mark Maclosky, Eric Mathisen, and Ken Leiphon	
9. Performing Organization Name and Address	10. Work Unit No. (TRAIS)
Honeywell International 1860 W. Rose Garden Lane Phoenix, AZ 85027	11. Contract or Grant No. DTFACT-09-C-00001 Amendment 0004
12. Sponsoring Agency Name and Address	13. Type of Report and Period Covered
U.S. Department of Transportation Federal Aviation Administration Northwest Mountain Region – Transport Airplane Directorate 1601 Lind Avenue, SW Renton, WA 98057	Final Report
	14. Sponsoring Agency Code ANM-113

15. Supplementary Notes

The Federal Aviation Administration William J. Hughes Technical Center Aviation Research Division CORs were Charles Kilgore and Robert McGuire.

16. Abstract

This research initiated as a multiphase project with the goal of emphasizing the benefits that would accrue to industry and government organizations adopting advanced Flight Guidance & Control (FG&C) technology. Task 2 of the project launched with the primary objective of conducting a detailed evaluation of previously developed, representative advanced functionally integrated FG&C system (Total Energy Control System (TECS) and Total Heading Control System (THCS)) algorithms in a part-task simulation. The ease of reuse and the associated performance achievable with the generic design when applied to an actual production aircraft was of particular interest.

In Task 1 of the project, a limited evaluation of the generic TECS outer loop (OL) design was evaluated for reuse and robustness. In Task 2, the intent was to demonstrate the full capability of the TECS/THCS control law through a comprehensive evaluation and analysis of both the inner loop (IL) and OL TECS/THCS algorithms implemented in a high-fidelity simulation environment. The evaluation included a linear stability analysis and six degrees of freedom, nonlinear, full-envelope simulation used to evaluate airplane response to simultaneous path, speed commands, and the effectiveness of multi-axis coordinated control in calm air, as well as in the presence of turbulence or wind shear.

A series of flight scenarios were run to compare the performance of the applied TECS/THCS IL/OL design with the performance of the reference airplane TECS/THCS design provided by the Federal Aviation Administration via the check case time history plots. The relative performance of the two systems was of particular interest. Since the reference airplane used for comparison assumed less transport lag than the Autoflight system, a good response match of the two systems would indicate good adaptability as a general FG&C control solution. The absolute performance of the systems was deemed meaningful as many real-world factors were introduced through the use of a high-fidelity simulation environment, providing a good stress test of the TECS/THCS control algorithm. Improved TECS/THCS performance, over and above what is presented in this report, would likely be achieved when applying this to a fly-by-wire system with less transport lag than in the applied Autoflight system evaluated.

17. Key Words	18. Distribution Statement
Total energy control system, Total heading control system, Inner loop, Outer loop, Autoflight	This document is available to the U.S. public through the National Technical Information Service (NTIS), Springfield, Virginia 22161. This document is also available from the Federal Aviation Administration William J. Hughes Technical Center at actlibrary.tc.faa.gov.

19. Security Classif. (of this report)	20. Security Classif. (of this page)	21. No. of Pages	22. Price
Unclassified	Unclassified	127	

Form DOT F 1700.7 (8-72) Reproduction of completed page authorized

ACKNOWLEDGEMENTS

The authors would like to acknowledge the overall contributions of Tony Lambregts, Charles Kilgore, and Robert McGuire of the Federal Aviation Administration for their contributions to this project and report. S pecial thanks to Tony Lambregts for his extensive technical contributions to this project and for the considerable content provided in various areas of this report including, but not limited to, the "Background: Flight Guidance and Control Systems History and the Evolution of TECS/THCS" section.

TABLE OF CONTENTS

		Page
EXECUTIVE SUMMARY		ix
1.	INTRODUCTION	1
	1.1 Total Energy Control System	4
	1.2 Total Heading Control System	6
	1.3 Application of TECS/THCS on Air Transport and General Aviation Airplanes	7
2.	PART TASK SIMULATION	8
3.	SAFETY STUDY	9
4.	EVALUATION METHOD	10
	4.1 Analysis	11
	4.2 Real-Time Simulation	11
	4.3 Control Law Development	15
	4.3.1 Inner Loop	15
	4.3.2 Outer Loop	27
	4.4 REAL-TIME SIMULATION EVALUATION	32
	4.4.1 Option 1 Results	32
	4.4.2 Option 2 Results	33
5.	CONCLUSIONS	36
6.	FUTURE STUDIES	37
7.	REFERENCES	38
APPENDICES		
	A—Honeywell Advanced Flight Guidance and Control Inner Loop Linear Analysis	
	B—Total Energy Control System/Total Heading Control System Inner Loop Linear Analysis	
	C—Test Case Scenarios	

LIST OF FIGURES

Figure		Page
1	The TECS Generalized Mode Architecture	4
2	The THCS Generalized Mode Architecture	6
3	Top-Level PC Sim and SoftBench Architecture	12
4	Primary Guidance Control Panel	12
5	Secondary Cockpit Control Panel	13
6	Cockpit Primary Flight Display	13
7	Advanced FG&C—Option 1	14
8	Advanced FG&C—Option 2	15
9	The HAFGC Control Law Block Diagram	16
10	The TECS Pitch IL	18
11	The TECS Longitudinal Axis Static Inversion	19
12	The TECS Pitch IL Control Law	20
13	The TECS Pitch IL Analytical Model	20
14	The THCS Lateral Directional IL	22
15	The THCS Lateral Directional Static Inversion	23
16	The THCS Coupled Lateral Directional IL Control Law	24
17	The THCS Side Slip Complementary Filter	25
18	The THCS Lateral Directional IL Analytical Model	26
19	The OL	28
20	The TECS Pitch OL	29
21	The TECS Core	30

LIST OF TABLES

Table		Page
1	The HAFGC Elevator Path IL Stability Margin Summary	17
2	The HAFGC Aileron Path IL Stability Margin Summary	17
3	The HAFGC Rudder Path IL Stability Margin Summary	17
4	The TECS Pitch IL Gains	20
5	The TECS Pitch IL Stability Margin Summary	21
6	The THCS Lateral Directional IL Gains	25
7	The THCS Aileron IL Stability Margin Summary	27
8	The THCS Rudder IL Stability Margin Summary	27
9	The TECS Core Gains	32

LIST OF ACRONYMS

AC	Advisory Circular
AFE	Aircrew Flight Equipment
AFCS	Automatic Flight Control System
ALT	Altitude
ASRS	Aviation Safety Reporting System
ARAC	Aviation Rulemaking and Advisory Committee
CAS	Calibrated airspeed
CDU	Control and display unit
CFR	Code of Federal Regulations
c.g.	Center of gravity
DARPA	Defense Advanced Research Projects Agency
dB	Decibel
DLL	Dynamic Link Library
FAA	Federal Aviation Administration
FG&C	Flight Guidance and Control
FLC	Flight level change
FMC	Flight Management Computer
FPA	Flight path angle
GA	General aviation
GS	Glide slope
HAFGC	Honeywell Advanced Flight Guidance and Control
HI	Honeywell International
Hz	Hertz
IL	Inner loop
kt	Knots
L_{NAV}	Lateral navigation
LOC	Loss of control
MIMO	Multi-input/multi-output
ms	Millisecond
NASA	National Aeronautics and Space Administration
OL	Outer loop
PC	Personal computer
SISO	Single-input/single-output
TECS	Total Energy Control System
THCS	Total Heading Control System
UAV	Unmanned Aircraft Vehicle
V_{MAX}	Maximum airspeed
V_{MIN}	Minimum airspeed
V_{NAV}	Vertical navigation
V_{stall}	Aircraft stall speed

EXECUTIVE SUMMARY

Advanced Flight Guidance and Control (FG&C) systems are characterized by fully integrated, multi-axis, multi-input/multi-output designs in which all modes are designed to work seamlessly with each other through all phases of flight, avoiding mode confusion and potential integration errors in the final implementation that can lead to operational hazards and handling quality issues. Advanced FG&C systems, if designed properly, are safer and operationally more effective than the current generation of FG&C systems onboard transport airplane, which typically evolved from single-input/single-output (SISO) independent control loops and are not fully integrated or designed to work in harmony with each other.

This project is the second phase of a multiphase project intended to clear the obstacles to the introduction and certification of advanced, functionally integrated FG&C systems in commercial airplanes. This report presents the Task 2 results of this ongoing project to evaluate the suitability of functionally integrated FG&C systems for commercial use. The primary focus for this project is the evaluation of the previously developed Total Energy Control System (TECS) and the Total Heading Control System (THCS).

Task 1 evaluated the reuse and robustness of the generic TECS outer loop (OL) design. The conclusions from this effort were that the performance results from the TECS generalized control approach were very favorable and, therefore, warranted a more in-depth evaluation of both TECS and THCS on a commercial airplane.

Task 2 expanded the scope to include a comprehensive evaluation of both vertical and lateral directional axis. A primary objective for this evaluation was the replacement of the application specific inner loops (IL) with generalized designs that could be more easily adapted to other applications with the goal of minimizing the need for extensive flight test activity to achieve desired levels of performance. Two approaches were considered.

First, the Honeywell Advanced Flight Guidance and Control (HAFGC) approach was used to implement the IL control laws in all three axes. HAFGC is a reusable guidance and control law that has been successfully employed in other applications; it was chosen for the program as it was believed to be suitable for meeting the Federal Aviation Administration (FAA) objectives of the generalized IL design. This approach was adopted to reduce program risk by allowing designers to work with a familiar control design approach. Significant technical difficulties were experienced while attempting to integrate HAFCG with the TECS OL control laws, and it was decided to pursue a second approach.

The second approach considered was the replacement of the legacy IL with the TECS/THCS pitch and lateral directional IL control laws plus static inversion. This approach was selected for the final demonstration and evaluation. The final evaluation included a linear stability analysis and a six degrees of freedom, nonlinear, full-envelope simulation used to evaluate airplane response to simultaneous path and speed commands and the effectiveness of multi-axis coordinated control in calm air, as well as in the presence of turbulence and wind shear.

Functionality and performance of the evaluation aircraft control system, adapted to include the TECS, was compared with vertical check case scenarios from a reference airplane supplied by the FAA. These scenarios included climbs and descents in a variety of modes (flight path angle, flight level change, glide slope, and general aviation) and configurations.

The real-time simulation results indicate that the objective of demonstrating the pilot-like energy management capability that is the fundamental advantage of TECS was achieved. In all cases, the energy management strategy that provides simultaneous coordinated elevator and thrust control to achieve an efficient in a decoupled command response was clearly demonstrated. For all multi-axis command scenarios considered, altitude was maintained to within 15 ft of the target altitude and airspeed was maintained to within 3 knots of the target airspeed.

In the lateral axis, the combination of the Honeywell International legacy OL control laws and the THCS IL design was successfully demonstrated using the heading, track, and localizer modes. The THCS IL was shown to provide simultaneous coordinated aileron and rudder commands while achieving smooth/well-damped heading control response with excellent turn coordination and yaw damping. For all lateral check cases performed, side slip angle was limited to 0.5°.

The primary objective of this project was to clear the obstacles to the introduction and certification of advanced, functionally integrated FG&C systems in commercial airplanes. The use of a high-fidelity airplane simulation introduced real-world technical challenges to the project. The successful demonstration of good performance in the high-fidelity environment supports the suitability of TECS/THCS for commercial use.

1. INTRODUCTION.

To evaluate the suitability of functionally integrated Flight Guidance and Control (FG&C) systems for commercial use, the Task 2 objectives were to:

- Conduct a detailed evaluation of previously developed, representative, advanced, functionally integrated FG&C system (Total Energy Control System (TECS) and Total Heading Control System (THCS)) algorithms in a part-task simulation, and assess the performance via in-depth effectiveness and safety evaluation. This research uses simulation and other methods to analyze the TECS/THCS system concept.

- Demonstrate a simplified process for adaptation and validation of the TECS/THCS algorithms in a part-task simulation including a representative target airplane.

- Develop appropriate requirements, objectives, performance standards, and identify potential certification process issues and avenues to resolve them.

The current advances in automatic FG&C is the result of more than 75 years of piecemeal evolution, mainly by a process of minimal change/minimal cost addition of more functions with each generation of airplane design. As a result of this historic evolutionary process, highly capable automatic FG&C systems have evolved. These systems have become exceedingly complex from the viewpoint of design, maintenance, and operation by the flight crew. This design tradition has resulted in too many modes and submodes, functional overlap, and inconsistencies of operation between modes; this results in flight crew mode confusion and errors and general difficulties in understanding automatic FG&C systems and maintaining situational awareness. Nevertheless, airlines and flight crews regard many of FG&C functions as mission critical, although most functions were designed and certified under the rules for noncritical systems. Such noncritical systems were originally intended to assist flight crews who are responsible for the correct and safe operation of those systems. Today, flight crews expect modern FG&C systems to operate correctly and with functional integrity in all flight conditions and to provide proper flight crew alerting in the case of failure or unsafe operating conditions.

Many reported deficiencies have been known for decades, and their root causes lie in the historic and traditional design concepts that propagated through many design generations without establishing a new design baseline that uses updated technologies and design integration techniques. Today, most of the earlier hardware technology constraints of analog electronics and mechanical instruments have been eliminated by the introduction of digital-processing and electronic-flight instrument technologies. Also, the knowledge for designing simpler, better integrated FG&C systems and man-machine interfaces has been available for decades. Unfortunately, early design practices are deeply entrenched in the industry, and a paradigm shift in the FG&C design approach away from the minimum change/minimum cost approach has been difficult. As a result, current systems are unnecessarily complex, very costly to develop and own, and still do not provide all desired safety and operational features. A more comprehensive discussion on this subject can be found in reference 1. Many of these automation safety

concerns are also addressed in reference 2. Thus, the deficiencies in operational effectiveness, safety, and performance associated with the current generation FG&C systems are well documented.

These deficiencies have led to a number of incidents and accidents involving flight deck automation. Many of these incidents and accidents involve situations in which pilots have difficulty understanding how the system operates and how to properly and timely interact with the system to assure their safe operation. Flight crew mode confusion, operational errors, and unwarranted trust that these systems will inherently operate safely, surprisingly led to a frequent occurrence of loss of control (e.g., stalls, disconnects that are badly out of trim), some with catastrophic consequences. As a result of the safety issues, the Aviation Rulemaking Advisory Committee (ARAC) commissioned a group consisting of cognizant personnel from the Federal Aviation Administration (FAA), the Joint Aviation Authorities, and the industry to rewrite the basic automatic FG&C certification safety regulations, Title 14 Code of Federal Regulations (CFR) 25.1329/1335 [2], and Advisory Circular (AC) 25.1329 [3]. As a result, the updated CFR and AC were issued by the FAA. These updated certification requirements are expected to precipitate relatively far-reaching changes in future automatic FG&C system design, including the application of multivariable control technology, a much higher degree of function sophistication and integration, flight and performance envelope protection features, and a reassessment of the design criticality of certain functions.

In the mid-1970s, as an outgrowth of the cancelled Supersonic Transport program, The Boeing Company delivered an advanced FG&C system to the National Aeronautics and Space Administration (NASA) Langley Research Center under the Terminal Configured Vehicle Program. It included the first prototype digital flight control computers, digital Cathode Ray Tube primary flight and navigation displays, and a prototype flight management computer (FMC). This NASA program contributed much to the evolution of the current modern automated flight deck, but also to its complexity, as the new operational capabilities were added onto an existing FG&C architecture. For example, the FMC not only incorporated new automatic navigation capabilities, but also a new batch of automatic control modes for controlling the airplane on waypoint defined flight paths in the horizontal plane, the lateral navigation (L_{NAV}) plane, the vertical navigation (V_{NAV}) plane, and airspeed control. It introduced a new keyboard-based control and display unit (CDU) that functioned more like a general office machine than a traditional interface. Although the new FMC and CDU provided many new capabilities, the complexities of how to operate the variety of system interfaces and the need to remember the correct syntax for programming and executing a desired automated maneuvering sequence made the flight crew's job more challenging. Pilots experienced difficulties in managing and understanding the operation of each subsystem. By the late 1970s, the NASA terminal area operations research using this system had clearly revealed a number of operational, control performance, and safety deficiencies. During this program, many attempts were made to make the systems operationally acceptable and to improve the basic interaction of the control laws. It was concluded that this control law architecture, with its multitude of historically evolved overlapping single-input/single-output (SISO) control modes and complex mode logic, would never provide the desired user-friendly system operation and optimal performance.

The objectives of this program were to:

- Develop a generalized reusable multi-input/multi-output (MIMO) control algorithm and system functional architecture that accommodates all needed modes for automatic and augmented airplane control operations.

- Eliminate functional overlap between modes and provide operational performance consistency for all modes and flight conditions.

- Provide decoupled vertical flight path and speed command responses by proper coordination of thrust and elevator control.

- Provide flight envelope protection that covers all flight modes.

- Provide operational effectiveness to the flight crew by simplifying the mode logic and man-machine interfaces.

- Reduce overall system complexity, eliminate hardware subsystems (e.g., autothrottle, flight management system control laws, yaw damper, thrust asymmetry compensator, etc.) and, where possible, reduce software.

The first phase of this research, performed by Boeing, addressed the functional integration of all automatic and augmented manual control modes for airplane control in the vertical plane. This research resulted in a Total Energy Control System (TECS). NASA and Boeing invested more than $5 million in the development and flight demonstrations of the TECS FG&C concept. The second phase of the research, which addressed the functional integration of all automatic lateral-directional control, was also performed by Boeing as part of the Condor Unmanned Air Vehicle (UAV) High Altitude Long Endurance Technology Demonstration program (1983-1990), and was jointly funded by Defense Advanced Research Projects Agency (DARPA) and Boeing and resulted in a THCS. Collectively, NASA, DARPA, and Boeing invested more than $20 million in the TECS/THCS FG&C system development. Both TECS and THCS were used in the Condor Flight Demonstration program.

The TECS/THCS concepts were developed to satisfy the functional, performance, and economic requirements discussed in this section.

- A minimum set of operationally required and preferred modes was defined.

- Generalized MIMO FG&C strategies were identified for airplane control in the vertical and horizontal planes, and the corresponding functionally integrated systems architectures were developed.

1.1 TOTAL ENERGY CONTROL SYSTEM.

The TECS was developed for airplane control in the vertical plane. This concept uses an energy-based control strategy to realize all needed mode functions. The general TECS architecture is shown in figure 1.

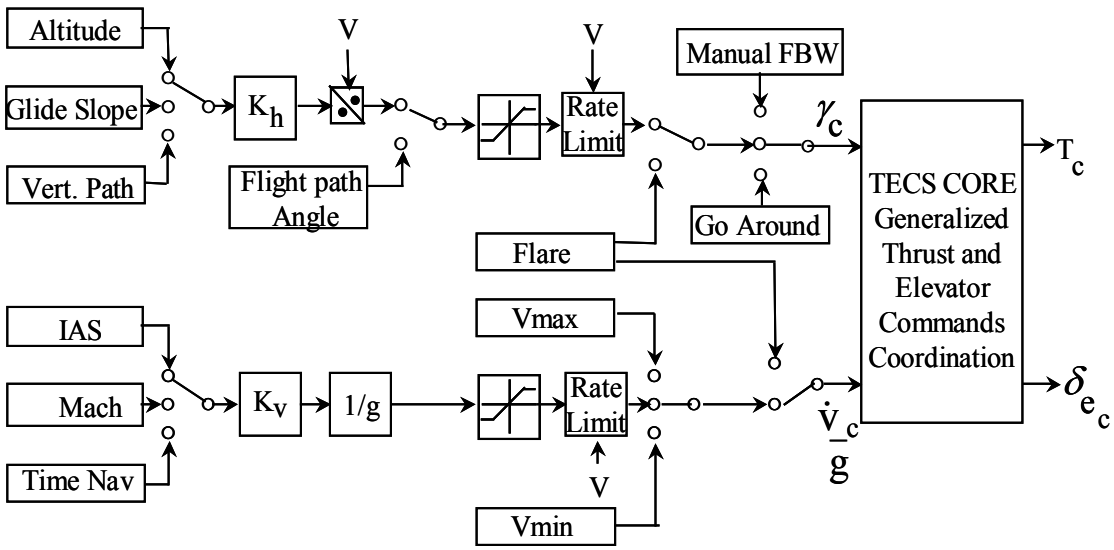

FBW = Fly by Wire
IAS = Indicated Airspeed
Vmin = Minimum airspeed

Figure 1. The TECS Generalized Mode Architecture

Thrust is used to control the airplane's total energy requirement based on flight path and speed targets. The elevator is used to control the channeling of energy to flight path or speed, or between flight path and speed. For any vertical path mode, the command and feedbacks are normalized into a flight path angle command (γc), which is the vertical flight path-related component of the airplane's specific energy rate. Likewise, for any speed mode, the command and feedbacks are normalized into a dimensionless, longitudinal, acceleration command ($\frac{\dot{V}_c}{g}$), which is the airspeed-related component of the airplane's specific energy rate. These commands are input to the TECS core algorithm, where the sum of flight path angle error and normalized longitudinal acceleration error signals are formed to develop the net thrust command, and the difference of flight path angle error and the normalized longitudinal acceleration error signals are formed to develop the elevator command. The TECS strategy provides simultaneous coordinated elevator and thrust commands to achieve energy-efficient, pilot-like control with decoupled command responses. Here, decoupled control means that the airplane will only respond, as intended, to a control command without causing significant unintended responses in the other command state variable. The result is a generalized reusable design, applicable to all conventional airplanes, that supports all necessary automatic and augmented manual control mode functions and provides performance consistency between modes.

The total net thrust command is scaled in proportion to the actual airplane weight. The energy distribution control dynamics and total energy control dynamics are designed to be identical. This is a prerequisite to ensure that the delta energy produced in the case of a single flight path or speed command goes entirely toward satisfying the new command and does not spill over onto the variable with an associated constant command. This is the mechanism for providing very simple and effective control command response decoupling. Simultaneous flight path and speed commands with opposing energy demands are executed by first exchanging energy to the extent possible using elevator control only, before commanding a thrust change to satisfy the final total energy demand. Thus, maneuvers are always executed in the most energy-efficient way possible, while also eliminating undesirable engine control activity. The TECS energy control concept makes the flight path and speed control modes fully generic/reusable, yielding the same performance in any airplane application.

Only the thrust and elevator control inner loops (ILs) need to be adapted to the specific airplane application to match thrust and flight path angle/longitudinal acceleration control dynamics. A flight path angle rate command/flight path angle hold augmented manual control algorithm is also provided and seamlessly integrated with the TECS core algorithm, by developing a flight path angle command based on the pilot's stick input, along with appropriate feed forward commands to shape the control responses for the desired handling qualities.

Envelope protection strategies are implemented as part of the TECS core algorithm to provide protection against excessive angle of attack, underspeed, overspeed, and normal load factor, appropriate for each mode. These features are implemented seamlessly as part of the basic modes. For the automatic modes, normal load factor control is implemented as an integral part of energy management control.

Extensive pilot-in-the-loop simulator development and final evaluations were conducted over the course of more than 5 years. An estimated 25 Boeing and NASA pilots took part in its development and evaluation. The TECS program culminated in a very successful flight test evaluation and demonstration program in mid-1985 on the NASA's B-737 airplane, covering all of the integrated automatic flight path and speed mode operations, as well as the augmented manual fly-by-wire control mode and all envelope protection functions. The system performed so well, it was determined that no design changes or system retuning were needed during this flight test program. The amount of software needed to implement all the TECS functions was less than 40% of the amount of software for the B-757 longitudinal control mode, although the B-757 did not feature full envelope protection. The TECS concept was used on the Condor UAV program because its generic, reusable design was ideally suited for low-budget, low-development effort applications. It was also chosen because the risk of losing the airplane in flight test due to an immature flight control system was considered substantially less than for a more traditional flight control system. All mode functionality and mode logic was considered highly mature and its generic software could be reused directly without significant specific development for the Condor. The TECS application risk due to differences between the airplane models used for designing the system and the actual airplane dynamics are confined to the IL only. This was considered more manageable than when airplane dependencies appear throughout the design, as is the case in a more traditional design.

1.2 TOTAL HEADING CONTROL SYSTEM.

Because of the success with TECS, a functionally integrated lateral-directional control for the Condor UAV was developed. This system, the THCS, uses a MIMO control strategy that is completely analogous to TECS. The general THCS architecture is shown in figure 2.

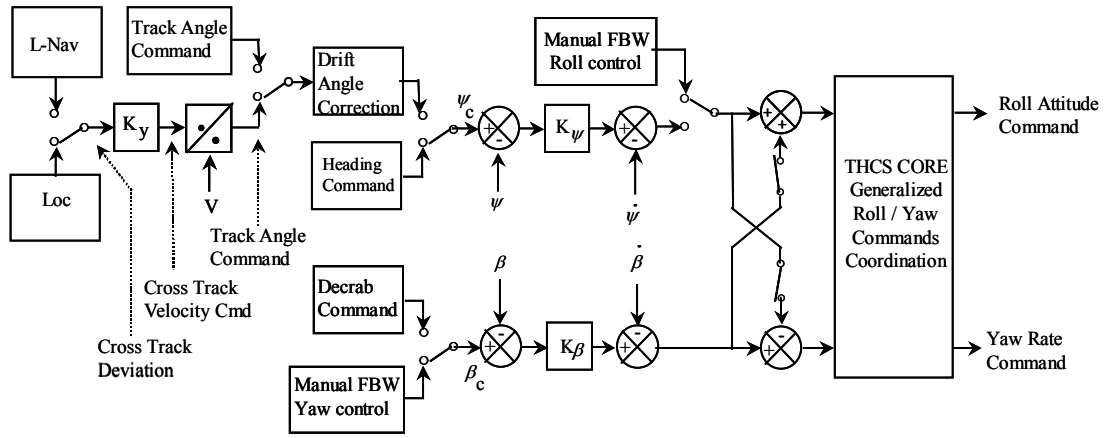

FBW = Fly by Wire
Loc = Localizer

Figure 2. The THCS Generalized Mode Architecture

In this THCS concept, the horizontal flight path control error of any outer loop (OL) mode is normalized into a heading error. A sideslip error is also developed. For normal operations, the sideslip command is zero. Nonzero sideslip commands are used for crosswind landing/decrab and as a result of rudder pedal inputs in the augmented manual control mode. The normalized heading and sideslip angular errors are input to a core lateral directional control algorithm, where the roll command is computed to null the sum of heading and sideslip errors; and a yaw rate command is computed to null the difference between heading and sideslip errors. The THCS core algorithm provides simultaneous coordinated aileron and rudder commands to achieve a smooth, well-damped heading control response with near perfect turn coordination (insignificant sideslip). It also provides inherent yaw damping, turn coordination, engine out yaw control, and automatic roll and yaw trim, without the need for separate/dedicated sensors and control/mode logic software. Thus, the THCS concept supports all needed automatic and augmented manual control mode functions.

All OL modes and core roll and yaw rate command coordination functions, as well as the mode logic, are fully generalized and can be used directly on any conventional airplane. Only the roll and yaw ILs need to be adapted to the specific airplane characteristics to produce properly coordinated roll and yaw dynamics.

1.3 APPLICATION OF TECS/THCS ON AIR TRANSPORT AND GENERAL AVIATION AIRPLANES.

There has been renewed focus on automatic FG&C safety, and new design safety regulations are expected. These new regulations include requirements for envelope protection and improved man-machine interfaces and operations concepts. Implementing most of the new design requirements in the existing FG&C system architectures is a possibility; but doing so results in greater design complexity without making progress in system modernization and cost reduction of future designs. Development and ownership costs of overly complex, custom designed FG&C systems will no longer be competitive when compared to generic reusable and functionally integrated designs such as TECS/THCS.

On the Condor flight test program, the TECS/THCS design performed as intended and greatly enhanced the flight safety for the failures encountered without the need for further development. TECS/THCS provided fully automatic control, from its first takeoff through its last landing and successfully managed a number of serious failure conditions, including two engine-out automatic landings and an inadvertent in-flight, full-reverse thrust condition while operating close to V_{stall}.

Application of the generalized/reusable TECS/THCS algorithms has the potential to reduce FG&C system development, and validation and flight test efforts, because all desired modes share major functional (possibly precertified) components. These algorithms also provide for simple, effective operational envelope protection and simpler, more flight crew-friendly, man-machine interfaces. The approach eliminates traditional separate subsystems that provide autothrottle, yaw damper, turn coordination, and thrust asymmetry compensation functions. Instead, these functions are integrally and generically provided by the multi-axes TECS and THCS control algorithms. Thus, TECS/THCS hold the potential for providing simpler, safer and less costly FG&C systems. TECS and THCS have very successfully gone through the final stages of a technology readiness demonstration, including flight tests, and have been shown to successfully address virtually all known FG&C automation issues.

Thus, advanced guidance and control technologies that promise safer, more capable, and more effective FG&C designs exist and have been adequately demonstrated in piloted simulations and flight tests, but these technologies have not been incorporated into U.S.-certified air transport and general aviation (GA) airplanes. It is clear that availability of the technologies is not enough to assure their application. Application of these technologies has been impeded by industry concerns about the perceived risks and uncertainties associated with a design changeover to the new integrated FG&C system, including:

- Operational suitability and performance
- Flight crew system acceptance
- Flight crew training needs
- Effort required for comprehensive FG&C redesign and change-over
- Certification issues and efforts required to resolve the issues
- Safety and cost benefit

The potential benefits include a simpler, better-integrated generic design that can be reused on many future airplane programs with little additional development. This should translate into significant reductions in future FG&C systems costs. Therefore, this project has been structured to help overcome the impediments for introducing more advanced, functionally integrated FG&C systems in Air Transport and GA airplanes.

2. PART TASK SIMULATION.

The outcome of the Task 1 study [2] resulted in a hybrid simulation that included some elements of TECS and many components taken from a legacy Honeywell International (HI) business jet application. Only the pitch OL used the TECS design. Mode logic, OL lateral control laws, and both the lateral directional and vertical IL were all based on the legacy business jet design.

In Task 2, the intent was to provide additional control law capability that would further demonstrate the advantages of generalized reusable advanced FG&C algorithms. To reduce development costs and risk, the decision was made to retain the mode logic and lateral OL control laws from the Task 1 study and focus on enhancements to the pitch and lateral directional ILs.

The simulation environment used by HI to demonstrate the TECS/THCS technology provided a close imitation of the target hardware and real-time operating system environment. This simulation environment required using software components that were compiled for the target hardware. Therefore, the autopilot algorithms evaluated were directly usable in flight hardware without modification and provided direct traceability from the analysis environment to a production environment.

The TECS OL algorithms were implemented using the same HI development tools typically used for autopilot development at HI. The airplane model, control system model, sensor models, and autopilot/autothrottle software models used in this environment are based on a certified autopilot except for the modifications that were made to integrate the TECS/THCS algorithms into the system. This approach was used to provide demonstration in an environment that is realistic to a certified aircraft. An exception to that approach was with respect to transport delays that were reduced towards a goal of 50 milliseconds (ms). This goal was achieved in the pitch and roll axes. The yaw axis transport delay was reduced but complexity of the modeling in the yaw axis would have required a prohibitively large effort to achieve 50 ms. A transport delay of 50 ms is readily achievable in a FG&C system, and therefore, this modification did not degrade the simulation environment in terms of making a judgment on the suitability of the results for future applications.

The IL control algorithms for this research were initially chosen to be implemented by generating a dynamic link library (DLL) from a proprietary tool that provides a control law structure using dynamic inversion. The proprietary tool works directly with the nonlinear airplane model to generate the dynamic inversion equations for the autopilot control law structure. Although this tool had been used to provide real-time software for actual flight tests in the past, it had not been used to generate software for the same target as used in this study. Due to software compatibility

issues, the task of incorporating the software from this dynamic inversion control law tool into the emulated real-time operating system environment proved to be significantly more difficult than anticipated, and an integrated software solution was not achieved. An alternate method that implemented the ILs as a DLL in the aircraft simulation partition (i.e., as a windows-based DLL) was achieved. However, this method does not preserve the timing relationships between the OL control laws, IL loop control laws, and control system actuators.

When it became clear that this first approach resulted in a significant impact to the program in terms of time and budget and that no working solution had yet been achieved, a decision was made to revert to the TECS/THCS IL design.

Manual translation of the FAA-provided IL algorithms allowed implementation within the same emulated real-time environment as the rest of the Automatic Flight Control System (AFCS) software. This preserved the timing relation among OL, IL, and actuator control signals. Analytic models were modified to incorporate the FAA-provided IL algorithms to determine the terms required for the static inversion and to analyze the margins for the feedback loops. As a result of discrepancies between analytic predictions and real-time response observed while working with Honeywell Advanced Flight Guidance and Control (HAFGC), the accuracy of the analytic modeling of the AFCS was also revisited. This effort identified and addressed several issues. An error was found in the real-time implementation of the TECS mode logic that contributes to allocating control to the flight path angle versus thrust control paths. The analytic models did not account for all of the transport delay in the system.

Modifications were made to the real-time simulation environment to reduce transport delays toward the 50-ms goal. The goal was achieved for the pitch and roll axes, but not the yaw axis, where the transport delay remained above 50 ms. The complexity of the real-time simulation prevented further reduction without extensive additional effort that would have further impacted the program. With the noted corrections and modifications implemented, the overall system performance was significantly improved.

Due to resource constraints, no attempt was made to reevaluate the original approach with the reduced transport delays. Final evaluations were conducted only with the revised FG&C architecture based on a hybrid of legacy HI business jet application (mode logic and lateral OL control laws) and TECS/THCS (TECS/THCS pitch OL and both pitch and lateral directional ILs).

3. SAFETY STUDY.

The resources used for the safety study and literature search include:

- National Transportation Safety Board Accident Database
- FAA Accident/Incident Data System (AIDS)
- Aviation Safety Reporting System (ASRS)
- NASA Aviation Safety Program
- Other aviation safety-related websites

Accidents and incidents were reviewed, particularly those most recently classified as loss of control (LOC). A general and consistent trend noticed in many of the LOC incidents and accidents was the pilot's loss of situational awareness, which resulted in an inappropriate aircraft energy state for the desired trajectory and path of the airplane. Often, this loss of situational awareness results in

- Destabilized approaches.
    - High and hot (resulting in overshooting of runway)
    - Low and slow (resulting in failure to reach runway)
- Aerodynamic stall.

In many scenarios, weather was stated as a contributing factor.

Several highly publicized accidents indicate that envelope protection features merit improving aircraft energy state and resulting safety margins, including:

- US Airways Flight 1549 successful ditching in the Hudson River (A320)
- Continental Connection Flight 3407 accident in Buffalo (Dash8-Q400)
- Turkish Airlines Flight 1951 accident in Amsterdam (B-737-800)

Numerous incidents are reported in the ASRS regarding altitude, heading, or speed deviations or anomalies attributed to limitations or deficiencies of current generation FG&C systems and/or the ability of the crew to timely monitor and manage these automated systems. Most findings had contributing factors such as distractions, workload, training, or simply failing to follow procedures.

From a qualitative perspective, the numerous reports in the ASRS indicate that design improvements and features that reduce reliance on flight crew interventions for safety are justified. The findings cited could result in significantly more serious consequences anticipated in the NextGen air traffic environment given the expected increase in operational density.

Based on the findings of this research, it is clear that advanced guidance and control systems, such as those evaluated as part of this project, can be an effective means of maintaining an appropriate aircraft energy state, avoiding these types of incidents and accidents, and ensuring safer operation.

4. EVALUATION METHOD.

This section provides a description of the two methods, namely analysis and real-time simulation, used to evaluate the various advanced FG&C control laws considered in this study.

4.1 ANALYSIS.

To adapt the generic FG&C control laws for use on a specific airplane application, all configuration-dependent aspects of the ILs and OLs must be specifically tailored. Both IL control law architectures considered in this study include algorithms that are dependent on accurate knowledge of actual airplane parameters. In cases where linear model approximations depart significantly from the true airplane behavior due to nonlinearity, special considerations may be necessary to achieve the desired performance for all flight conditions and vehicle configurations. Additional considerations may be necessary to account for traditional factors that limit the performance capabilities of the IL (such as discrete delays and actuator bandwidth limitations). The TECS/THCS OL was designed with the intent that it be 100% reusable with no need for airplane-specific adjustments. However, it was discovered during the course of this research that adjustments were warranted to optimize performance.

Control law analysis and gain selection for the ILs and OLs were performed using non-real-time MATLAB® simulations and linear analysis techniques. This analysis effort used models for all components relating to control law performance. This includes the IL and OL control laws, the nonlinear aircraft model, the mechanical flight control system (including all nonlinear effects), subsystems that provide sensor data feedback, and the surface actuators. The effects of time delays due to discrete data processing and transmission must also be included. Frequency analysis using linear models was performed to examine stability margins and sensitivities of the design to due to actuator bandwidth and transport delays for both the ILs. Time domain analysis was used to evaluate response characteristics. The task of tuning the configurable gains proved to be an iterative process that was completed when a gain set was identified that provided acceptable performance in both the time and frequency domain.

4.2 REAL-TIME SIMULATION.

Once the analysis phase was complete, the analysis-based design was then converted to a real-time software implementation or operational flight code. The flight code was then evaluated using a real-time hardware-in-the-loop simulation that included the best available (high-fidelity) models for all system components.

HI used SoftBench, a previously developed personal computer (PC)-based simulation tool for this purpose. SoftBench is an integrated environment that includes emulation of the target processor and operating system environment. The SoftBench environment includes the following capabilities:

- Runs actual real-time flight control software DLLs
- Integrates custom HI flight test tools that allow data collection and parameter stimulation for the real-time flight control software DLLs
- Simulates the digital data bus communications for an Epic flight control system
- Simulation of the real-time aircraft model (PC Sim)

The PC Sim is a general purpose dynamic airplane simulation program designed to support on-ground development of avionics equipment.

In this study, an existing PC Sim platform for a certified GA class business jet was used as baseline environment for control law development purposes. The platform contains high-fidelity nonlinear models for the mechanical control system, surface actuators, propulsion system, and the aerodynamic models that are supplied by the original equipment manufacturer. This environment replicates the functionality and performance of the true airplane to a level of confidence that is accepted for use in the certification process.

Figure 3 shows the top-level PC Sim functionality and data flow.

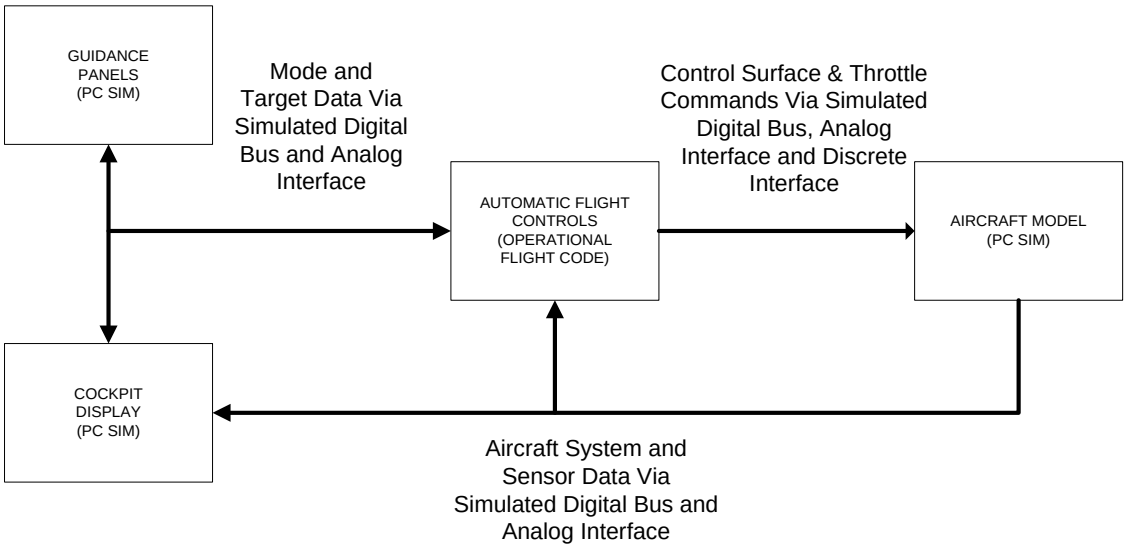

Figure 3. Top-Level PC Sim and SoftBench Architecture

The user interface consists of a primary mode guidance panel, a secondary control panel, and a simple cockpit display.

The primary guidance panel shown in figure 4 allows the user to enter AFCS engagement and mode commands as well as control law target information. Active selected and armed system modes and target information are also annunciated on the guidance panel.

Figure 4. Primary Guidance Control Panel

A secondary cockpit panel, shown in figure 5, displays information relating to the navigation radio tuning and allows for control of the throttles, flaps, and gear.

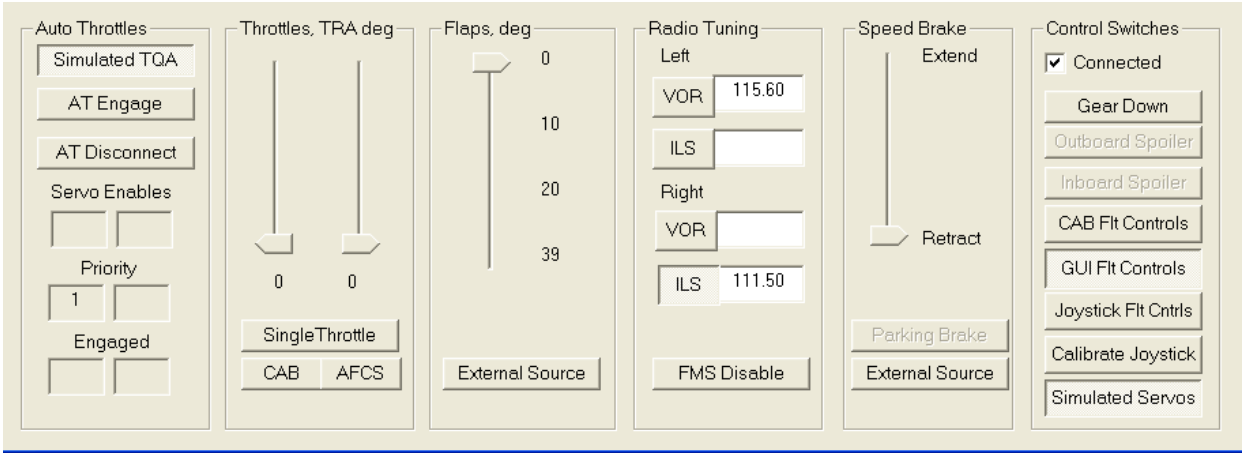

Figure 5. Secondary Cockpit Control Panel

The cockpit primary flight display contains basic flight instrumentation including an attitude direction indicator, horizontal situation indicator, course deviation indicator, airspeed indicator, altimeter, and vertical-speed indicators, as shown in figure 6.

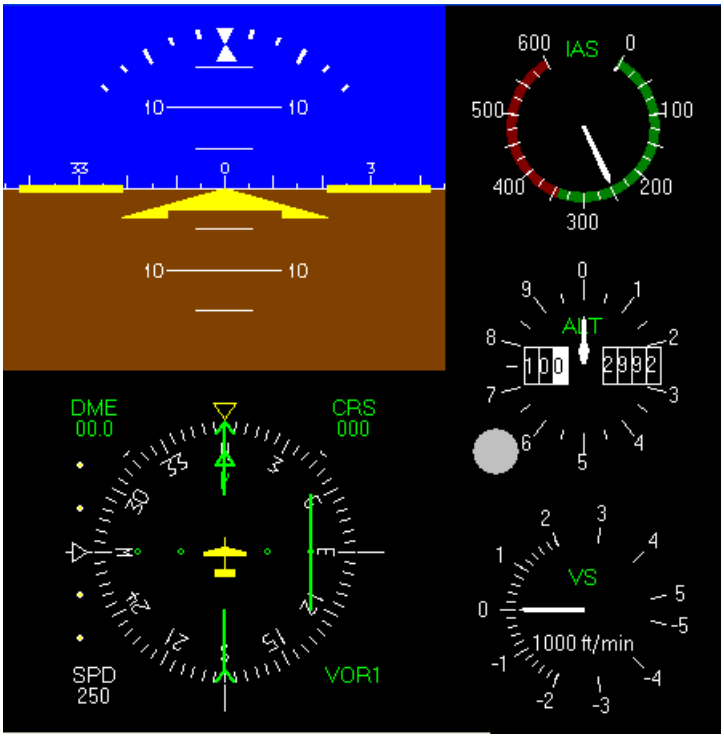

Figure 6. Cockpit Primary Flight Display

The aircraft model includes the equations of motion, the aerodynamic and propulsion models, models for the physical flight control system and models for all avionic subsystems that provide data used by the AFCS.

The subsystem under evaluation is the automatic flight controls, which includes the flight code for the FG&C control laws and associated mode logic. Two configurations were considered in this study.

The first configuration is shown in figure 7.

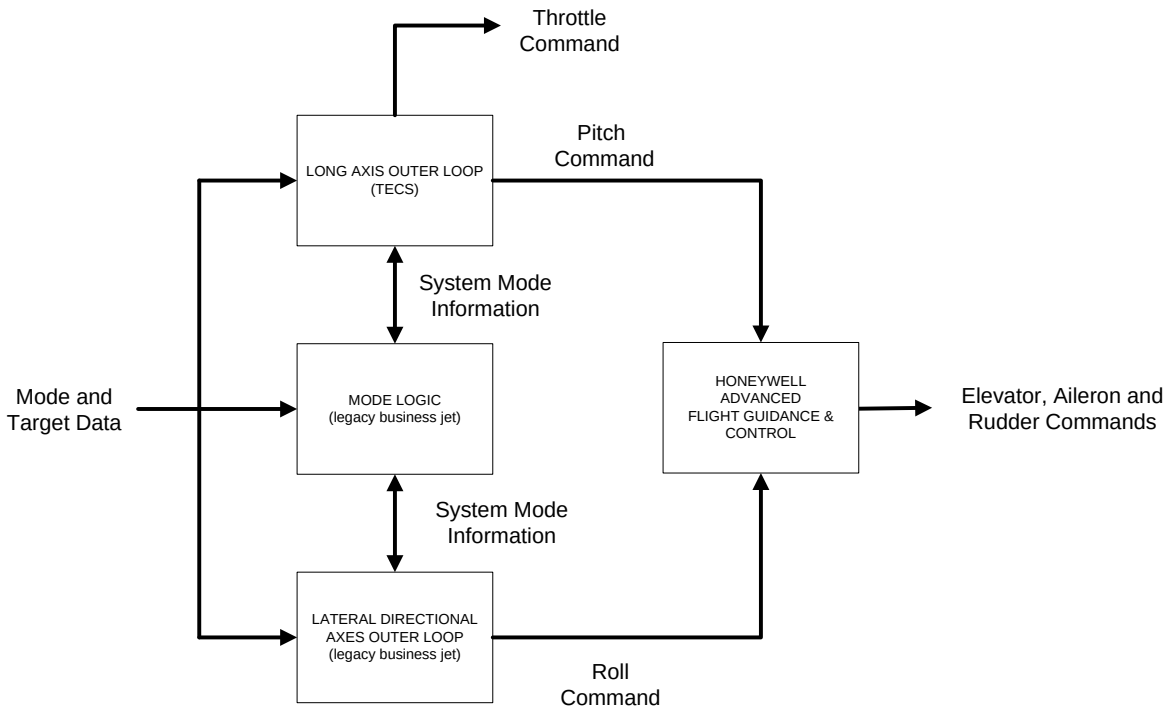

Figure 7. Advanced FG&C—Option 1

The first configuration used the outcome of the Task 1 study as a baseline, but replaced the legacy business jet IL control laws with a HI FG&C system configured to perform the IL function in all three axes. The pitch OL is implemented using the TECS vertical axis control laws. The lateral OL and mode logic of the legacy business jet used in this study were retained.

The second configuration is shown in figure 8.

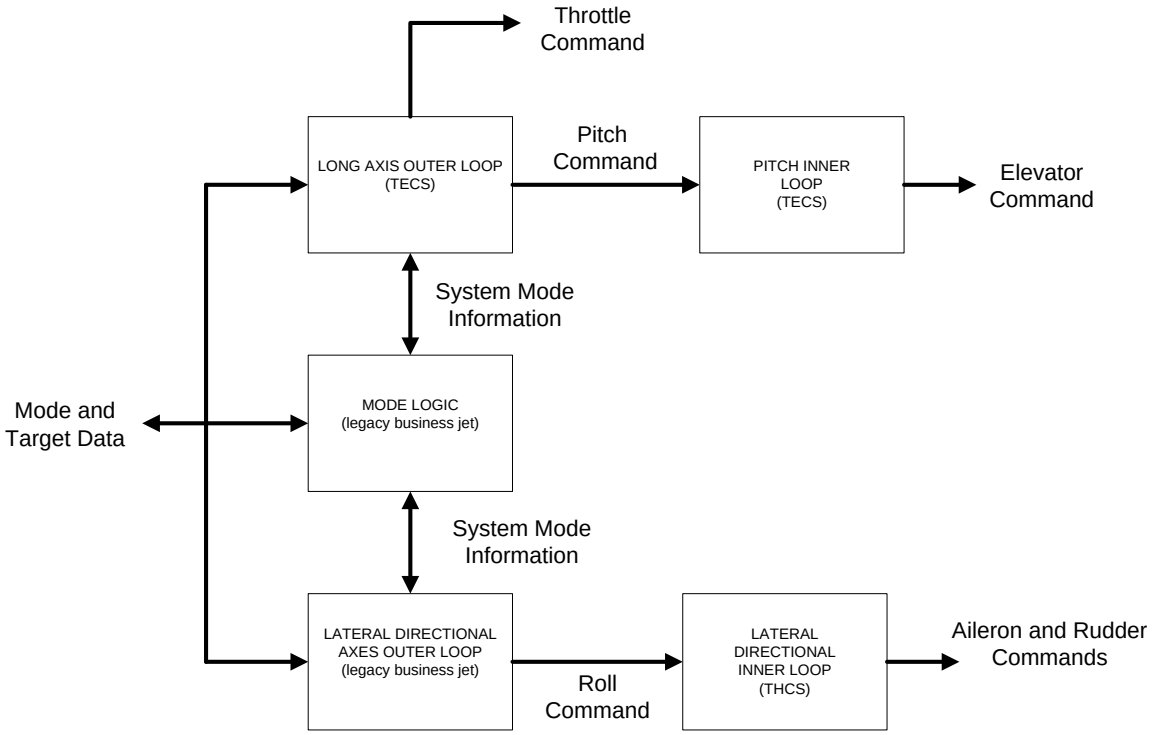

Figure 8. Advanced FG&C—Option 2

The second option also used the outcome of the Task 1 study as a baseline, but the IL control laws were replaced with the TECS and THCS ILs. The pitch OL was implemented using the TECS vertical axis control laws. Again, the lateral OL and mode logic functionality of the legacy business jet application were retained.

4.3 CONTROL LAW DEVELOPMENT.

This section provides a discussion of the analysis and development activities used to evaluate and, ultimately, articulate the IL and OL FG&C MIMO control laws considered for this study.

4.3.1 Inner Loop.

Two design approaches were considered for the IL control laws. The first method used a generic, reusable, advanced FG&C control law product developed by HI, and the second method was the expansion of the Task 1 TECS/THCS design to include the FAA-provided TECS/THCS IL implementation.

4.3.1.1 The HAFGC System Architecture.

The HAFGC system was developed with a similar objective as the TECS/THCS concept. HAFGC is a reusable vehicle FG&C law that has been successfully employed in several types of applications, including fighter aircraft, space vehicles, and unmanned vehicles.

The FG&C algorithms are parameterized in terms of the following items:

- Vehicle mass properties, aerodynamics, and actuation system constraints
- Control data, such as proportional and integral gains and axis prioritization
- Additional constraints, such as those related to envelope protection

HAFGC includes the capability for both OL and IL vehicle control. The HAFGC approach also uses an aircraft inversion methodology that separates aircraft control dynamics from the IL controller gains and, thereby, promotes the concept of a more generalized design.

The generic HAFGC control law consists of an attitude and a trajectory and position controller, as shown in figure 9.

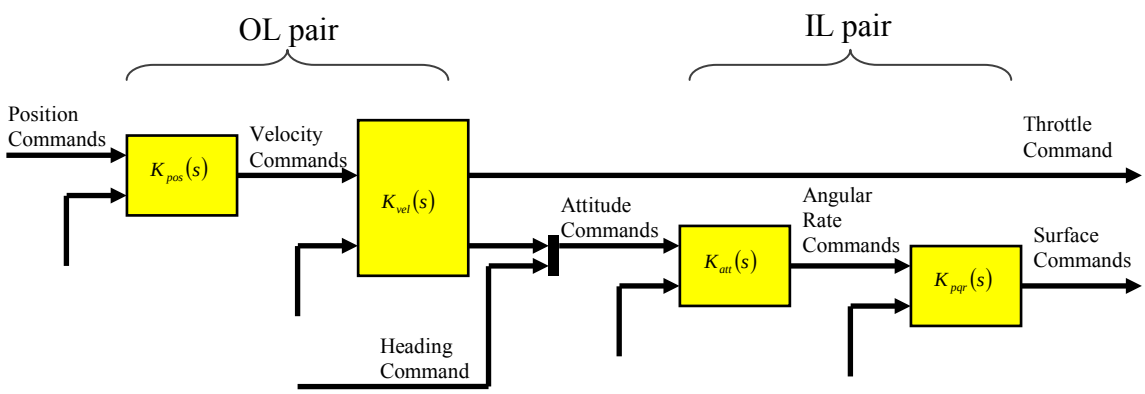

Figure 9. The HAFGC Control Law Block Diagram

For this study, the OL pair (position and velocity) is bypassed and only the IL (attitude and rate) pair is used to serve as the IL for the pitch, roll, and yaw axes.

Appendix A contains the detailed Bode plots (figures A-1 through A-4, A-8 through A-11, and A-12 through A-15) and step responses (figures A-5 through A-7 and A-16 through A-22) for a single flight condition. The flight condition is altitude 10,000 feet (ft) and airspeed 250 knots (kt), and the vehicle configuration is mid weight, mid center of gravity (c.g.).

Tables 1 through 3 summarize the resulting elevator, aileron, and rudder path stability margins, respectively, for the four values of transport delay evaluated at a single flight condition.

Table 1. The HAFGC Elevator Path IL Stability Margin Summary

Transport Delay (ms)	Gain Margin	Phase Margin
25	10.0 dB at 2.1 Hz	74.6 degrees at 0.7 Hz
50	8.3 dB at 1.8 Hz	68.1 degrees at 0.7 Hz
75	6.9 dB at 1.5 Hz	61.5 degrees at 0.7 Hz
100	5.7 dB at 1.4 Hz	55.0 degrees at 0.7 Hz

Table 2. The HAFGC Aileron Path IL Stability Margin Summary

Transport Delay (ms)	Gain Margin	Phase Margin
25	14.6 dB at 2.0 Hz	73.7 degrees at 0.26 Hz
50	11.7 dB at 1.7 Hz	71.4 degrees at 0.26 Hz
75	9.3 dB at 1.4 Hz	69.1 degrees at 0.26 Hz
100	7.5 dB at 1.3 Hz	66.7 degrees at 0.26 Hz

Table 3. The HAFGC Rudder Path IL Stability Margin Summary

Transport Delay (ms)	Gain Margin	Phase Margin
25	9.7 dB at 2.0 Hz	57.0 degrees at 0.8 Hz
50	7.4 dB at 1.6 Hz	49.6 degrees at 0.8 Hz
75	5.7 dB at 1.4 Hz	42.3 degrees at 0.8 Hz
100	4.4 dB at 1.3 Hz	34.9 degrees at 0.8 Hz

At a 50-ms transport lag, stability margins are greater than the selected guideline of 6 decibel (dB) and 45 degrees for all three axes. The rudder control path margins drop below the guideline at 75 ms.

The time responses due to pitch and roll steps show reasonably damped response for all parameters for transport lags up to 50 ms. As expected, the yaw axis parameters (yaw rate, lateral acceleration, and rudder) show the most sensitivity to transport lag beyond 50 ms of transport lag.

4.3.1.2 The TECS/THCS IL.

The TECS/THCS IL control laws consist of an independent pitch axis IL and a coupled lateral directional IL.

4.3.1.2.1 The TECS Pitch IL.

The top-level pitch axis IL is shown in figure 10.

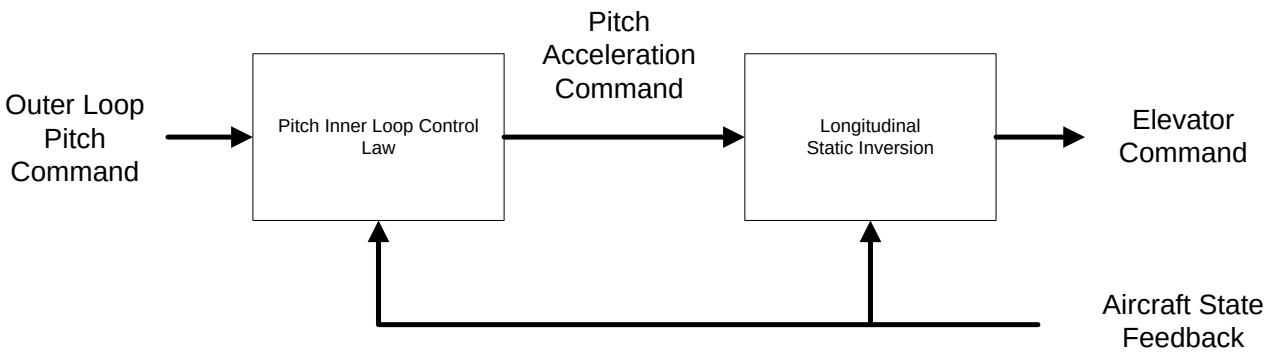

Figure 10. The TECS Pitch IL

The pitch IL control law computes a pitch acceleration command based on the OL pitch command and aircraft state feedback. The elevator command necessary to produce the desired angular acceleration is computed using a static inversion technique.

4.3.1.2.2 The TECS Longitudinal Static Inversion.

The longitudinal static inversion makes use of the equation of motion that defines the relationship between the rate of change of angular rate ($\dot{q}$) in the pitch axis and the external moments acting upon the airplane and the current airplane state.

$$I_{yy} * \dot{q} = M_A + M_T - (I_{xx} - I_{zz}) * p * r - I_{xz} * (p^2 - r^2)$$

Ignoring cross coupling terms due to roll rate and yaw rate and expanding the aerodynamic pitch moment term yields

$$I_{yy} * \dot{q} = \overline{q} S c * c_m + M_T$$

The total pitching moment is approximated using stability derivative estimates for those terms that are determined to be the most significant.

For the airplane used in this study, c_m is approximated as

$$c_m = c_{m_a} * \alpha + c_{m_q} * q + c_{m_{etab}} * etab + c_{m_{stab}} * stab + c_{m_{elev}} * elev$$

The selected derivatives include the standard set of terms related to vehicle dynamics and trim activity.

Given a desired pitch acceleration ($\dot{q}_{des}$), the required elevator command is computed as

$$elev_{cmd} = \left(\frac{\dot{q}_{des} * \left(\frac{I_{yy}}{\bar{q}Sc} \right) - \left[c_{m_a} * \alpha + c_{m_q} * q + c_{m_{etab}} * etab + c_{m_{stab}} * stab + \left(\frac{M_T}{\bar{q}Sc} \right) \right]}{c_{m_{elev}}} \right)$$

The static inversion equation is shown implemented in block diagram form in figure 11.

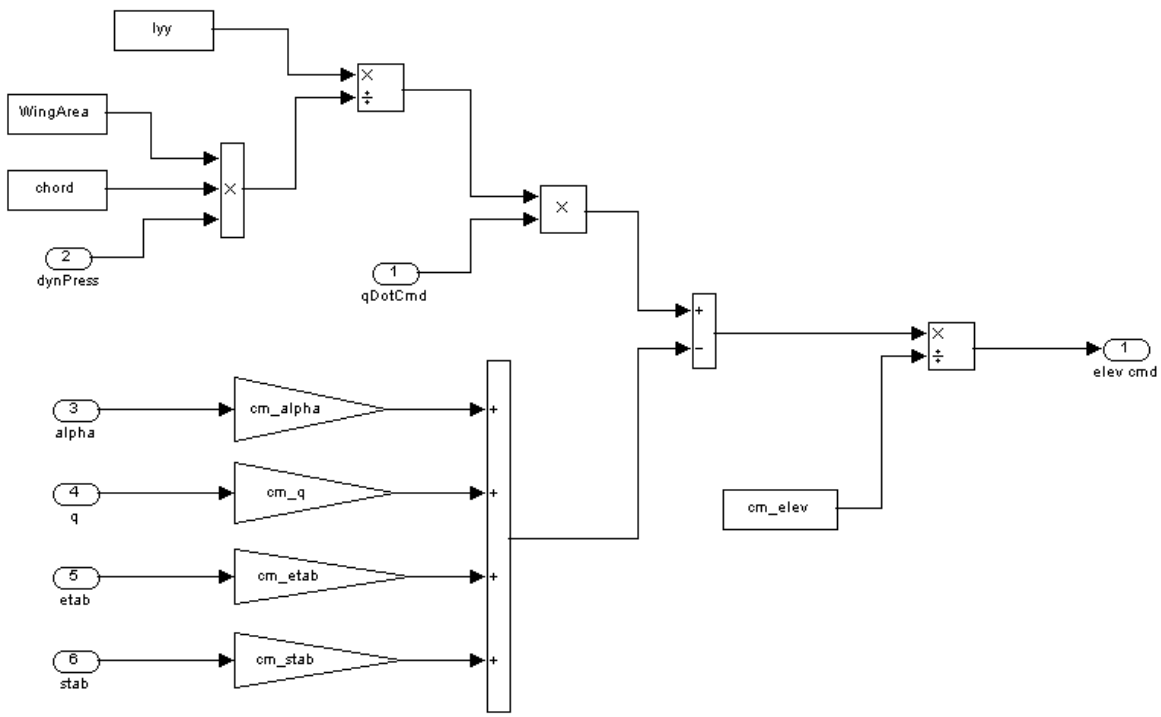

Figure 11. The TECS Longitudinal Axis Static Inversion

This implementation neglects the pitching moment (M_T) due to engine thrust and the moment arm between the location of the engines and the aerodynamic reference point with only a minor penalty in the accuracy of the inversion for the aircraft model being used in this study.

4.3.1.2.3 The TECS Pitch IL Control Law.

The pitch IL control law is shown in figure 12.

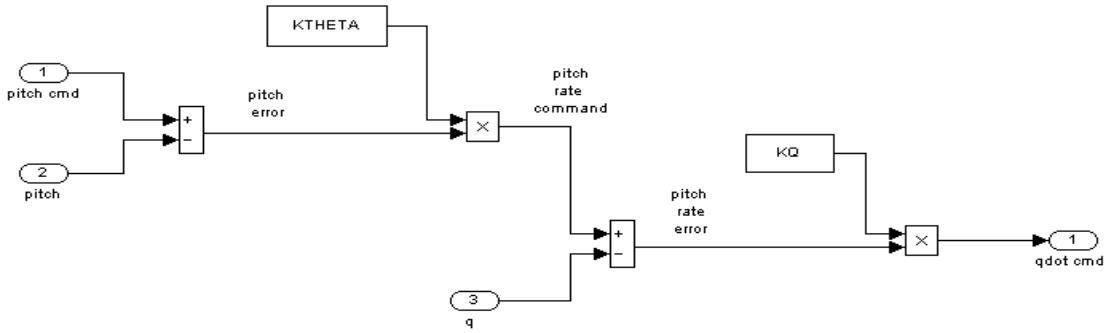

Figure 12. The TECS Pitch IL Control Law

The control law computes a pitch acceleration command based on an OL pitch attitude command with loop closure on pi tch attitude and pitch rate. T he OL command is rate-limited and magnitude-limited depending on the active vertical flight director mode. There is no m ode dependency in the IL.

The pitch IL control law gains are set, as shown in table 4.

Table 4. The TECS Pitch IL Gains

Gain	Value
KTHETA	1.6
KQ	6.4

Initial evaluations were conducted with transport delays in the elevator path that were greater than the design guideline of 50 ms, and the resulting performance was lightly damped. Once the transport lag was reduced to 50 ms, performance improved significantly, and it was determined that the baseline gains provided adequate time domain response characteristics and stability margin for the airplane used in this study.

4.3.1.2.4 The TECS Pitch IL Linear Analysis.

The closed-loop sytem shown in figure 13 was used to analyze the time and frequency domain characteristics of the pitch IL design.

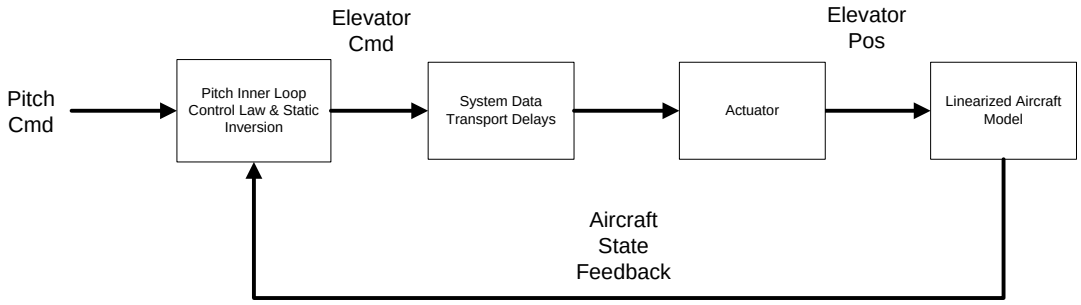

Figure 13. The TECS Pitch IL Analytical Model

The model shown includes the pitch IL and static inversion, a model for the control surface actuator, a linearized model of the airplane, and a model to account for the system transport delays.

The total system transport delay is defined to be the sum of all the delays associated with the synthesis of the control law command, the transmission of the command to the control surface, and the subsequent measurement and transmission of the appropriate aircraft sensor data feedbacks that complete the closed-loop control law. A range of values were considered for total system transport lag from an optimistic value of 25 ms to a pessimistic value of 100 ms.

The elevator hydraulic actuator is modeled as a linear second-order transfer function with a 3-dB bandwidth of 3.5 hertz (Hz).

Using the above assumptions, time and frequency responses were examined for multiple flight conditions to assess the performance of the IL control law. Appendix B contains the detailed Bode plots (figures B-1 through B-4) and step responses (figures B-5 through B-7) for a single flight condition. The flight condition is altitude 10k and airspeed 250 kt, and the vehicle configuration is mid weight and mid c.g.

Table 5 summarizes the stability margin sensitivity to transport delay.

Table 5. The TECS Pitch IL Stability Margin Summary

Transport Delay (ms)	Gain Margin	Phase Margin
25	10.4 dB at 2.6 Hz	58.7 degrees at 1 Hz
50	7.8 dB at 2.1 Hz	49.5 degrees at 1 Hz
75	5.8 dB at 1.8 Hz	40.3 degrees at 1 Hz
100	4.2 dB at 1.5 Hz	31.1 degrees at 1 Hz

The goal of meeting 6 dB of gain margin and 45 degrees of phase margin is achieved with a transport delay of 50 ms or less.

The time response due to a pitch step input also shows adequate damping for transport delays up to 50 ms. Above 50 ms, damping begins to deteriorate significantly.

4.3.1.3 The THCS Lateral Directional IL.

The lateral directional IL control law consists of a coupled roll and yaw axis control law followed by a static inversion, as shown in figure 14.

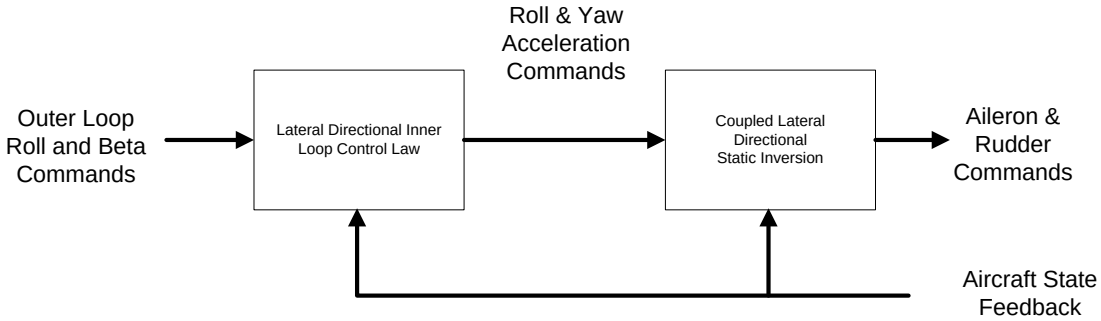

Figure 14. The THCS Lateral Directional IL

The OL command for roll attitude command and a side slip command of zero drive the control law to compute roll and yaw acceleration commands. These commands are converted to aileron and rudder commands using the static inversion method.

4.3.1.3.1 The THCS Lateral Directional Static Inversion.

The lateral directional static inversion makes use of the equations of motion that define the rate of change of angular rate ($\dot{p}$ and $\dot{r}$) in the roll and yaw axes.

$$I_{xx} * \dot{p} - I_{xz} * \dot{r} = L_A + L_T - \left(I_{zz} - I_{yy}\right) * r * q + I_{xz} * p * q$$

$$I_{zz} * \dot{r} - I_{xz} * \dot{p} = N_A + N_T - \left(I_{yy} - I_{xx}\right) * p * q - I_{xz} * r * q$$

Ignoring cross-coupling terms with q and I_{xz}, neglecting roll and yaw moments due to engine thrust and expanding the aerodynamic moment term yields

$$I_{xx} * \dot{p} = \overline{q} S b * c_r$$

$$I_{zz} * \dot{r} = \overline{q} S b * c_n$$

where

$$c_r = c_{r_p} * p + c_{r_r} * r + c_{r_\beta} * \beta + c_{r_{ail}} * ail + c_{r_{rud}} * rud$$

$$c_n = c_{n_p} * p + c_{n_r} * r + c_{n_\beta} * \beta + c_{n_{ail}} * ail + c_{n_{rud}} * rud$$

Given a desired $\dot{p}$ and $\dot{r}$, the required aileron and rudder commands can be computed as

$$ail_{cmd} = \left(\frac{\dot{p}_{desired} * \left(\frac{I_{xx}}{\bar{q}Sb} \right) - \left(c_{r_p} * p + c_{r_r} * r + c_{r_\beta} * \beta + c_{r_{rud}} * rud \right)}{c_{r_{ail}}} \right)$$

$$rud_{cmd} = \left(\frac{\dot{r}_{desired} * \left(\frac{I_{zz}}{\bar{q}Sb} \right) - \left(c_{n_p} * p + c_{n_r} * r + c_{n_\beta} * \beta + c_{n_{ail}} * ail \right)}{c_{n_{rud}}} \right)$$

Figure 15 shows the coupled static inversion in block diagram form.

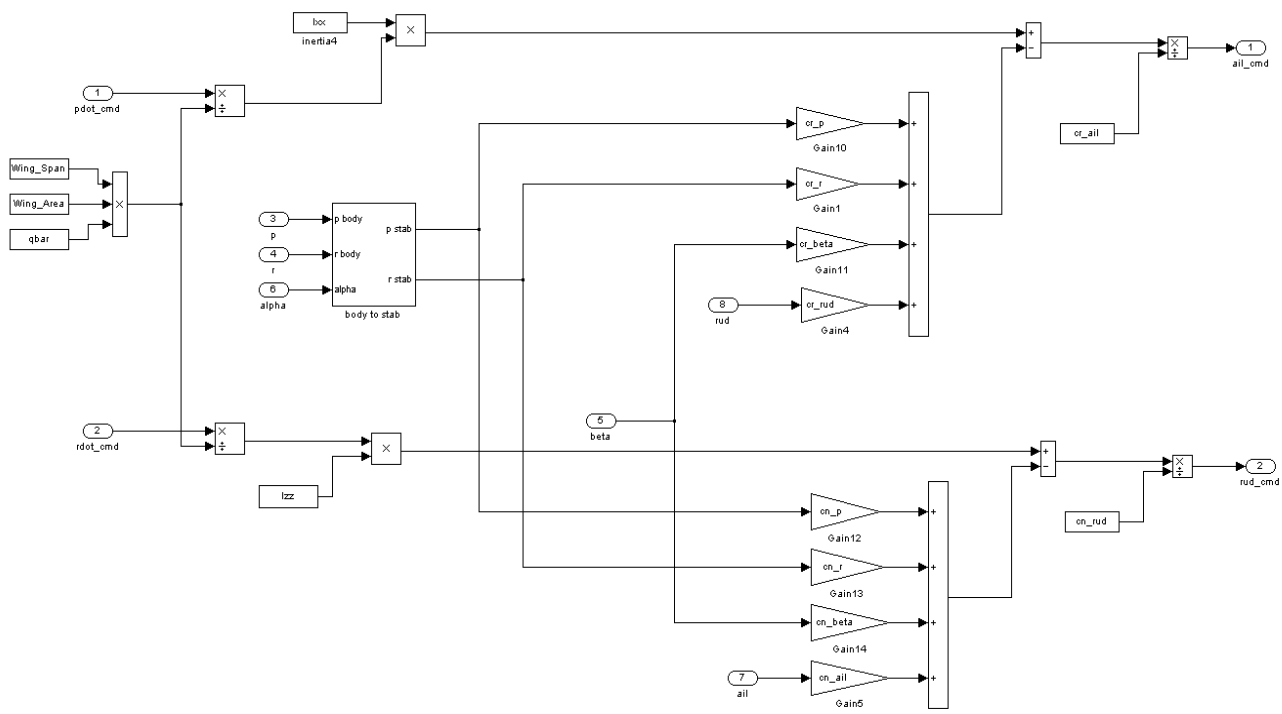

Figure 15. The THCS Lateral Directional Static Inversion

4.3.1.3.2 The THCS Lateral Directional IL Control Law.

Figure 16 shows the THCS lateral directional IL control law.

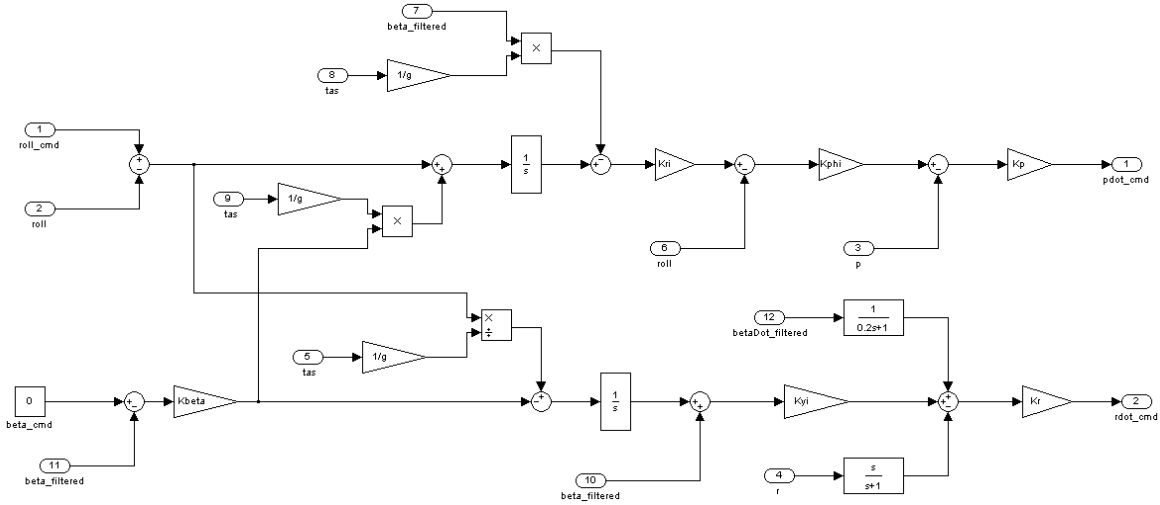

Figure 16. The THCS Coupled Lateral Directional IL Control Law

The roll axis loop computes a roll acceleration command that nulls the sum of the roll attitude error and the side slip error. The yaw axis loop computes a yaw acceleration command that nulls the difference between the roll error and the side slip error.

It should be noted that there is a difference between the implementation shown in figure 16 and the FAA-supplied THCS control laws. The decision to retain the existing lateral OL control laws resulted in the need to make alterations to the THCS IL control law.

In the standard THCS OL/IL interface, the various THCS lateral OL control laws (heading, track, localizer, and LNAV) produce a heading or ground track error which is used by the lateral directional THCS IL to synthesize a magnitude and rate-limited roll command. The heading/track error gain and subsequent roll rate limits and roll magnitude limits are mode independent.

Each legacy OL control law computes rate-limited and magnitude-limited roll commands that are also based on heading/track error, but the heading/track error gains, roll rate limits, and roll magnitude limits vary for each OL control law. For this reason, the THCS IL was modified to accept roll commands directly, and there is no standard heading/track error gain, roll rate limit or roll magnitude limit used in the IL. This mode-dependent functionality is performed in the OLs.

The complementary filter used to produce the filtered side slip and the side slip rate (based on measured beta and inertial data) is shown in figure 17.

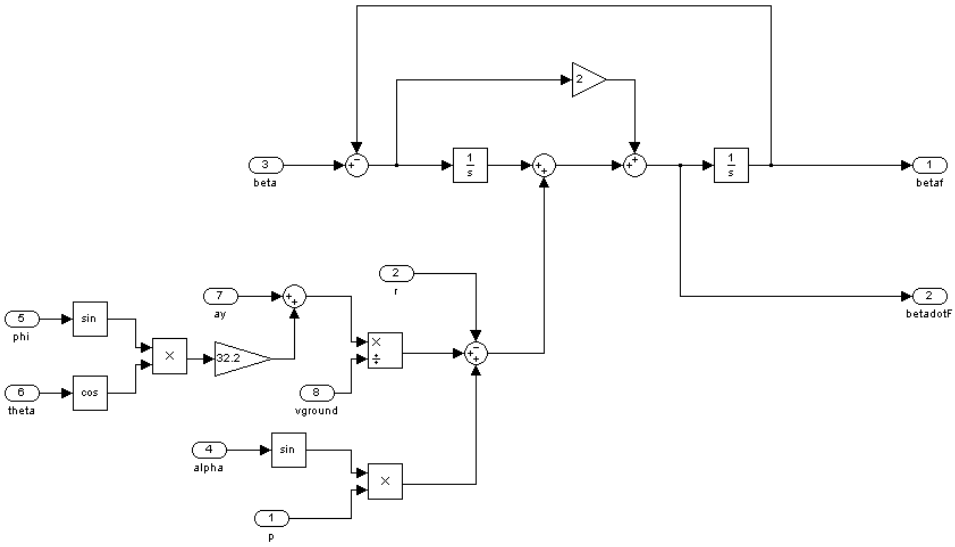

Figure 17. The THCS Side Slip Complementary Filter

The baseline implementation of the lateral directional IL did not use a washed-out beta dot feed forward term, and the yaw rate feedback in the rudder control loop was not filtered.

Initial performance was evaluated without these elements and also with transport lags in both the aileron and rudder path that were larger than the design goal of 50 ms. The resulting performance was lightly damped in the yaw axis. Attempts to improve performance with gain reductions alone were not successful and resulted in secondary performance issues in the roll axis. Upon discovering the larger than expected transport delays in both axes, the simulation environment was modified to reduce the aileron path transport lag to 50 ms and the rudder path transport lag to 75 ms. This resulted in improved, but still less than desirable, performance. Upon recommendations from the FAA, the IL gains were modified, and the beta dot feed forward and yaw rate low-pass filter were added. This provided further improvement in performance, but still there were issues. Finally, a combination of time domain and frequency domain analysis while varying the IL gains yielded a solution that delivered acceptable performance.

The final gain set, as well as the original gains and the updated gains, both provided by the FAA are summarized in table 6.

Table 6. The THCS Lateral Directional IL Gains

Gain	FAA Original Value	FAA Updated Value	Honeywell Adjusted Value
kRI	0.4	0.4	0.4
KPHI	1.6	1.6	1.6
KP	6.4	4.0	5.0
KBETA	0.125	0.15	0.15

Table 6. The THCS Lateral Directional IL Gains (Continued)

Gain	FAA Original Value	FAA Updated Value	Honeywell Adjusted Value
KYI	0.45	0.4	0.4
KR	6.6	1.6	4.0
TAU LAG	NA	1.5	0.2
TAU WASH	NA	1.5	1.0

The primary change from the original gain set was the introduction of the filter elements and a reduced KP and KR. The final values for KP and KR determined to be appropriate for the airplane used in this study were closer to the original gain set. Filter time constants were also significantly altered to maximize performance.

4.3.1.3.3 The THCS Lateral Directional Linear Analysis.

The closed-loop sytem shown in figure 18 was used to analyze the time and frequency domain characteristcs of the lateral directional IL design.

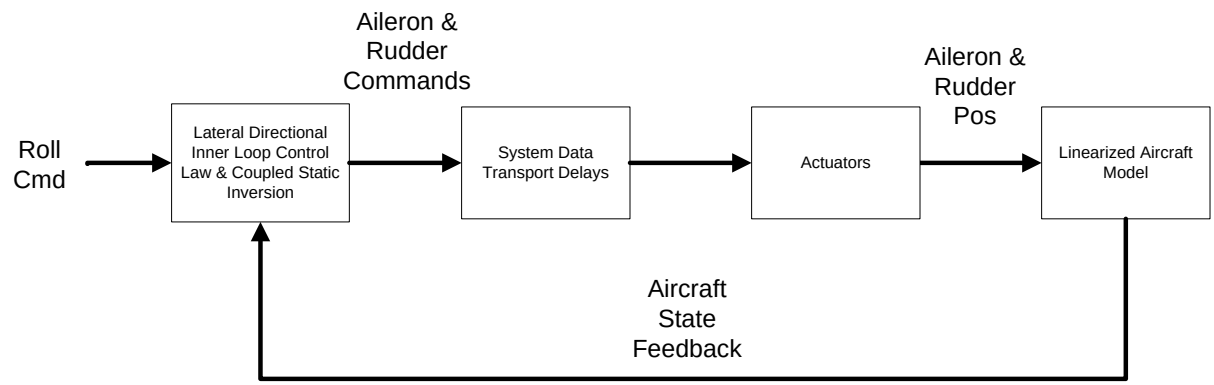

Figure 18. The THCS Lateral Directional IL Analytical Model

The model shown includes the lateral directional IL and coupled static inversion, a model for the control surface actuators, a linearized model of the airplane, and a model to account for the system transport delays.

The aileron and rudder actuators were modeled as linear, second-order transfer functions with a 3-dB bandwidth of 4.5 and 3.75 Hz, respectively. A range of values were considered for total system transport lag from an optimistic value of 25 ms to a pessimistic value of 100 ms.

Using the above assumptions, time and frequency responses were examined for multiple flight conditions to assess the performance of the IL control law. Appendix B contains the detailed Bode plots (figures B-8 through B-11 and B-12 through B-15) and step responses (figures B-16

through B-22) for a single flight condition. The flight condition is altitude 10,000 ft and 250 kt airspeed, and the vehicle configuration is mid weight, mid c.g.

Tables 7 and 8 summarize the sensitivity to transport delay for the aileron and rudder control loops.

Table 7. The THCS Aileron IL Stability Margin Summary

Transport Delay (ms)	Gain Margin	Phase Margin
25	24.8 dB at 3.6 Hz	61.9 degrees at 0.2 Hz
50	21.4 dB at 2.7 Hz	59.6 degrees at 0.2 Hz
75	15.8 dB at 0.64 Hz 18.9 dB at 2.2 Hz	57.2 degrees at 0.2 Hz
100	11.9 dB at 0.58 Hz 16.8 dB at 1.9 Hz	54.6 degrees at 0.2 Hz

Table 8. The THCS Rudder IL Stability Margin Summary

Transport Delay (ms)	Gain Margin	Phase Margin
25	-9.7 dB at 0.24 Hz 17.6 dB at 3.0 Hz	50.7 degrees at 0.7 Hz
50	-9.5 dB at 0.24 Hz 12.1 dB at 2.0 Hz	46.1 degrees at 0.7 Hz
75	-9.3 dB at 0.24 Hz 8.6 dB at 1.6 Hz	41.7 degrees at 0.7 Hz
100	-9.0 dB at 0.25 Hz 6.2 dB at 1.3 Hz	37.3 degrees at 0.7 Hz

Tables 7 and 8 show that the goal of meeting 6 dB of gain margin and 45 degrees of phase margin is achieved in both axes for transport lag values of 50 ms or less.

The time response due to a roll step sequence shows a well-damped response for transport lags up to and including 100 ms.

4.3.2 Outer Loop.

The hybrid TECS/legacy HI OL consists of the vertical axis and lateral axis control laws and the associated mode logic function. Figure 19 shows the structure of the OL.

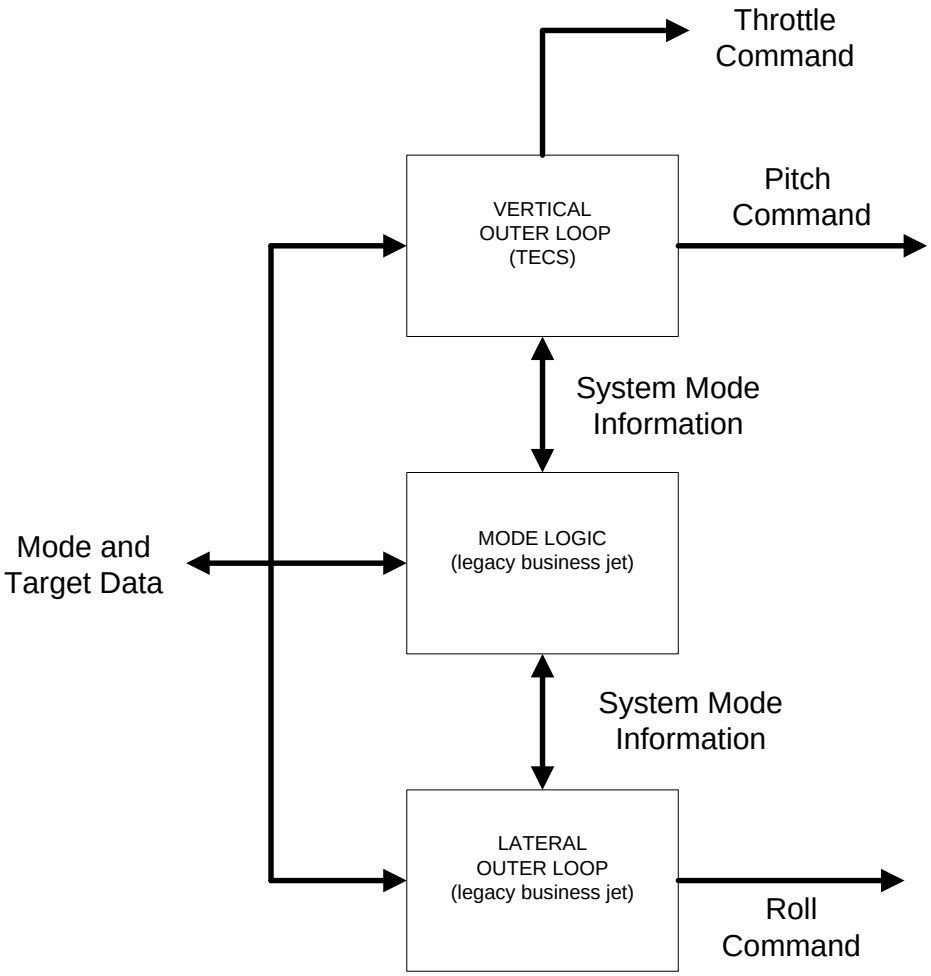

Figure 19. The OL

As stated in section 2, the vertical axis TECS OL control laws are the only reusable FG&C OL elements that are under consideration for evaluation in this study. The mode logic and lateral axis OL control laws of a legacy business jet were used to provide a means for evaluating the lateral FG&C ILs only. Because it is not an objective within this study to evaluate these legacy elements for reusability, no in-depth discussion of these OL functions is included in this section.

The TECS vertical axis outer FG&C control laws were implemented in Task 1 of this study, but were not evaluated in terms of the need for gain adjustments in order to achieve desired performance. Although the TECS control laws were developed with the intent to provide a reusable standardized OL design that would not require aircraft specific modifications, it was determined that this was a necessary step.

4.3.2.1 Vertical Axis.

The TECS is used to control the airplane longitudinal axis. The concept uses an energy-based control strategy. Thrust is used to control the airplane's total energy requirement based on flight path and speed targets. The elevator is used to control the channeling of energy to flight path or

speed, or both. T he TECS strategy provides simultaneous, coordinated pitch and thrust commands to achieve energy efficient/pilot-like control with decoupled command responses. The airplane will only respond as intended to a control command, without causing significant unintended responses in the other command state variable.

The TECS pitch OL consists of mode logic, a flight path control function, an airspeed control function, and a core algorithm that converts flight path and airspeed commands to pitch and thrust commands. Figure 20 shows the general structure of the TECS pitch OL.

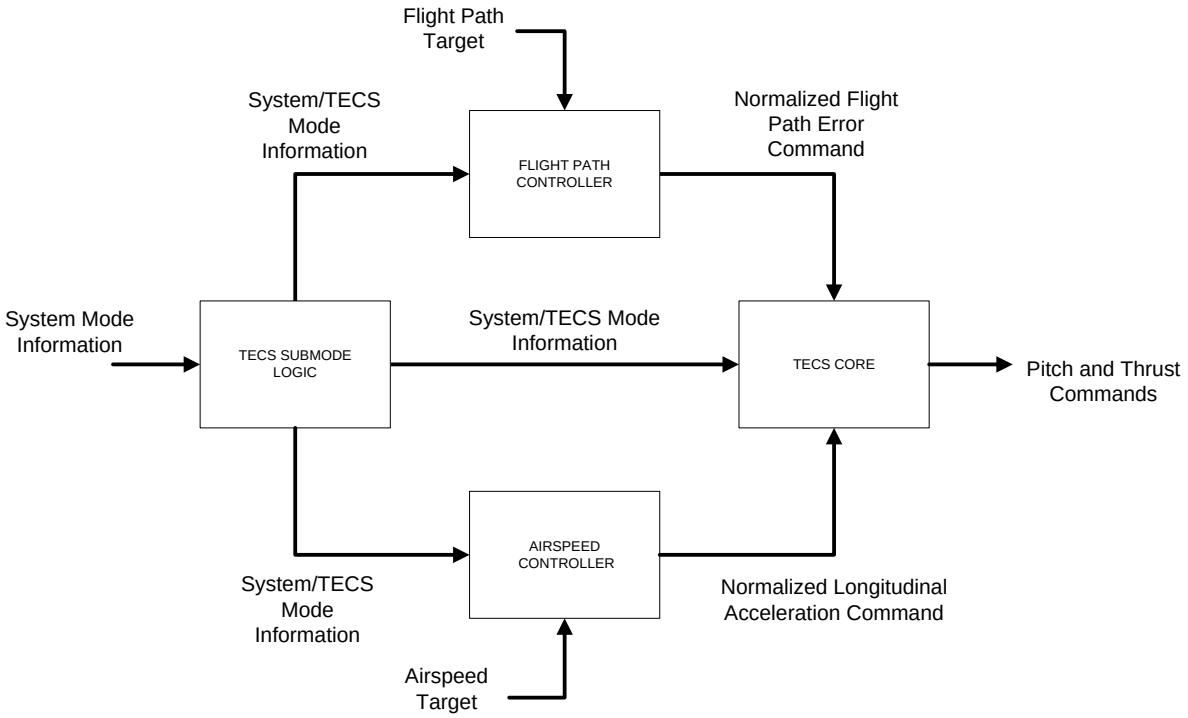

Figure 20. The TECS Pitch OL

The mode control block uses high-level system mode information, engine status, and control law internal information to determine the active TECS submode. The submode is nominally MIMO, but will revert to PATH or SPEED priority based on the existing conditions. In general, when engine thrust has reached idle or max thrust, speed control using the throttles is no l onger possible, and the choice must be made to control airspeed using pitch or path control. When the airplane is within the normal flight envelope, SPEED control is selected when the airplane is climbing or descending using the Flight Management Computer (FMC) mode. All other vertical modes (flight path angle (FPA), vertical speed, go around, altitude capture, altitude hold, and glide slope) are considered to be PATH control modes. If V_{MIN} or V_{MAX} is reached with the engine in saturation, then a reversion to SPEED control is activated for envelope protection.

The flight path controller computes a normalized flight path command, which is the vertical flight path-related component of the airplane's specific energy rate. A flight rate-limited flight path error is computed that imposes the selected mode-dependent g-limit.

The airspeed controller computes a normalized, dimensionless, longitudinal acceleration command, which is the airspeed-related component of the airplane's specific energy rate ($\frac{\dot{V}_c}{g}$). This acceleration command is then used to compute rate-limited command error. These commands are input to the TECS core processing algorithm, as shown in figure 21.

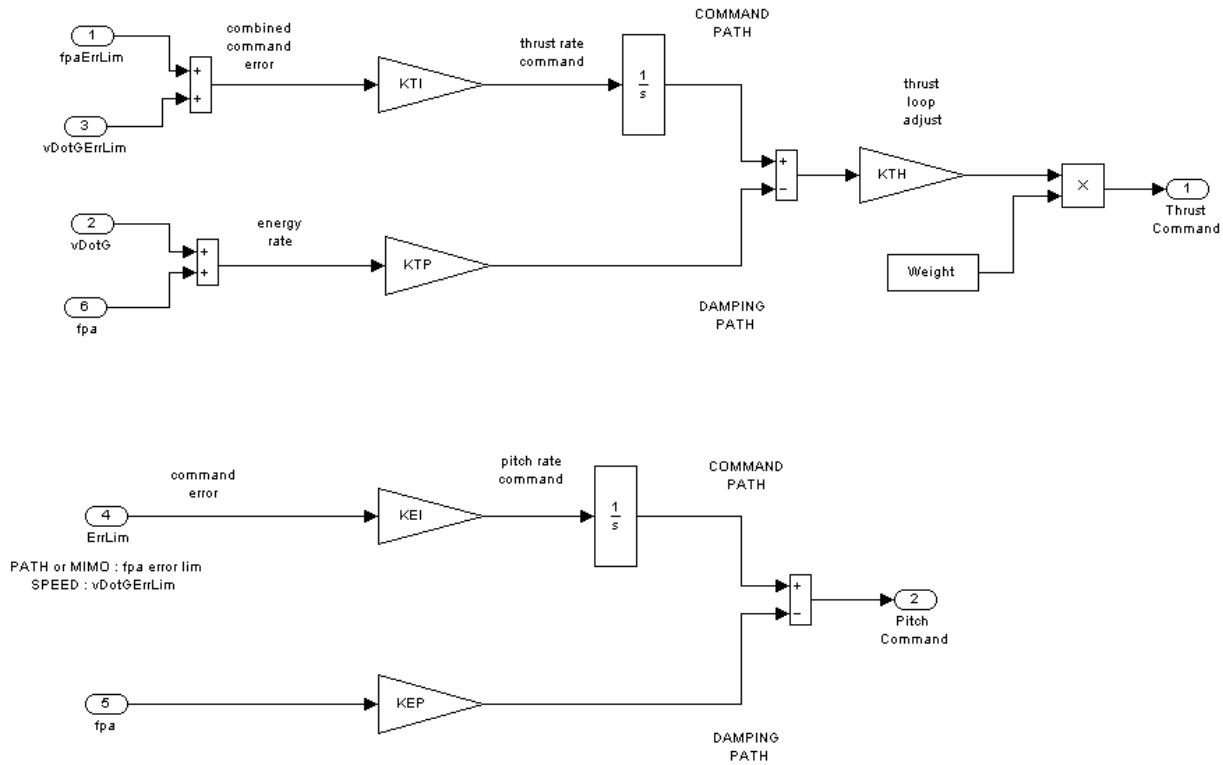

Figure 21. The TECS Core

Each control path includes an integrated command path and a damping path. The sum of the flight path angle error and normalized longitudinal acceleration error signals are formed to develop the net thrust command. Damping in the thrust loop is achieved using the estimated energy rate. The final net thrust command is scaled in proportion to the actual airplane weight and an adjustment scale factor. The scale factor adjustment is provided for the purpose of balancing the thrust and flight path angle/longitudinal acceleration control dynamics.

When the TECS submode is MIMO or PATH, the flight path angle error is used to develop the pitch command. When the submode is SPEED, the normalized longitudinal acceleration error signal is used. Damping in the pitch loop is achieved using flight path angle.

For proper TECS functionality, the energy distribution and total energy control dynamics must be equally balanced. This is a prerequisite for assuring that the delta energy produced in case of a single flight path or speed command goes entirely toward satisfying the new command and does not spillover onto the variable with an associated constant command. This is the mechanism for

providing very simple and effective control command response decoupling. Simultaneous flight path and speed commands with opposing energy demands are executed by first exchanging energy to the extent possible using elevator control only, before commanding a thrust change to satisfy the final total energy demand. Thus, maneuvers are always executed in the most energy efficient way possible, while also eliminating undesirable engine control activity.

Upon recommendation from the FAA, an evaluation was performed to establish that the thrust and flight path loop were, in fact, balanced properly. This test consisted of a series of flight path and airspeed step responses at multiple flight conditions. Small flight path angle steps of ±3° in FPA mode and small airspeed steps of ±5 kt in altitude ALT HOLD mode were used. Steps were performed at four flight conditions (5-kt calibrated airspeed (CAS) at 140 kt, 10-kt CAS at 200 kt, 10-kt CAS at 250 kt, and 10-kt at CAS 300 kt) to ensure that acceptable performance could be achieved with a single gain set independent of flight condition.

The performance objectives established for this test to ensure proper loop balancing included:

- Response time—A target value of 10 seconds was used for flight path steps of ±3° and 20 seconds for airspeed of ±5 kt.

- Overshoot—Minor overshoot (<5%) is acceptable.

- Damping—Overdamped response with no oscillations in any parameters.

Cross-coupling objectives included:

- Speed variance—no more than 0.5 kt for flight path steps
- Altitude variance—no more than 5 ft for airspeed steps

If required, the thrust path IL gain (KTH) could be adjusted to optimize the balancing of the loop dynamics, but the command and damping path gains were not expected to vary from the FAA-provided values.

From the results of these tests, however, it was concluded that both the command and damping path gains, as well as the thrust loop balancing gain, required adjustments to provide matched loop dynamics that would meet the performance objectives established above.

The gains were varied to optimize the dynamic response for both axes, and the resulting TECS core gains determined from this exercise (as well as the FAA-provided gains) are listed in table 9.

Table 9. The TECS Core Gains

Gain	FAA Original Value	HI Adjusted Value
KTI	0.4	0.30
KTP	0.3	0.60
KEI	0.4	0.30
KEP	1.6	0.60
KTH	1.0	1.12

In contrast to the original FAA-provided gains, it was determined that optimal performance was achieved with identical command and damping gains used in both the thrust and flight path loops. Command path gains were reduced by 25% in both paths. Damping was significantly reduced in the flight path loop while being significantly increased in the thrust loop. An overall thrust loop gain of 12% was also required.

The selected gains result in satisfactory OL performance and meet the objectives listed for response time, overshoot, and damping ratio.

In the case of ±3° flight path steps, airspeed variance was 0.3 kt or less for most flight conditions. The one exception was the low speed +3° step scenario, in which the peak airspeed variation was 0.9 kt.

For airspeed steps of ±5 kt, altitude variance was 2 ft or less for most flight conditions. At the low speed, the altitude change for a -5 kt step was 6 ft.

4.4 REAL-TIME SIMULATION EVALUATION.

Section 3.1.2 defined the two configurations of FG&C control architectures that were considered for evaluation in this study. The primary difference between the two methods is the implementation of the IL control laws. Option 1 used the Honeywell method, and option 2 used the TECS/THCS approach.

4.4.1 Option 1 Results.

Initial attempts to integrate and evaluate the option 1 approach in the high-fidelity simulation environment resulted in significant performance issues relating to the IL, which were not fully understood at the time. The decision was made to proceed with the integration and evaluation using the option 2 approach.

Due to resource constraints, the option 1 architecture was not reevaluated with the improved real-time simulation environment. However, it is believed that, based on the success ultimately

achieved with the option 2 mechanization, the option 1 mechanization would also perform well in the revised real-time simulation environment.

4.4.2 Option 2 Results.

Initial attempts to integrate the option 2 architecture also experienced less than satisfactory results during first evaluation. After further investigation, it was determined that the overall system transport delays were not completely represented in the analytic models. The linear analysis performed previously indicated that values closer to 50 ms were needed to ensure good performance; the high-fidelity environment confirmed that this was the case for both options. The decision was made based on FAA guidance to make modifications to the simulation models to reduce the transport delays to values closer to 50 ms, a value that should be readily achievable in an FG&C system.

The elevator and aileron path transport lags were reduced to 50 ms, and the rudder path transport lag was reduced to 75 ms. Due to complexities of the simulation environment, the cost of modifying the simulation for further reduction was judged to be unacceptable for the program, and the remaining limitations were accepted.

Upon making this adjustment to the simulation architecture, IL performance was significantly improved for the option 2 mechanization, but some issues remained in the rudder control axis. Section 3.2 describes the final adjustments that were made to the THCS IL to achieve the desired level of performance.

The following sections give a summary of the evaluation tests performed for the vertical and lateral axis and the results of this test activity.

4.4.2.1 Vertical Evaluation Summary.

To validate that the implementation of the TECs design performs as expected, the FAA supplied Honeywell with a series of vertical test scenarios, or check cases, to use as a reference. The check cases consisted of a variety of vertical axis airplane maneuvers that exercise the energy management capabilities of TECS. In each example, the expected behavior was documented as a series of time recordings of altitude, airspeed, attitude, elevator, and thrust. The FAA-provided data were produced using a MATLAB simulation of a generic air transport airplane.

The comparison of the results was not expected to match precisely due to the significant differences in the FAA reference aircraft model and the business jet reference model used in this study.

Appendix C gives the results of the comparison of the performance recorded using the Honeywell PC Sim and the reference FAA simulation.

The objectives for the vertical test cases were to:

- Demonstrate the decoupled pilot-like command responses in which the airplane responds to single axis control commands without causing significant unintended response in the other axis.

- Demonstrate the energy efficient coordinated response to simultaneous flight path and air speed change requests.

- Demonstrate that flight path and airspeed commands with opposing energy demands are executed by first exchanging energy to the extent possible using elevator control only before commanding a thrust change to satisfy the final total energy demand.

Check cases 1 through 4 (figures C-1 through C-16) are all examples of a single-axis command designed to illustrate the minimization of energy spillover when executing a command in one axis (flight path or speed only).

Check cases 1 and 3 consisted of a simple flight level change (climb 5000 and 500 ft) while holding a fixed airspeed (250 kt). The altitude profile of the Honeywell airplane compared very well with the reference FAA airplane. Airspeed was controlled to within ±0.5 kt in both cases.

Check cases 2 and 4 consisted of a simple airspeed change (25 and 100 kt) while holding altitude (10,000 ft). The airspeed profile of the Honeywell airplane compared favorably with the reference FAA airplane. Altitude was controlled to within ±10 ft in both cases.

Check cases 5 (figures C-17, C-18, C-19, and C-20) and 7 (figures C-25, C-26, C-27, and C-28) are examples in which airspeed reduction was requested during climb. These cases are both examples of conflicting energy requirements. In case 5, the airspeed decrease requested was large enough that the throttles were not used at first and all the energy needed to initiate the climb was taken from the airplane's kinetic energy. The throttles were advanced when the point at which the available energy was exhausted. In check case 7, the airspeed reduction was less and throttle movement was required sooner.

In check case 6 (figures C-21, C-22, C-23, and C-24), an airspeed increase was requested during climb. In this case, there was no conflict in energy requirements and the throttles were moved to maximum and held until the airplane to leveled off at the desired altitude.

In check case 8 (figures C-29, C-30, C-31, and C-32), an airspeed reduction during descent was required. In this case, the airspeed reduction request was delayed until after the throttles were already in the idle position. To satisfy the objective to reduce the aircraft energy state in a configuration where the thrust levels are already at minimum, the control laws elect to level off the airplane to slow down. Once the excess energy was burned off by drag, the airplane could resume descent to the target altitude.

In check case 9 (figures C-33, C-34, C-35, and C-36), the airplane was slowed to V_{MIN} (1.2 V_{stall}) and then the flaps were deployed incrementally. With each flap increment, V_{MIN} dropped and the control laws reduced the airspeed to stay on target. In this case, the behavior of the two airplane was similar, but not identical. In the case of the Honeywell airplane, there was slightly more altitude variation in response to flap motion.

Check case 10 (figures C-37, C-38, C-39, and C-40) was a glide slope capture and track from 1500 ft above ground level. At 500 ft above ground level go around was selected with a target altitude of 3000 ft. The airplane climbed rapidly and then captures the target altitude. The altitude and airspeed profiles were very similar for the two airplanes. When go around was activated, there was airspeed variation from the target of ±1 to 3 kt for both airplanes.

Check case 11 (figures C-41, C-42, C-43, and C-44), exercised the flight path mode in descent and then climb. Airspeed was controlled to within ±0.5 kt of the target for both airplanes.

In check case 12 (figures C-45, C-46, C-47, and C-48), the airplane flew near the ground (2000 ft) and slow (127 kt) with flaps deployed and gear extended. The airplane was then exposed to a horizontal wind shear of 2 kt/sec. The altitude loss was less than 15 ft for both airplanes and the airspeed loss was less than 20 kt for both aircraft.

In check case 13 (figures C-49, C-50, C-51, and C-52), the airplane was also flying low and slow (2k ft 127 kt) with flaps deployed and gear up. The airplane was exposed to moderate turbulence that is intended to be single-axis, 5-ft/sec root mean square. The PC Sim Honeywell Dryden model applied the turbulence on all three axes so the response of the Honeywell airplane is more severe. However, the purpose of this test was to demonstrate that there is no excessive activity on the elevator. In this sense, both simulations agreed.

4.4.2.2 Lateral Evaluation Summary.

Three additional check cases were developed to evaluate the basic performance of the THCS Lateral Directional IL control laws coupled with the legacy Honeywell lateral outer control laws.

The objectives of these check cases were to:

- Demonstrate the coordinated IL performance in the roll and yaw axes with smoothly executed well-damped turns.
- Demonstrate turn coordination.
- Demonstrate yaw damping.

Appendix C gives the results for the three lateral scenarios using the Honeywell PC Sim.

Check case 20 (figures C-53 through C-64) was a heading select test case in which the airplane executed a 90° turn into a 20-kt crosswind. Altitude was 10k and airspeed was 250 kt for this

test. All lateral axis parameters behaved as expected for this maneuver with heading, bank angle, and side slip following the appropriate commands. There was no overshoot and no evidence of oscillation in any of the rate or acceleration terms. Altitude was controlled to within ±10 ft and airspeed was held to within ±0.5 kt during maneuvers.

Check case 21 (figures C-65 through C-76) was a track select in which the airplane executed a 90° ground track change into a 20-kt crosswind. The results for this test were identical to case 21 results except that the heading tracked the ground track instead of magnetic heading.

Check case 22 (figures C-77 through C-90) was a 60° localizer capture and track while turning into a 15-kt crosswind. The initial distance to station was 24 nautical miles when the localizer beam was captured. Altitude was 5k and airspeed was 160 kt. All lateral axis parameters behaved as expected for this maneuver with heading, bank angle, and side slip following the appropriate commands. There was minor overshoot and no evidence of oscillation in any rate or acceleration terms. Altitude was controlled to within ±20 ft and airspeed was held to within ±0.5 kt during maneuvers.

5. CONCLUSIONS.

This research effort is a multiphase project intended to determine the benefits to industry and government of adopting advanced FG&C technology. As part of this research both the Honeywell Advanced Flight Guidance and Control (HAFGC) and Total Energy Control System/Total Heading Control System (TECS/THCS) algorithms were evaluated.

The analytical evaluation of both the HAFGC and TECS/THCS inner loop (IL) control laws indicate that each method is a reusable generic IL design suitable for use in conjunction with the standardized TECS/THCS outer loop (OL) system. The linear analysis was an important and necessary step required in order to uncover any IL sensitivities to system limitations, such as actuator bandwidth or transport lag. Both control laws showed a sensitivity to transport lag and significant efforts were needed to adjust gains to achieve good performance in the time and frequency domain for a variety of flight conditions. In the final configuration, both methods delivered 6 decibels of gain margin and 45° of phase margin when the total transport delay was 50 milliseconds (ms) or less. In the case of the THCS IL, minor architecture changes were needed to achieve desired performance levels.

One unexpected finding that resulted from this study was the need to make aircraft-specific tuning adjustments to the TECS OL. Although the TECS OL was developed with the intent that it would be a standardized reusable design and that any aircraft-specific changes would be constrained to the ILs, a time domain evaluation of the TECS OL response to flight path and airspeed step inputs confirmed the need to make gain-tuning changes to the TECS core algorithm to optimize and balance the pitch and thrust loops. With minor adjustments, the goal of achieving equalized energy distribution dynamics and total energy control dynamics control was realized. Given that OL gains changes were made, a complete linear analysis of the OL modes is recommended for future study.

Damping performance issues were encountered while attempting to integrate HAFGC with the TECS/THCS OLs. The approach was shelved in favor of a second approach that used the TECS pitch and THCS lateral directional ILs. The second approach initially resulted in poor performance as well. An investigation into the source of the poor performance discovered several issues. An error was found in the real-time implementation of the TECS mode logic for allocating control to the flight path angle versus thrust control paths. The real-time implementation was corrected. The analytic models did not account for all transport delay in the system, explaining the difference between real-time simulation and expected results based on prior linear analysis. The simulation environment models were altered to reduce transport lag to be closer to 50 ms based on guidance from the Federal Aviation Administration (FAA). After this modification was implemented and control gains were adjusted for the remaining limitations on transport delay, the TECS/THCS mechanization delivered the expected performance for both the ILs and OLs.

The real-time simulation results indicate that the objective of demonstrating the pilot-like energy management capability, which is the fundamental advantage of TECS, was achieved. In all cases, the energy management strategy that provides simultaneous, coordinated elevator and thrust control to achieve an efficient command response was clearly demonstrated. For all multi-axis command scenarios considered, altitude was maintained to within 15 ft of the target altitude, and airspeed was maintained to within 3 kt of the target airspeed.

In the lateral axis, the combination of the Honeywell legacy OL control laws and the THCS IL design was successfully demonstrated using the heading, track, and localizer modes. The THCS IL was shown to provide simultaneous, coordinated aileron and rudder commands while achieving smooth, well-damped heading control response with excellent turn coordination and yaw damping. For all lateral check cases performed, side slip angle was limited to 0.5°.

The objective of this project was to enable the introduction and certification of advanced functionally integrated FG&C systems in commercial airplanes. The use of a high-fidelity aircraft simulation introduced real-world technical challenges to the project, which were successfully overcome, proving the viability of TECS/THCS as a control solution. This is a significant finding supporting suitability for commercial use.

6. FUTURE STUDIES.

To adapt a control law to a new airplane, the inverse model to be carried on the airplane must be developed. A standard format could simplify adapting control laws from one airplane to the next, assuming a common format can be determined that satisfies all user needs and not just the development of the automatic flight control systems; otherwise, the data will never be generated. To support the generalized control approach application, future research focused on the development of a generalized aircraft modeling approach supportive of the TECS/THCS control approach would enable industry adoption and application of the generalized control approach

evaluated in this research. The goal of the generalized simulation approach would be to develop a simulation model that is useful for the following activities:

- Development of models for airframe manufacturers' analysis of the airframe design
- Development of full-flight simulators
- Capturing wind tunnel test results
- Validation by flight test
- Modeling for linear and nonlinear analysis by airframe manufacturers and AFCS suppliers
- Simplified control law static inversion

To achieve a generic approach to applying the TECS/THCS control concepts, some other guidelines would benefit from further study. As a consequence of certain limitations of this study, tuning of the FAA control algorithms was required after modifications were made to the simulation to improve the transport delays from the fielded system. Although tuning a flight control law is not uncommon, the FAA goal is to achieve a generic algorithm than can reduce the variation across aircraft to that of changing the static inversion processing to match the new aircraft. To achieve that goal, additional studies are recommended. A comprehensive linear analysis of the TECS OL and TECS core algorithms is recommended to determine the sensitivities of the OL algorithms to the IL performance and develop guidelines for:

- The level of fidelity required in the inversion process.
- The targeted IL bandwidth, along with transport delay requirements and actuator bandwidth requirements that would be imposed on the flight control systems.
- The response required in the throttle controls and airplane response to thrust.
- A methodology to compute the gains that will balance the FPA control with the thrust control. (If the two preceding items can guarantee that a single set of gains in the TECS core will then work, then this study is not needed.)

7. REFERENCES.

1. Lambregts, A.A., "Automatic Flight Controls Concepts and Methods," Human Factors Team Report "The Interfaces Between Flight Crews and Modern Flight Deck Systems," June 18, 1996.

2. Eladl, M., Eltohamy, K., Hill, B., Horne, T., Krasnovskiy, B., Leiphon, K. and Taylor, S., "Advanced Guidance and Control—Operational and Safety Benefits," FAA report DOT/FAA/AR-08/27, June 2008.

3. Title 14 Code of Federal Regulations 25.1329/1335, "Flight Guidance System," Updated to January 1, 2011.

4. Advisory Circular 25.1329, "Approval of Flight Guidance Systems," July 17, 2006.

APPENDIX A—HONEYWELL ADVANCED FLIGHT GUIDANCE AND CONTROL INNER LOOP LINEAR ANALYSIS

A.1 Pitch Stability Analysis.

The Bode magnitude and phase response are given for a single flight condition and four values of system transport lag (25, 50, 75, and 100 milliseconds (ms)). The flight condition is altitude 10,000 feet (ft) and airspeed 250 knots (kt), and the vehicle configuration is mid weight, mid center of gravity (c.g.). The open-loop system analyzed is the pitch inner loop (IL) with the loop broken at the actuator input.

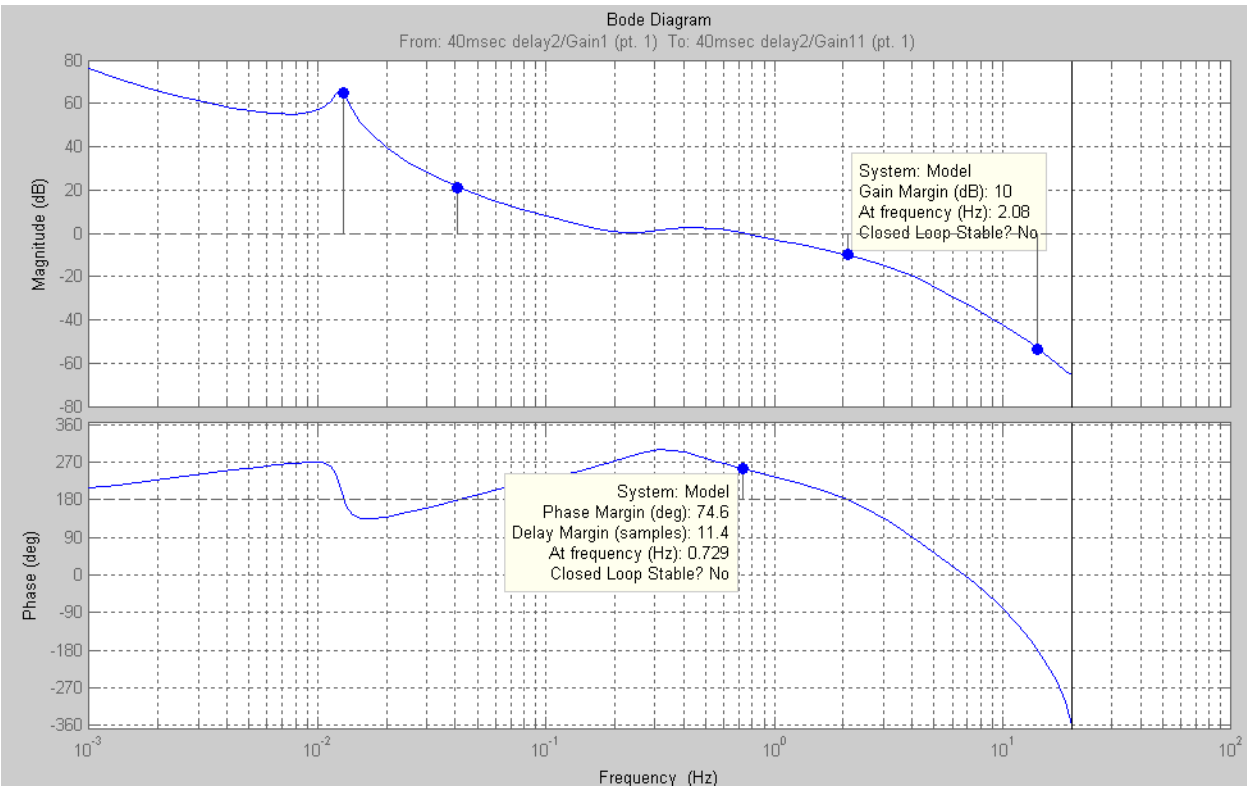

Figure A-1. Elevator Path Frequency Response—25-ms Transport Lag

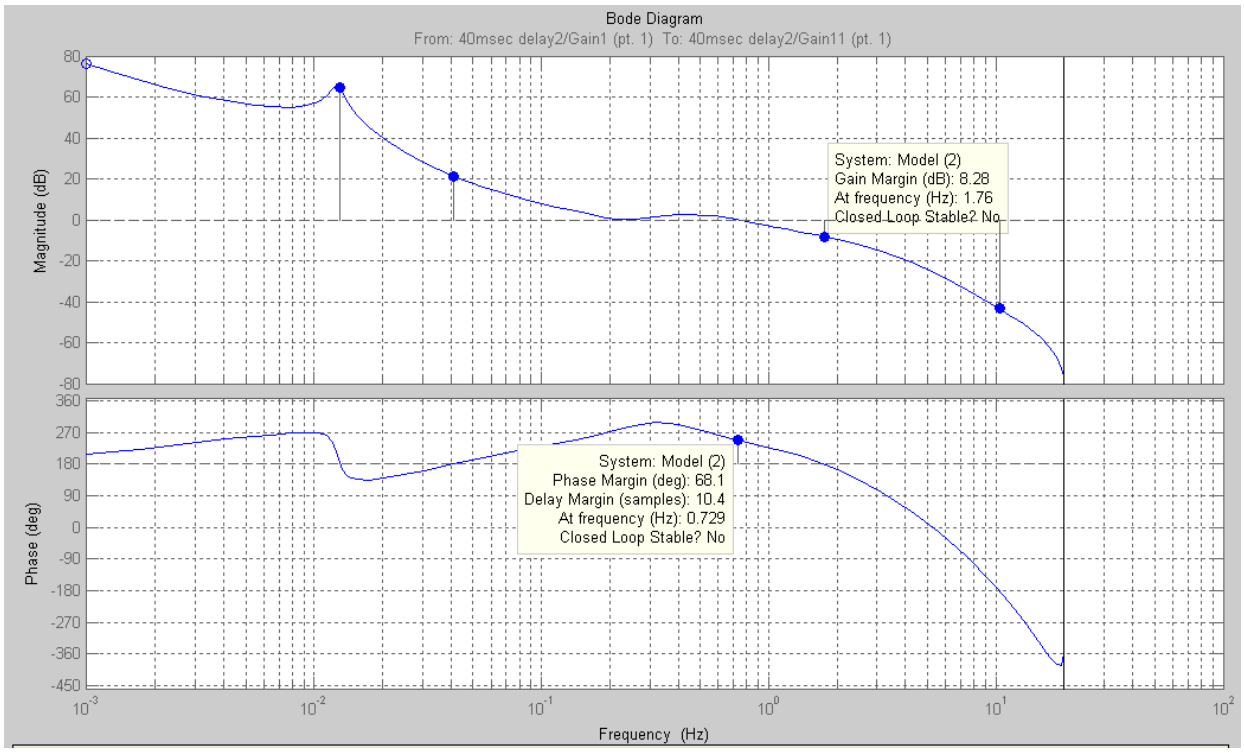

Figure A-2. Elevator Path Frequency Response—50-ms Transport Lag

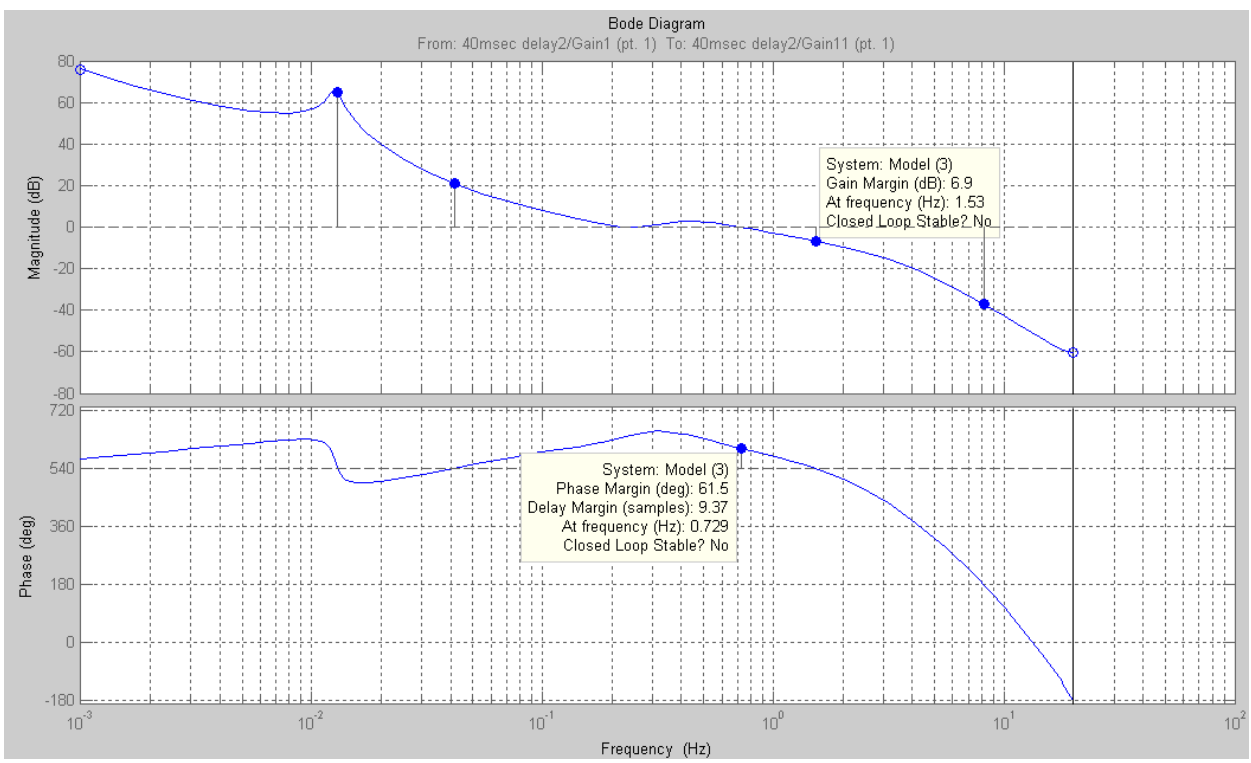

Figure A-3. Elevator Path Frequency Response—75-ms Transport Lag

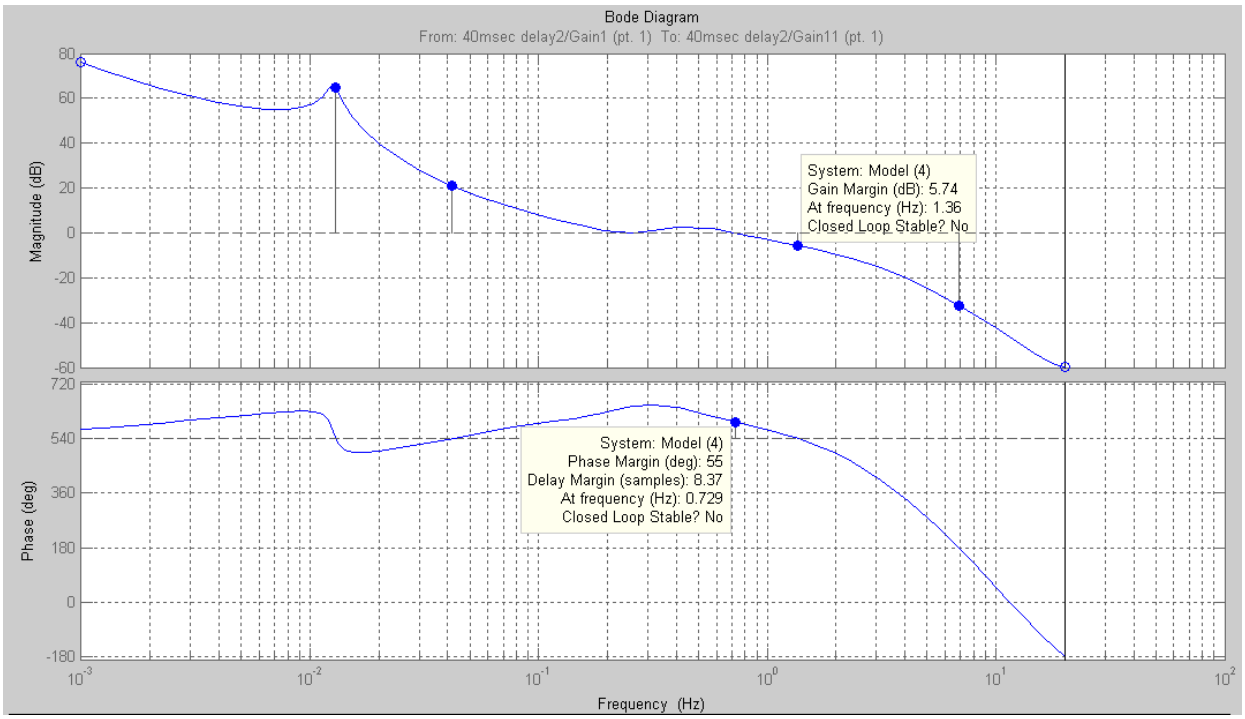

Figure A-4. Elevator Path Frequency Response—100-ms Transport Lag

Table A-1. Pitch IL Stability Margin Summary

Transport Delay (ms)	Gain Margin	Phase Margin
25	10.0 dB at 2.1 Hz	74.6 degrees at 0.7 Hz
50	8.3 dB at 1.8 Hz	68.1 degrees at 0.7 Hz
75	6.9 dB at 1.5 Hz	61.5 degrees at 0.7 Hz
100	5.7 dB at 1.4 Hz	55.0 degrees at 0.7 Hz

A.2 Time Response to Pitch Step.

The response of the pitch IL system to a 1° step in pitch attitude was recorded at a single flight condition. The flight condition is altitude 10k and airspeed 250 kt, and the vehicle configuration is mid weight, mid c.g. The response for four values of transport lag is shown below.

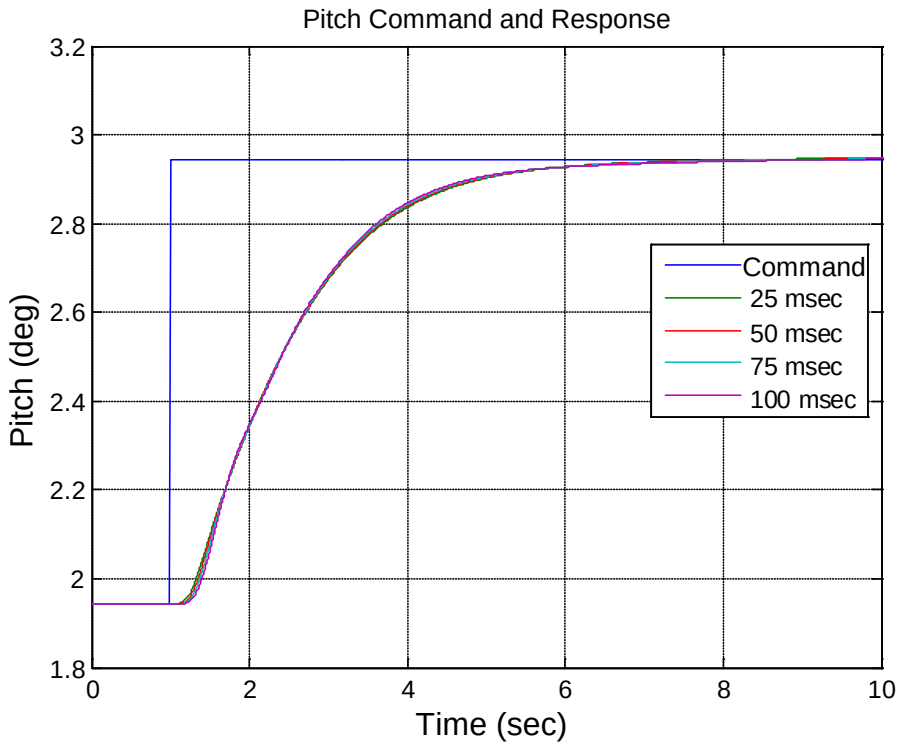

Figure A-5. Pitch Step—Pitch Attitude Response

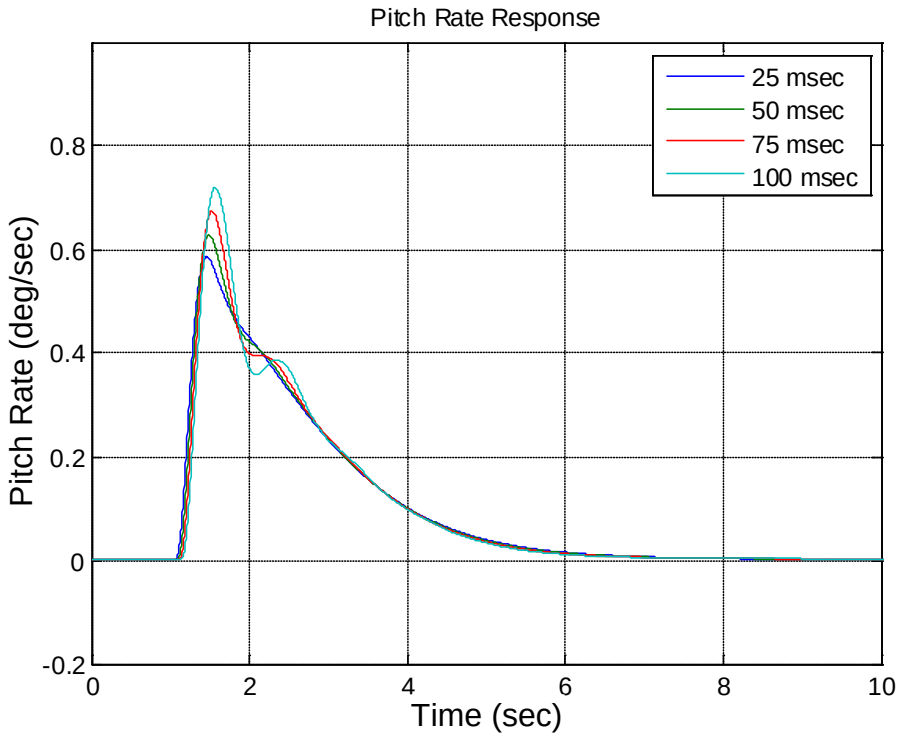

Figure A-6. Pitch Step—Pitch Rate Response

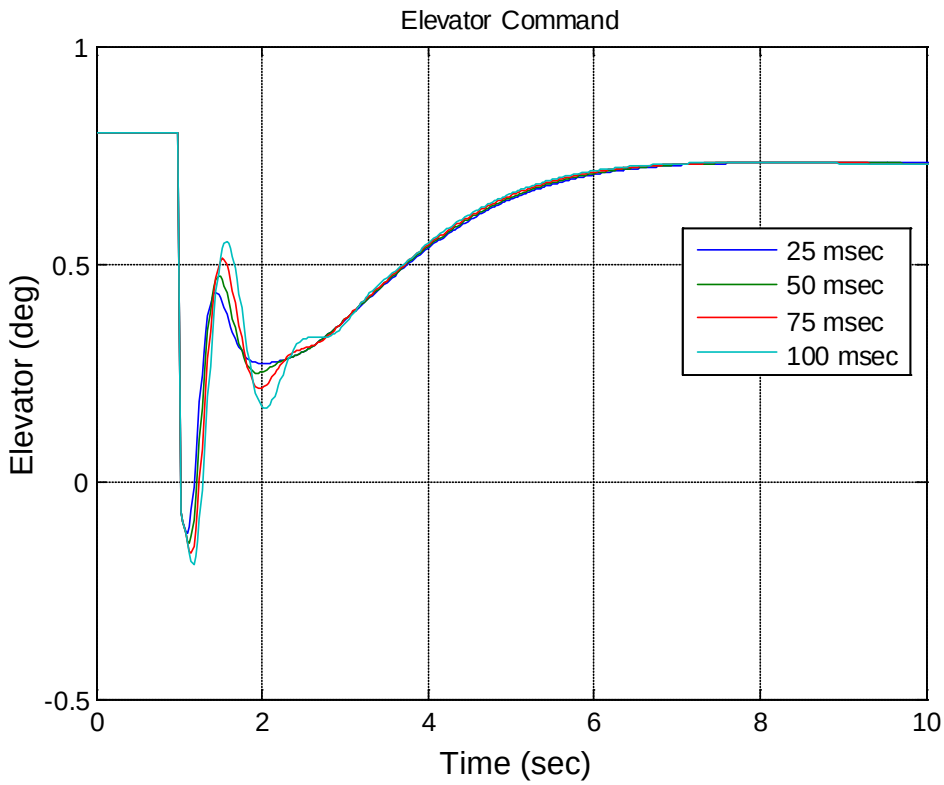

Figure A-7. Pitch Step—Elevator Response

A.3 Lateral Directional Stability.

The Bode magnitude and phase response are given for a single flight condition and four values of system transport lag (25, 50, 75, and 100 ms). The flight condition is altitude 10k and airspeed 250 kt, and the vehicle configuration is mid weight, mid c.g. The open-loop system analyzed is the lateral directional IL with the loop broken at the actuator input (aileron and rudder).

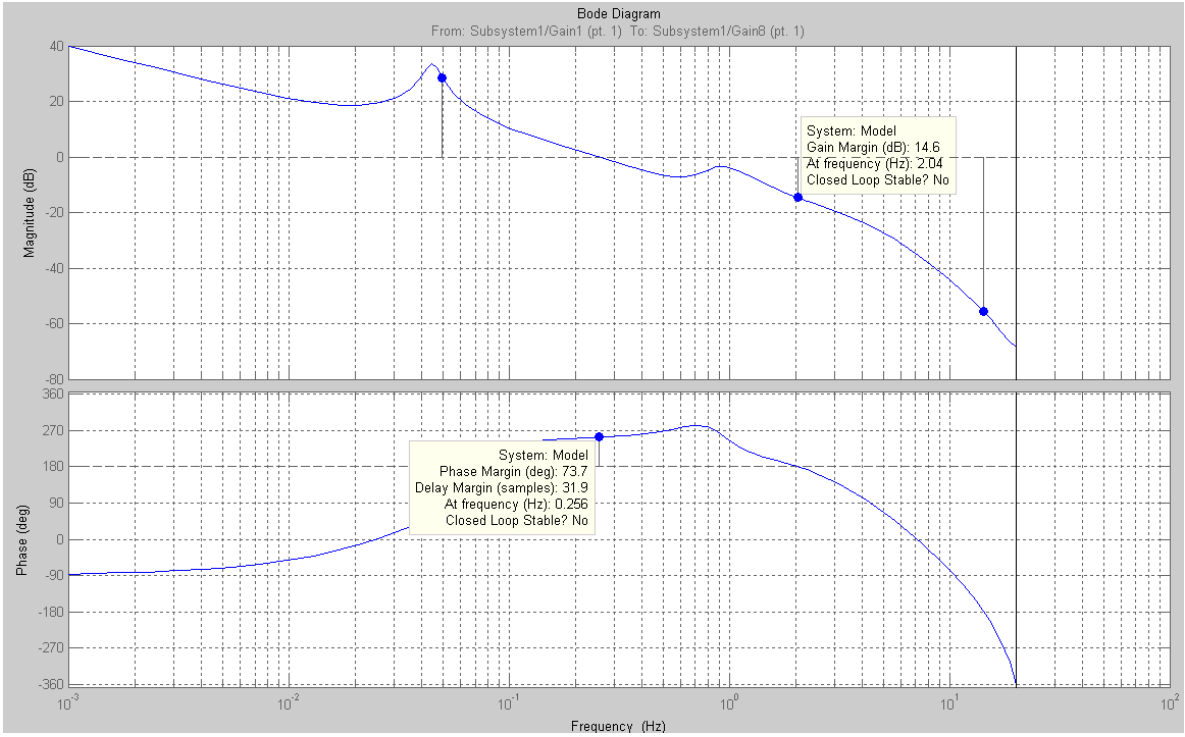

Figure A-8. Aileron Path Frequency Response—25-ms Transport Lag

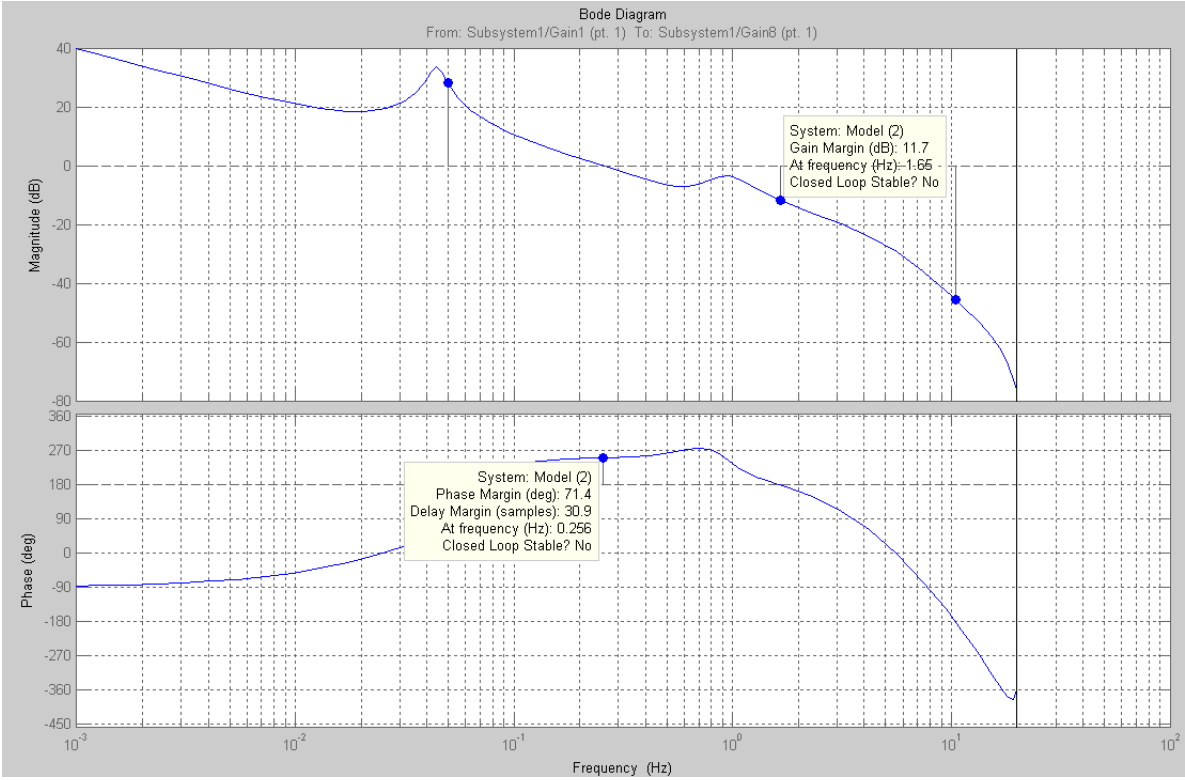

Figure A-9. Aileron Path Frequency Response—50-ms Transport Lag

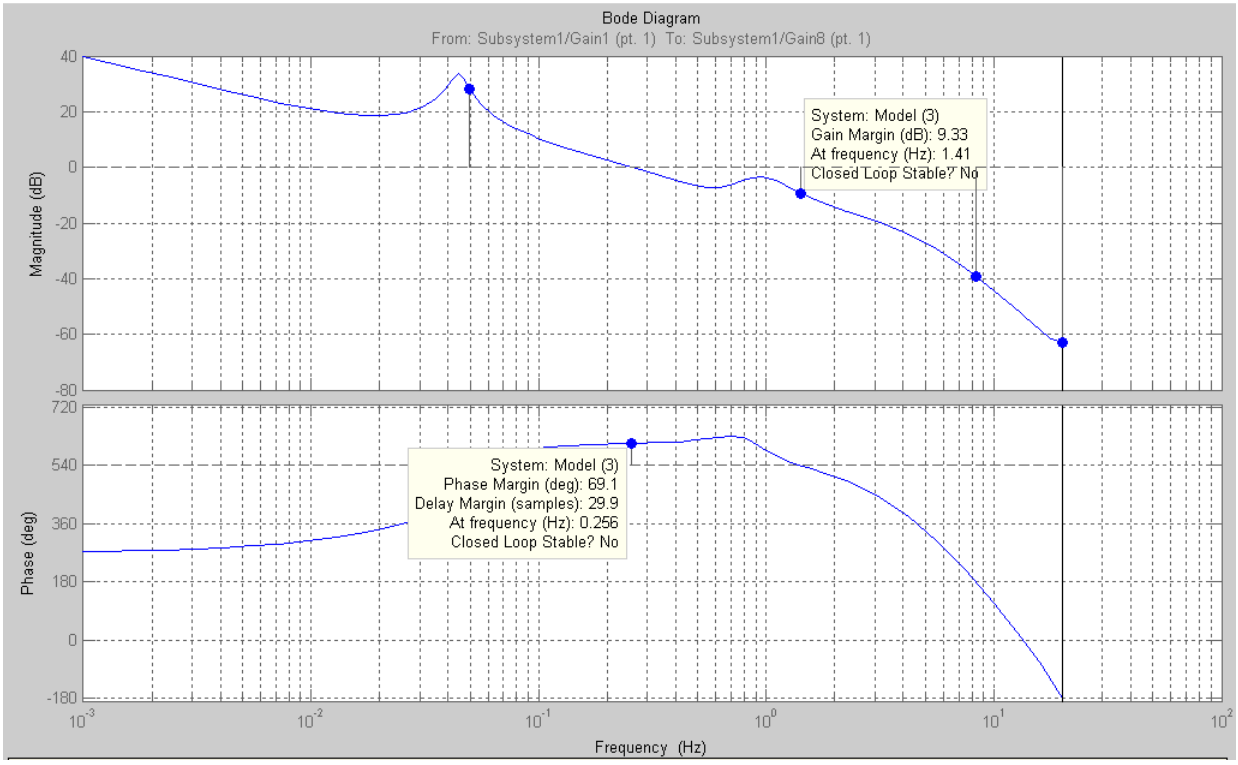

Figure A-10. Aileron Path Frequency Response—75-ms Transport Lag

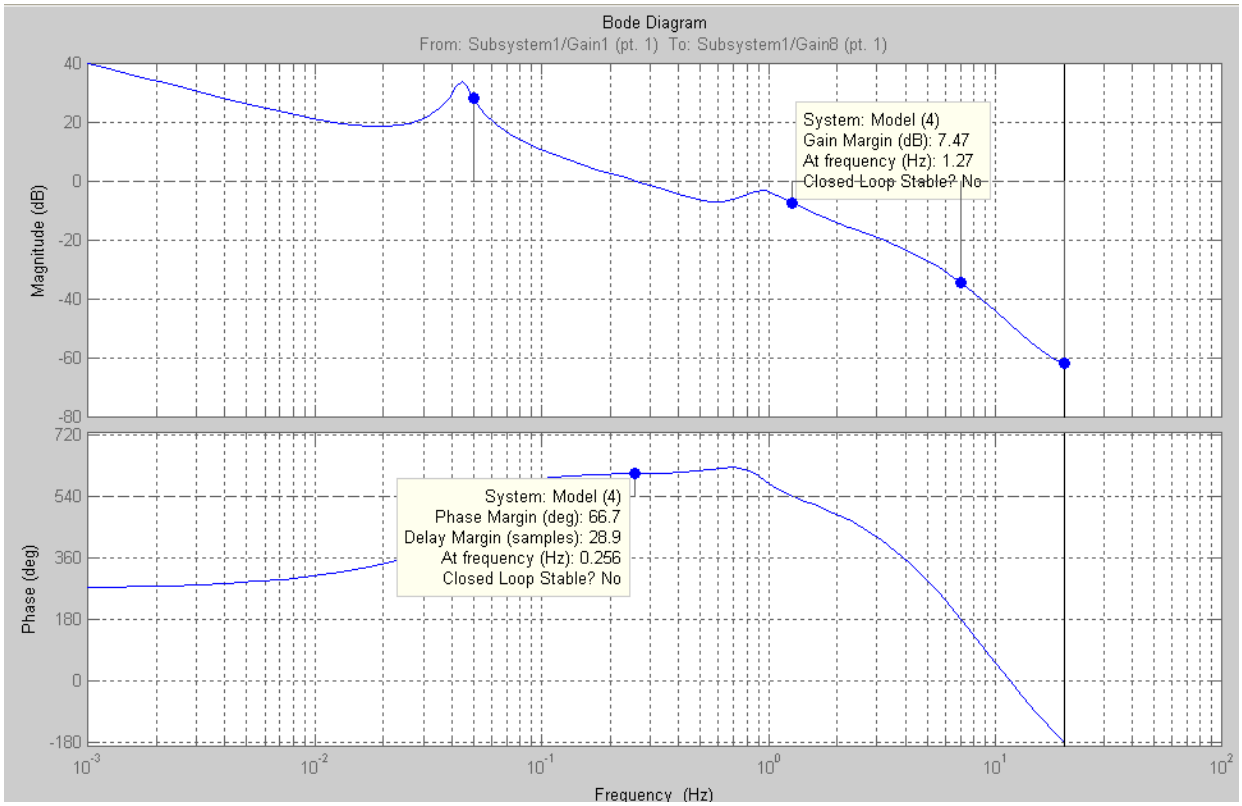

Figure A-11. Aileron Path Frequency Response—100-ms Transport Lag

Table A-3. Aileron Path IL Stability Margin Summary

Transport Delay (ms)	Gain Margin	Phase Margin
25	14.6 dB at 2.0 Hz	73.7 degrees at 0.26 Hz
50	11.7 dB at 1.7 Hz	71.4 degrees at 0.26 Hz
75	9.3 dB at 1.4 Hz	69.1 degrees at 0.26 Hz
100	7.5 dB at 1.3Hz	66.7 degrees at 0.26 Hz

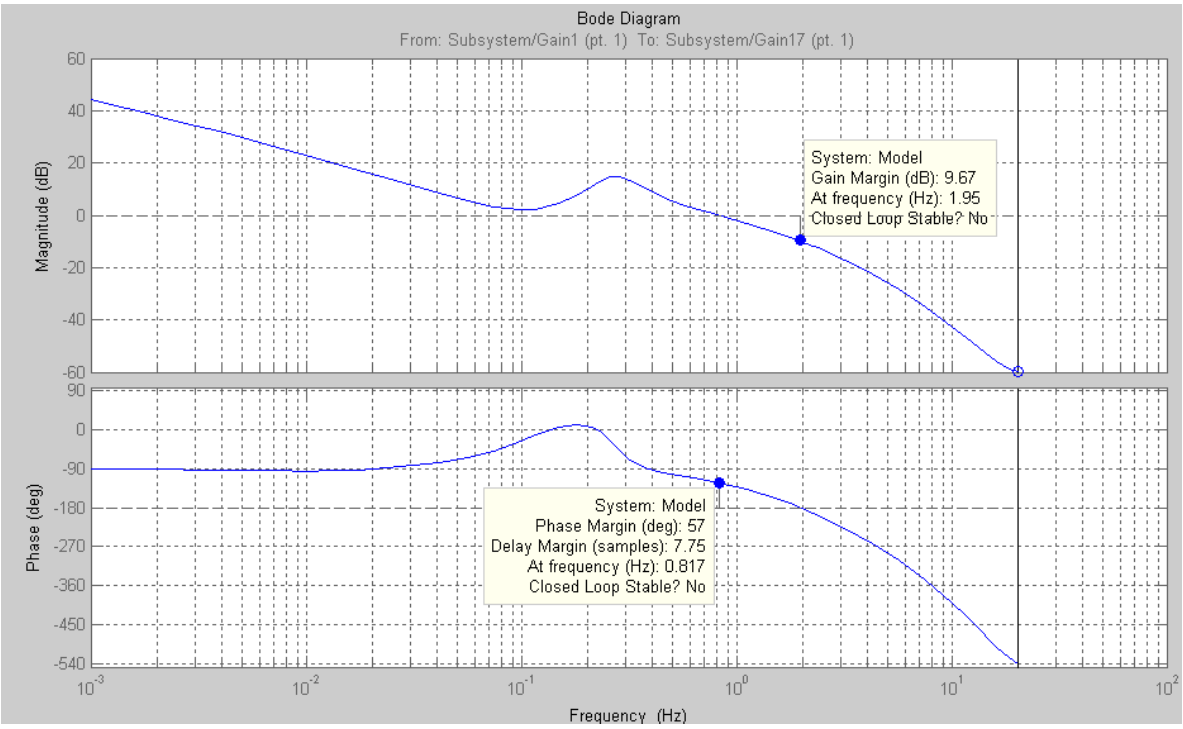

Figure A-12. Rudder Path Frequency Response—25-ms Transport Lag

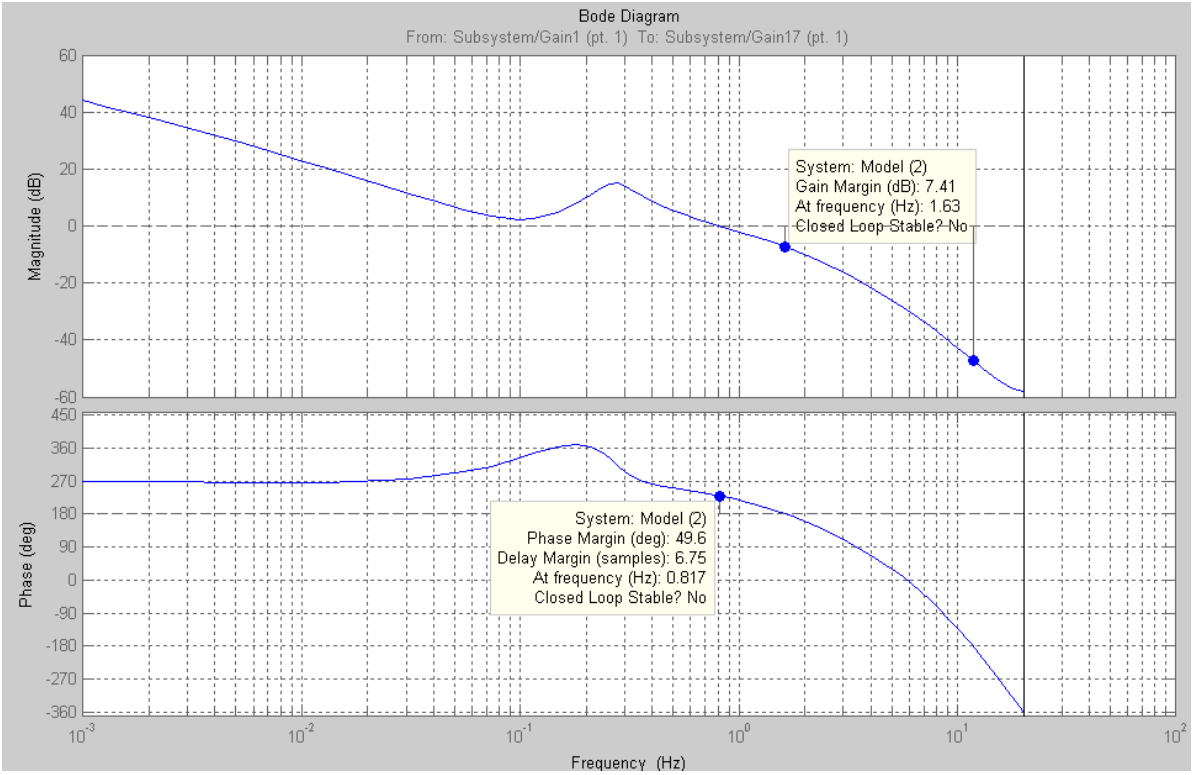

Figure A-13. Rudder Path Frequency Response—50-ms Transport Lag

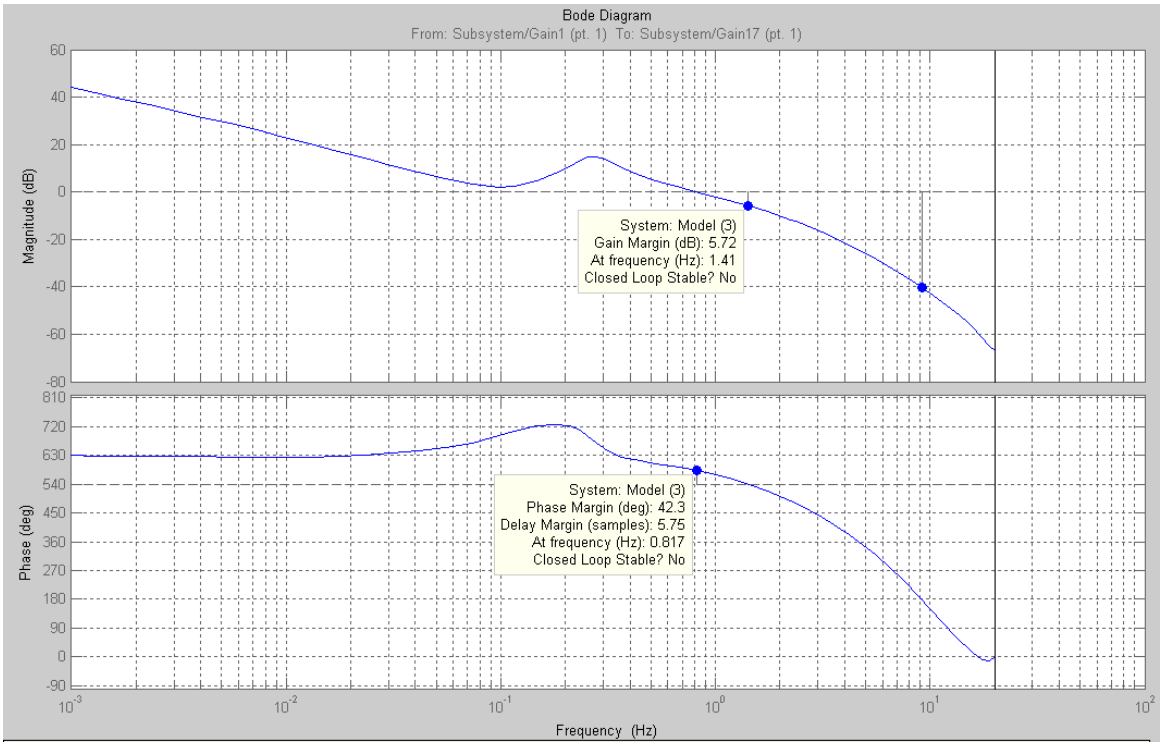

Figure A-14. Rudder Path Frequency Response—75-ms Transport Lag

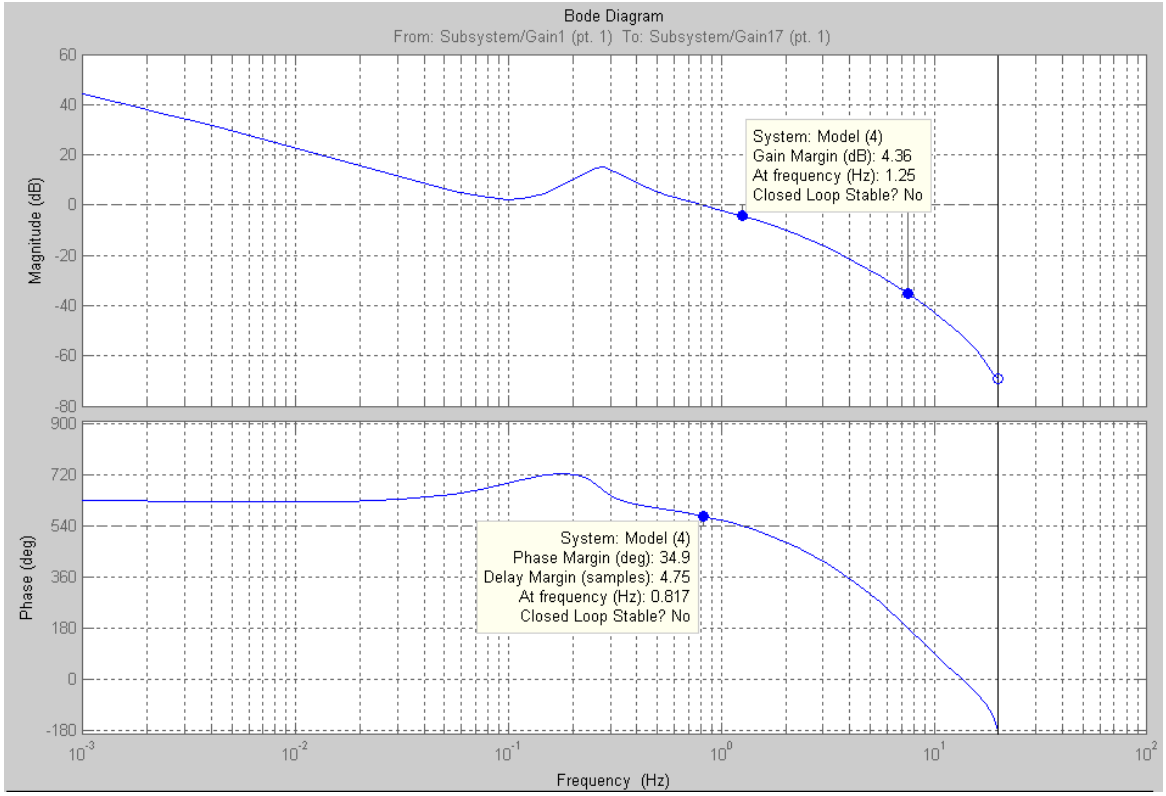

Figure A-15. Rudder Path Frequency Response—100-ms Transport Lag

Table A-3. Rudder Path IL Stability Margin Summary

Transport Delay (ms)	Gain Margin	Phase Margin
25	9.7 dB at 2.0 Hz	57.0 degrees at 0.8 Hz
50	7.4 dB at 1.6 Hz	49.6 degrees at 0.8 Hz
75	5.7 dB at 1.4 Hz	42.3 degrees at 0.8 Hz
100	4.4 dB at 1.3 Hz	34.9 degrees at 0.8 Hz

A.4 Time Response to Roll Step Sequence.

The response of the lateral-directional IL system to a 5° step sequence in pitch attitude was recorded at a single flight condition. The flight condition is altitude 10k and airspeed 250 kt, and the vehicle configuration is mid weight, mid c.g. The response for four values of transport lag is shown below.

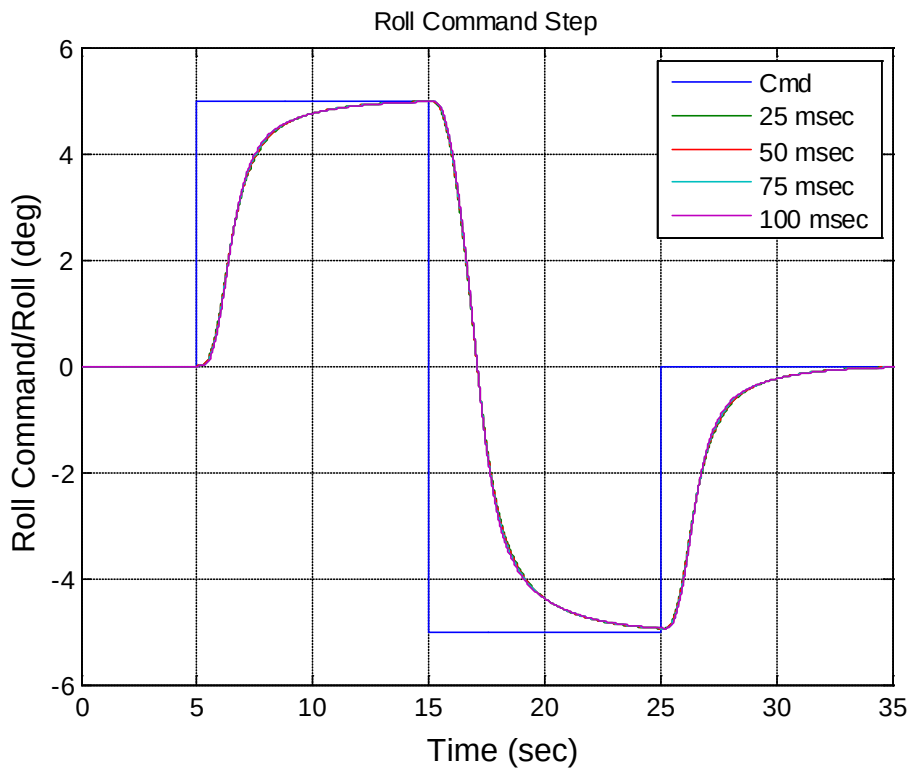

Figure A-16. Roll Step—Roll Attitude Response

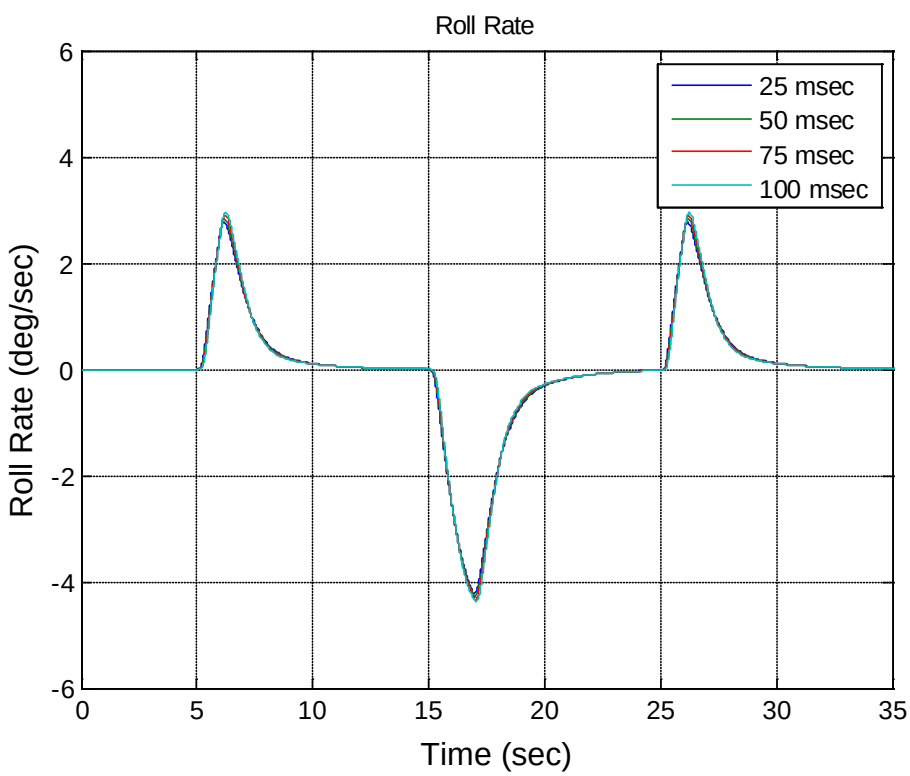

Figure A-17. Roll Step—Roll Rate Response

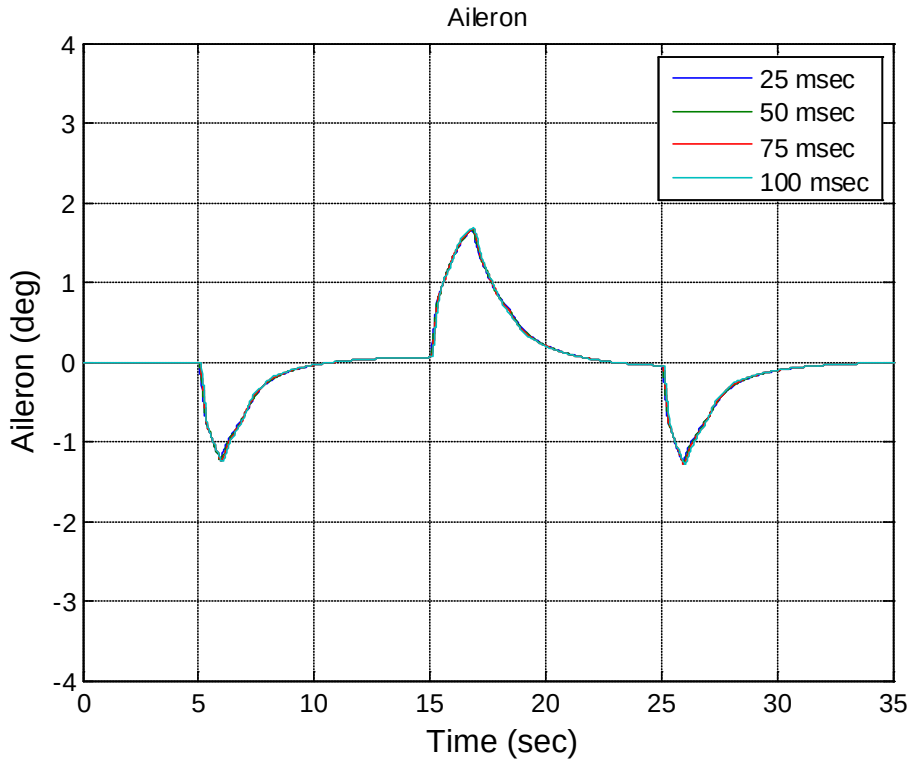

Figure A-18. Roll Step—Aileron Response

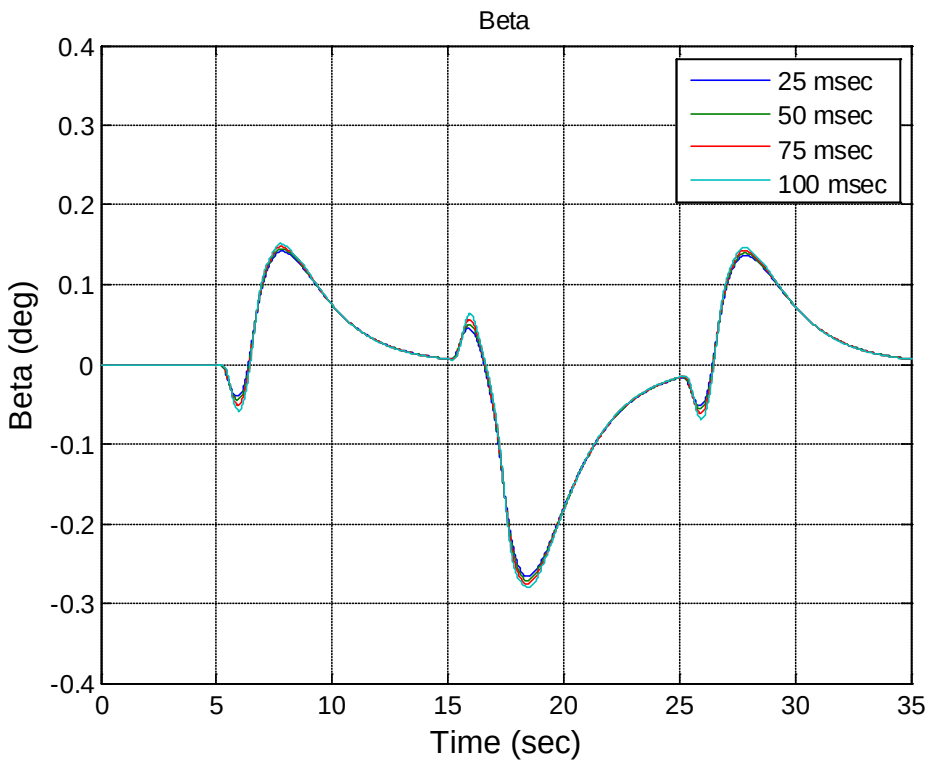

Figure A-19. Roll Step—Side Slip Response

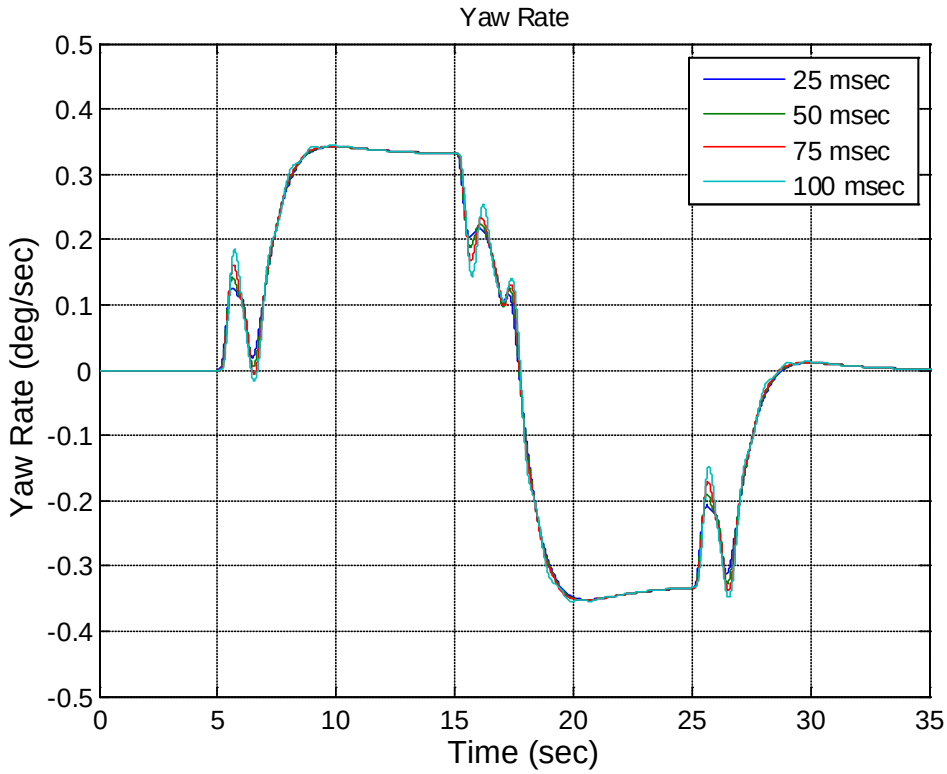

Figure A-20. Roll Step—Yaw Rate Response

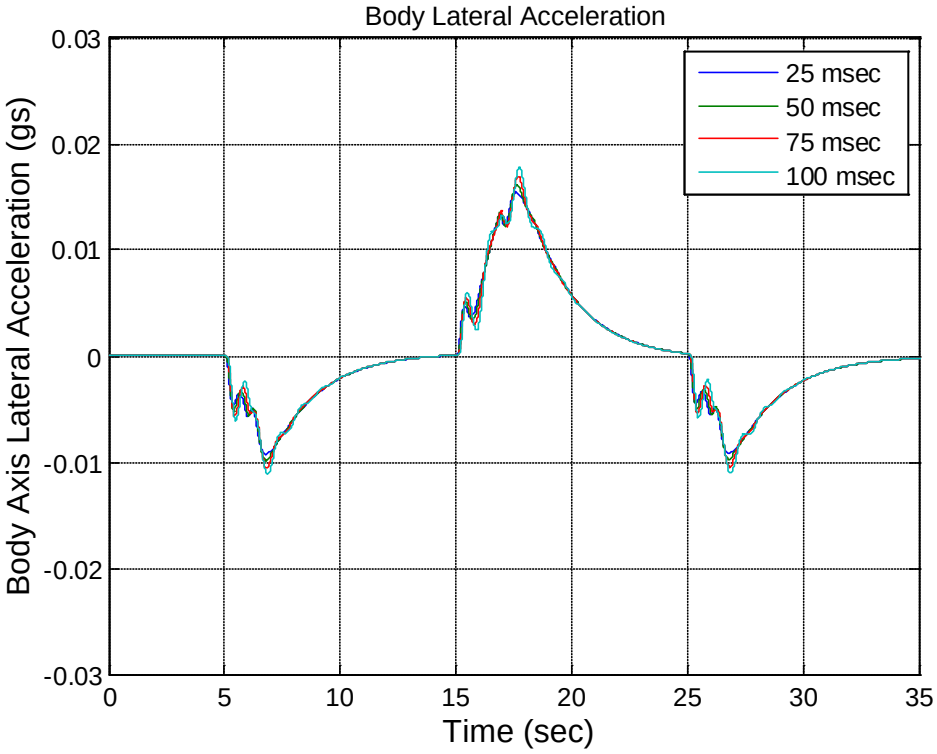

Figure A-21. Roll Step—Lateral Acceleration Response

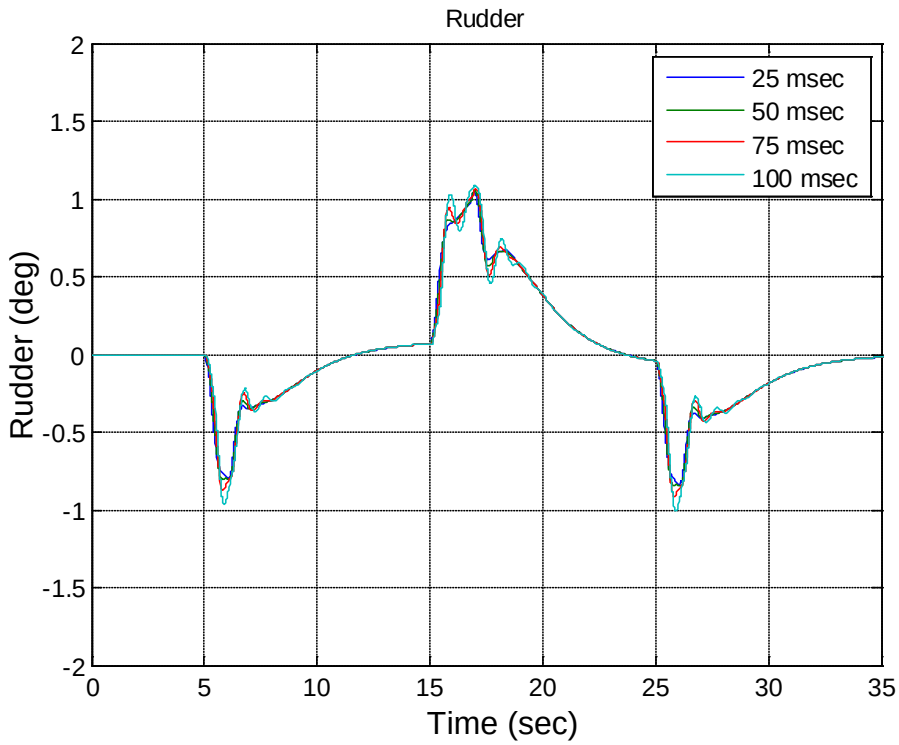

Figure A-22. Roll Step—Rudder Response

APPENDIX B—TOTAL ENERGY CONTOL SYSTEM/TOTAL HEADING CONTROL SYSTEM INNER LOOP LINEAR ANALYSIS

B.1 Pitch Stability Analysis.

Figures B-1 through B-4 and table B-1 give the Bode magnitude and phase response for the pitch inner loop (IL) (broken at the actuator input) using four different values for transport lag (25, 50, 75, and 100 milliseconds (ms)). The flight condition is altitude 10,000 feet (ft) and airspeed 250 knots (kt) and the vehicle configuration is mid weight, mid center of gravity (c.g).

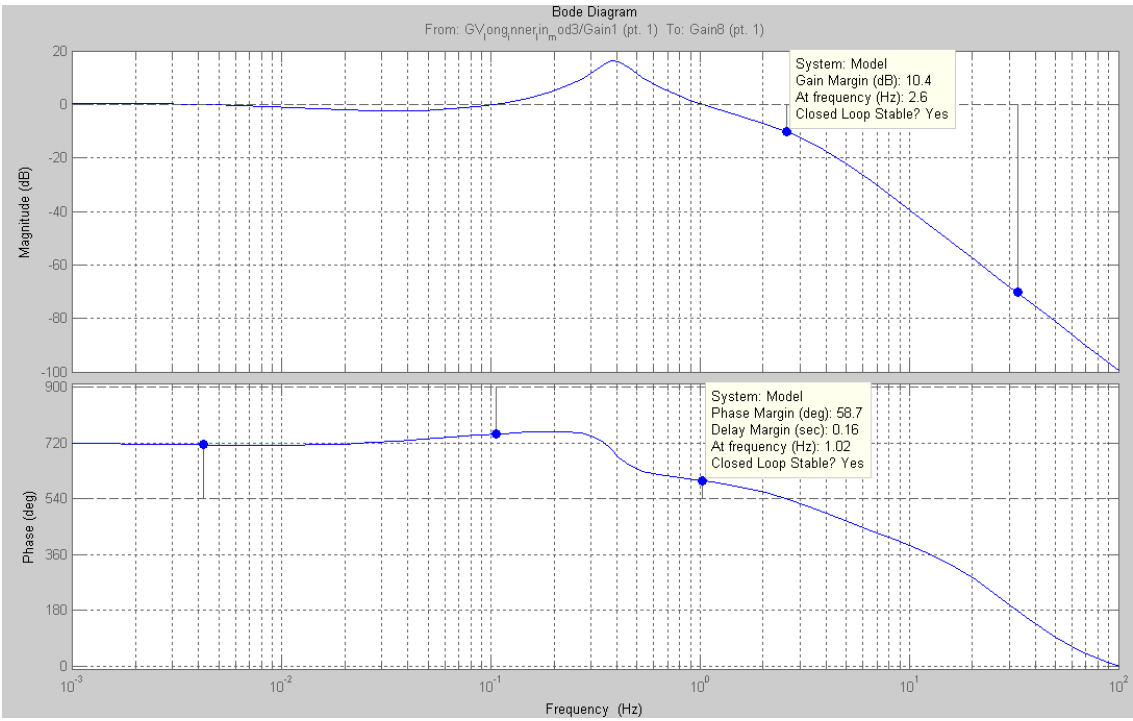

Figure B-1. Elevator Path Frequency Response—25-ms Transport Lag

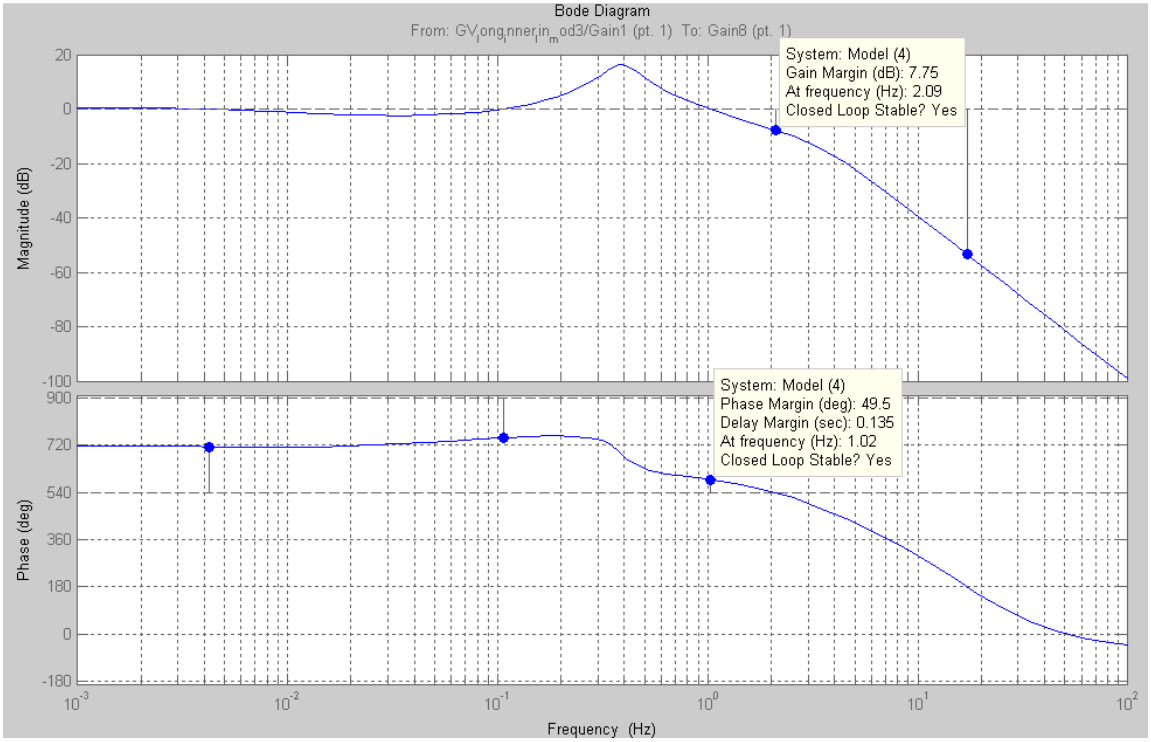

Figure B-2. Elevator Path Frequency Response—50-ms Transport Lag

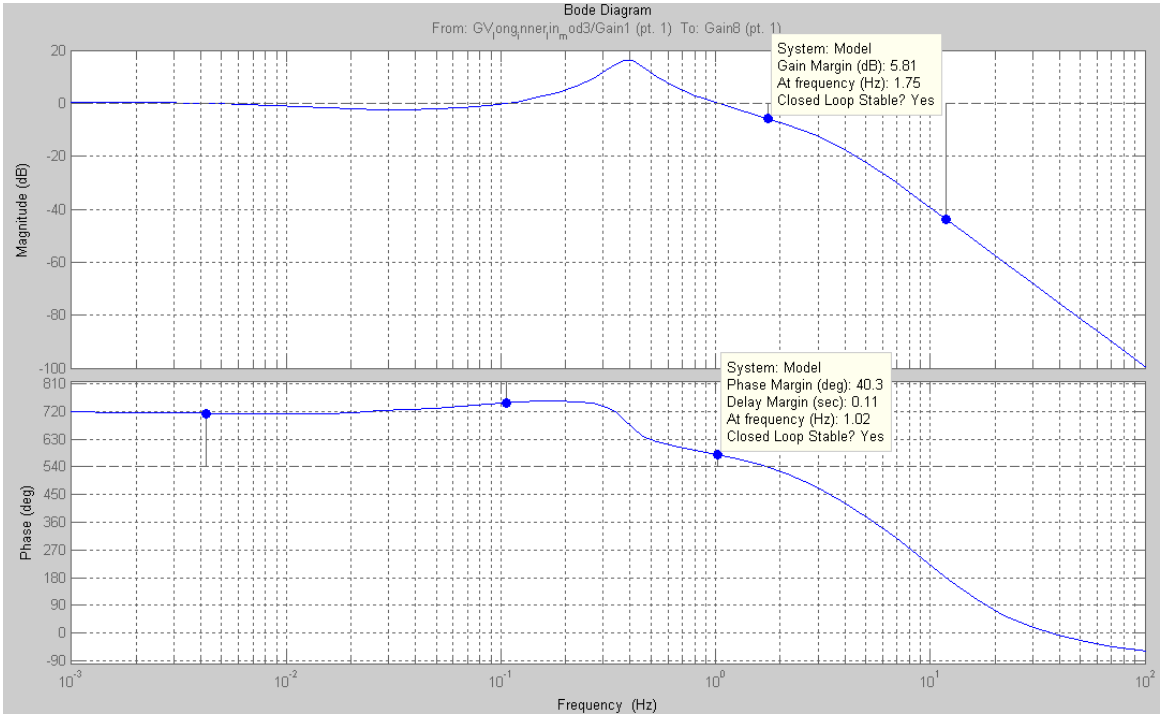

Figure B-3. Elevator Path Frequency Response—75-ms Transport Lag

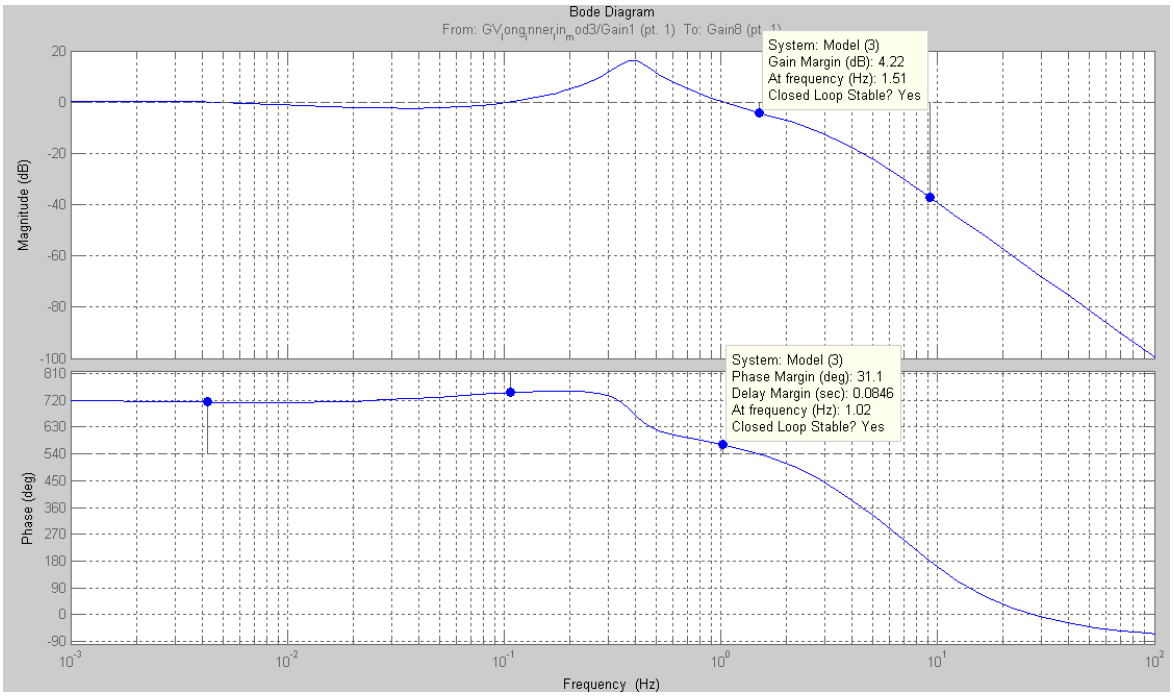

Figure B-4. Elevator Path Frequency Response—100-ms Transport Lag

Table B-1. Pitch IL Stability Margin Summary

Transport Delay (ms)	Gain Margin	Phase Margin
25	10.4 dB at 2.6 Hz	58.7 degrees at 1 Hz
50	7.8 dB at 2.1 Hz	49.5 degrees at 1 Hz
75	5.8 dB at 1.8 Hz	40.3 degrees at 1 Hz
100	4.2 dB at 1.5 Hz	31.1 degrees at 1 Hz

B.2 Response to a Pitch Step.

Figures B-5 though B-7 shows the step response of the pitch IL for four values of transport lag (25, 50, 75, and 100 ms). The flight condition is altitude 10k and airspeed 250 kt and the vehicle configuration is mid weight, mid c.g.

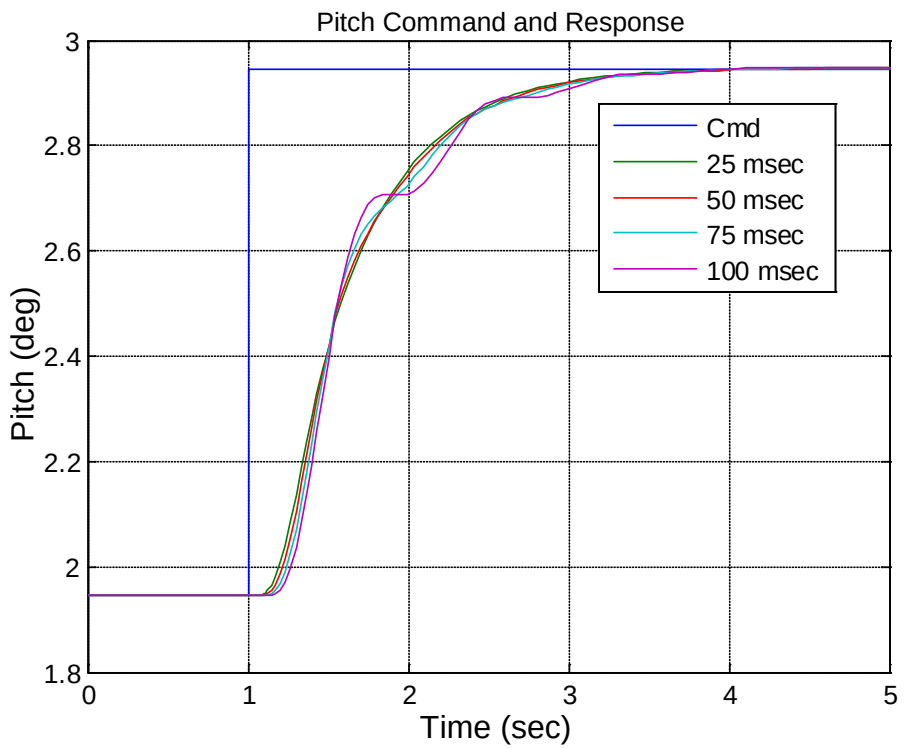

Figure B-5. Pitch Step—Pitch Attitude Response

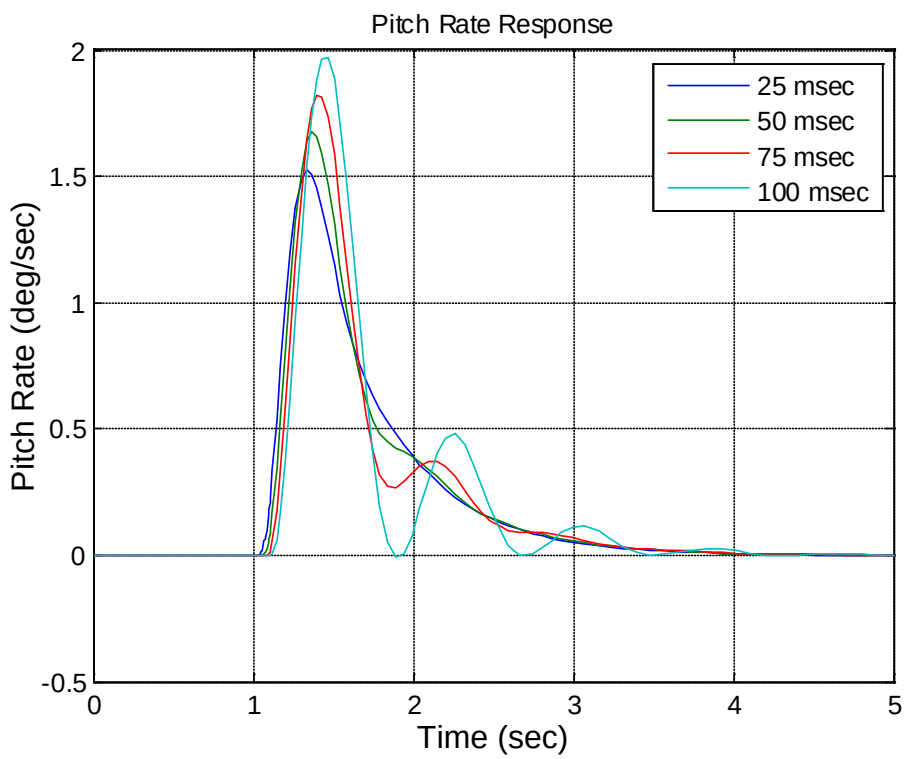

Figure B-6. Pitch Step—Pitch Rate Response

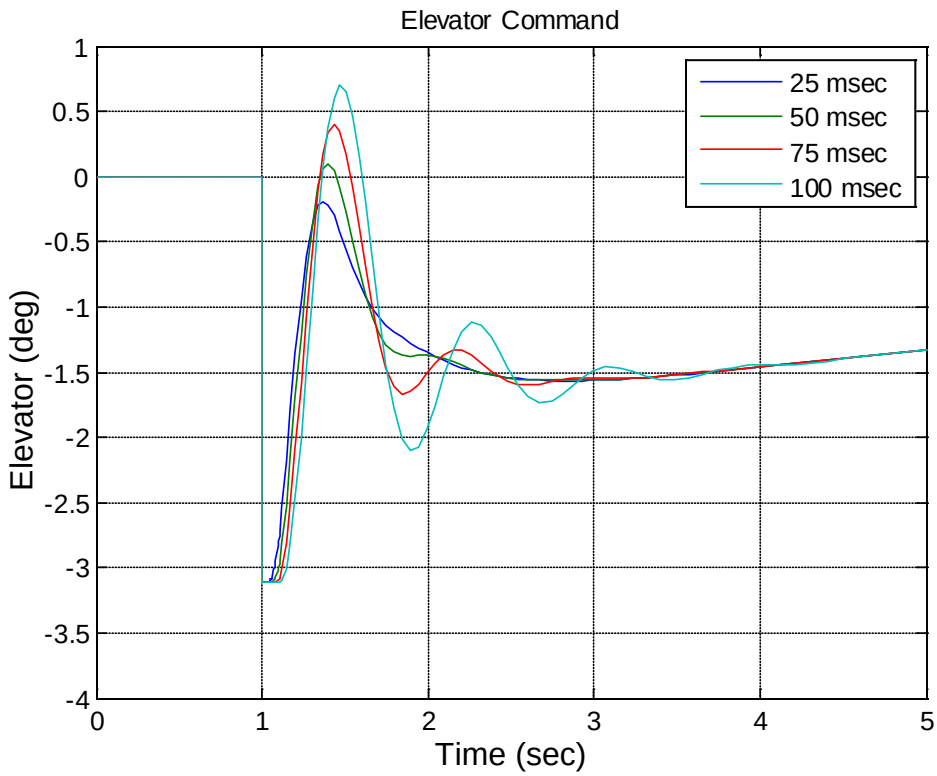

Figure B-7. Pitch Step—Elevator Response

B.3 Lateral Directional Stability Analysis.

Figures B-8 through B-15 and tables B-2 and B-3 give the Bode magnitude and phase response for the lateral directional IL (broken at the actuator input) using four different values for transport lag (25, 50, 75, and 100 ms). The flight condition is altitude 10k and airspeed 250 kt and the vehicle configuration is mid weight, mid c.g.

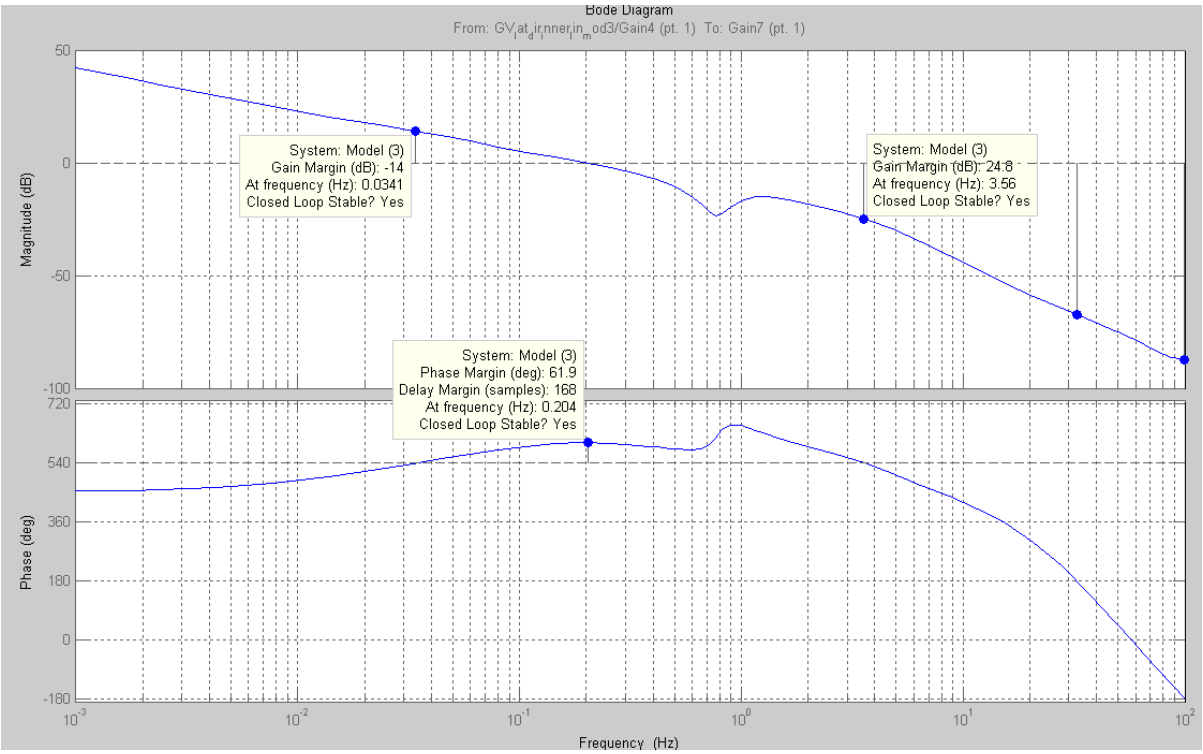

Figure B-8. Aileron Path Frequency Response—25 ms

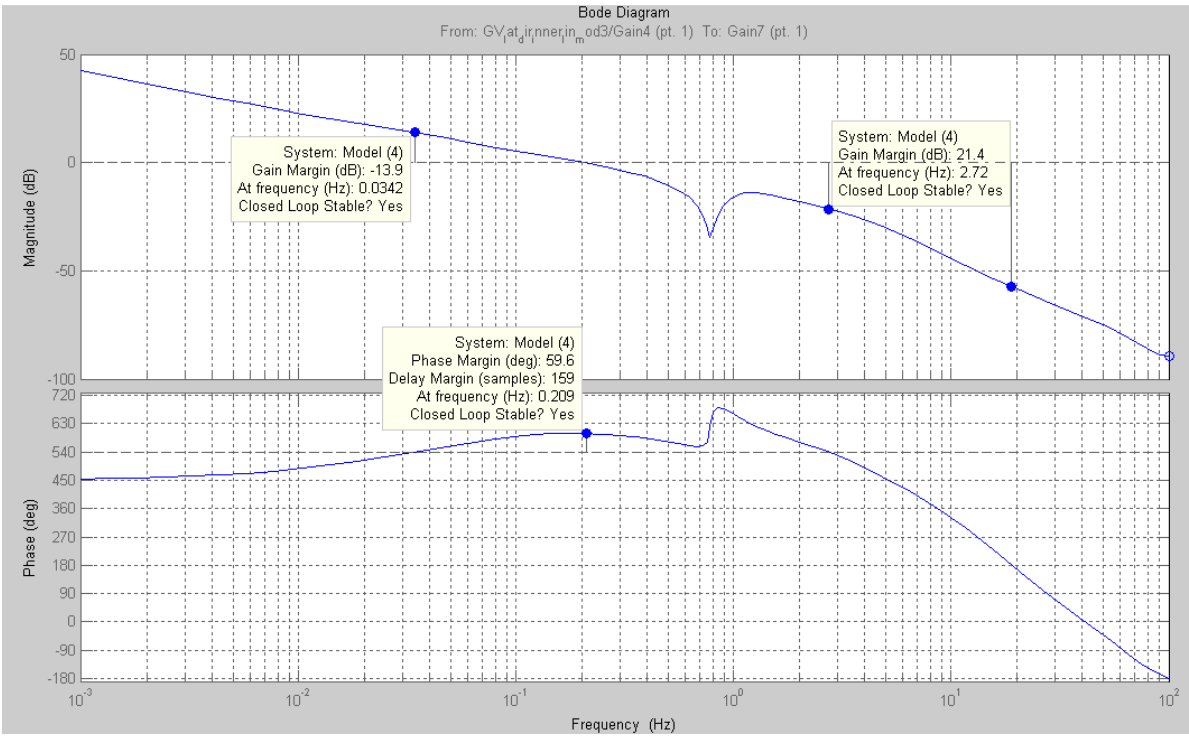

Figure B-9. Aileron Path Frequency Response—50 ms

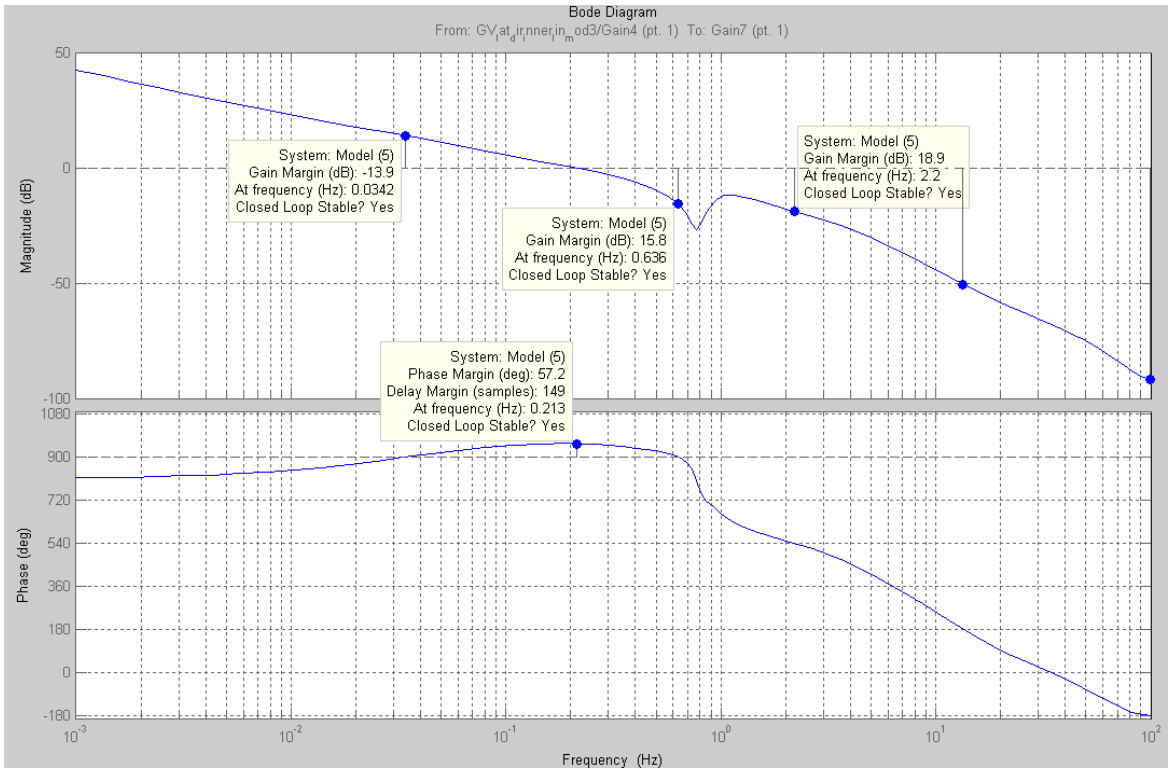

Figure B-10. Aileron Path Frequency Response—75 ms

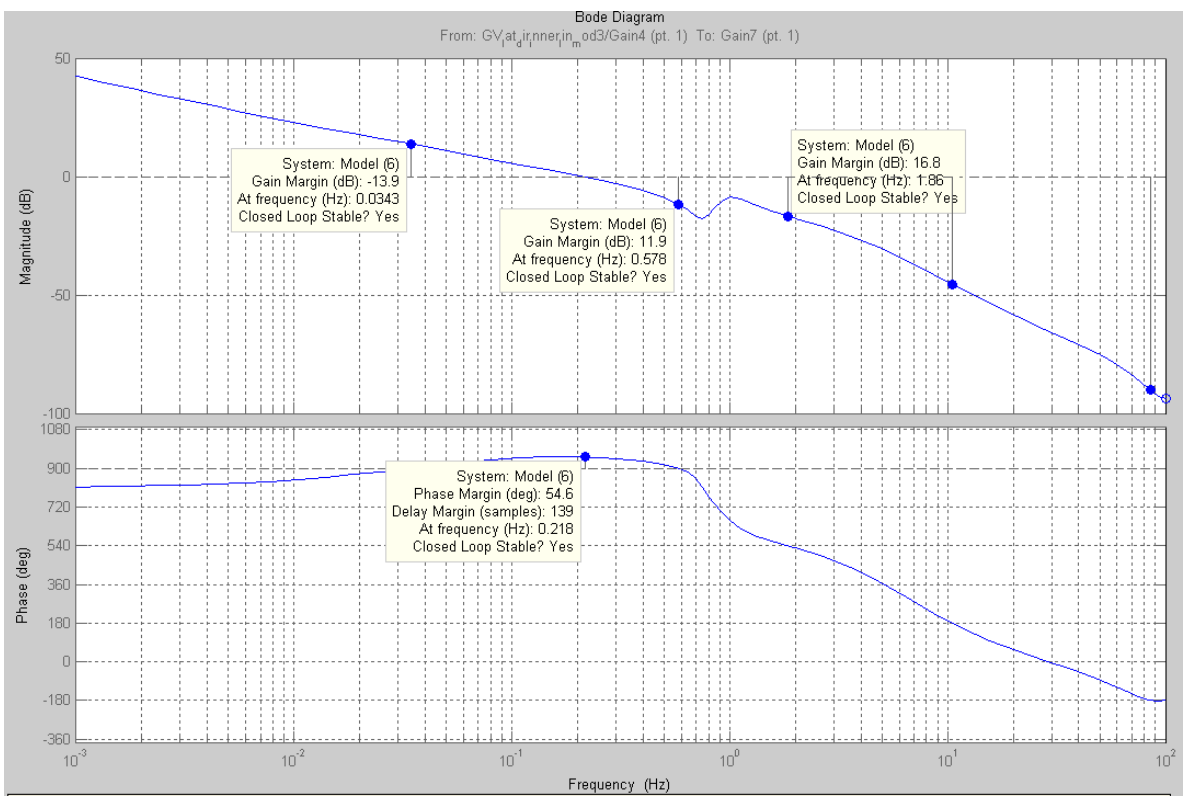

Figure B-11. Aileron Path Frequency Response—100 ms

Table B-2. Aileron Path IL Stability Margin Summary

Transport Delay (ms)	Gain Margin	Phase Margin
25	-14 dB at 0.03 Hz 24.8 dB at 3.6 Hz	61.9 degrees at 0.2 Hz
50	-13.9 dB at 0.03 Hz 21.4 dB at 2.7 Hz	59.6 degrees at 0.2 Hz
75	-13.9 dB at 0.03 Hz 15.8 dB at 0.64 Hz 18.9 dB at 2.2 Hz	57.2 degrees at 0.2 Hz
100	-13.9 dB at 0.03 Hz 11.9 dB at 0.58 Hz 16.8 dB at 1.9 Hz	54.6 degrees at 0.2 Hz

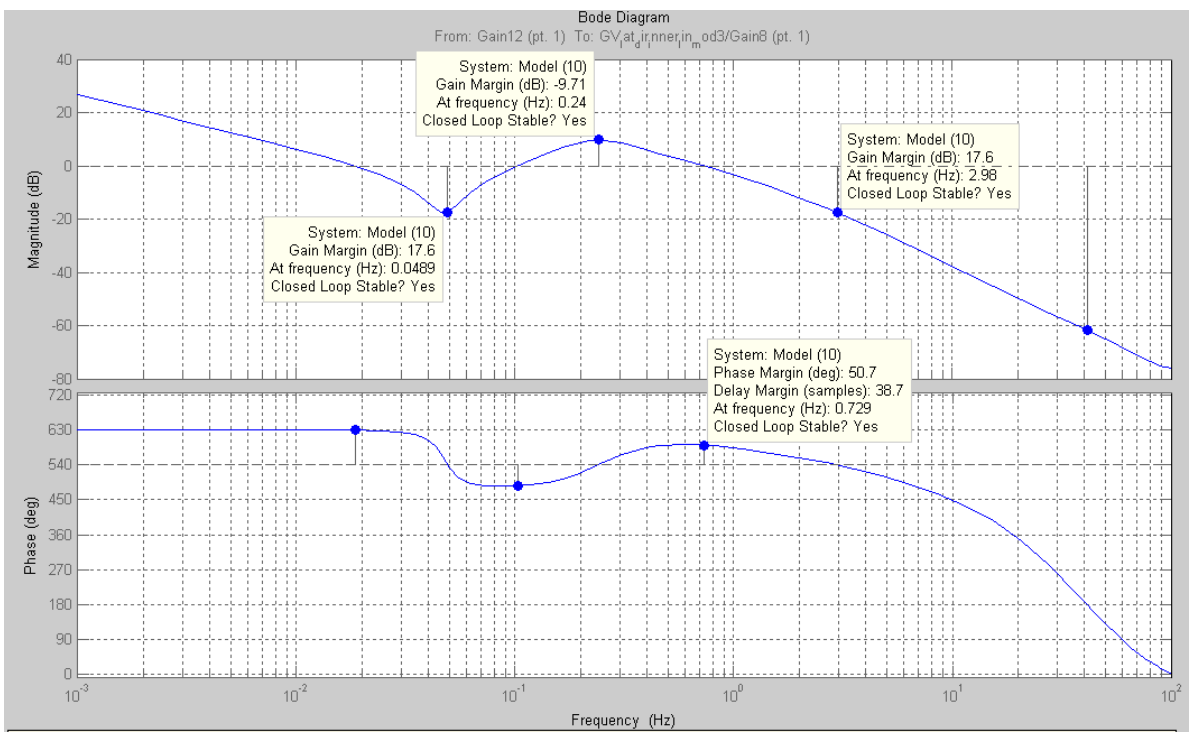

Figure B-12. Rudder Path Frequency Response—25 ms

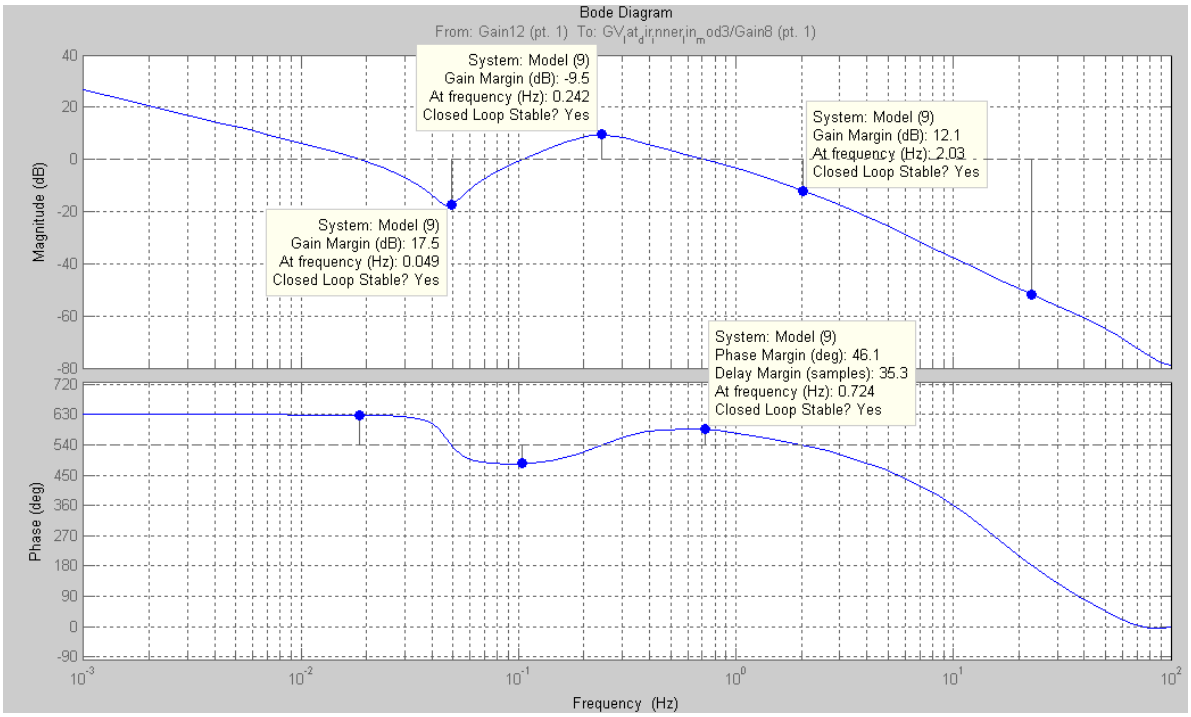

Figure B-13. Rudder Path Frequency Response—50 ms

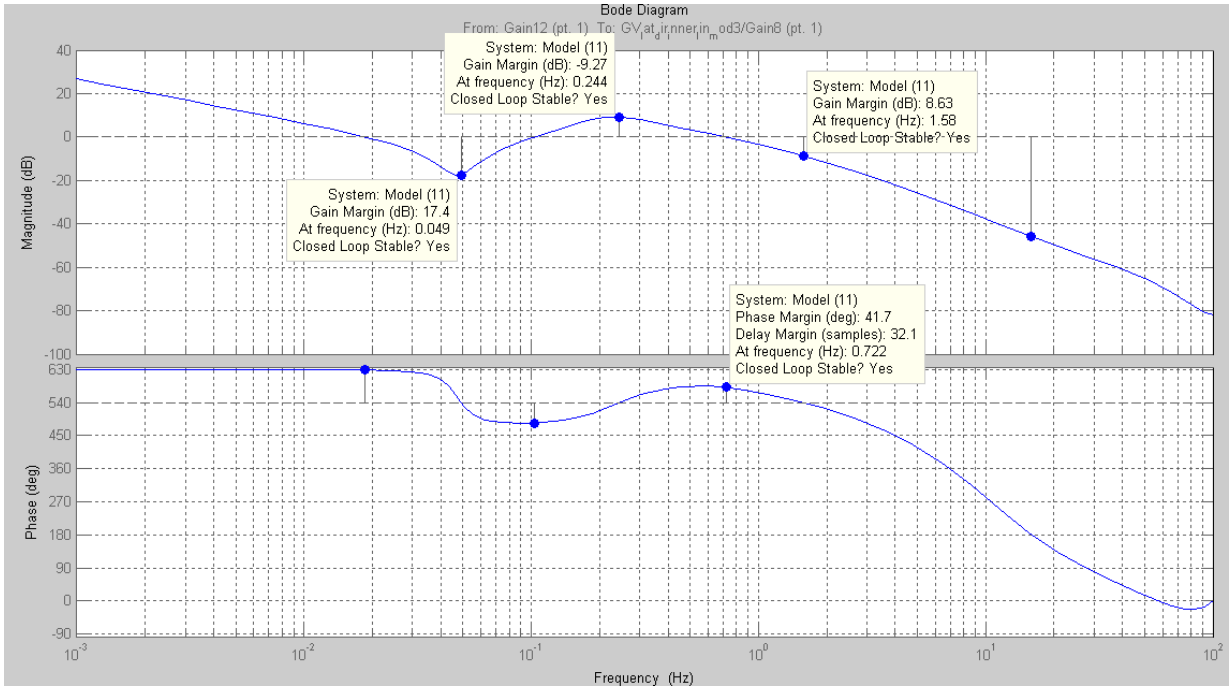

Figure B-14. Rudder Path Frequency Response—75 ms

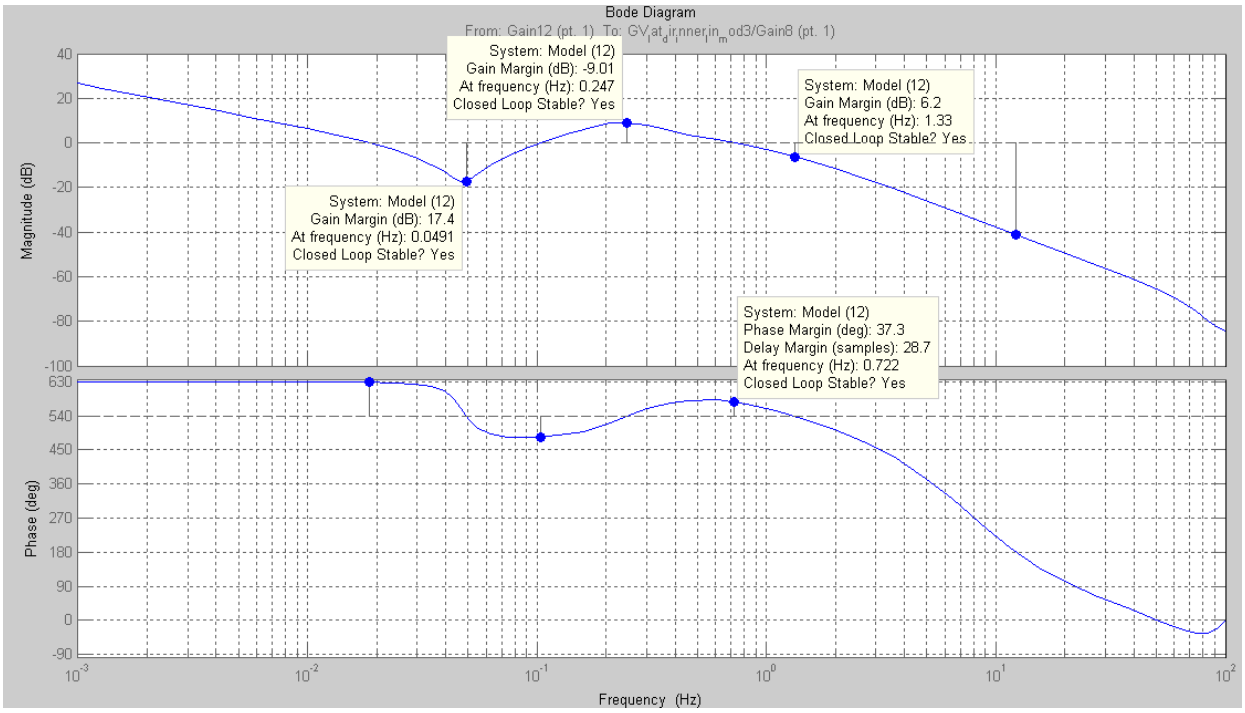

Figure B-15. Rudder Path Frequency Response—100 ms

Table B-3. Rudder Path IL Stability Margin Summary

Transport Delay (ms)	Gain Margin	Phase Margin
25	17.6 dB at 0.05 Hz -9.7 dB at 0.24 Hz 17.6 dB at 3.0 Hz	50.7 degrees at 0.7 Hz
50	17.5 dB at 0.05 Hz -9.5 dB at 0.24 Hz 12.1 dB at 2.0 Hz	46.1 degrees at 0.7 Hz
75	17.4 dB at 0.05 Hz -9.3 dB at 0.24 Hz 8.6 dB at 1.6 Hz	41.7 degrees at 0.7 Hz
100	17.4 dB at 0.05 Hz -9.0 dB at 0.25 Hz 6.2 dB at 1.3 Hz	37.3 degrees at 0.7 Hz

B.4 Response to a Roll Step Sequence.

Figures B-16 through B-22 show the lateral directional IL system response to a roll step sequence for four values of transport lag (25, 50, 75, and 100 ms). The flight condition is altitude 10,000 ft, calibrated airspeed (CAS) 250, and the vehicle configuration is mid weight, mid c.g.

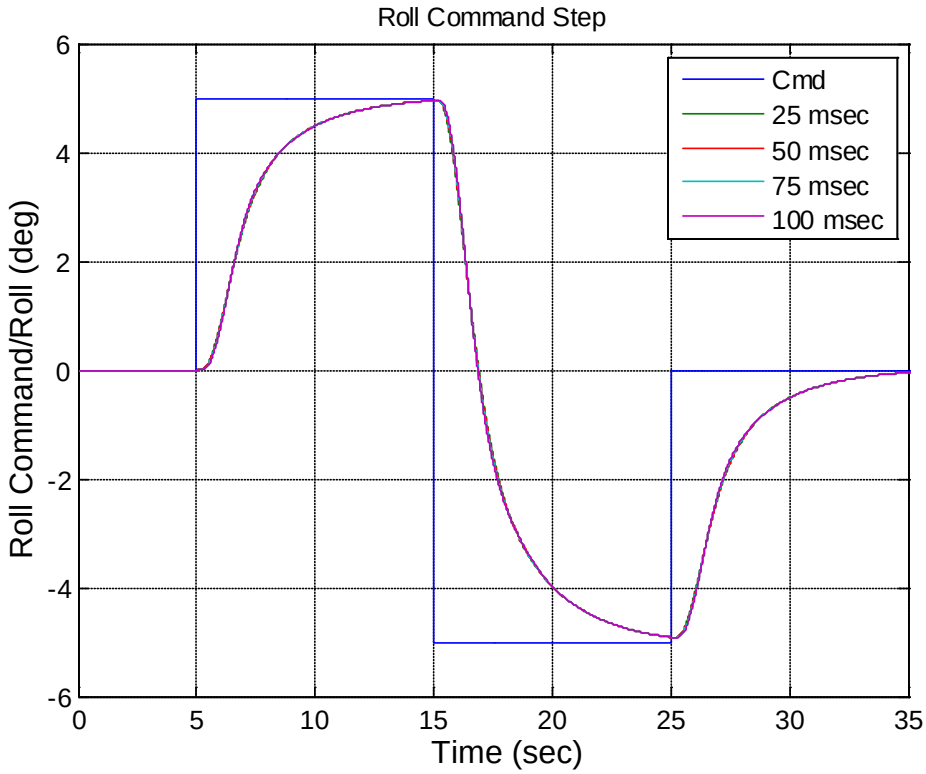

Figure B-16. Roll Step—Roll Attitude Response

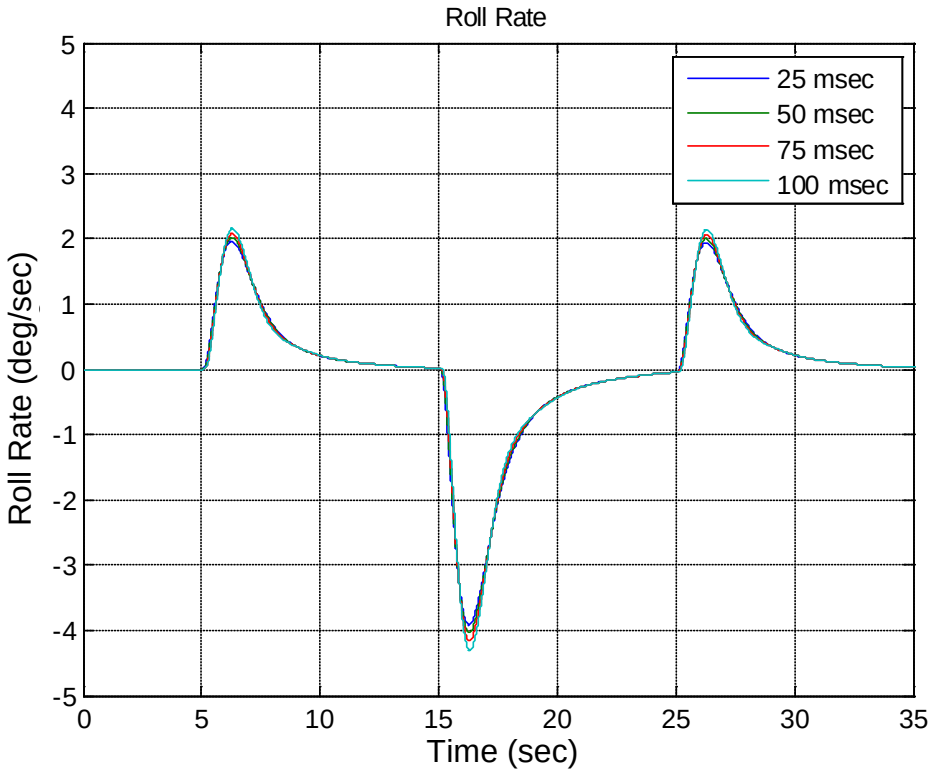

Figure B-17. Roll Step—Roll Rate Response

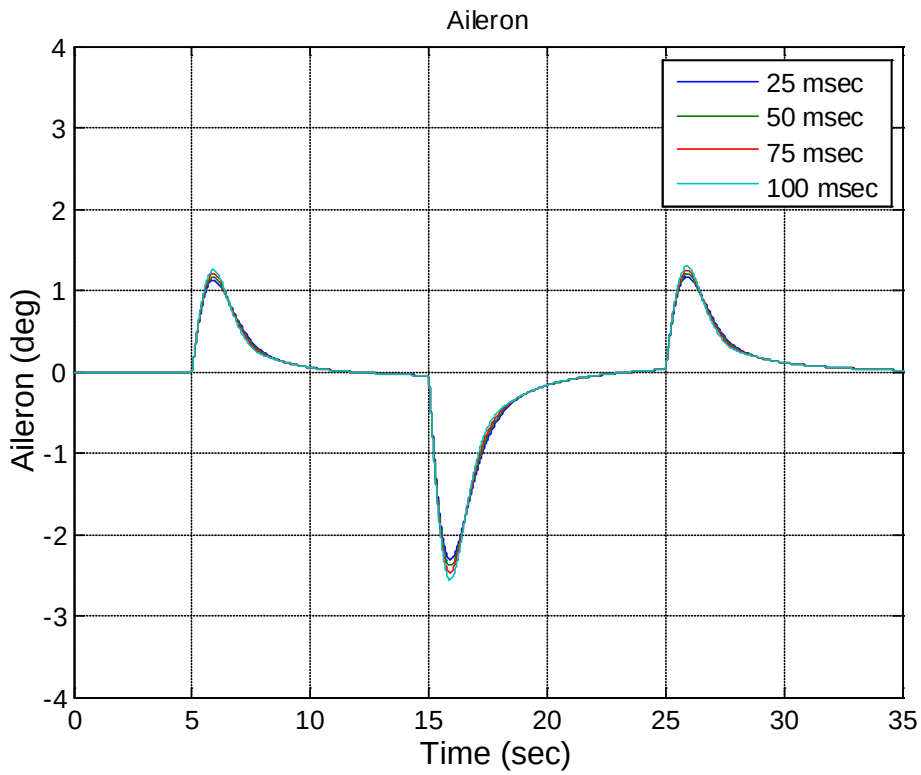

Figure B-18. Roll Step—Aileron Response

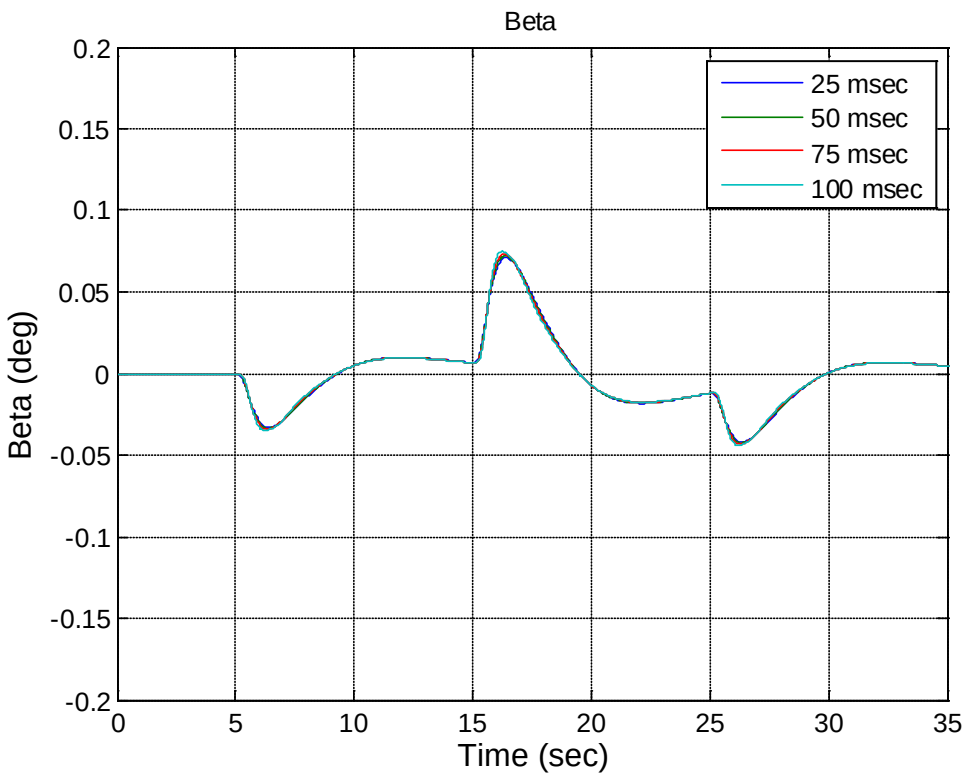

Figure B-19. Roll Step—Side Slip Response

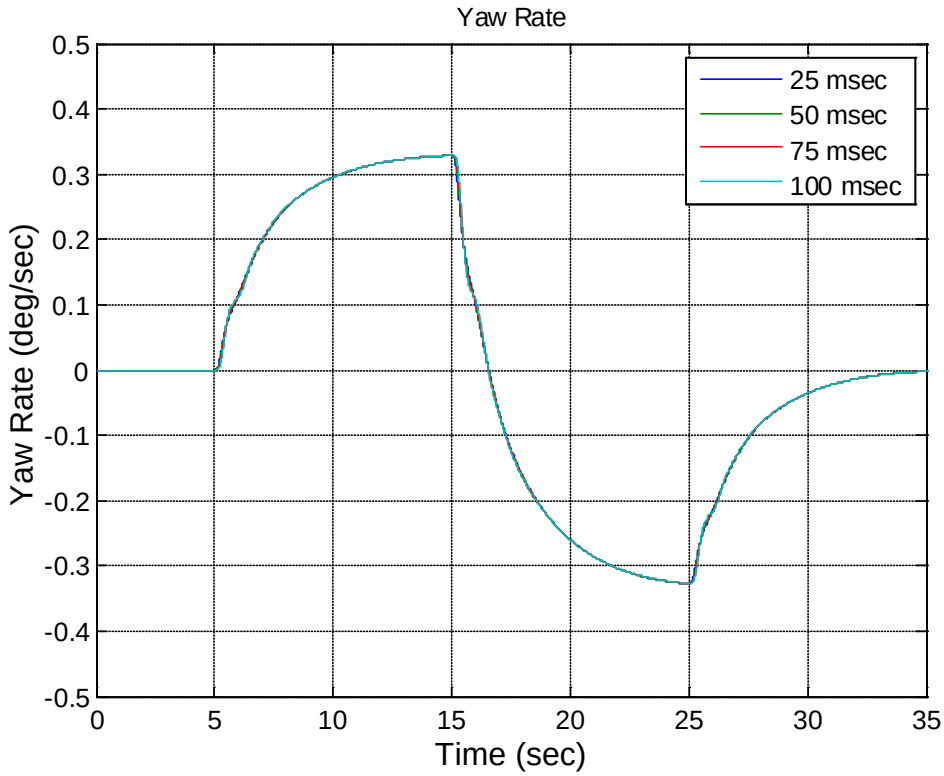

Figure B-20. Roll Step—Yaw Rate Response

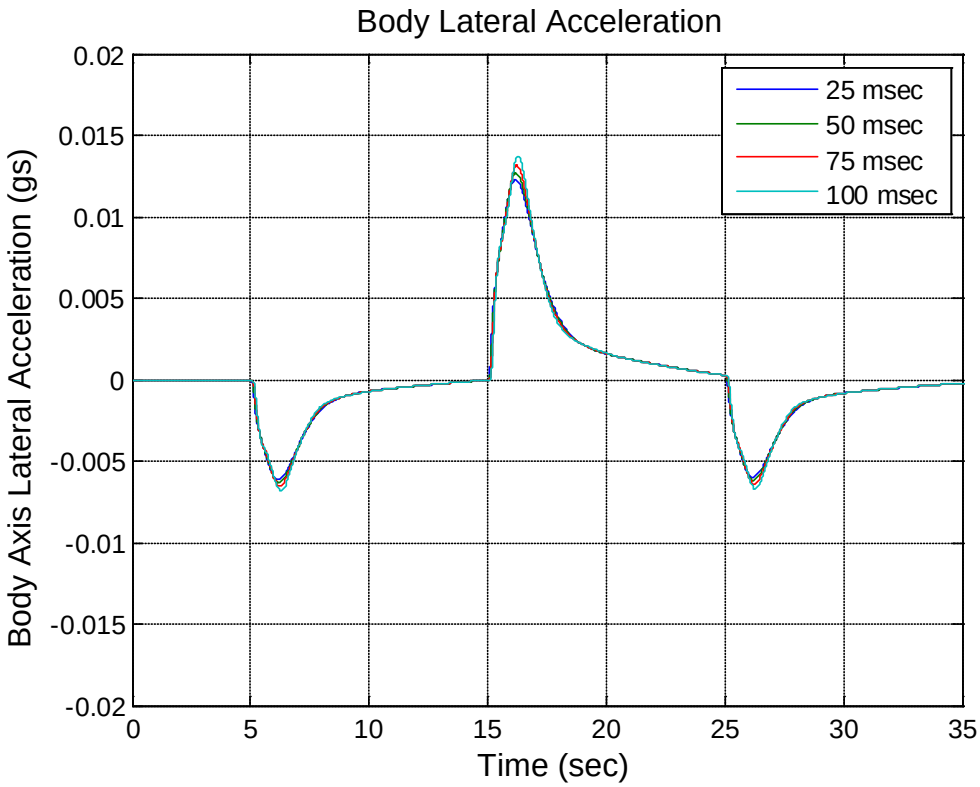

Figure B-21. Roll Step—Lateral Acceleration Response

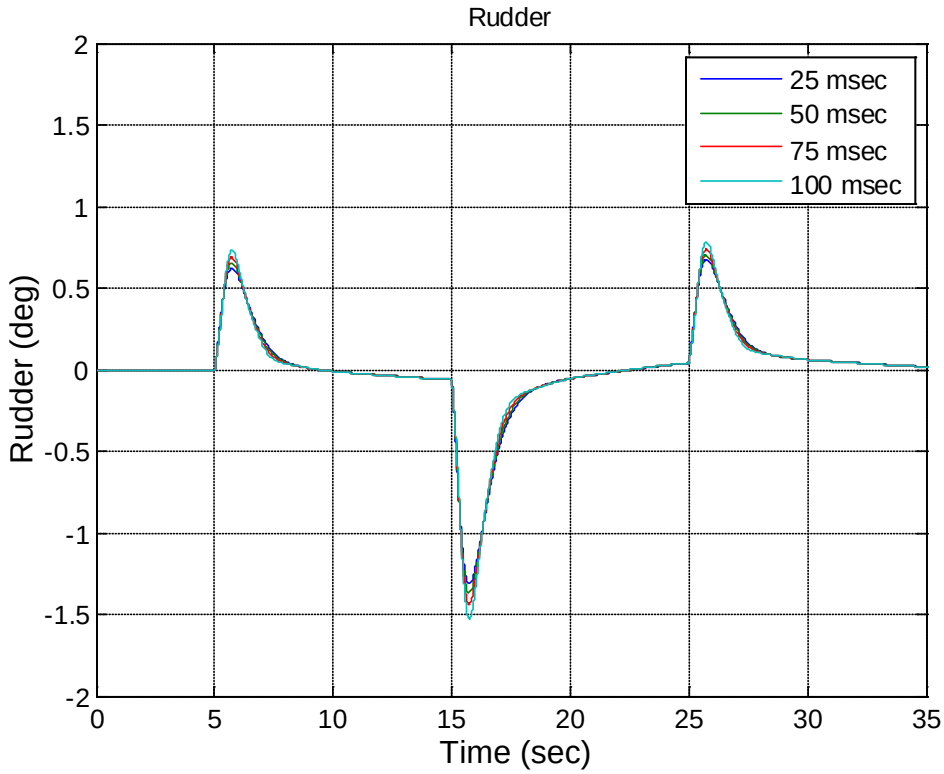

Figure B-22. Roll Step—Rudder Response

APPENDIX C—TEST CASE SCENARIOS

Table C-1. Check Case Descriptions for Federal Aviation Administration Total Energy Control System/Total Heading Control System Program

No.	Title 1	Title 2	y label 1	y label 2	y label 3	y label 4
1	Alt Acq, Alt-ic = 10,000 ft, Altcmd = 15,000 ft Flaps Up, Gear Up	Vecmd = 250 kt, Weight = 120,000 ft	Alt, Altcmd ~ft	Theta, Alpha, Gamin ~deg	Thrustcmd, Tmax, Tmin ~lb	Ve, Vecmd ~kt
2	Ve-mode, Ve-ic = 200 kt, Vecmd = 225 kt Flaps Up, Gear Up	Alt Hold, Altcmd = 10,000 ft, Weight = 120,000 lb	Ve, Vecmd ~kt	Theta, Alpha, Gamin, Elevatorcmd ~deg	Thrust, Tmax, Tmin ~lb	Alt, Altcmd ~ft
3	Alt Acq, Alt-ic = 10,000 ft, Altcmd = 10500 ft Flaps Up, Gear up	Vemode, Vecmd = 250 kt, Weight = 120,000 lb	Alt, Altcmd ~ft	Theta, Alpha, Gamin, Elevatorcmd ~deg	Ve, Vecmd ~kt	Thrustcmd, Tmax, Tmin ~lb
4	Ve-mode, Ve-ic = 200 kt, Vecmd = 300 kt Flaps up, Gear Up,	Alt Hold, Altcmd = 10,000 ft, Weight = 120,000 lb	Ve, Vecmd ~kt	Theta, Alpha, GAmin, Elevatorcmd ~deg	Throttlecmd, Tmax, Tmin ~lb	Alt, Altcmd ~ft
5	Dual cmds, Ve-mode, Ve-ic = 300 kt, Vecmd = 225 kt Weight = 120,000 lb, Flaps Up, Gear Up	Alt Acq, Alt-ic = 10,000 ft, Altcmd = 15,000 ft	Ve, Vecmd ~kt	Alt, Altcmd ~ft	Theta, Alpha, Gamin, Elevatorcmd ~deg	Thrustcmd, Tmax, Tmin ~lb
6	Accel cmd execution during Alt Acq climb at max thrust Ve-mode, Ve-ic = 200 kt, Vecmd = 250 kt	Alt Acq, Alt-ic = 10,000 ft, Altcmd = 15,000 ft Weight = 120,0000 lb, Flaps Up, Gear Up	Ve, Vecmd ~kt	Alt, Altcmd ~ft	Theta, Alpha, Gamin, Elevatorcmd ~deg	Thrustcmd, Tmax, Tmin ~lb
7	Decel cmd during Alt Acq climb at max thrust Ve-mode, Ve-ic = 300 kt, Vecmd = 250 kt	Alt Acq-mode, Alt-ic = 10,000 ft, Altcmd = 18,000 ft Weight = 120,000 lb, Flaps Up, Gear Up	Alt, Altcmd ~ft	Ve, Vecmd ~kt	Theta, Alpha, Gamin, Elevatorcmd ~deg	Thrustcmd, Tmax, Tmin ~lb
8	Decel cmd during Alt Acq descent at idle thrust Ve-mode, Ve-ic = 250 kt, Vecmd = 200 kt	Alt Acq-mode Alt-ic = 10,000 ft, Altcmd = 8000 ft Weight = 120,000 lb, Flaps Up, Gear Up	Alt, Altcmd ~ft	Ve, Vecmd ~kt	Theta, Alpha, Gamin, Elevatorcmd ~deg	Thrustcmd, Tmax, Tmin ~lb

Table C-1. Check Case Descriptions for Federal Aviation Administration Total Energy Control System/Total Heading Control System Program (Continued)

No.	Title 1	Title 2	y label 1	y label 2	y label 3	y label 4
9	Decel cmd in Alt Hold mode	Ve-mode, Ve-ic = 200 kt, Vecmd = 110 kt	Ve, Vecmd, Vmin ~kt	Theta, Alpha, Gamin, Elevatorcmd ~deg	Thrustcmd, Tmax, Tmin ~lb	Alt, Altcmd ~ft
	Alt Hold-mode, Altcmd = 10,000 ft	Flaps-ic = 0 deg, stepped dwn to 5, 15, 25, 30 deg				
	Gear Down, Weight = 100,000 lb					
10	Glide Slope and Go Around control mode operations	Go Around @ Alt = 426.5 ft, min Alt = 403.5 ft	Alt ~ft, VpathMode	Theta, Alpha, Gamin, Elevatorcmd ~deg	Thrustcmd, Tmax, Tmin ~lb	Ve, Vecmd, Vmin ~kt
	Ve-mode, Vecmd = 127 kt	Weight = 100,000 lb, Flaps = 30 deg, Gear Down				
11	FPA & Alt Acq mode operations	FPA-mode, Gamin-ic = 0 deg, FPAcmd = -3, +3 deg	Gamin, Fpacmd ~deg, VpathMode	Alt ~ft	Thrustcmd, Tmax, Tmin ~lb	Ve, Vecmd ~kt
	Alt Acq-mode, Altcmd = 11,000 ft	Ve-mode, Vecmd = 200 kt				
	Weight = 120,000 lb, Flaps Up, Gear Up					
12	Response to Hor Windshear Alt Hold & Ve control modes	Vecmd = 127 kt, Altcmd = 2,000 ft	Ve, Vecmd ~kt	Alt, Altcmd ~ft	Theta, Alpha, Gamin, Elevatorcmd ~deg	Thrustcmd, Tmax, Tmin ~lb
	Weight = 100,000 lb, Flaps = 30 deg, Gear Down					
13	Response to 5 ft/sec RMS Ugust, Alt Hold & Ve control modes	Vecmd = 127 kt, Altcmd = 2000 ft	Ve, Vecmd ~kt	Alt, Altcmd ~ft	Theta, Alpha, Gamin, Elevatorcmd ~deg	Thrustcmd, Tmax, Tmin ~lb
	Weight = 100,000 lb, Flaps = 30 deg, Gear Up					

C.1 Check Case 1.

Flight level change (FLC) from 10,000 to 15,000 feet (ft) (mode)
Maintain constant airspeed at 250 knots (kt)

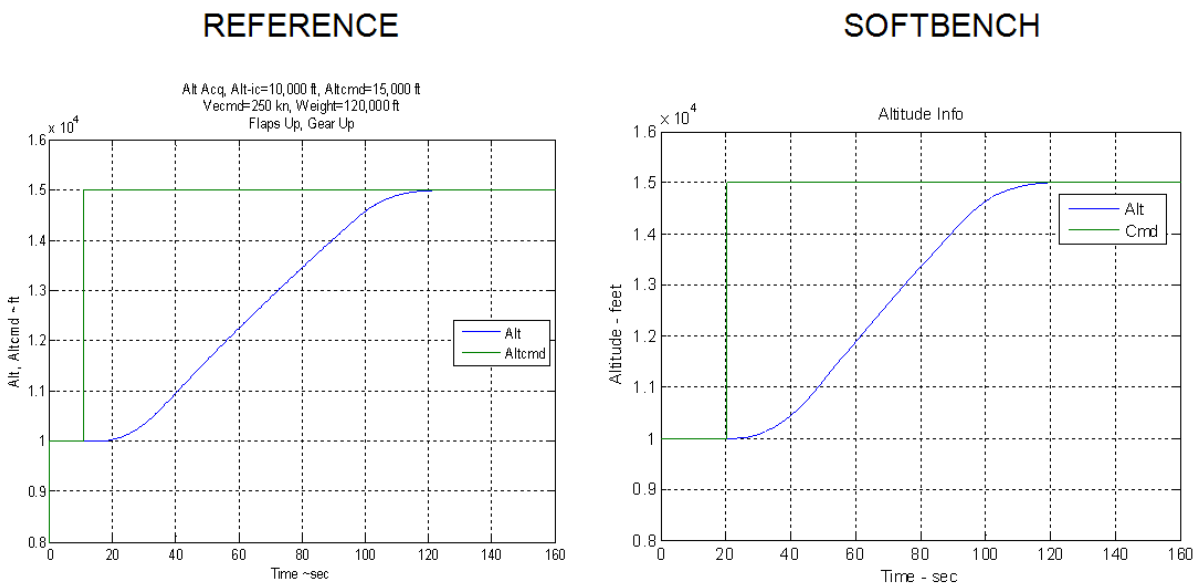

Figure C-1. Altitude Command and Altitude

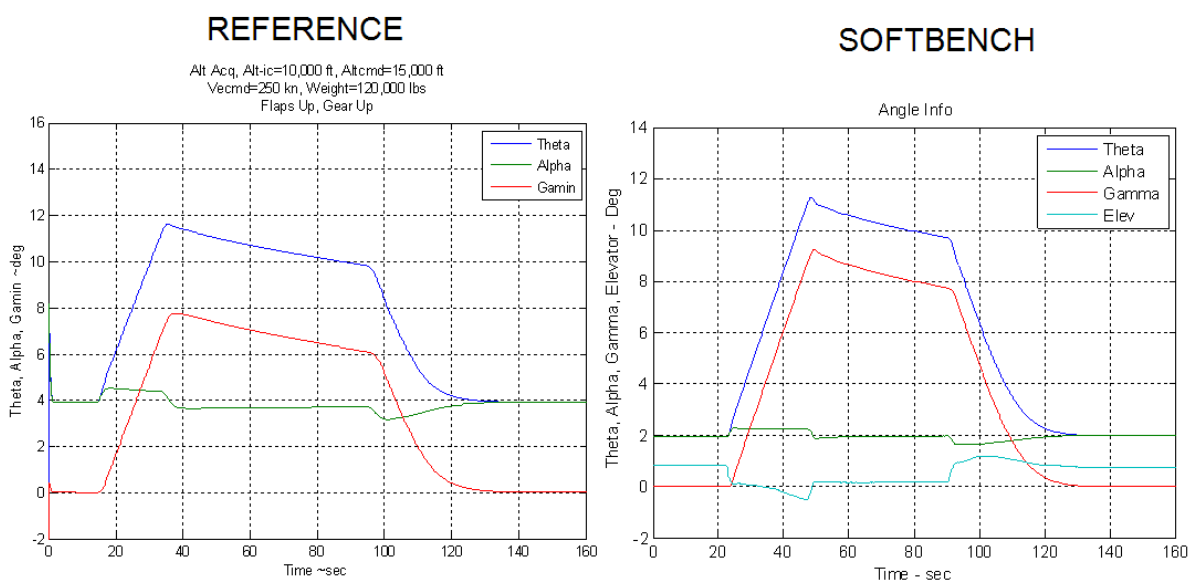

Figure C-2. Theta, Alpha, Gamma, and Elevator

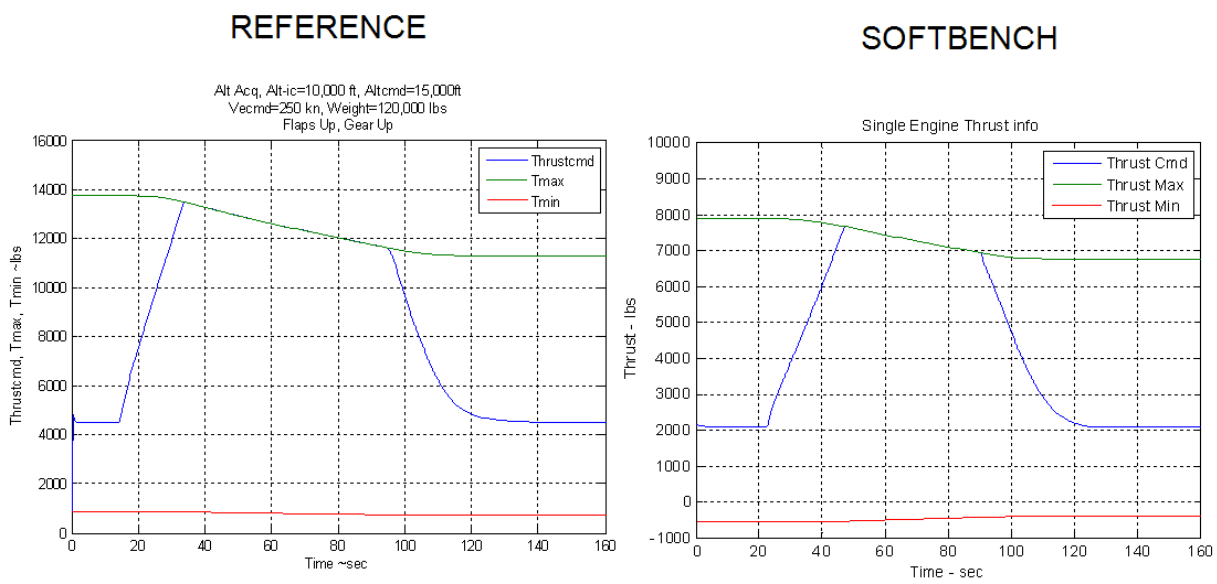

Figure C-3. Thrust Command, Thrust Minimum, and Thrust Maximum

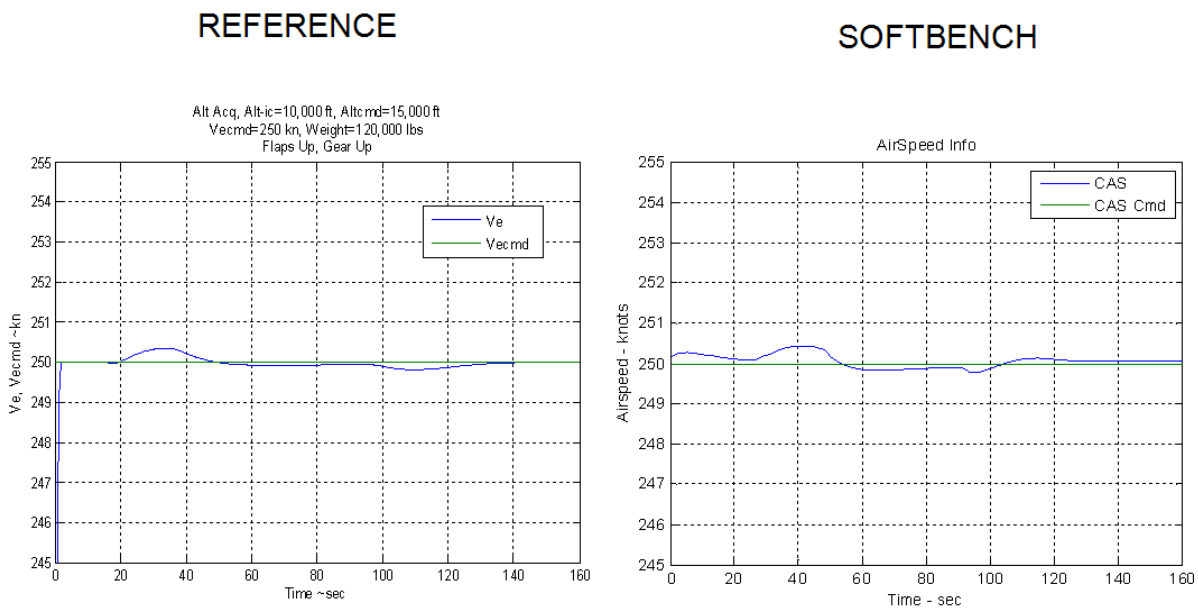

Figure C-4. Calibrated Airspeed Target and Calibrated Airspeed

C.2 Check Case 2.

Airspeed change from 200 to 225 kt (ALT HOLD)
Maintain altitude at 10,000 ft

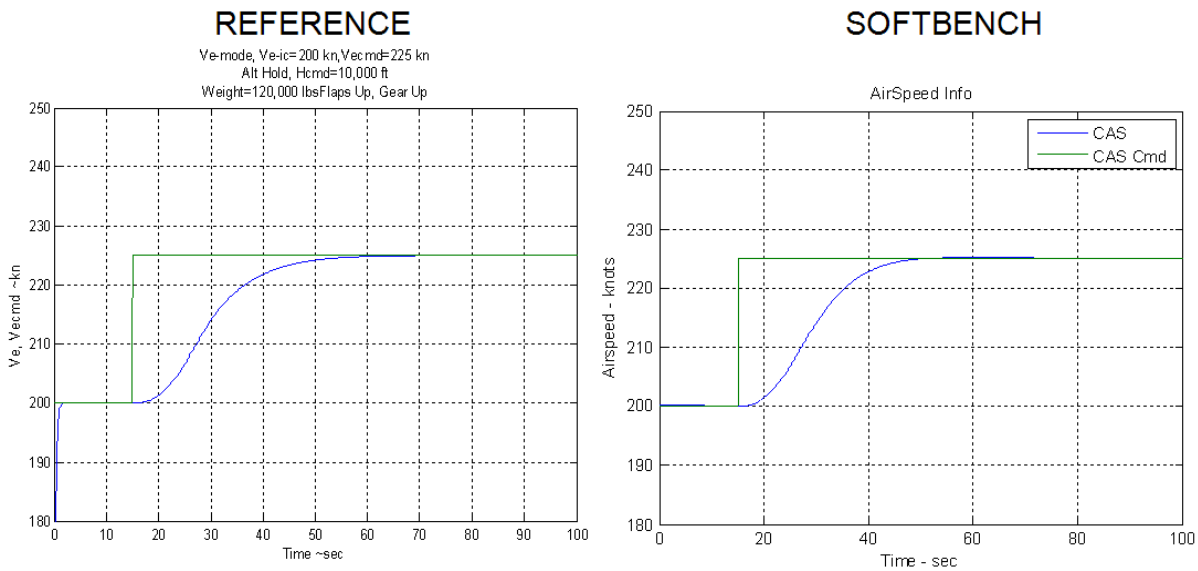

Figure C-5. Calibrated Airspeed Target and Calibrated Airspeed

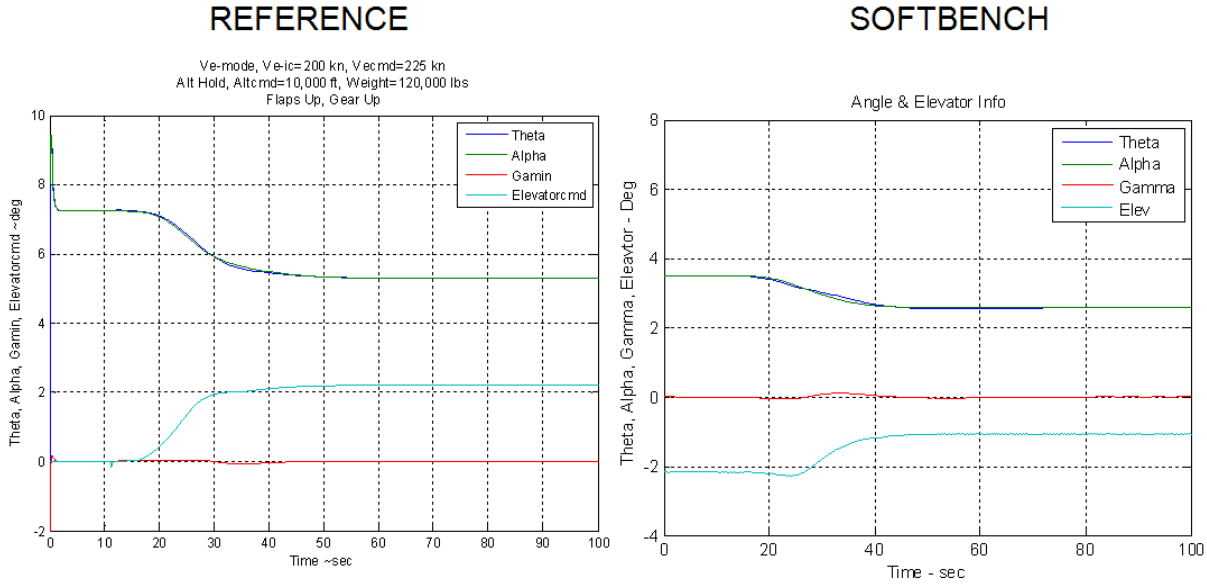

Figure C-6. Theta, Alpha, Gamma, and Elevator

REFERENCE SOFTBENCH

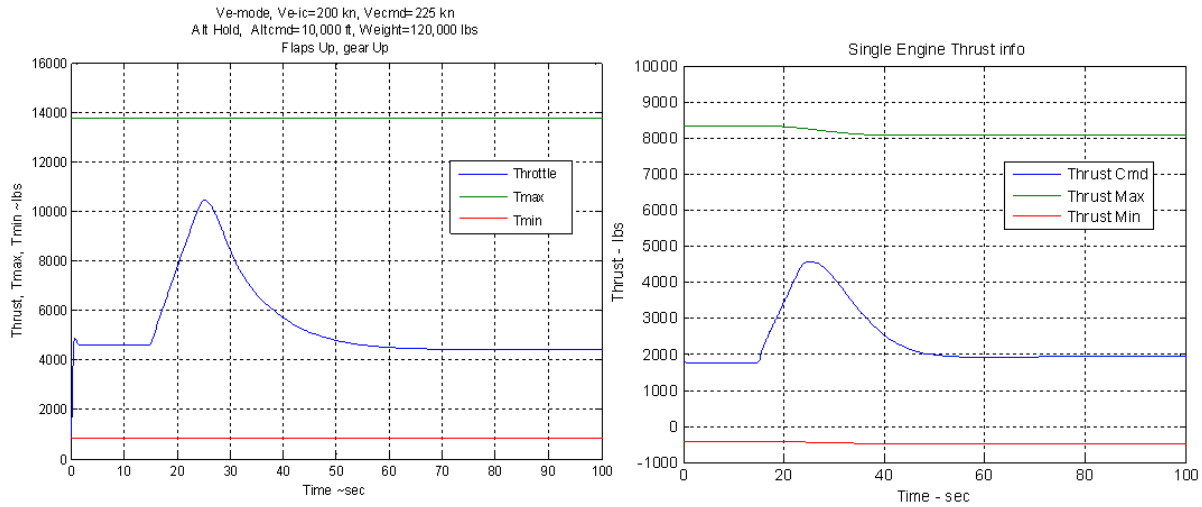

Figure C-7. Thrust Command, Thrust Minimum, and Thrust Maximum

REFERENCE SOFTBENCH

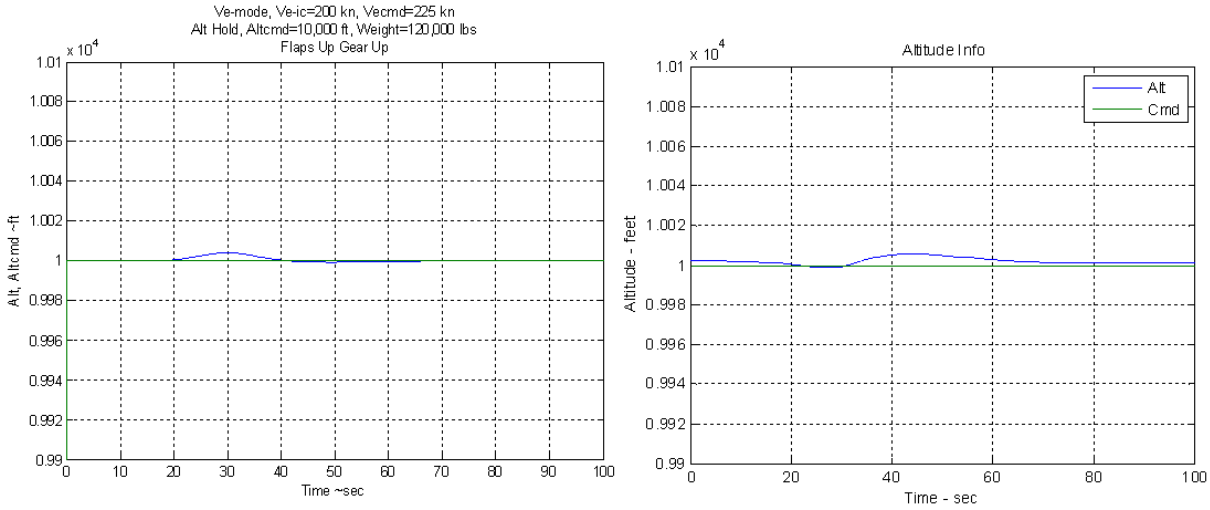

Figure C-8. Altitude Command and Altitude

C.3 Check Case 3.

FLC from 10,000 to 10,500 ft (mode)
Maintain constant airspeed at 250 kt

REFERENCE

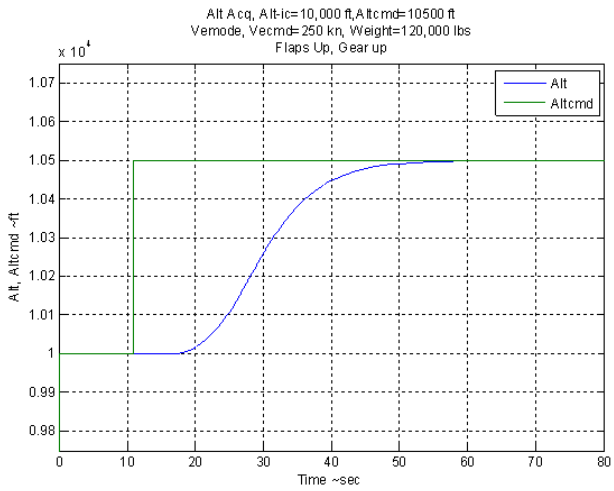

SOFTBENCH

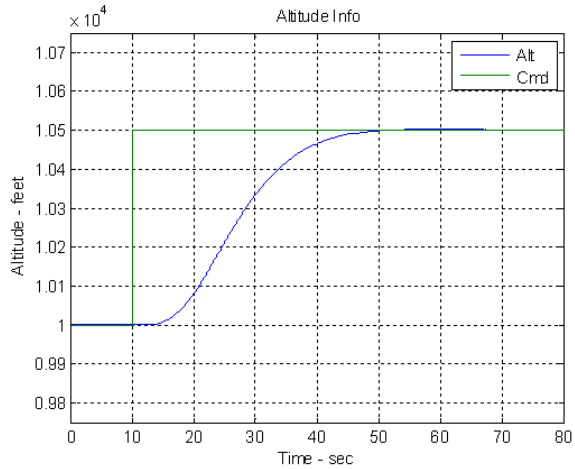

Figure C-9. Altitude Command and Altitude

REFERENCE

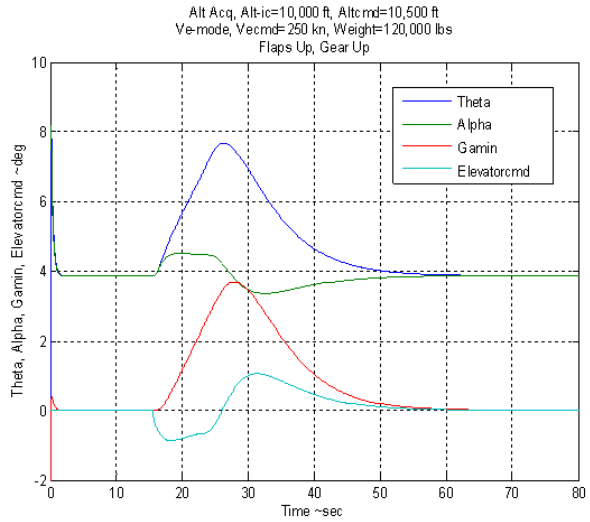

SOFTBENCH

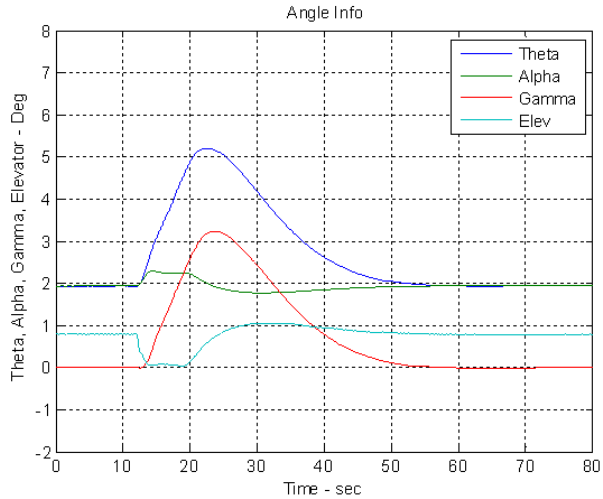

Figure C-10. Theta, Alpha, Gamma, and Elevator

REFERENCE SOFTBENCH

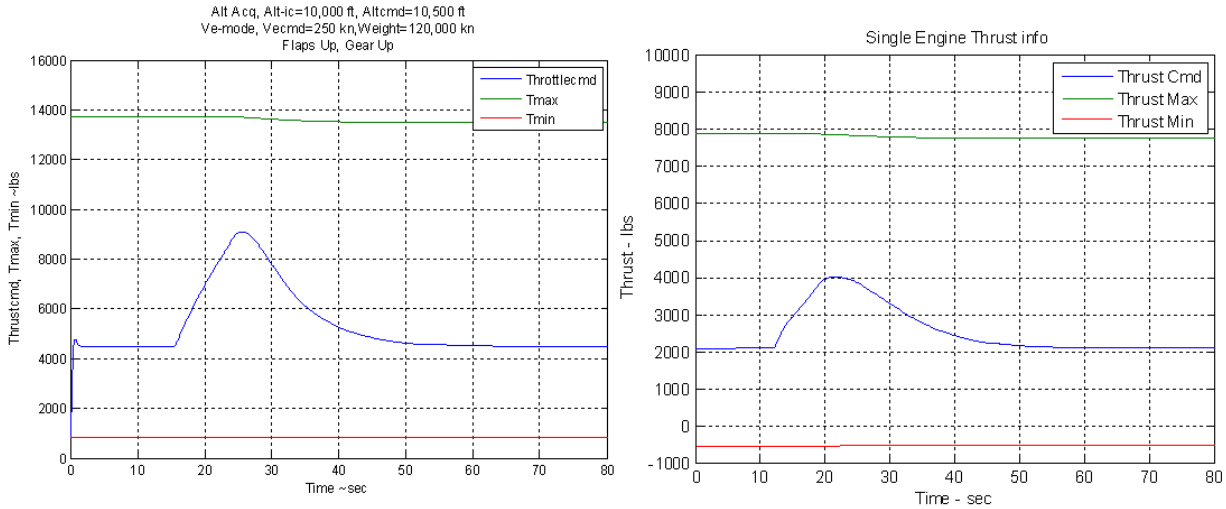

Figure C-11. Thrust Command, Thrust Minimum, and Thrust Maximum

REFERENCE SOFTBENCH

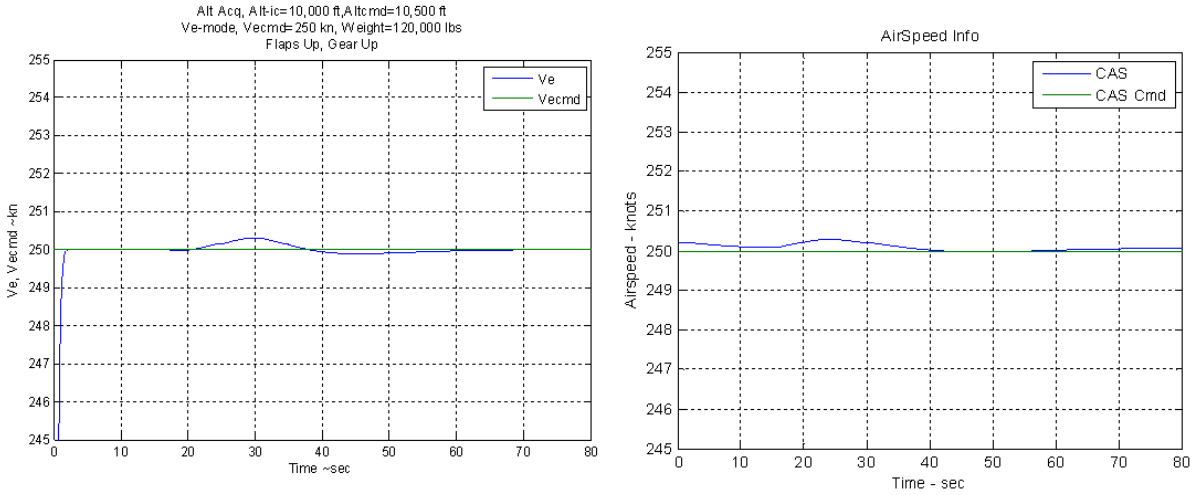

Figure C-12. Calibrated Airspeed Target and Calibrated Airspeed

C.4 Check Case 4.

Airspeed change from 200 to 300 kt (ALT HOLD)
Maintain altitude at 10,000 ft

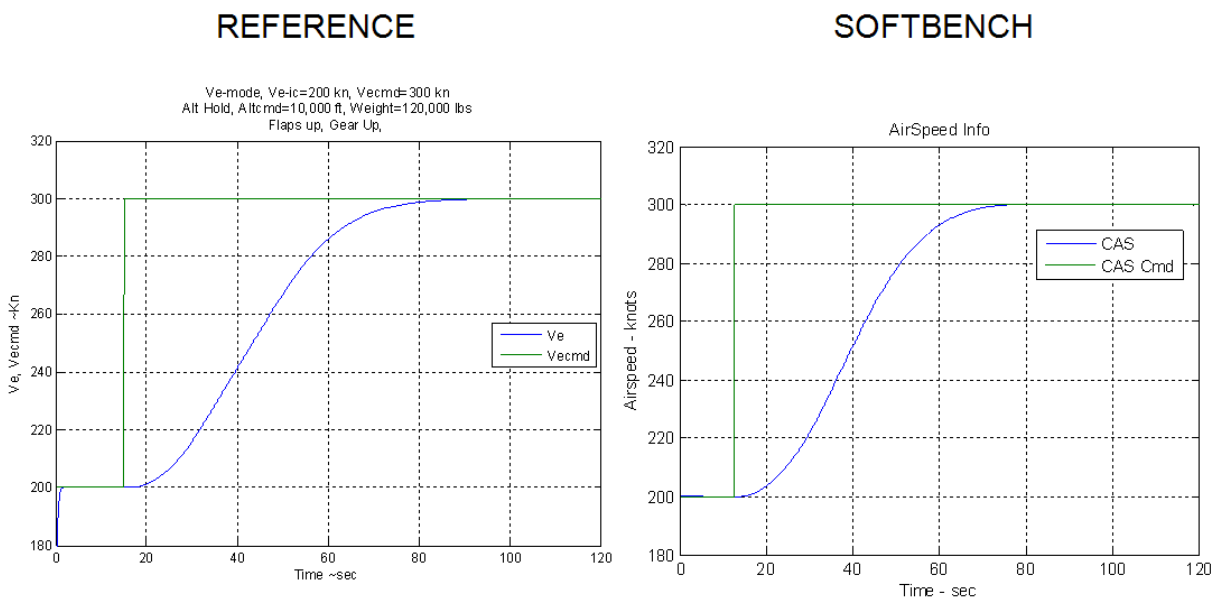

Figure C-13. Calibrated Airspeed Target and Calibrated Airspeed

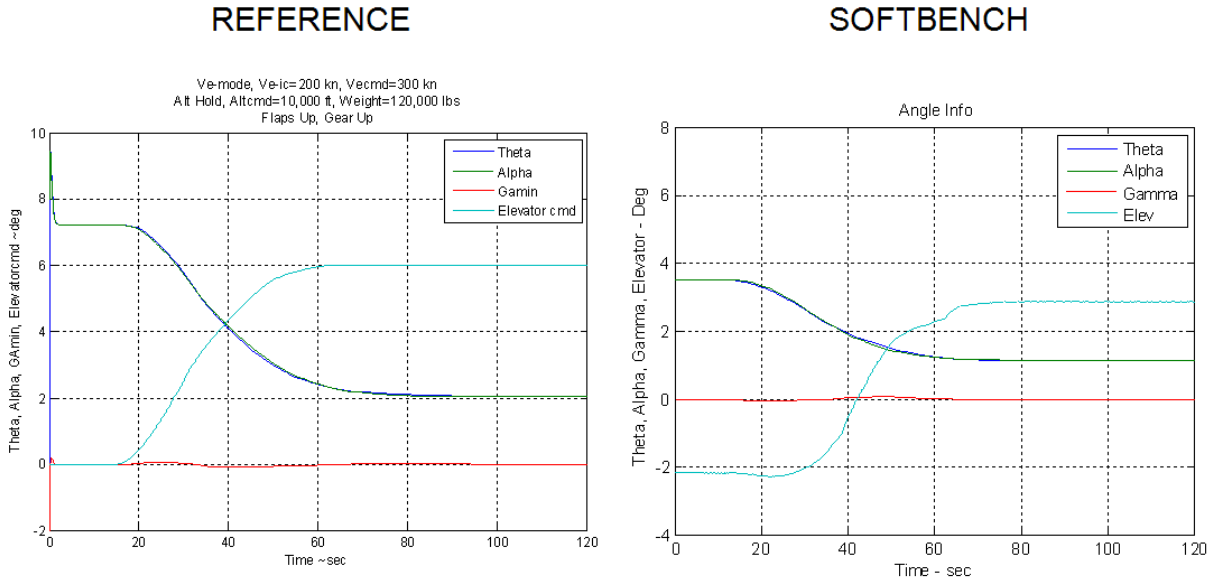

Figure C-14. Theta, Alpha, Gamma, and Elevator

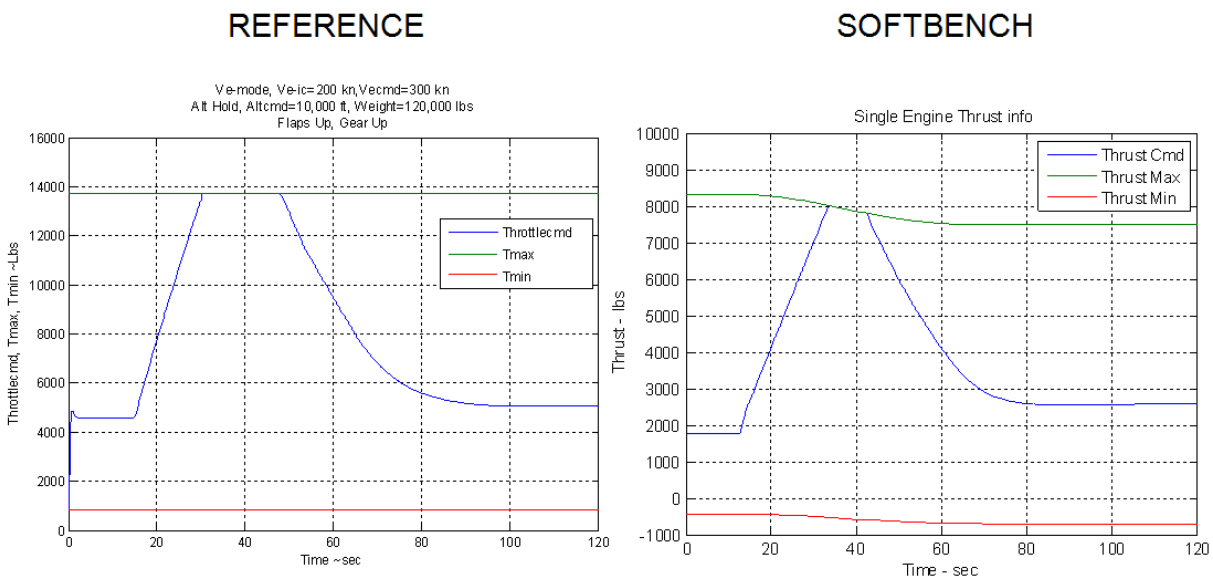

Figure C-15. Thrust Command, Thrust Minimum, and Thrust Maximum

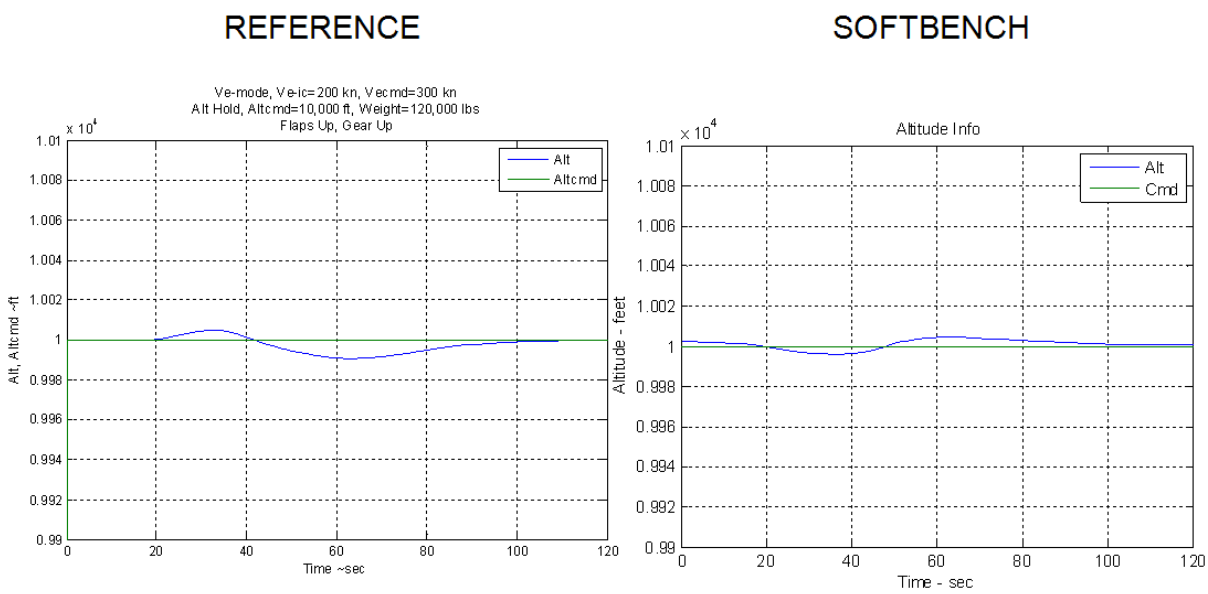

Figure C-16. Altitude Command and Altitude

C.5 Check Case 5.

FLC from 10,000 to 15,000 ft (mode)
Reduce airspeed from 300 to 225 kt during climb

REFERENCE SOFTBENCH

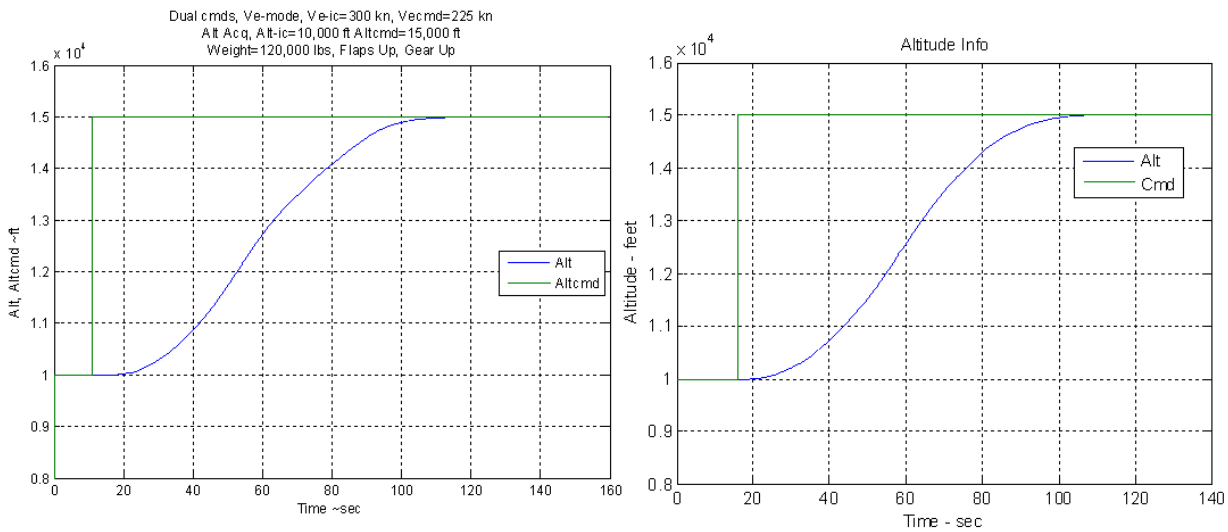

Figure C-17. Altitude Command and Altitude

REFERENCE SOFTBENCH

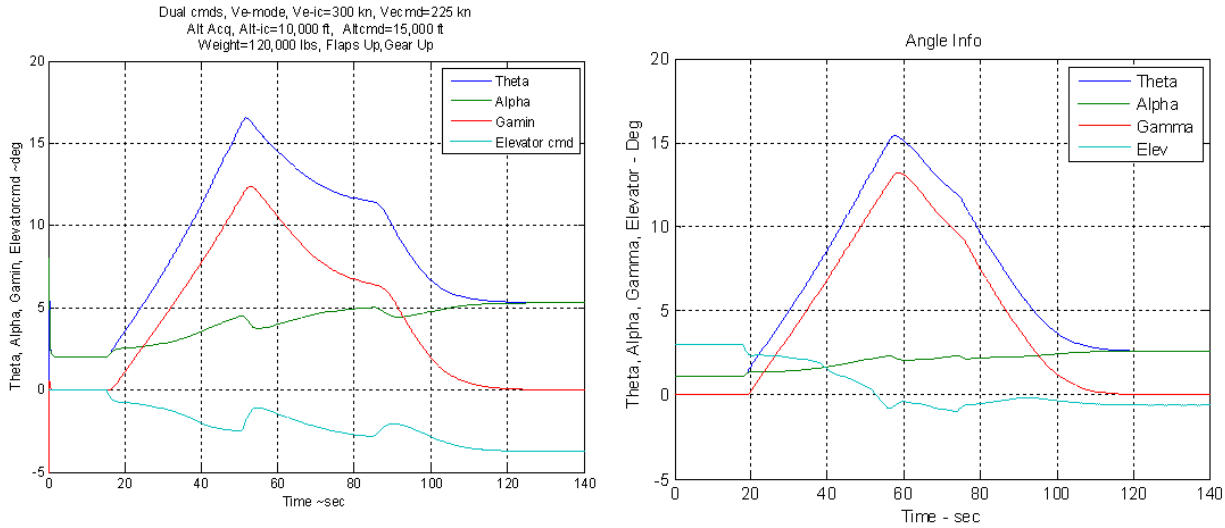

Figure C-18. Theta, Alpha, Gamma, and Elevator

REFERENCE SOFTBENCH

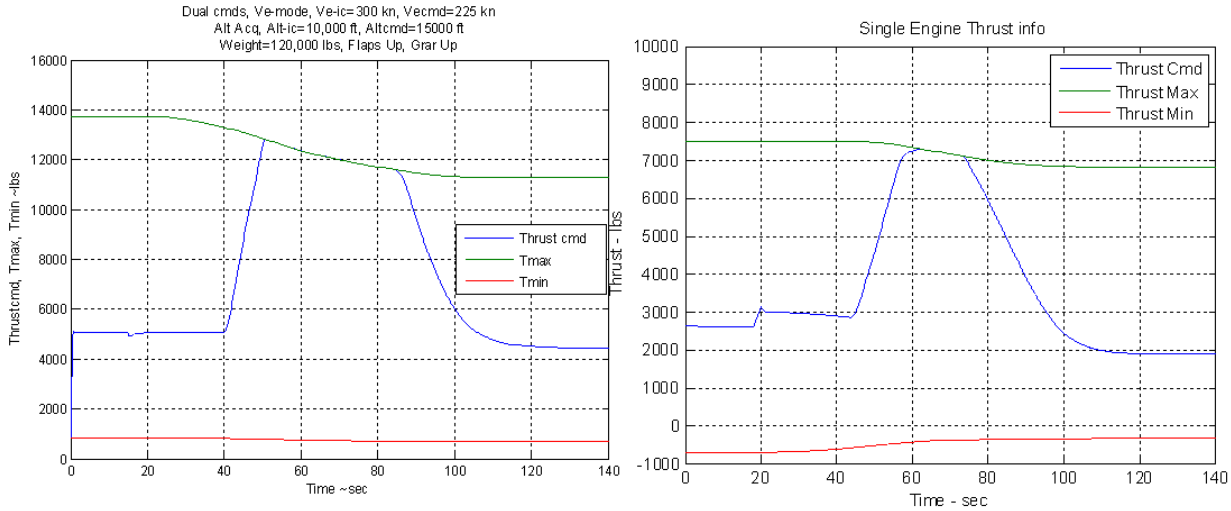

Figure C-19. Thrust Command, Thrust Minimum, and Thrust Maximum

REFERENCE SOFTBENCH

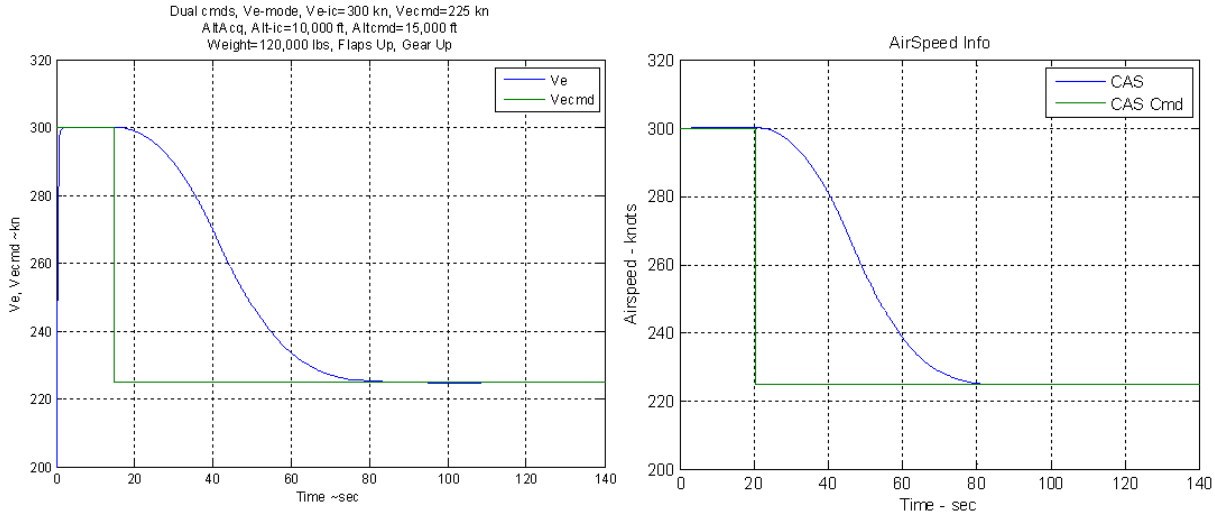

Figure C-20. Calibrated Airspeed Target and Calibrated Airspeed

C.6 Check Case 6.

FLC from 10,000 to 15,000 ft (mode)
Increase airspeed from 200 to 250 kt during climb

REFERENCE

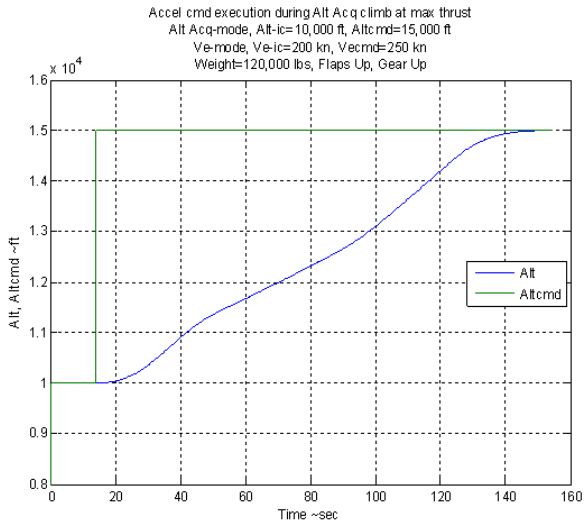

SOFTBENCH

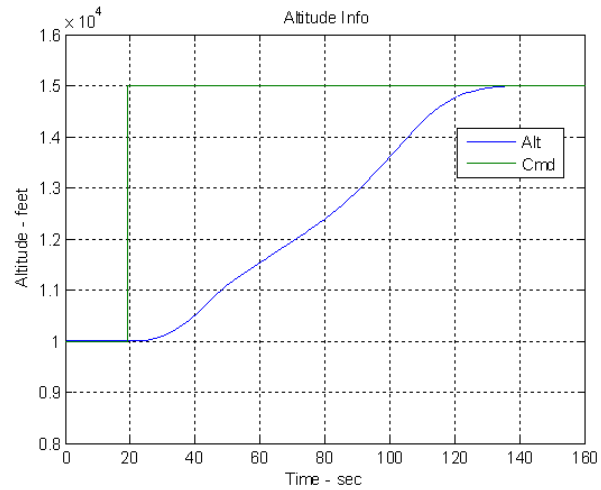

Figure C-21. Altitude Command and Altitude

REFERENCE

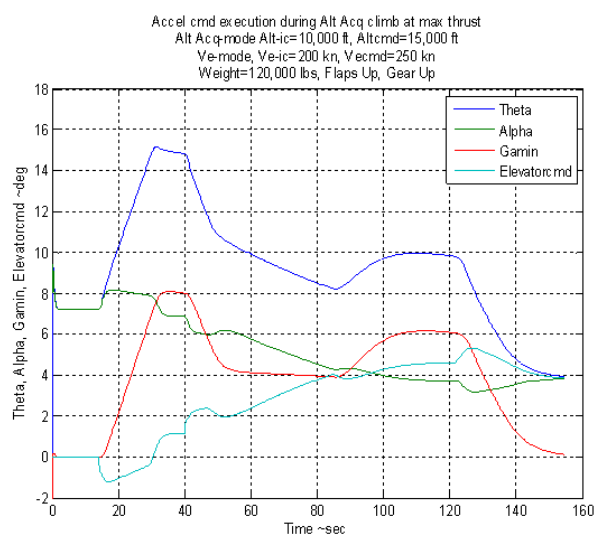

SOFTBENCH

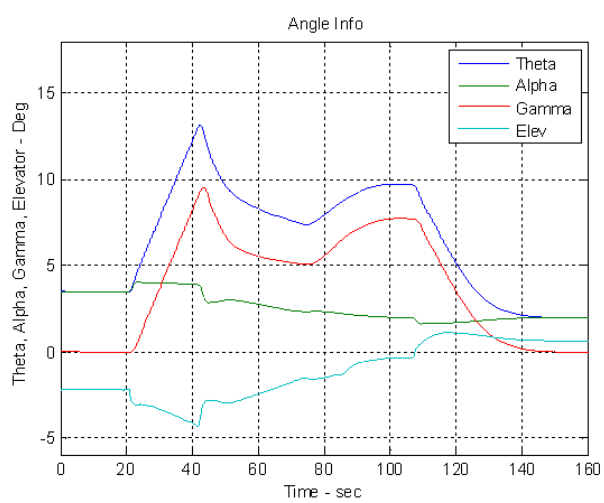

Figure C-22. Theta, Alpha, Gamma, and Elevator

REFERENCE SOFTBENCH

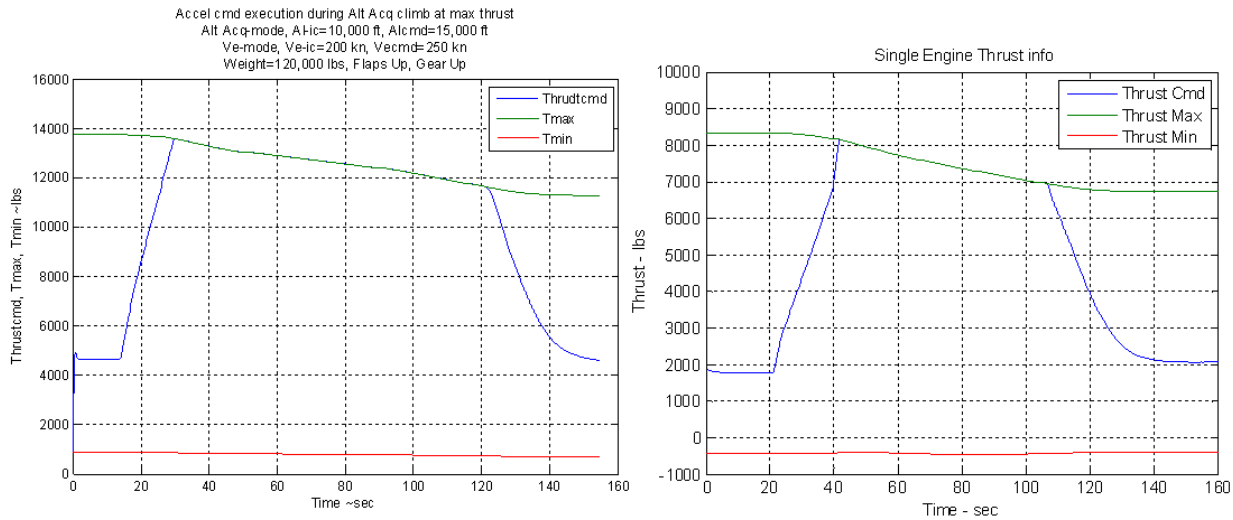

Figure C-23. Thrust Command, Thrust Minimum, and Thrust Maximum

REFERENCE SOFTBENCH

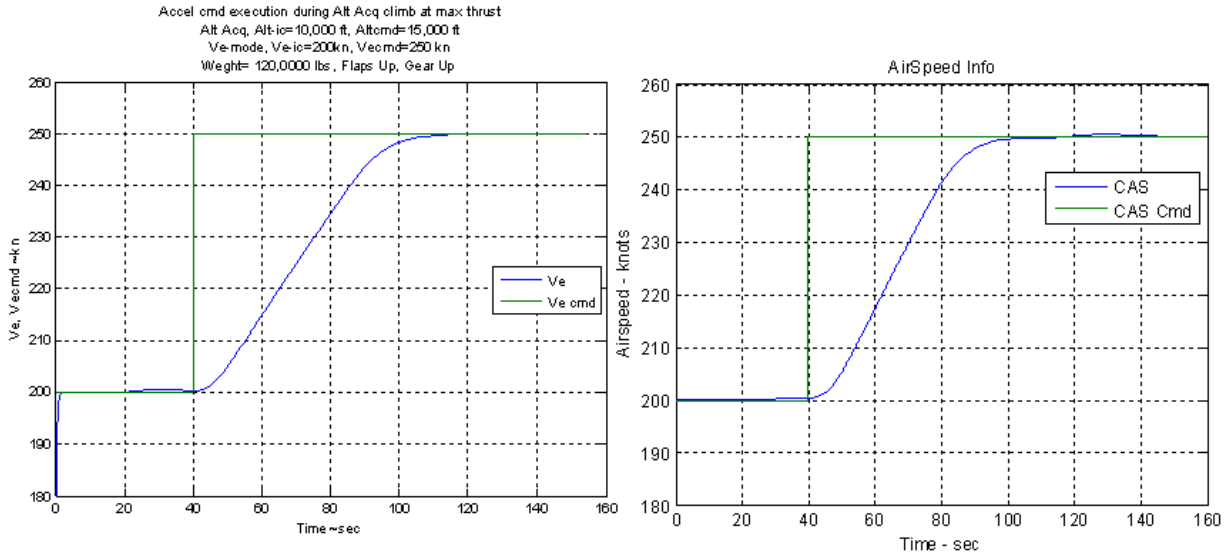

Figure C-24. Calibrated Airspeed Target and Calibrated Airspeed

C.7 Check Case 7.

FLC from 10,000 to 18,000 ft (mode)
Decrease airspeed from 300 to 250 kt during climb

REFERENCE SOFTBENCH

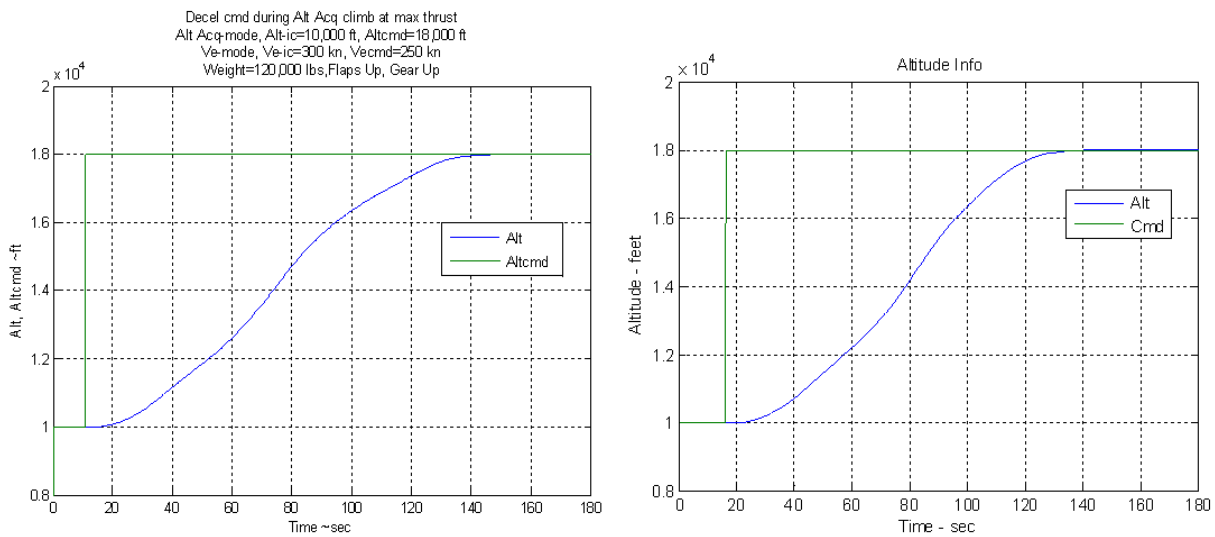

Figure C-25. Altitude Command and Altitude

REFERENCE SOFTBENCH

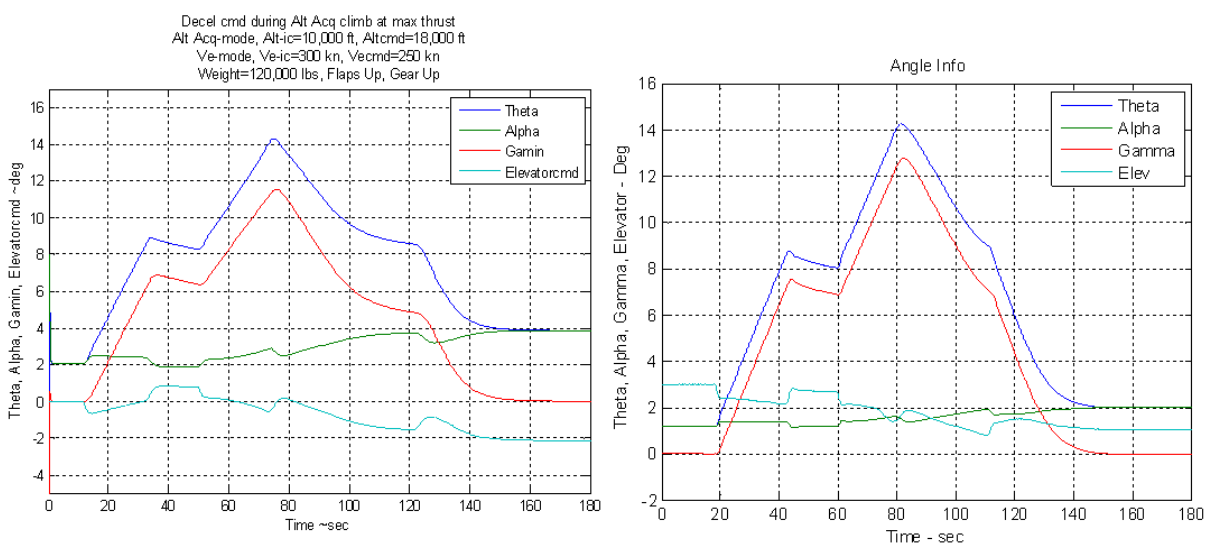

Figure C-26. Theta, Alpha, Gamma, and Elevator

REFERENCE SOFTBENCH

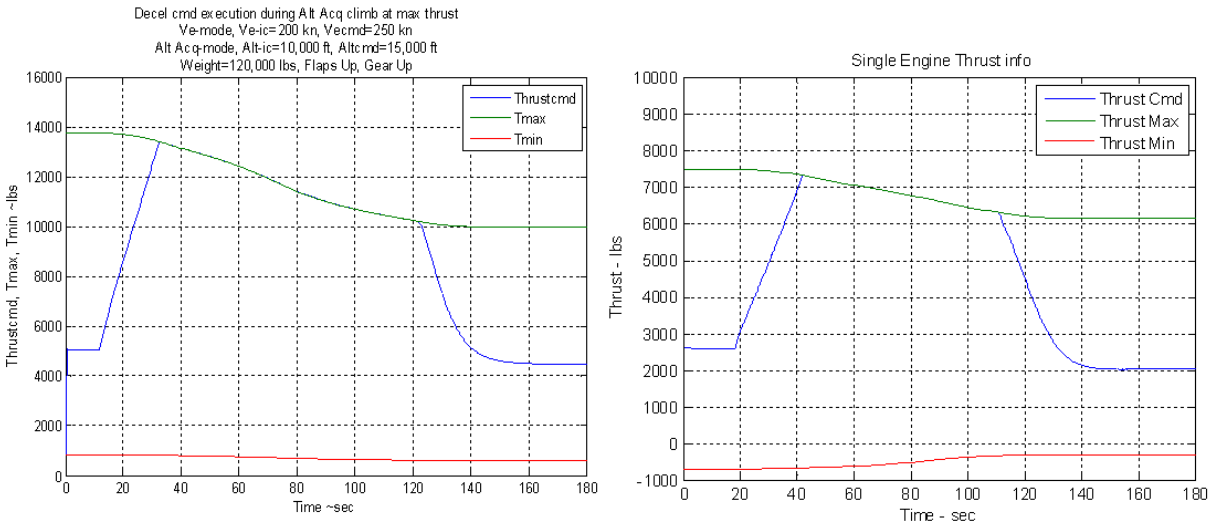

Figure C-27. Thrust Command, Thrust Minimum, and Thrust Maximum

REFERENCE SOFTBENCH

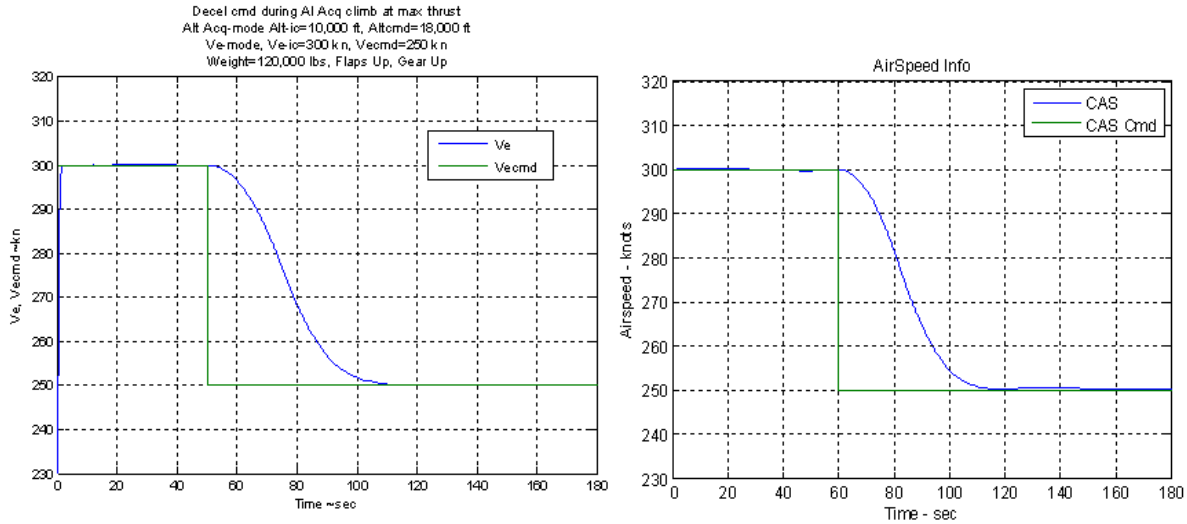

Figure C-28. Calibrated Airspeed Target and Calibrated Airspeed

C.8 Check Case 8.

FLC from 10,000 to 8,000 ft (mode)
Reduce airspeed from 250 to 200 kt during descent

REFERENCE SOFTBENCH

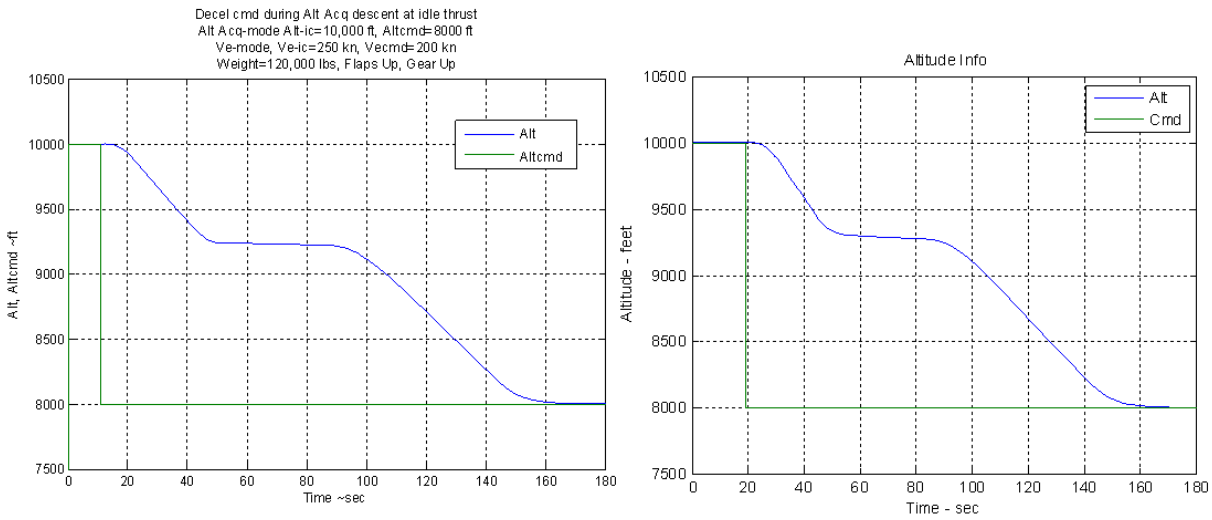

Figure C-29. Altitude Command and Altitude

REFERENCE SOFTBENCH

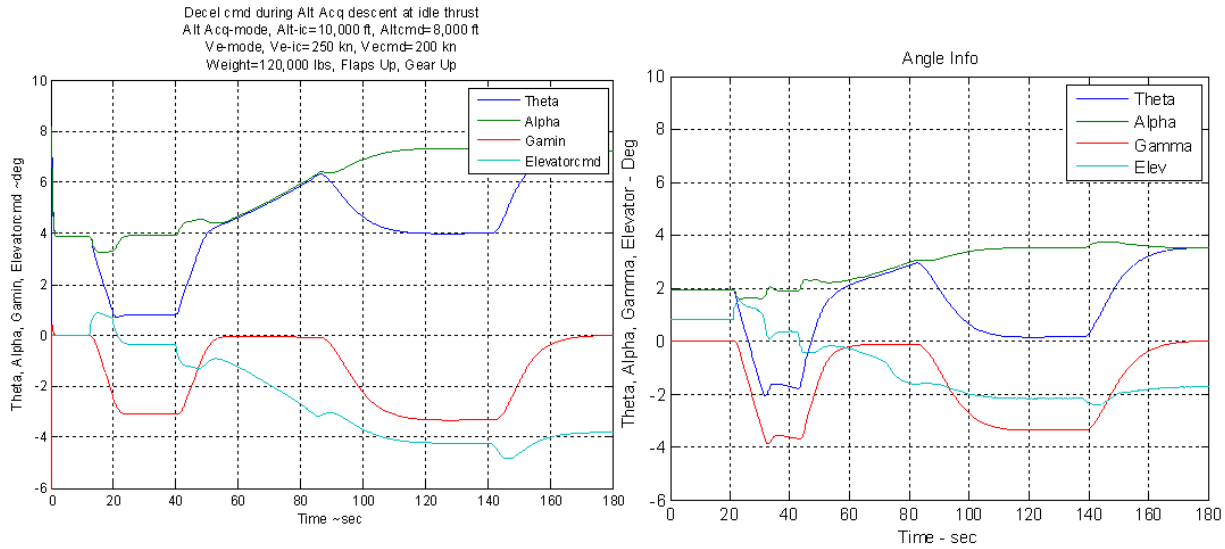

Figure C-30. Theta, Alpha, Gamma, and Elevator

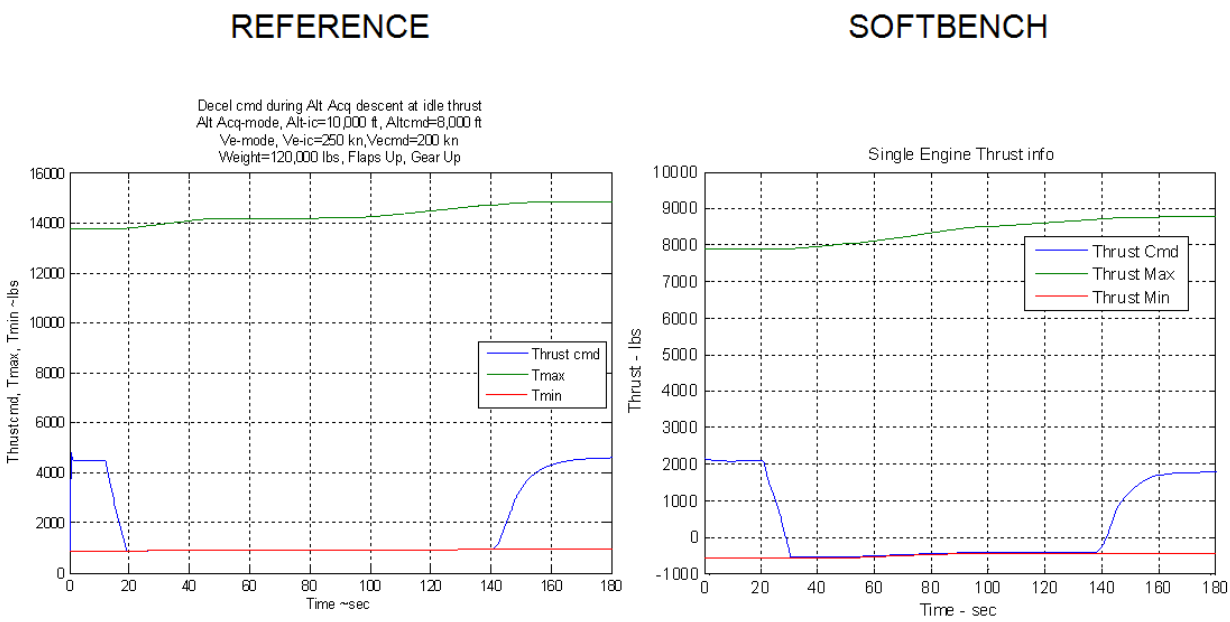

Figure C-31. Thrust Command, Thrust Minimum, and Thrust Maximum

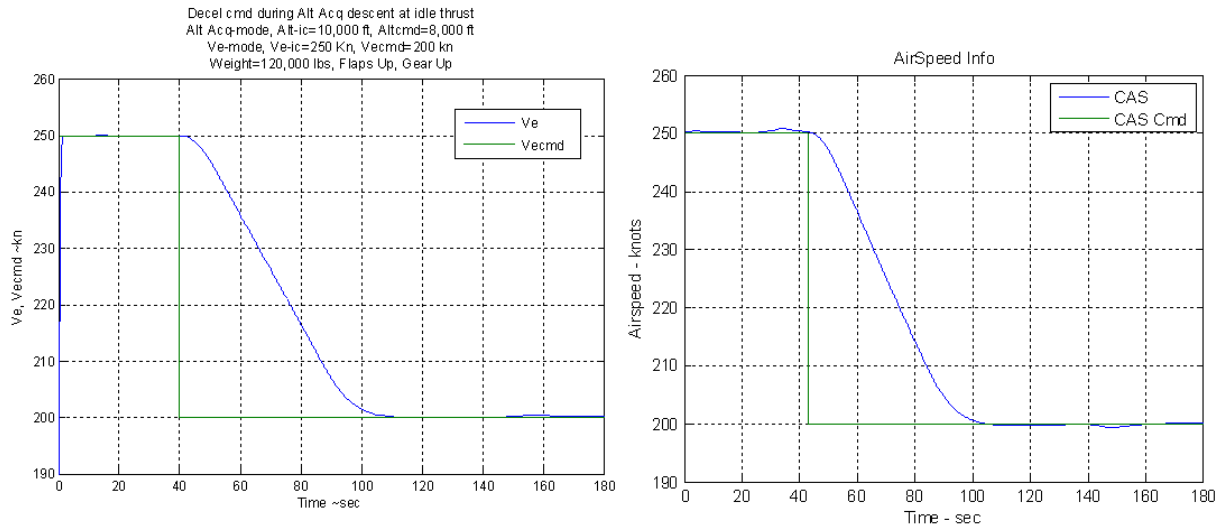

Figure C-32. Calibrated Airspeed Target and Calibrated Airspeed

C.9 Check Case 9.

Maintain altitude at 10,000 ft (ALT HOLD)
Reduce airspeed from 200 kt to 1.2 V_{stall}
Deploy Flaps

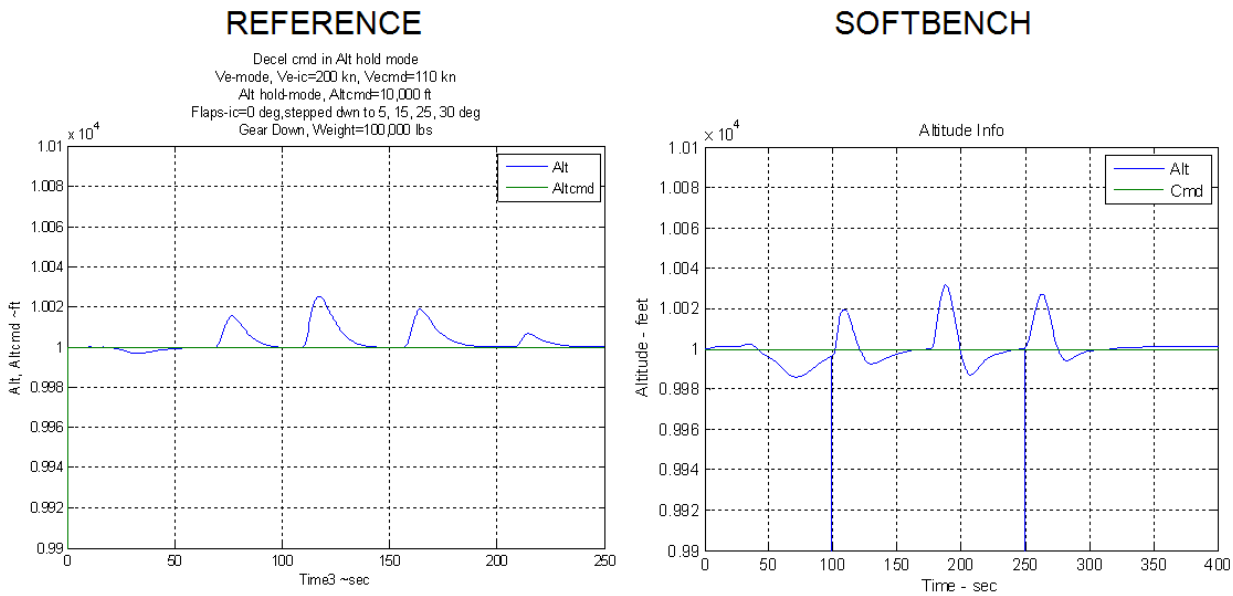

Figure C-33. Altitude Command and Altitude

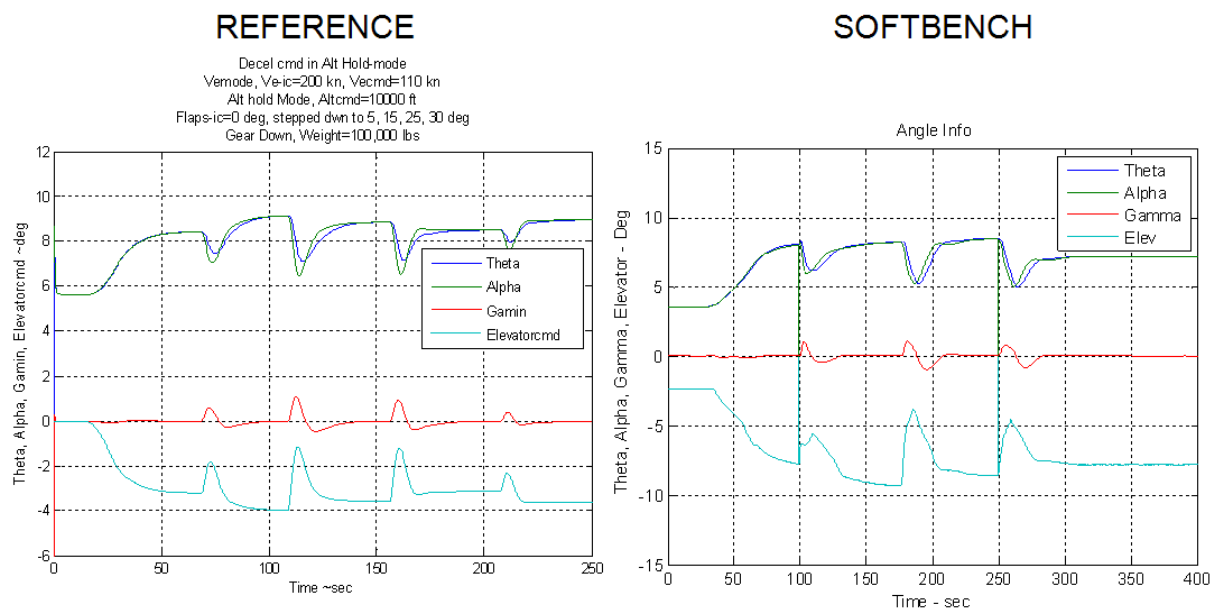

Figure C-34. Theta, Alpha, Gamma, and Elevator

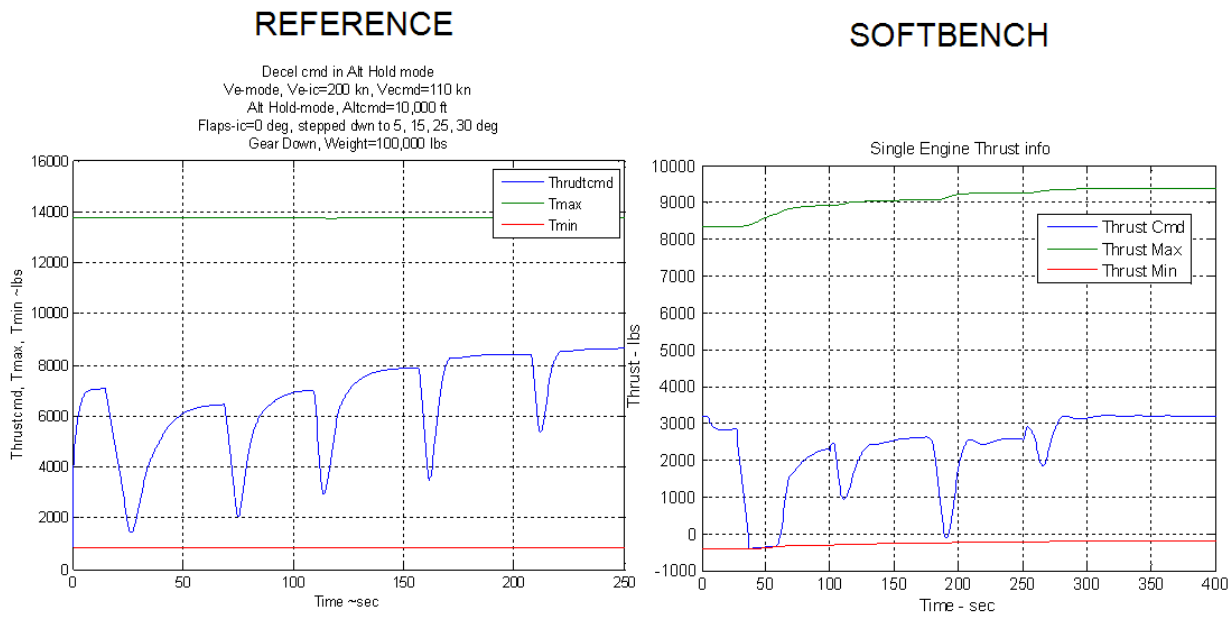

Figure C-35. Thrust Command, Thrust Minimum, and Thrust Maximum

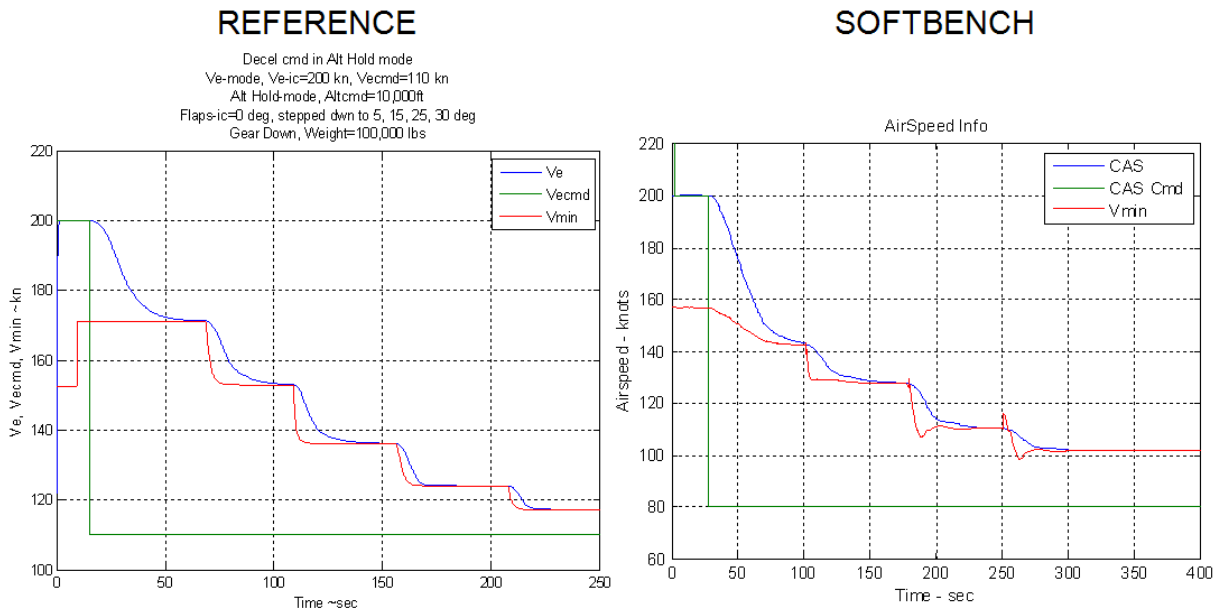

Figure C-36. Calibrated Airspeed Target and Calibrated Airspeed

C.10 Check Case 10.

Glide slope capture at 1500 ft (flaps deployed, gear down)
Descend to 500 ft, engage go around, climb to 3000 ft and capture altitude
Maintain airspeed at 127 kt

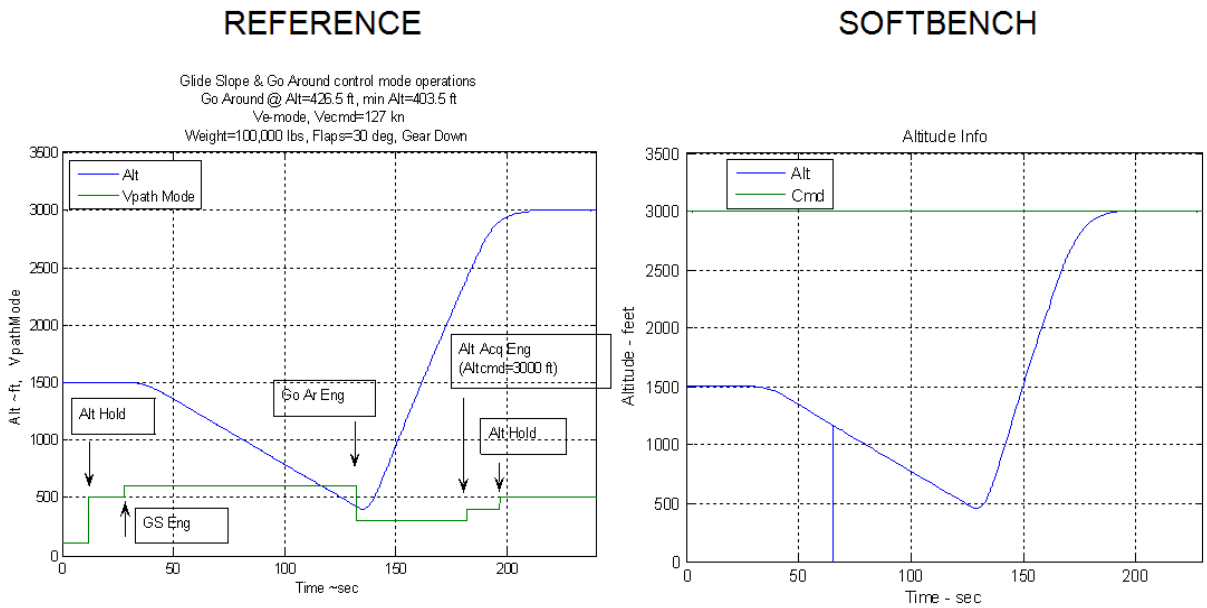

Figure C-37. Altitude Command and Altitude

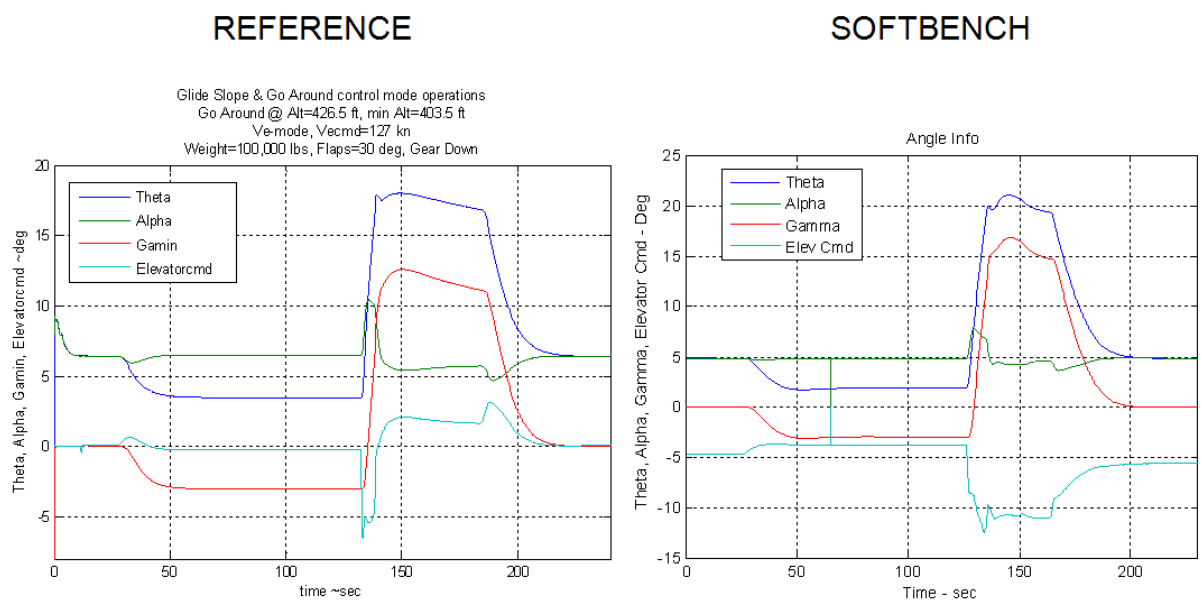

Figure C-38. Theta, Alpha, Gamma, and Elevator

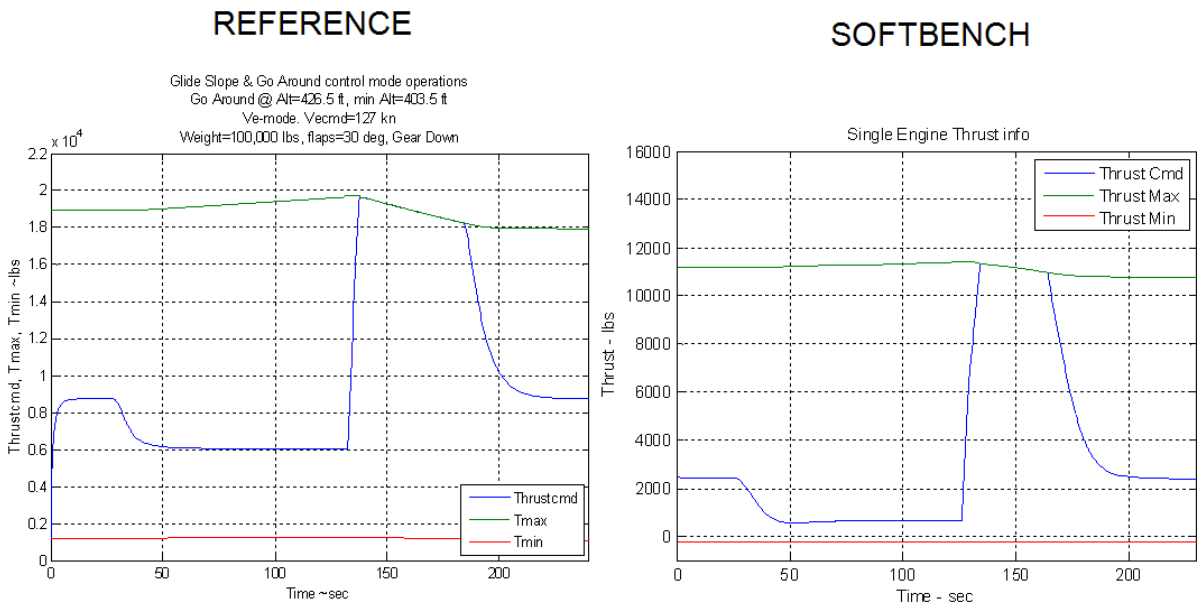

Figure C-39. Thrust Command, Thrust Minimum, and Thrust Maximum

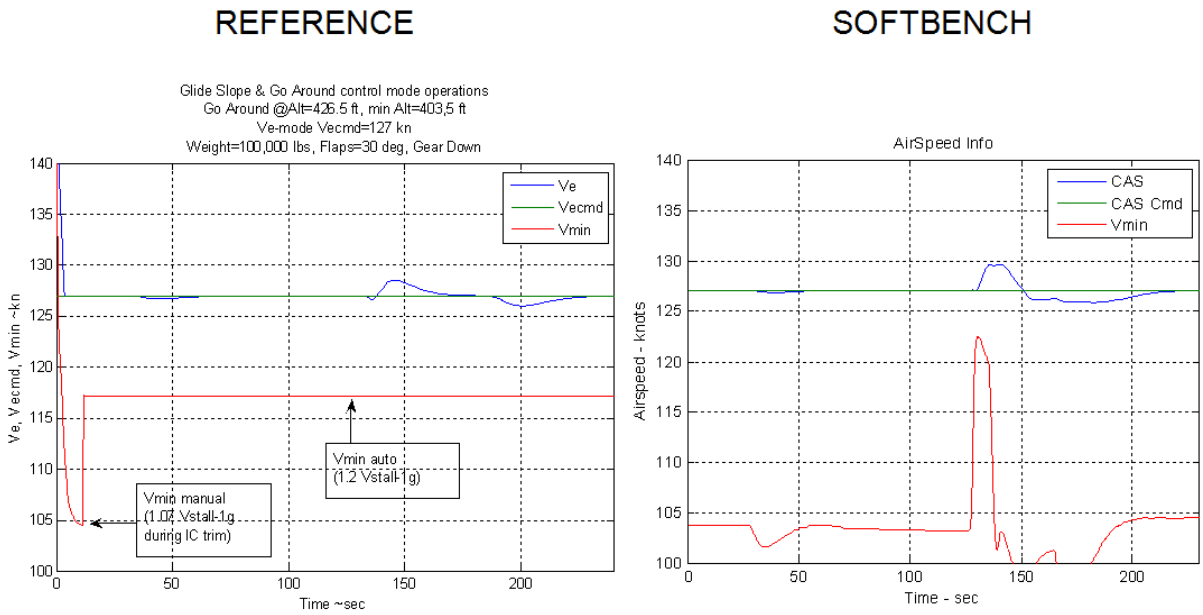

Figure C-40. Calibrated Speed Target and Calibrated Speed

C.11 Check Case 11.

Descend at -3° flight path starting from 10,000 ft (FPA Mode)
After 30 seconds, climb at +3° to 11,000 ft and capture altitude
Maintain airspeed at 200 kt during maneuvers

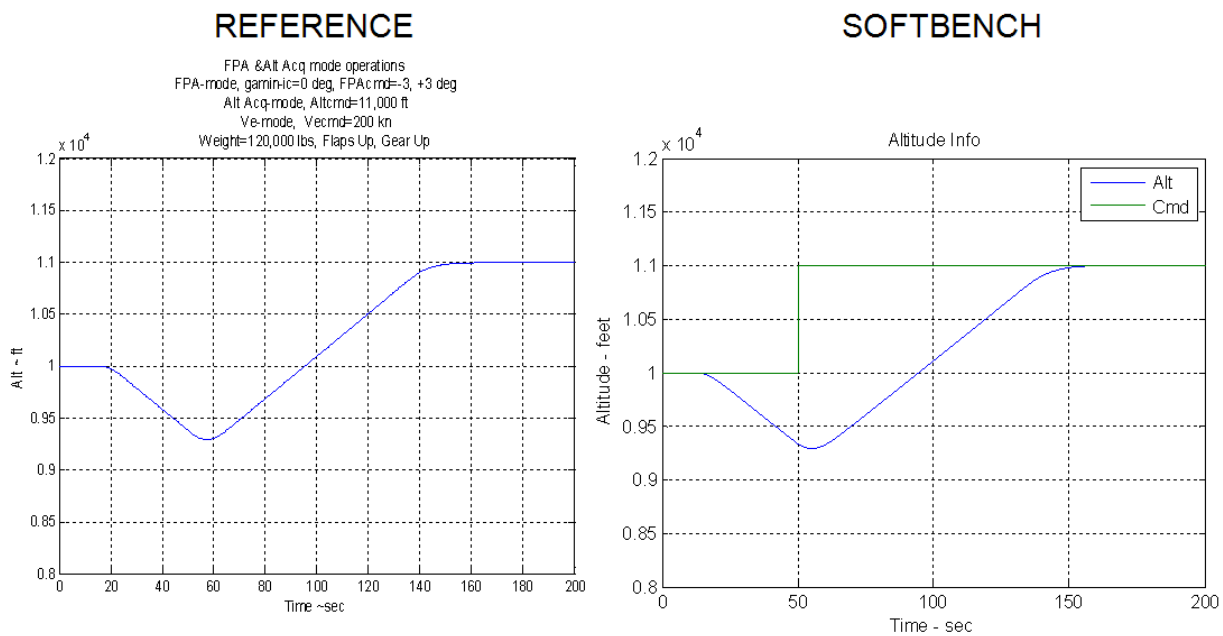

Figure C-41. Altitude Command and Altitude

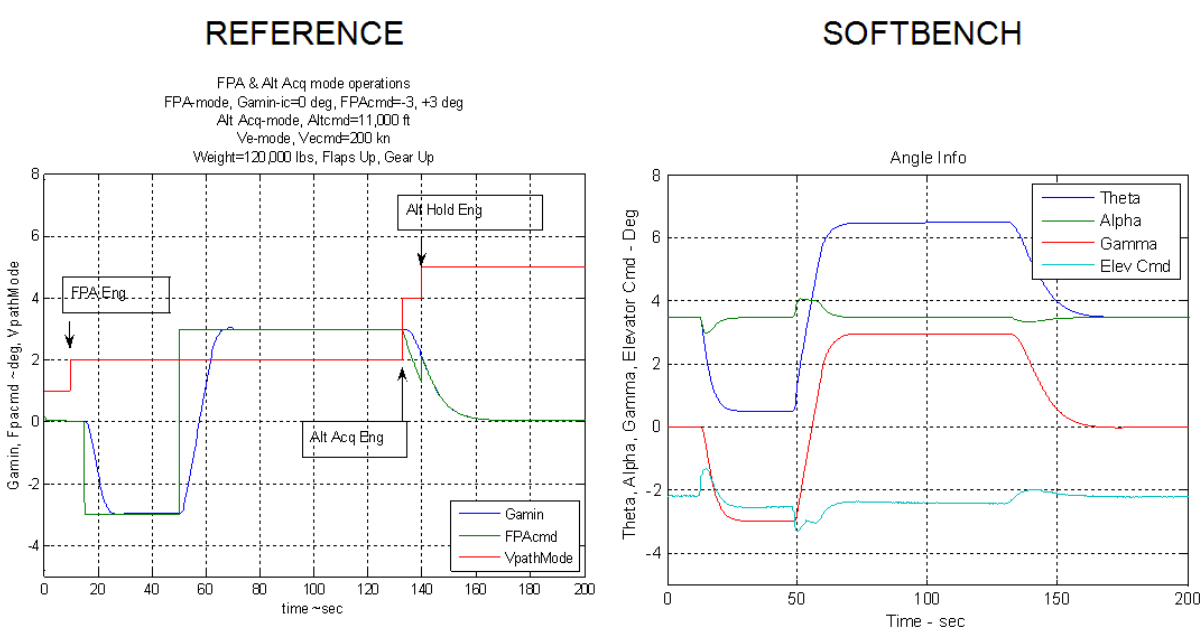

Figure C-42. Theta, Alpha, Gamma, and Elevator

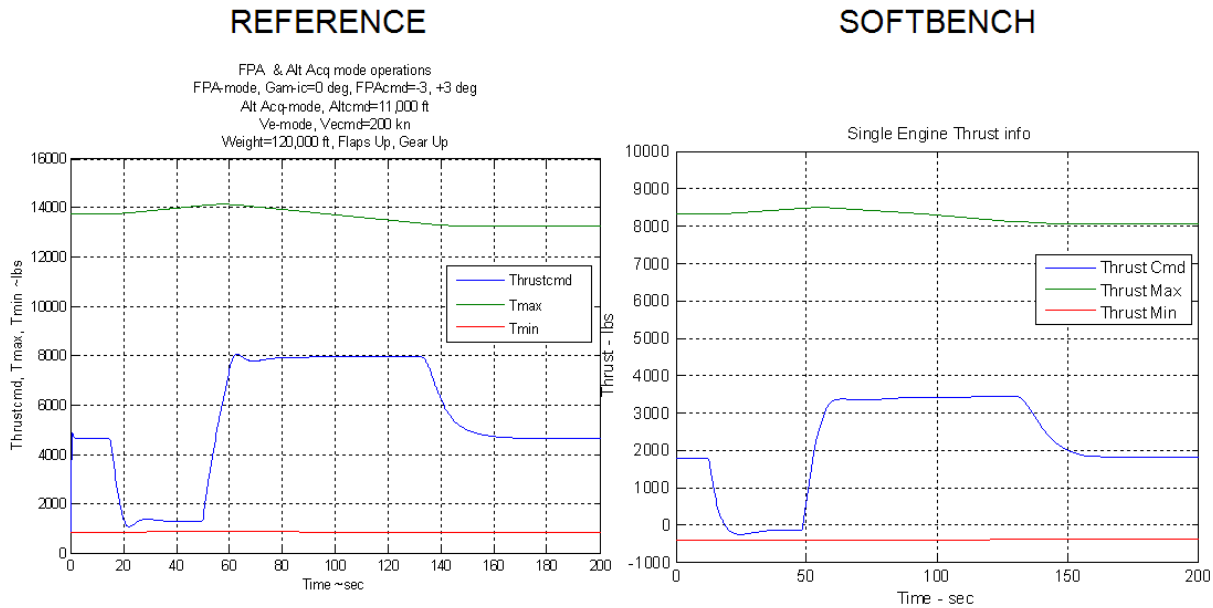

Figure C-43. Thrust Command, Thrust Minimum, and Thrust Maximum

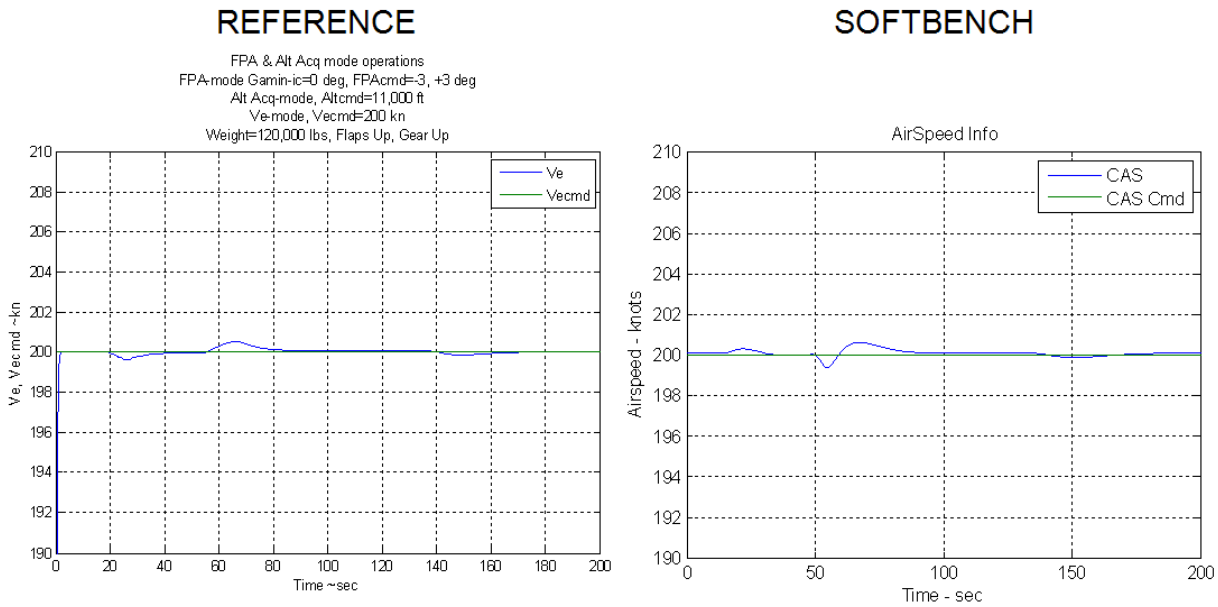

Figure C-44. Calibrated Airspeed Target and Calibrated Airspeed

C.12 Check Case 12.

Horizontal wind shear of 2000 ft/sec
Altitude Hold at 2000 ft
Maintain airspeed at 127 kt
Flaps deployed, gear down

REFERENCE

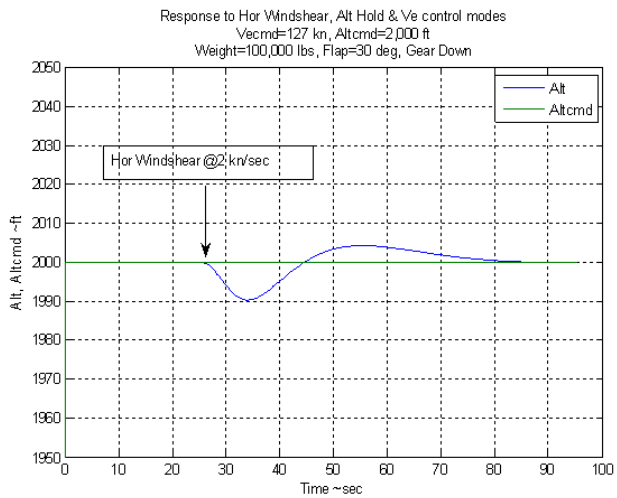

SOFTBENCH

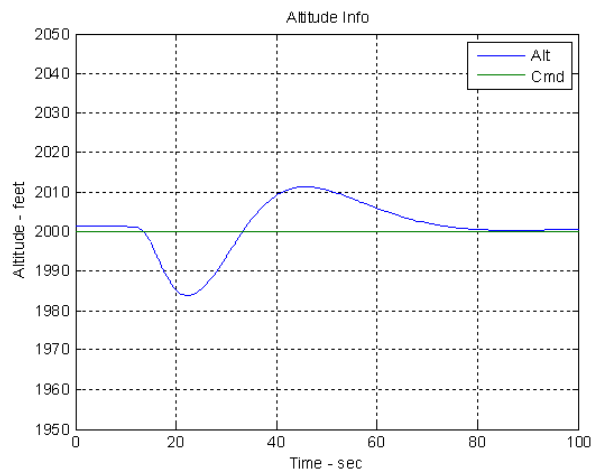

Figure C-45. Altitude Command and Altitude

REFERENCE

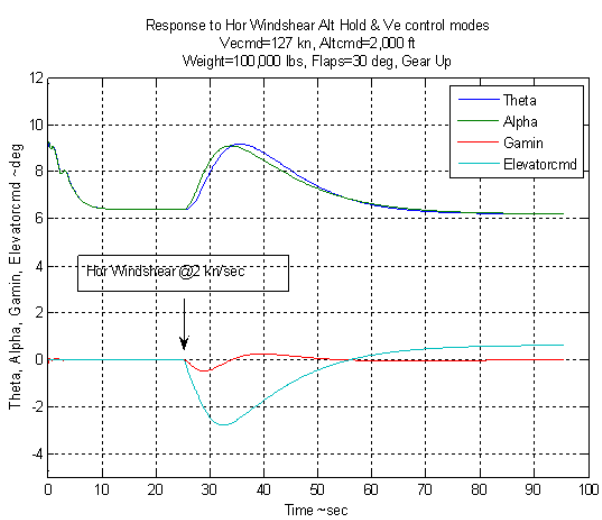

SOFTBENCH

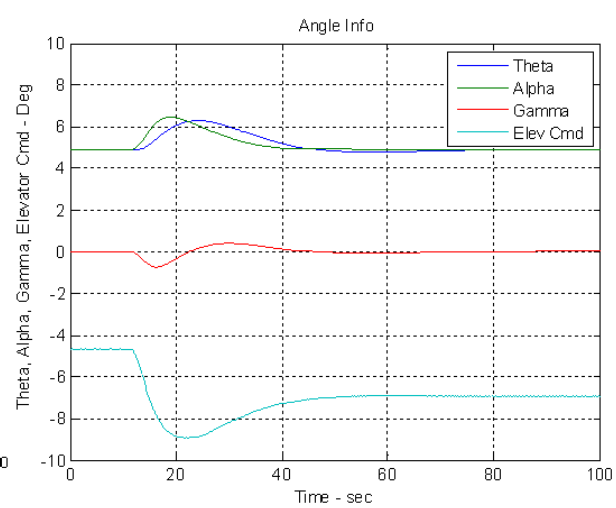

Figure C-46. Theta, Alpha, Gamma, and Elevator

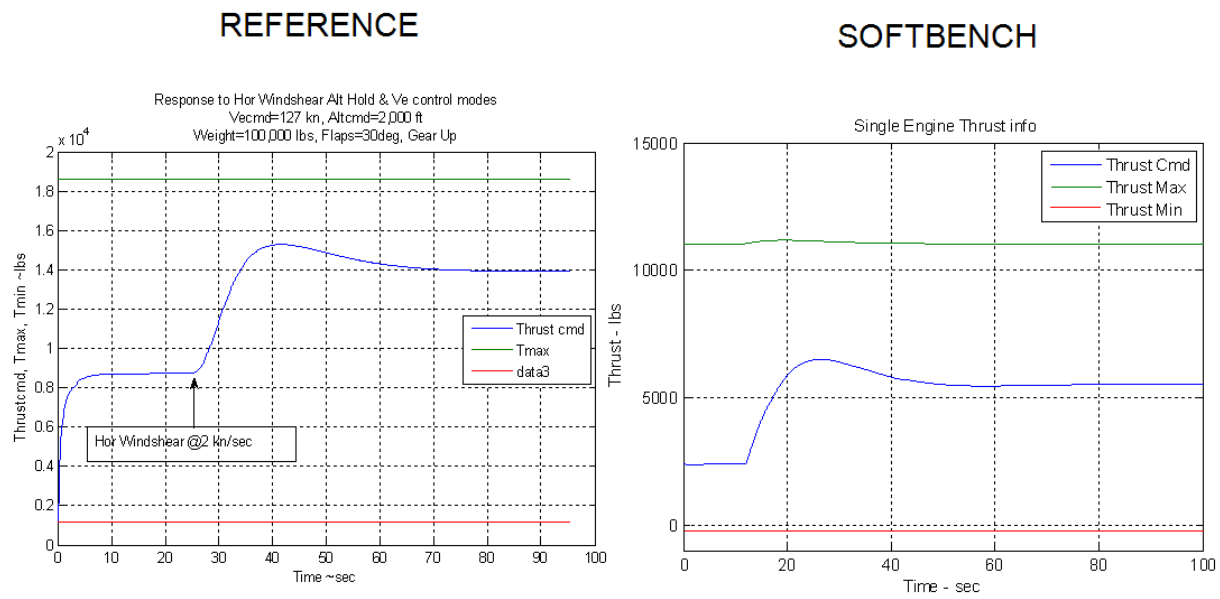

Figure C-47. Thrust Command, Thrust Minimum, and Thrust Maximum

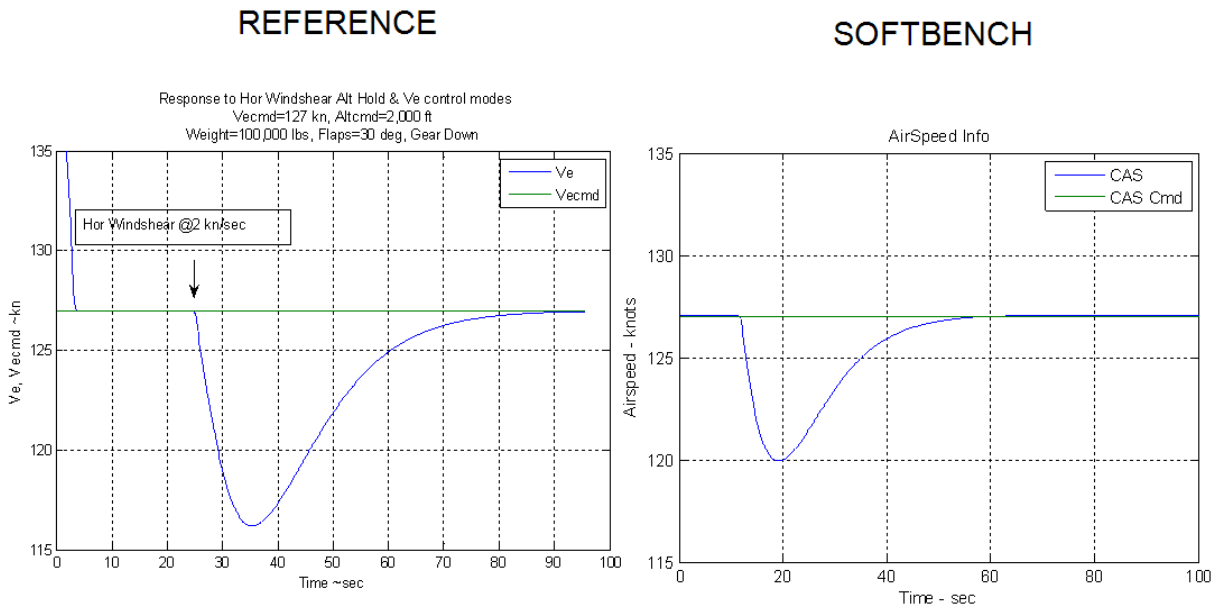

Figure C-48. Calibrated Airspeed Target and Calibrated Airspeed

C.13 Check Case 13.

Turbulence—5 ft/sec root mean square (RMS) (U axis only for reference, 3 axes on SoftBench)
Altitude hold at 2000 ft
Maintain airspeed at 127 kt
Flaps deployed

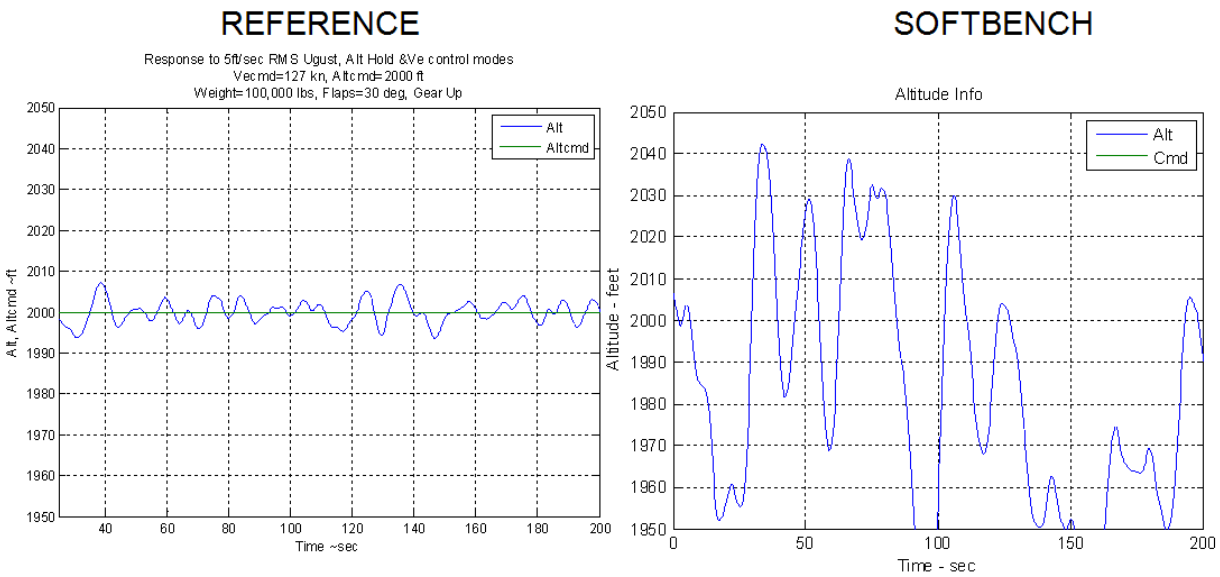

Figure C-49. Altitude Command and Altitude

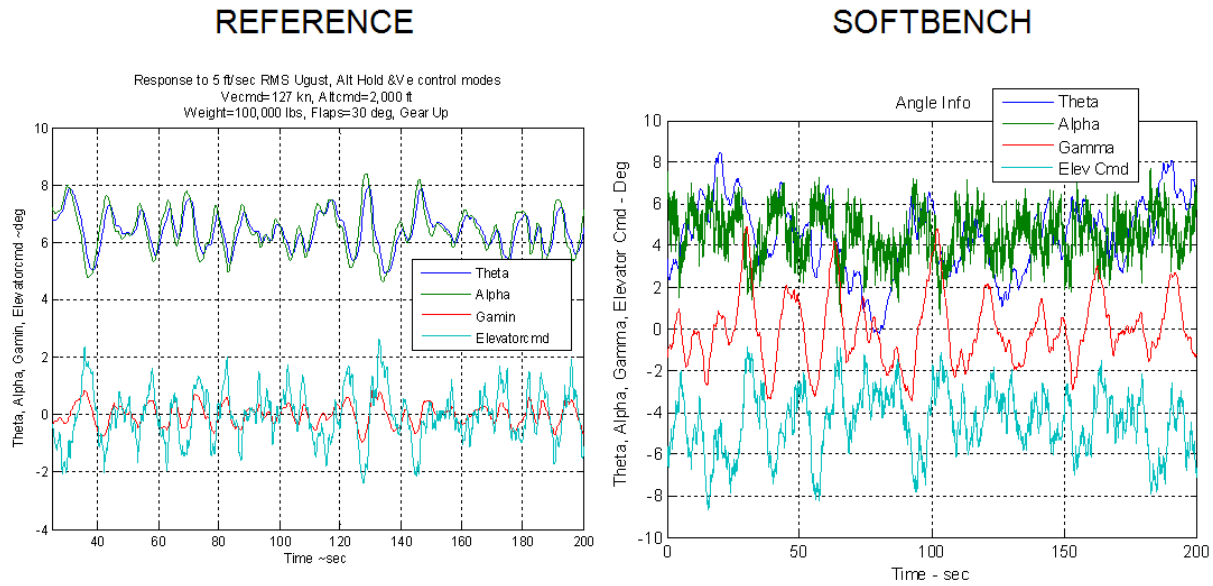

Figure C-50. Theta, Alpha, Gamma, and Elevator

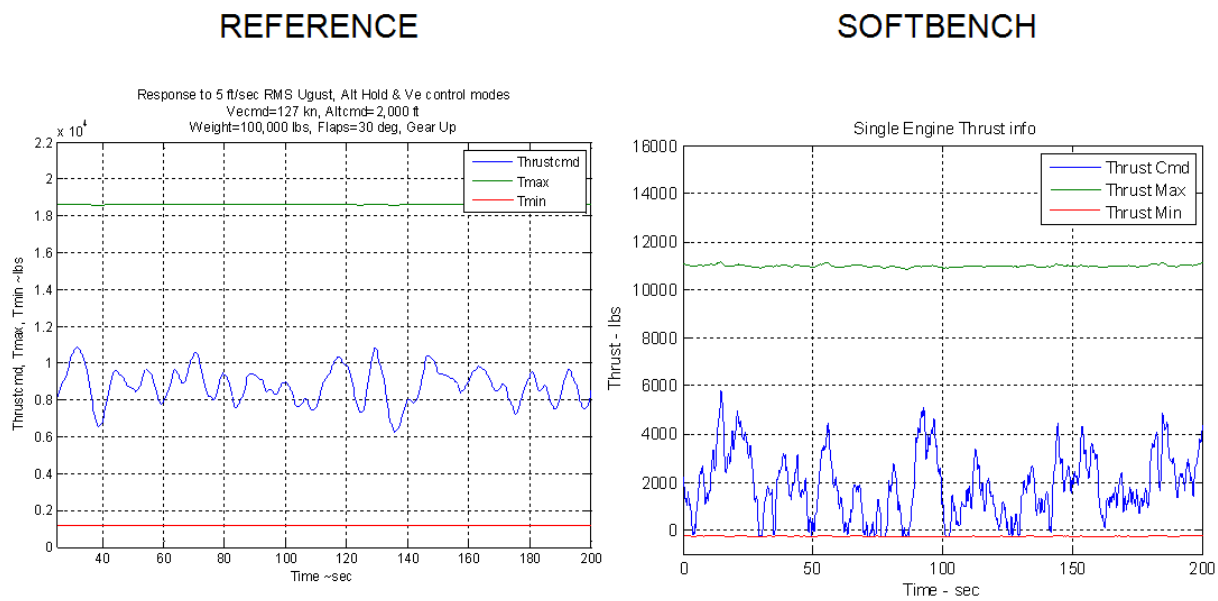

Figure C-51. Thrust Command, Thrust Minimum, and Thrust Maximum

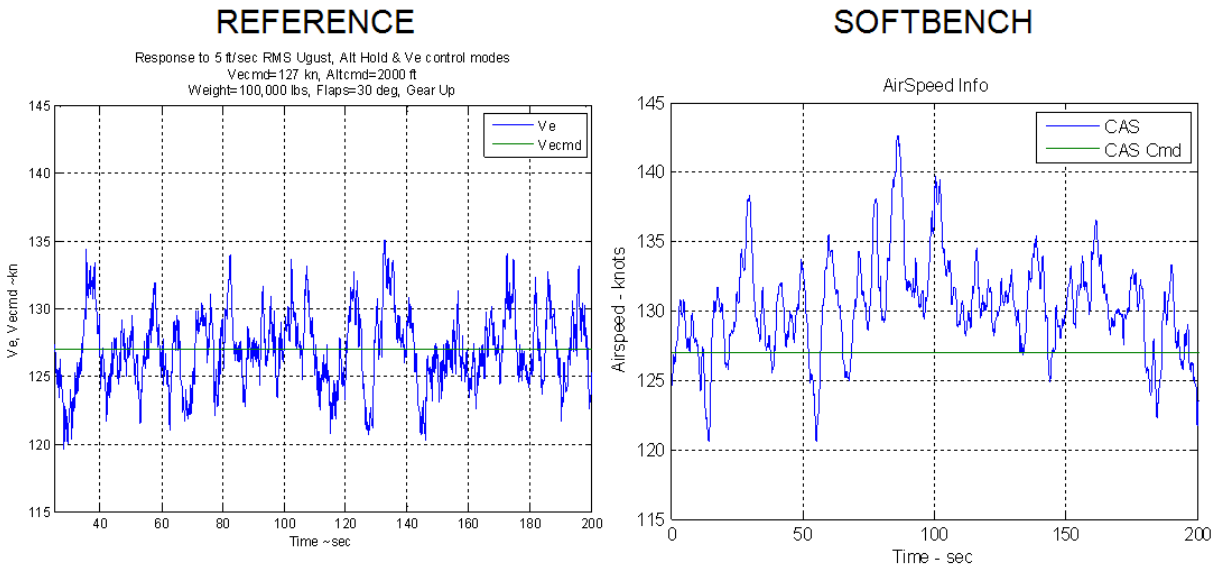

Figure C-52. Calibrated Airspeed Target and Calibrated Airspeed

C.14 Check Case 20—Lateral Axis Heading Select Mode.

Heading change (90°) in 20-kt crosswind
Maintain altitude at 10,000 ft and airspeed at 250 kt

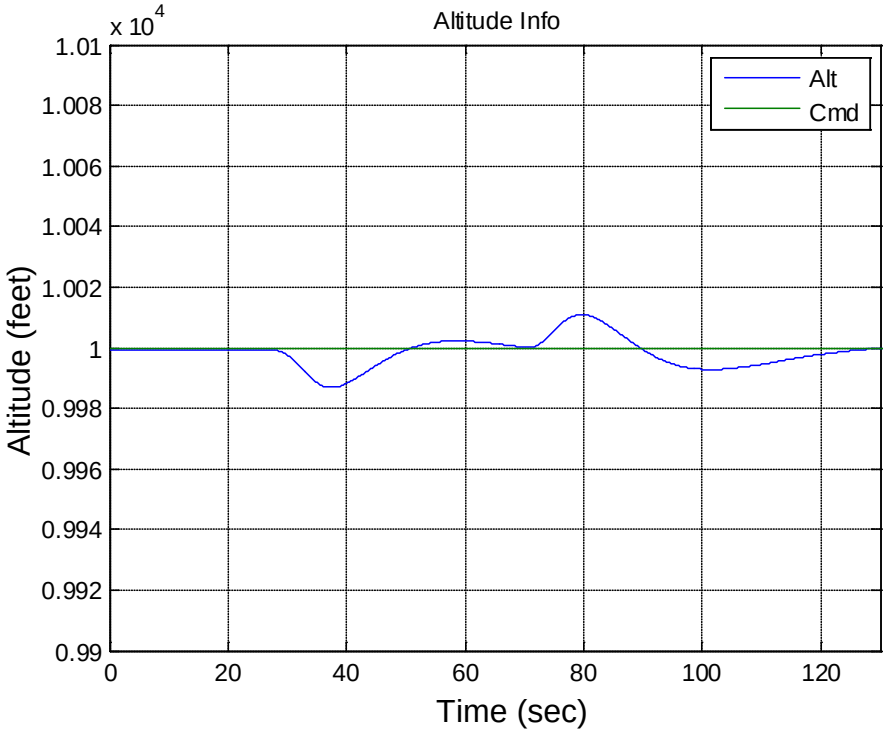

Figure C-53. Altitude Command and Altitude

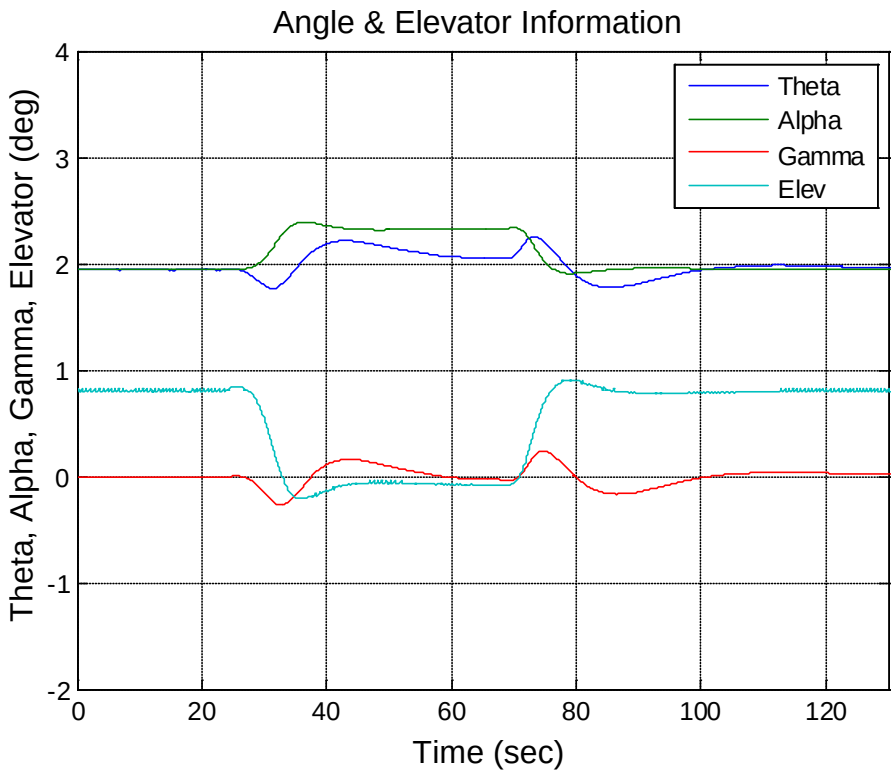

Figure C-54. Theta, Alpha, Gamma, and Elevator

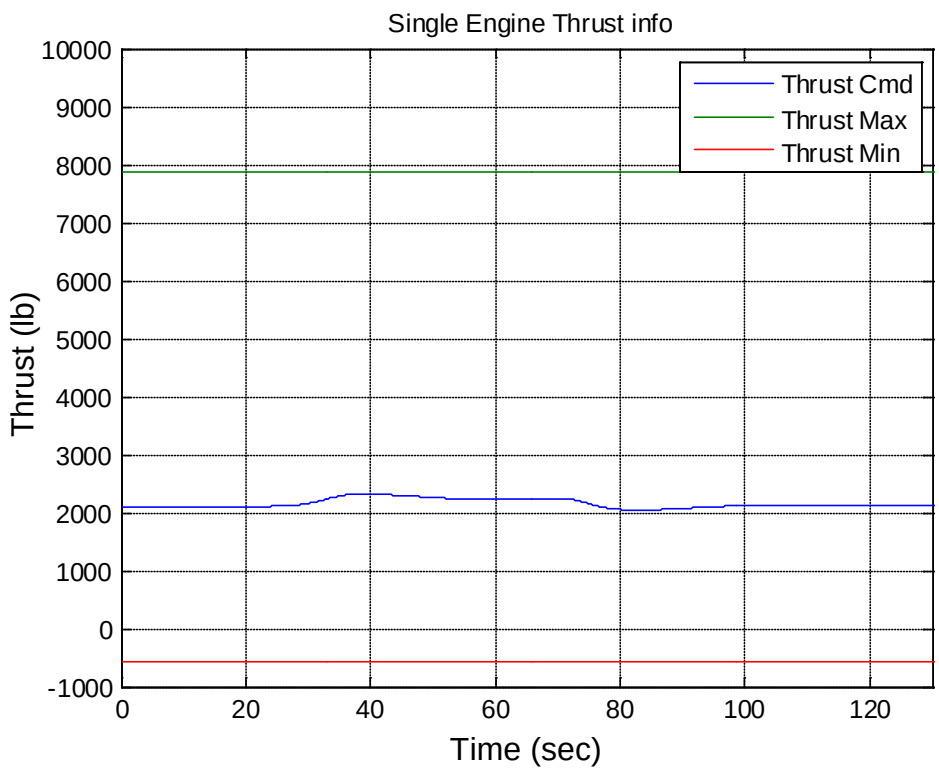

Figure C-55. Thrust Command, Thrust Minimum, and Thrust Maximum

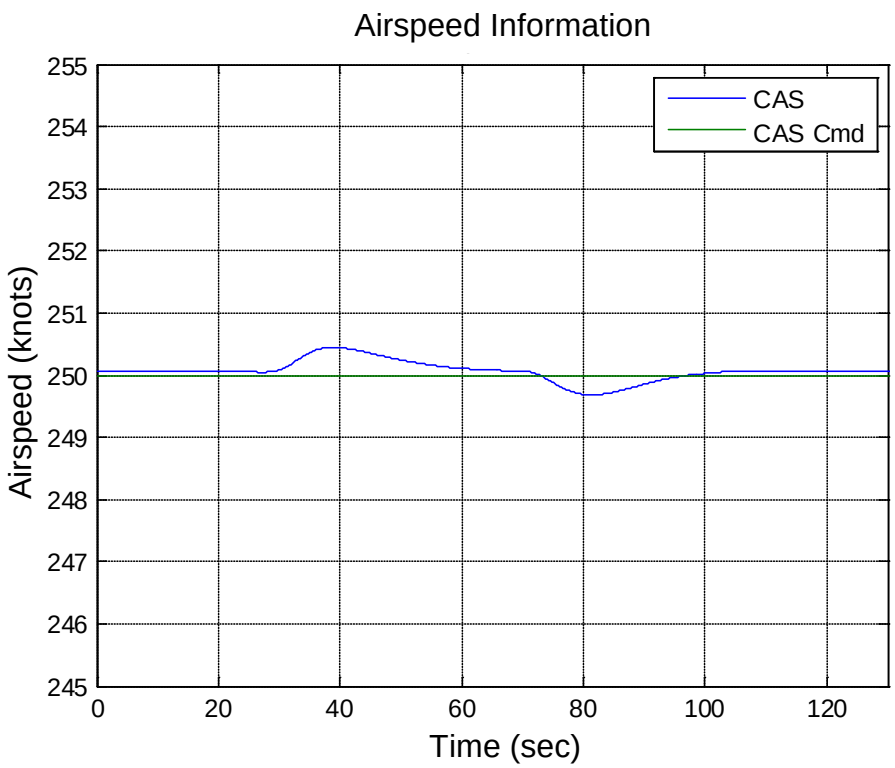

Figure C-56. Calibrated Airspeed Target and Calibrated Airspeed

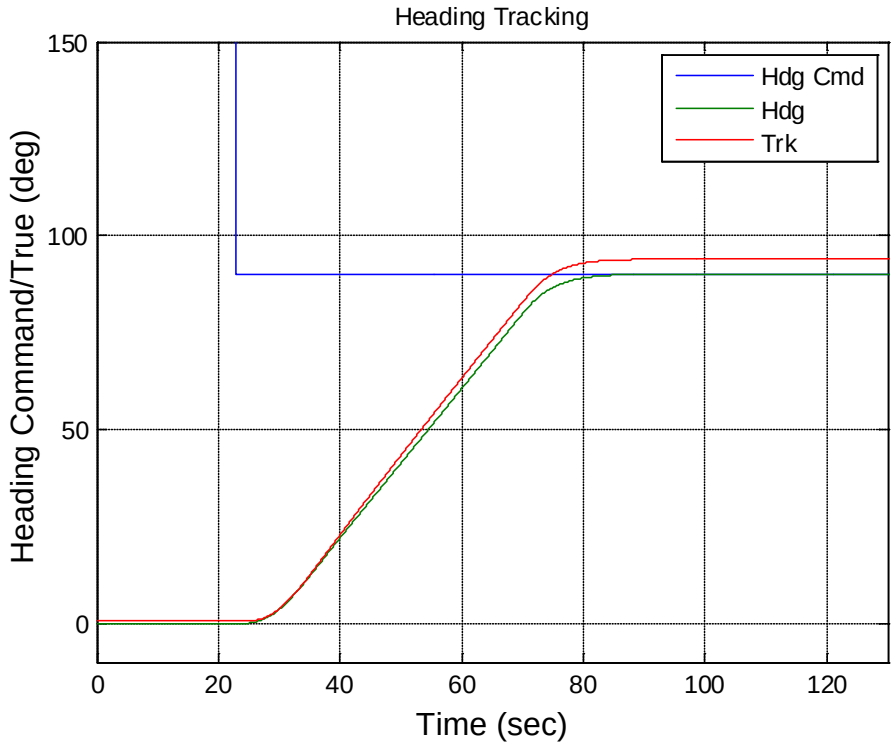

Figure C-57. Heading Target, Heading, and Ground Track

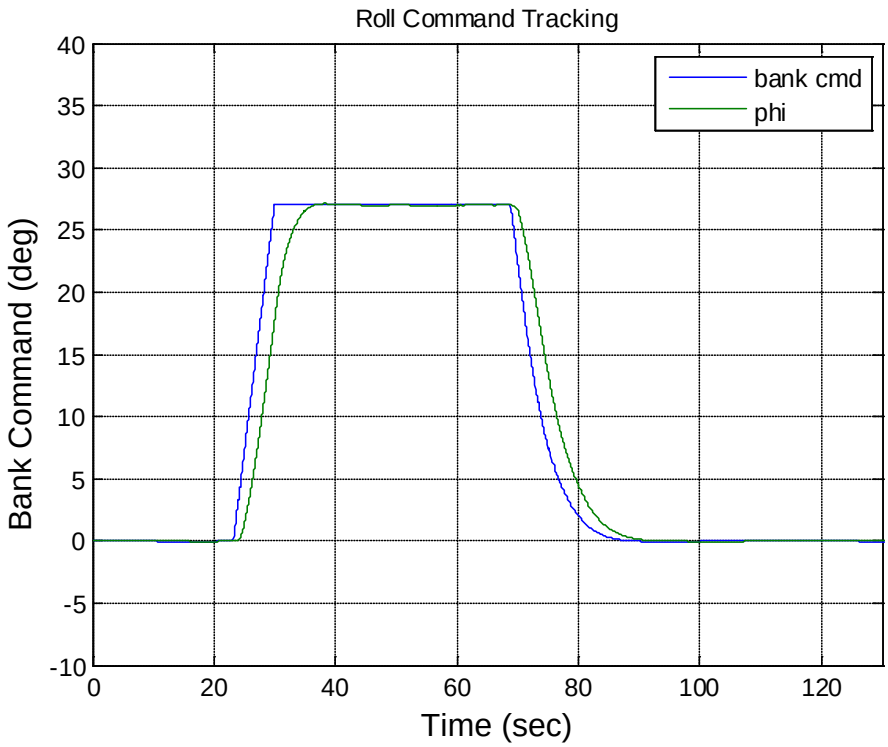

Figure C-58. Bank Command and Bank

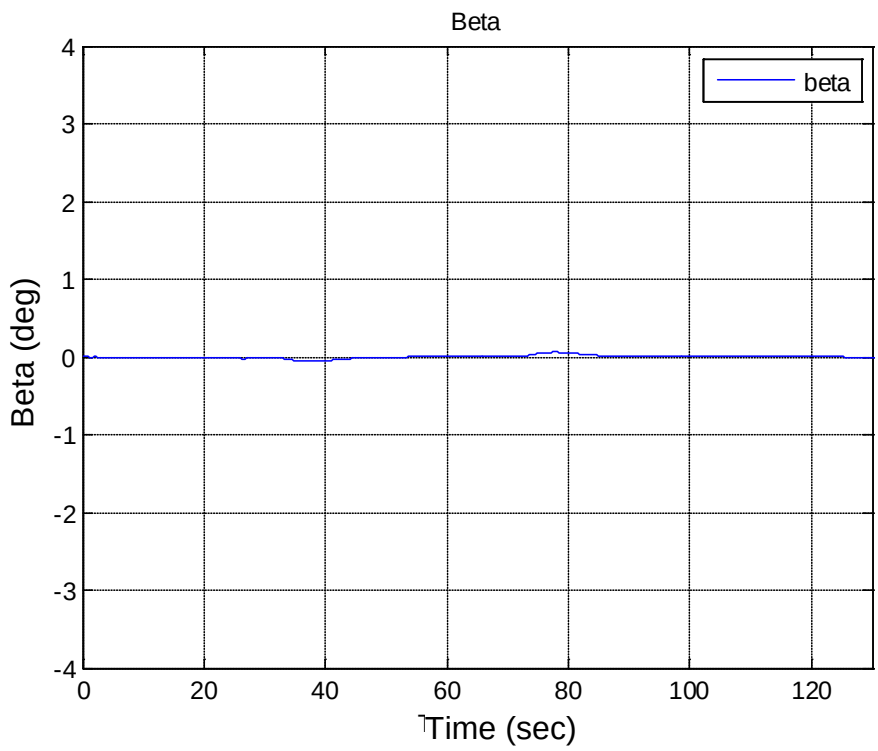

Figure C-59. Beta

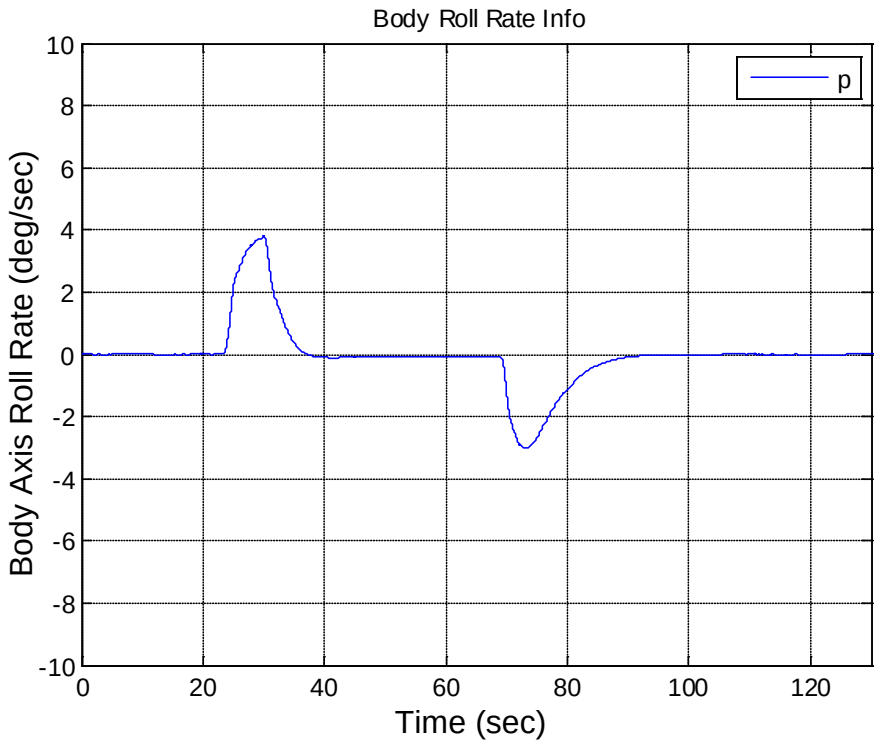

Figure C-60. Roll Rate

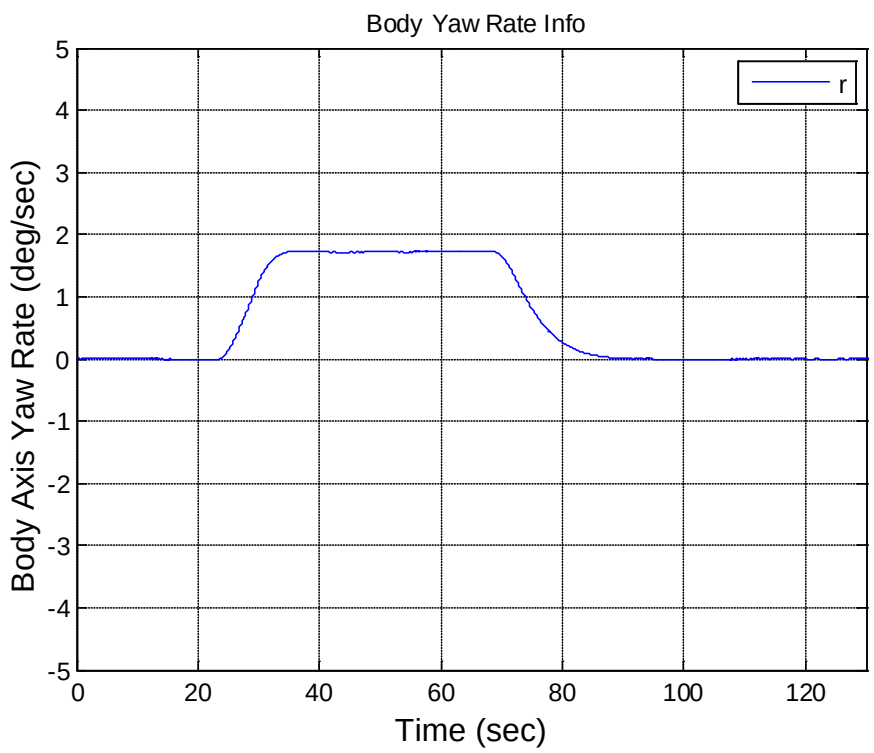

Figure C-61. Yaw Rate

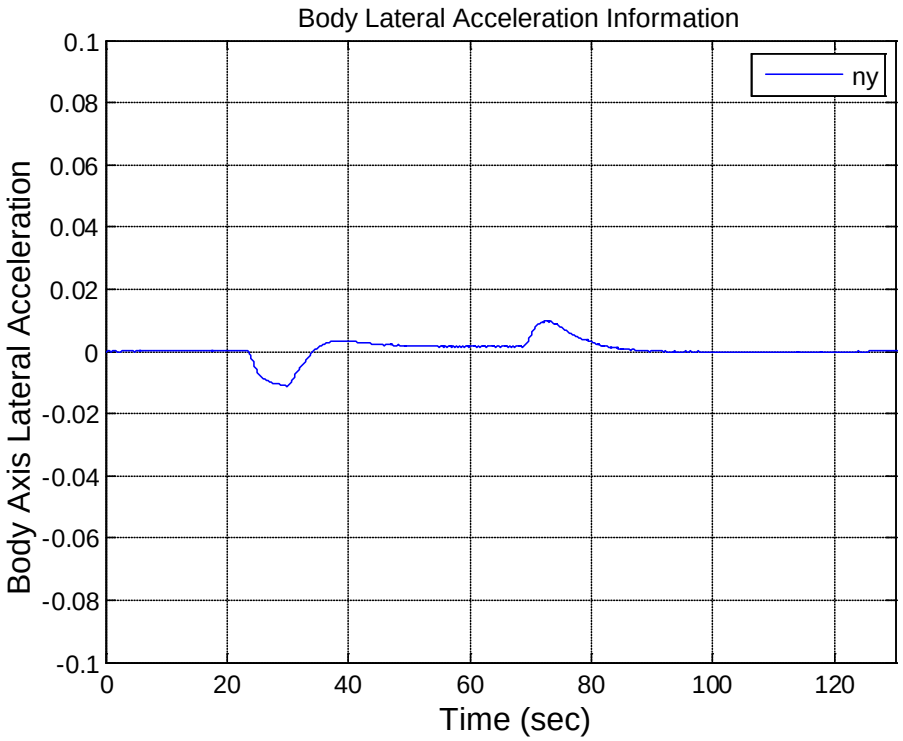

Figure C-62. Lateral Acceleration

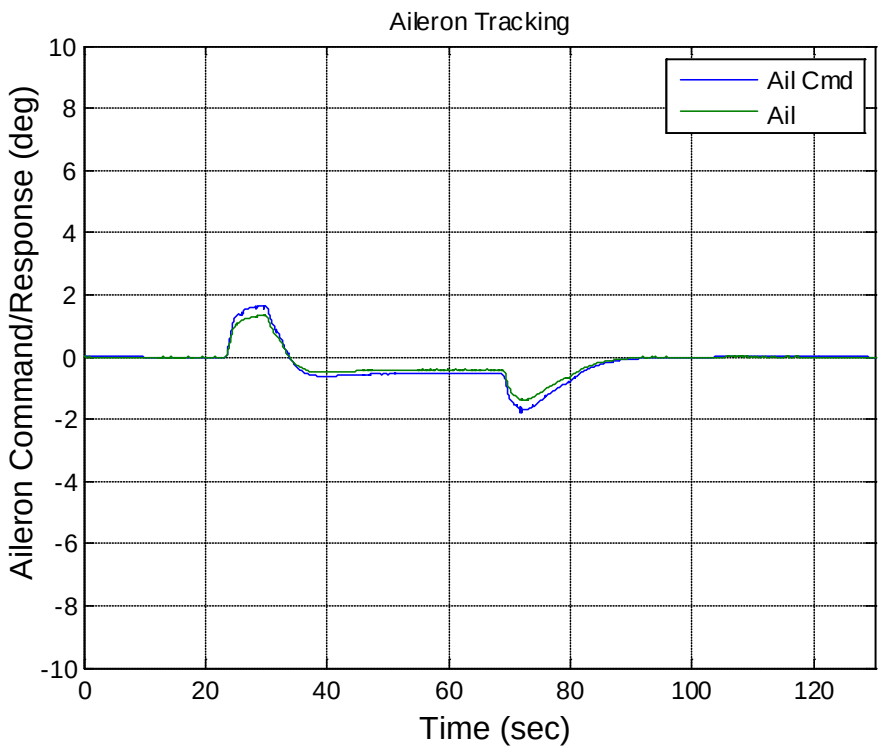

Figure C-63. Aileron Command and Aileron

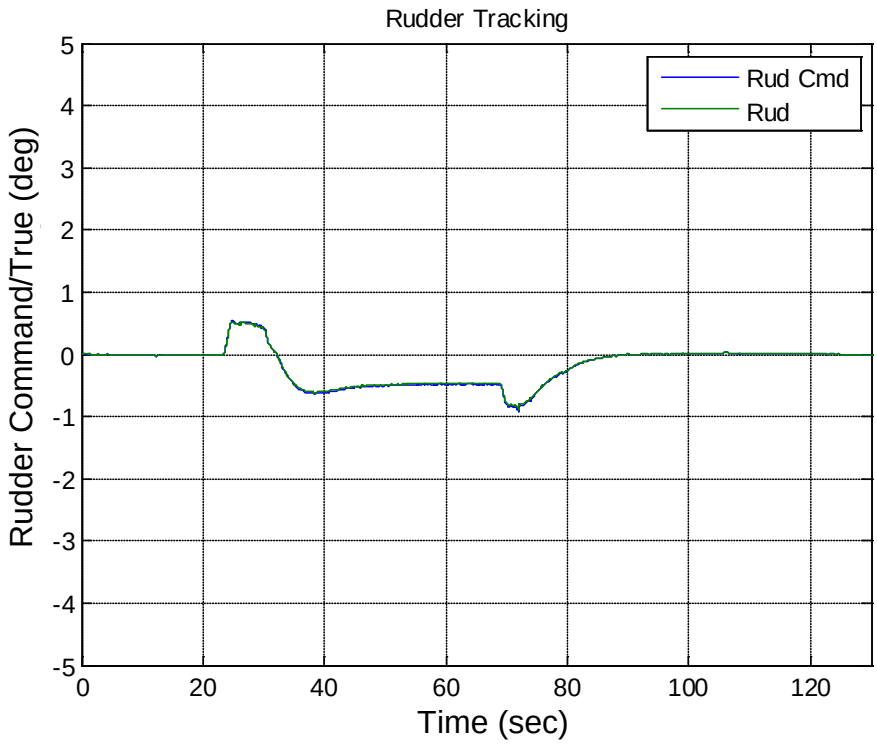

Figure C-64. Rudder Command and Rudder

C.15 Check Case 21—Lateral Axis Ground Track Select Mode.

Ground track change (90°) in 20-kt crosswind
Maintain altitude at 10,000 ft and airspeed at 250 kt

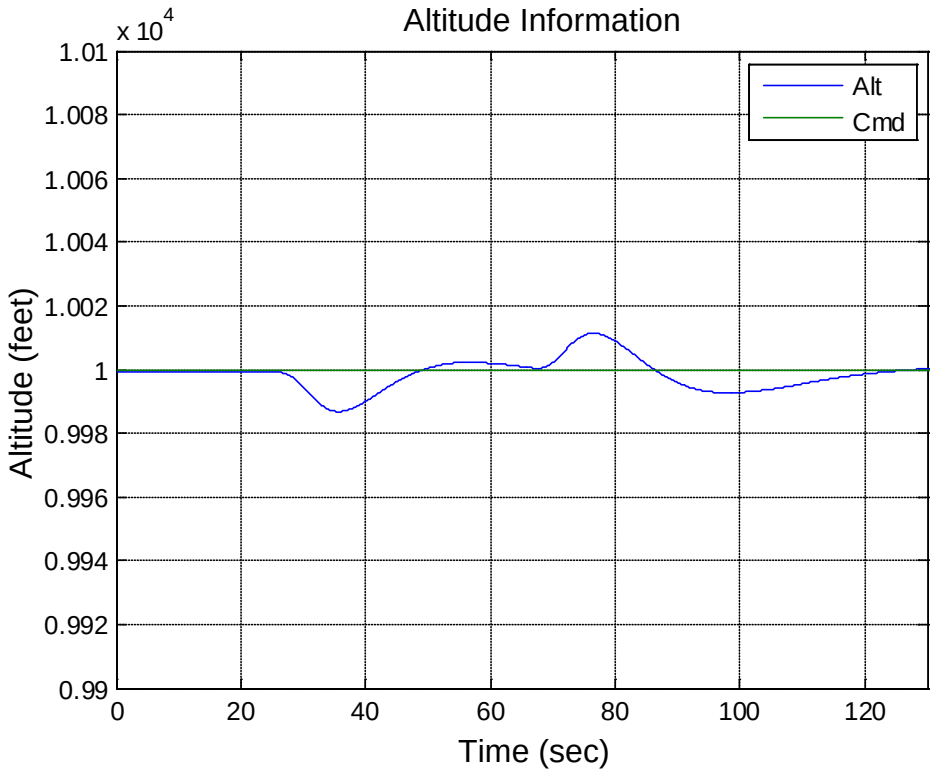

Figure C-65. Altitude Command and Altitude

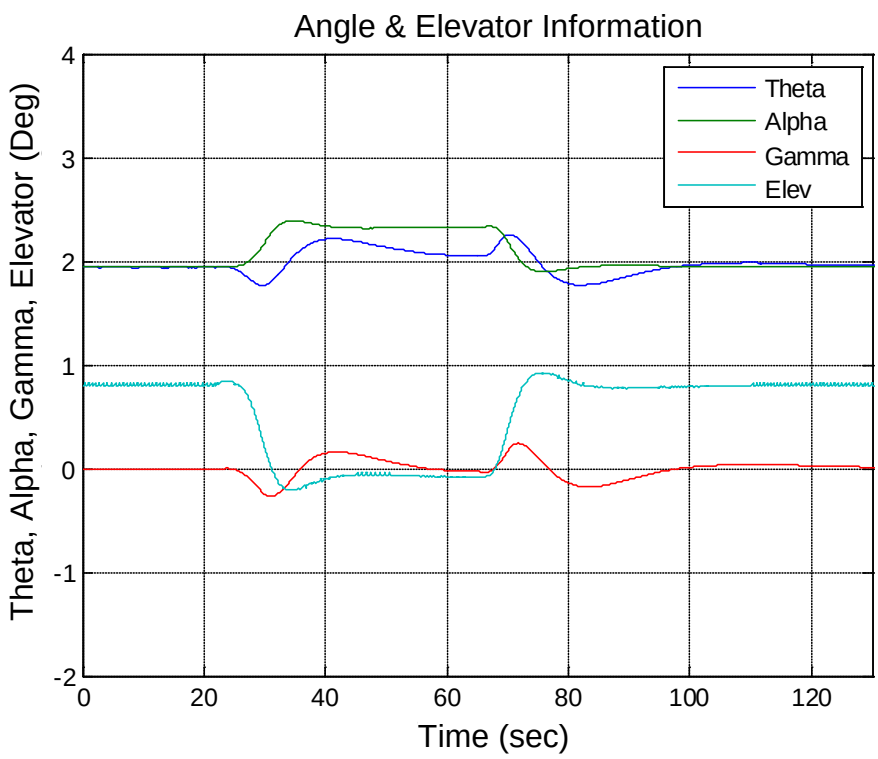

Figure C-66. Theta, Alpha, Gamma, and Elevator

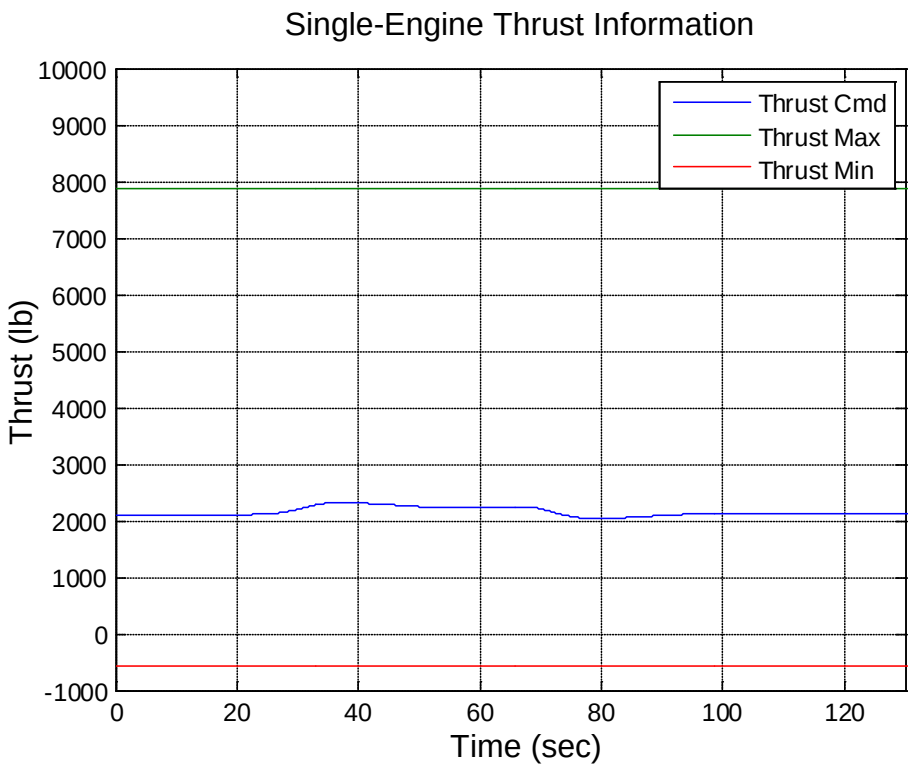

Figure C-67. Thrust Command, Thrust Minimum, and Thrust Maximum

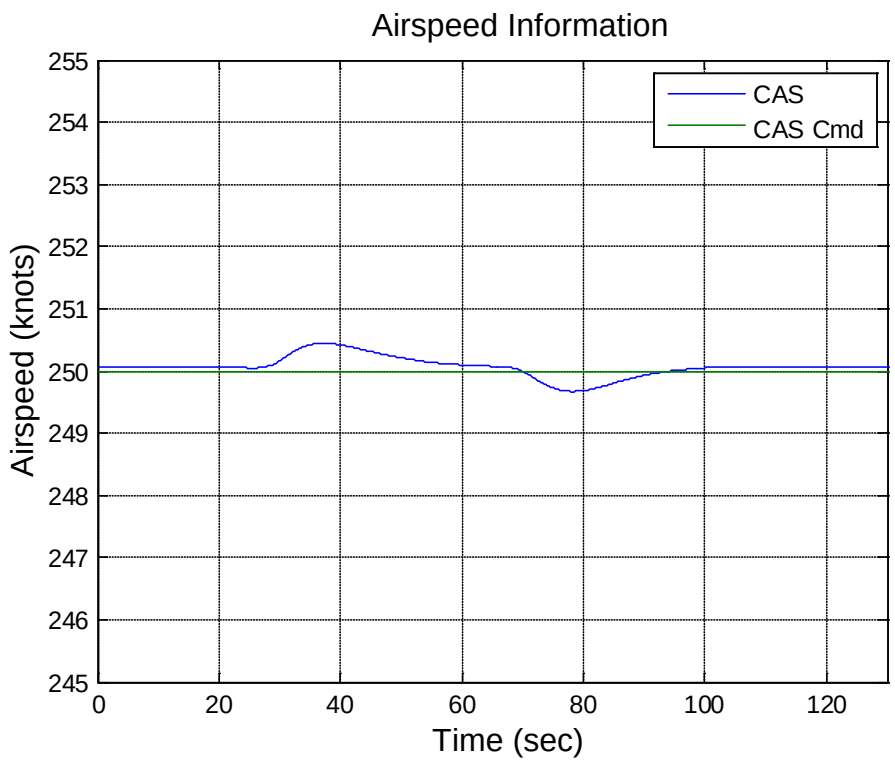

Figure C-68. Calibrated Airspeed Target and Calibrated Airspeed

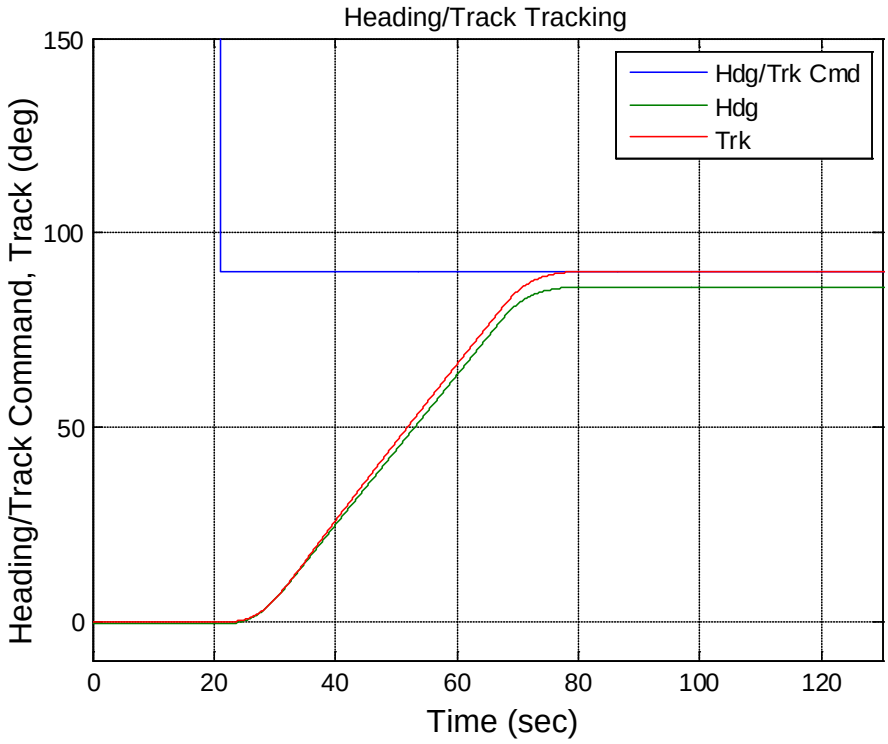

Figure C-69. Track Angle Target, Heading, and Ground Track

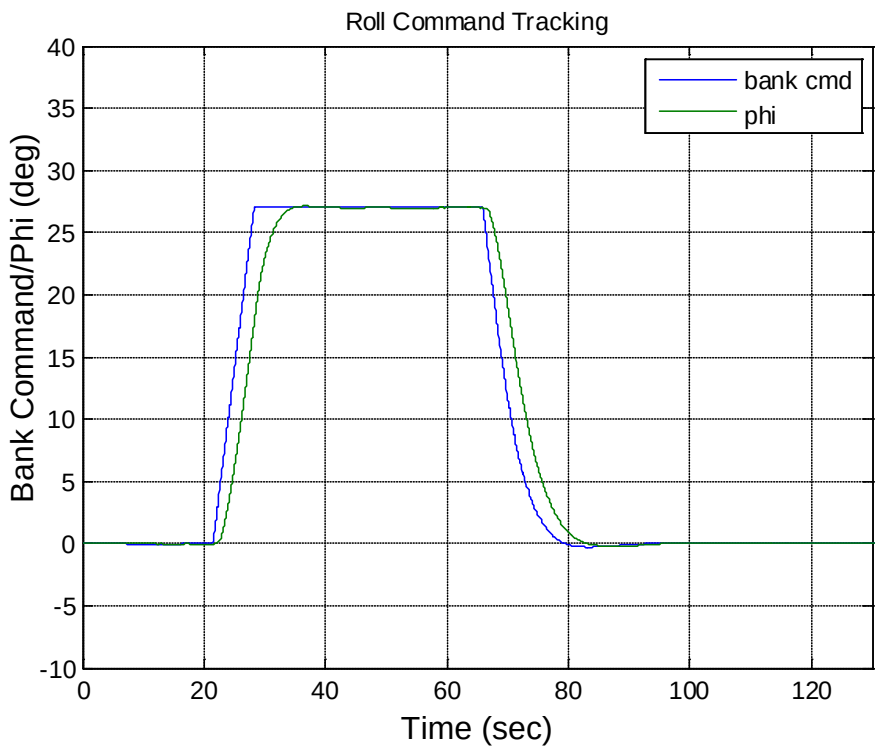

Figure C-70. Bank Command and Bank

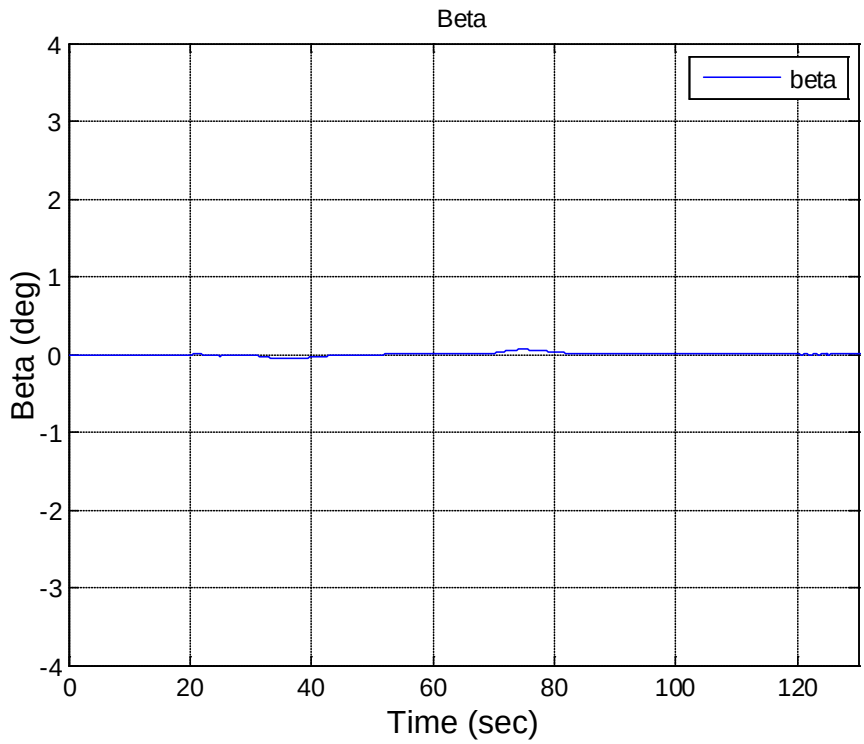

Figure C-71. Beta

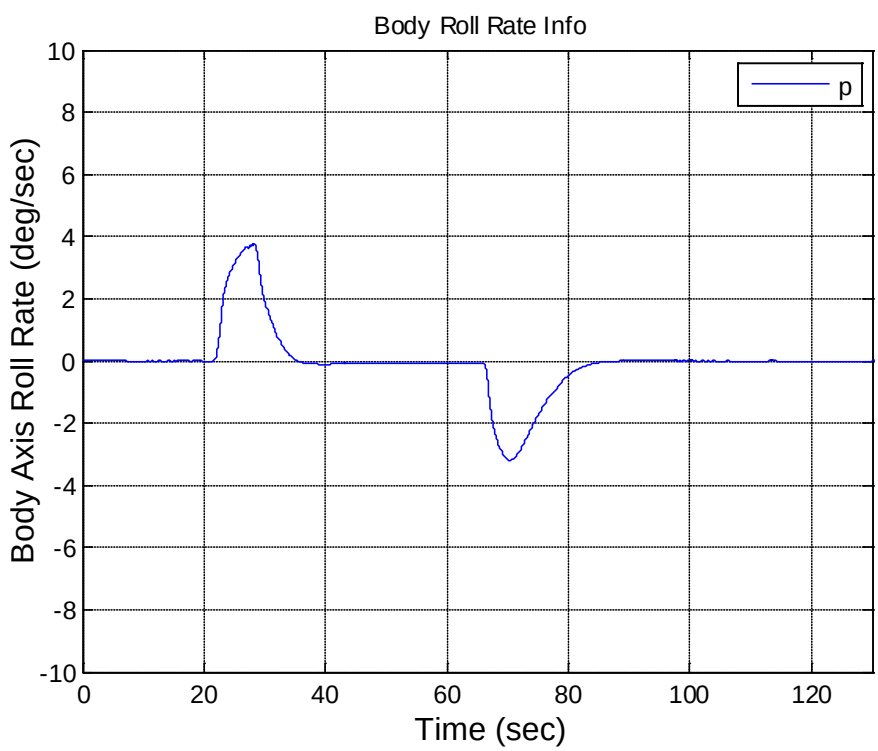

Figure C-72. Roll Rate

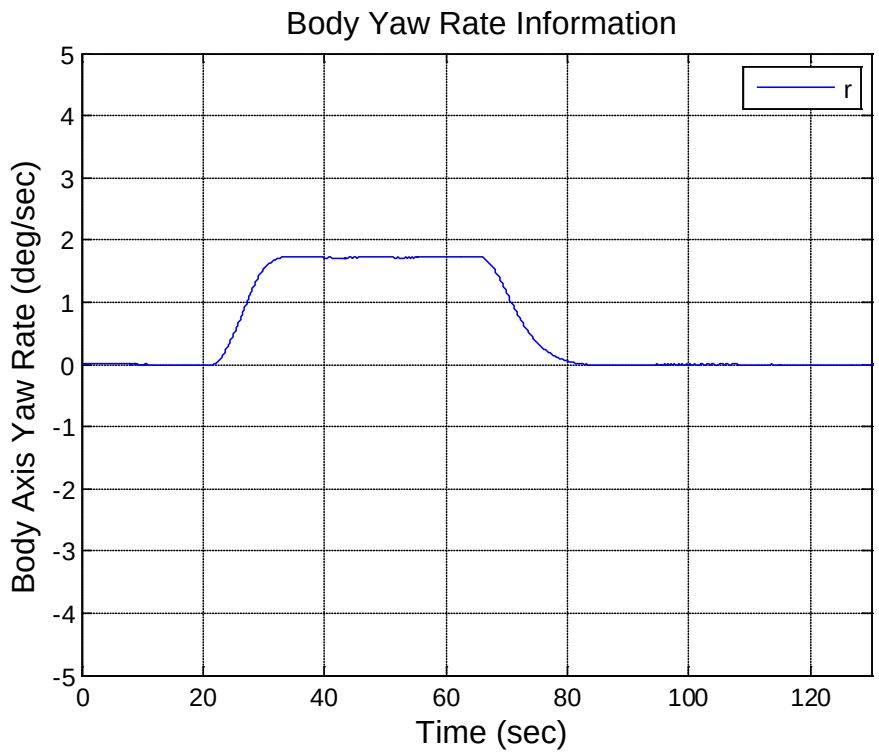

Figure C-73. Yaw Rate

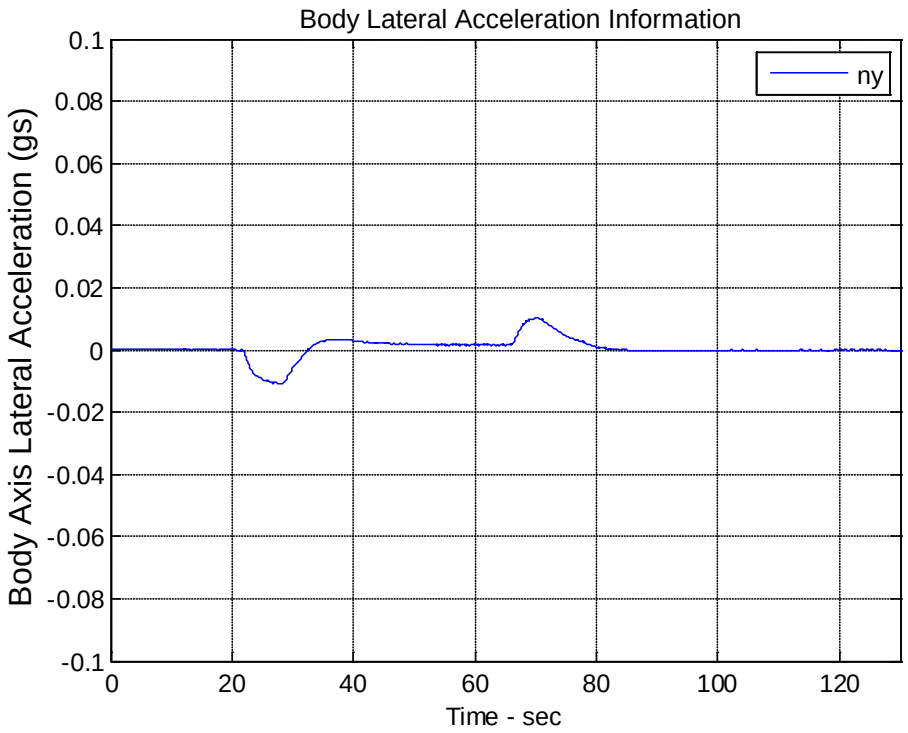

Figure C-74. Lateral Acceleration

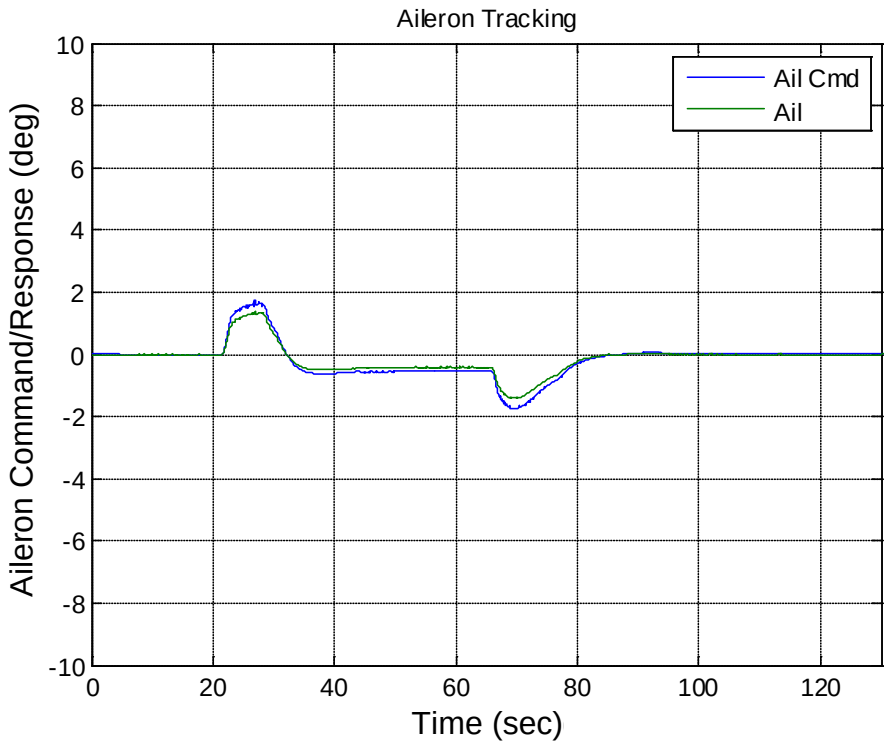

Figure C-75. Aileron Command and Aileron

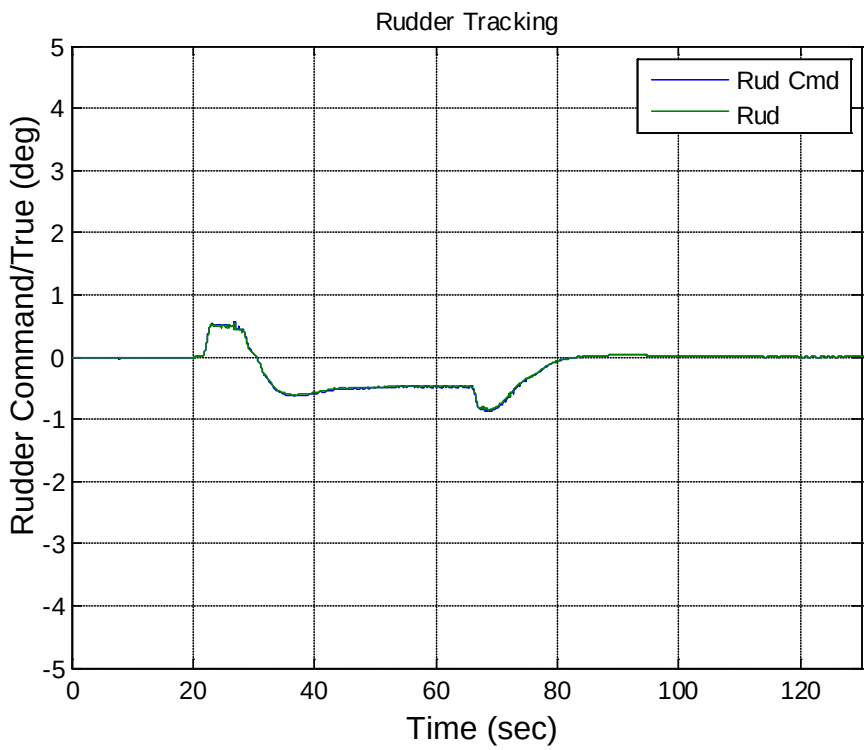

Figure C-76. Rudder Command and Rudder

C. 16 Check Case 22—Lateral Axis Localizer Mode.

Intercept (60° at 24 nautical miles), capture and track in 15-kt crosswind
Maintain altitude at 5000 ft and airspeed at 160 kt

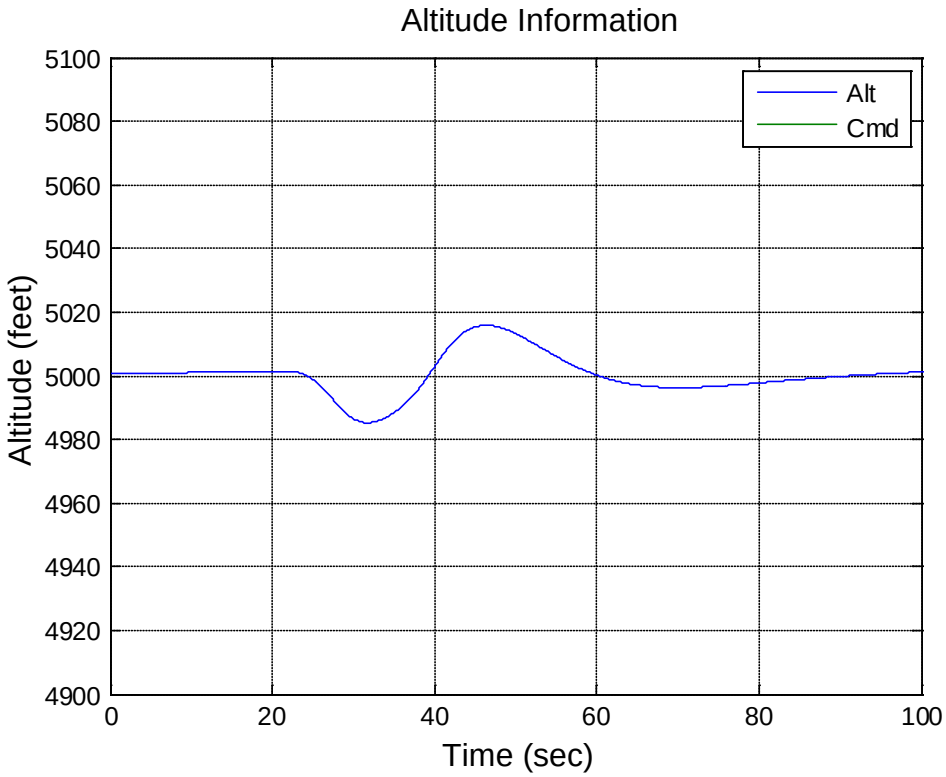

Figure C-77. Altitude Command and Altitude

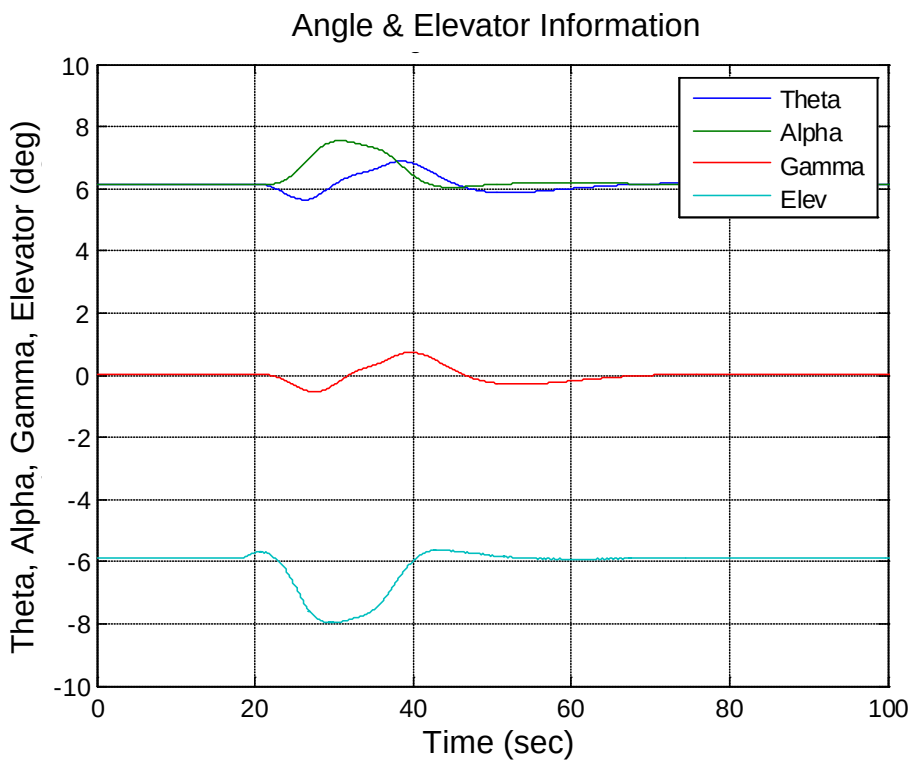

Figure C-78. Theta, Alpha, Gamma, and Elevator

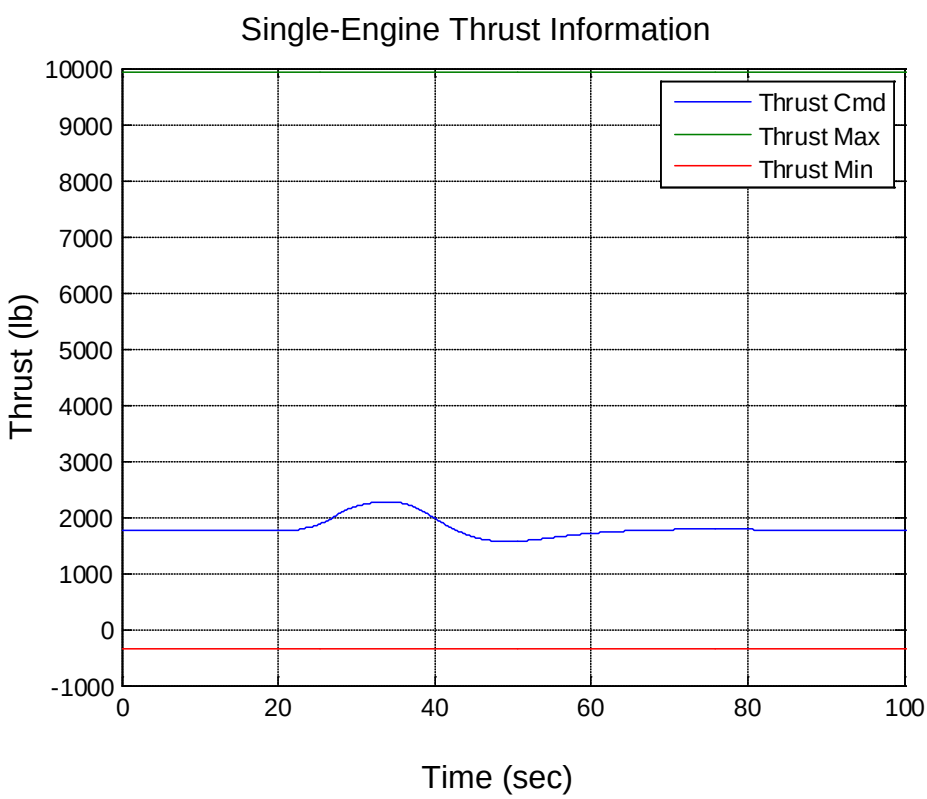

Figure C-79. Thrust Command, Thrust Minimum, and Thrust Maximum

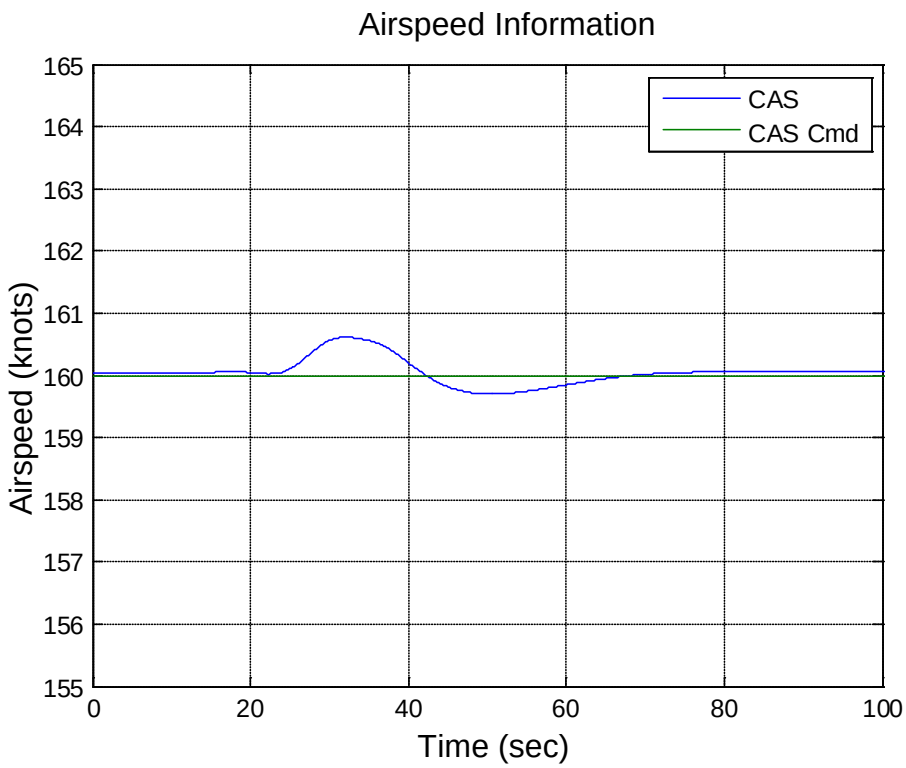

Figure C-80. Calibrated Airspeed Target and Calibrated Airspeed

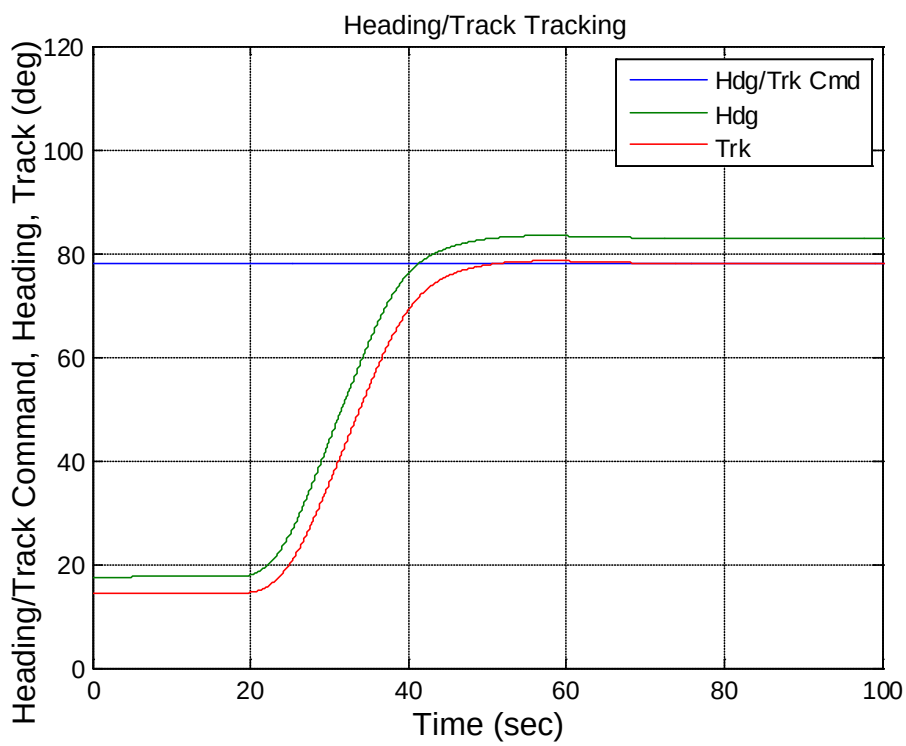

Figure C-81. Localizer Target, Heading, and Ground Track

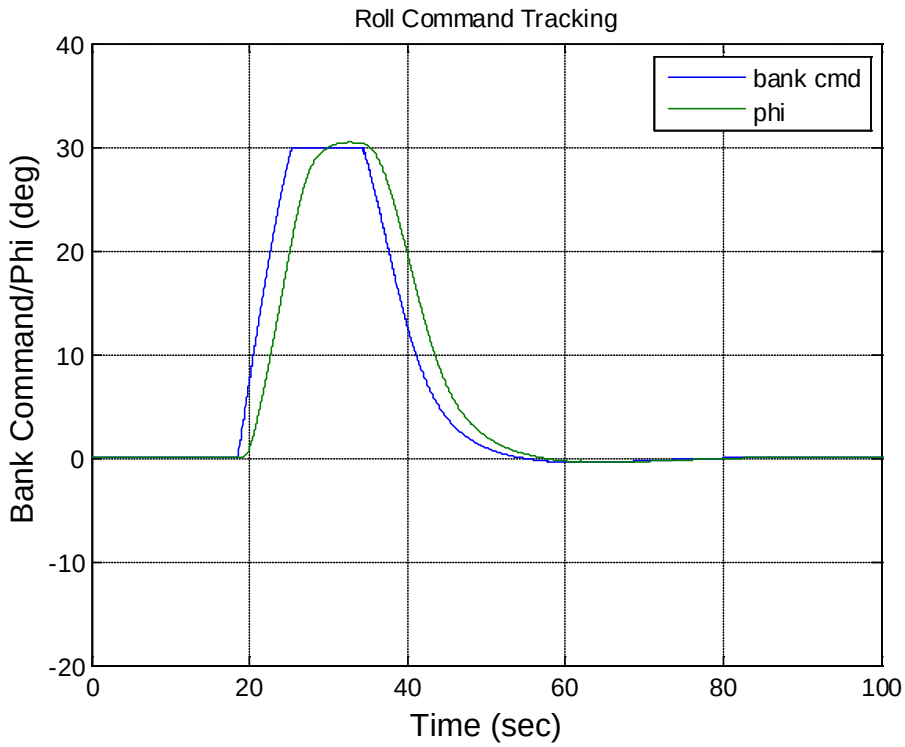

Figure C-82. Bank Command and Bank

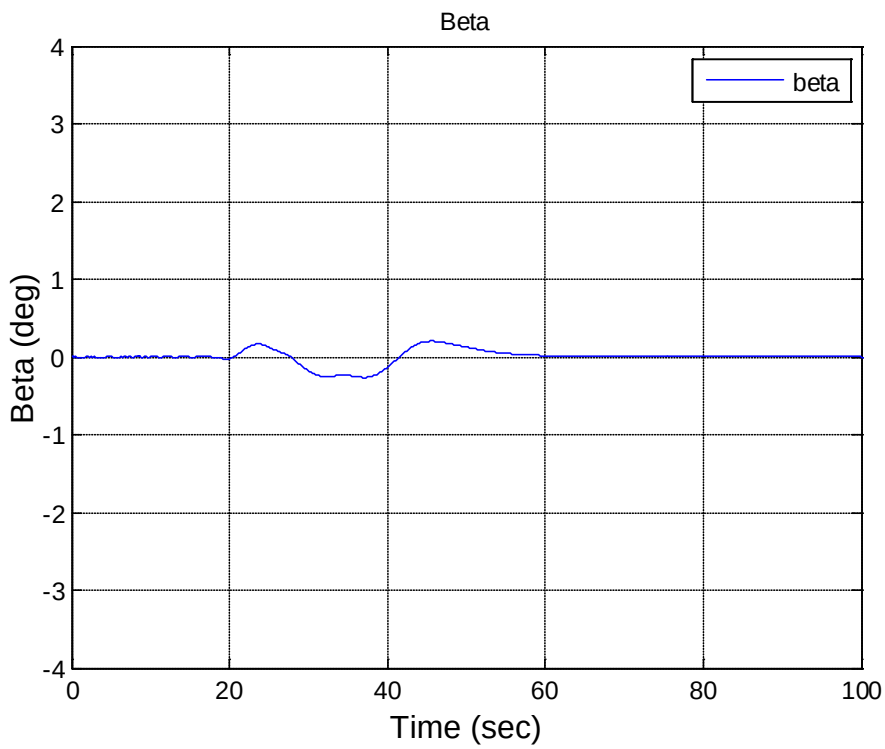

Figure C-83. Beta

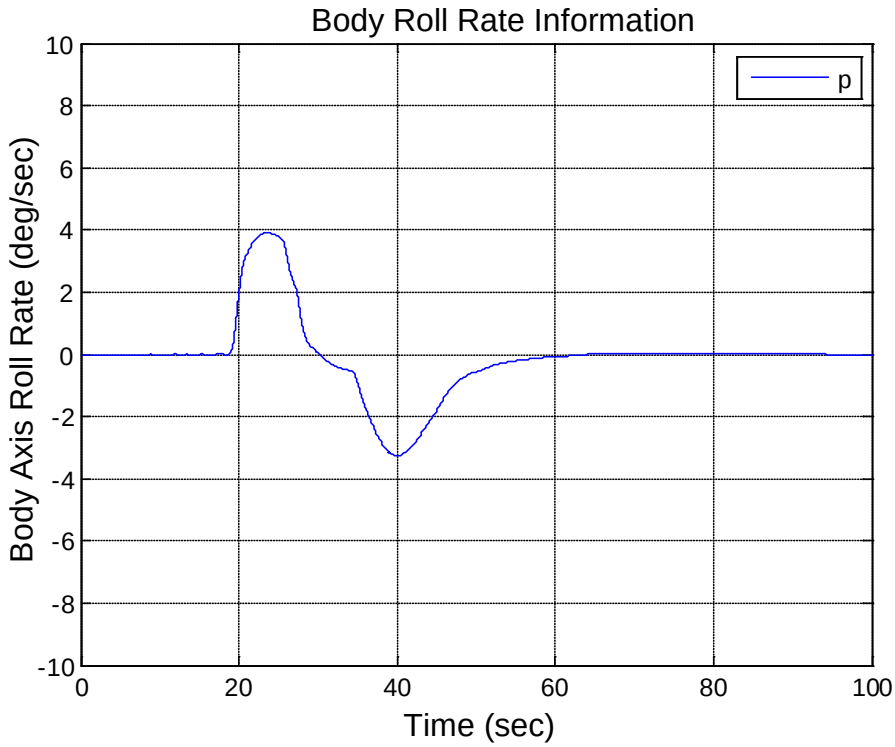

Figure C-84. Roll Rate

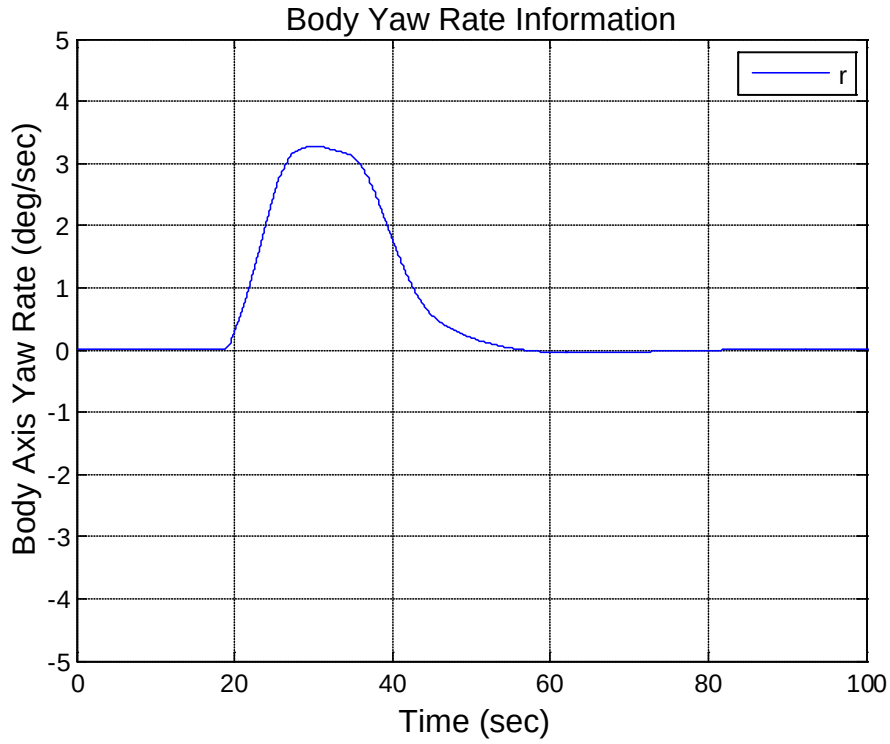

Figure C-85. Yaw Rate

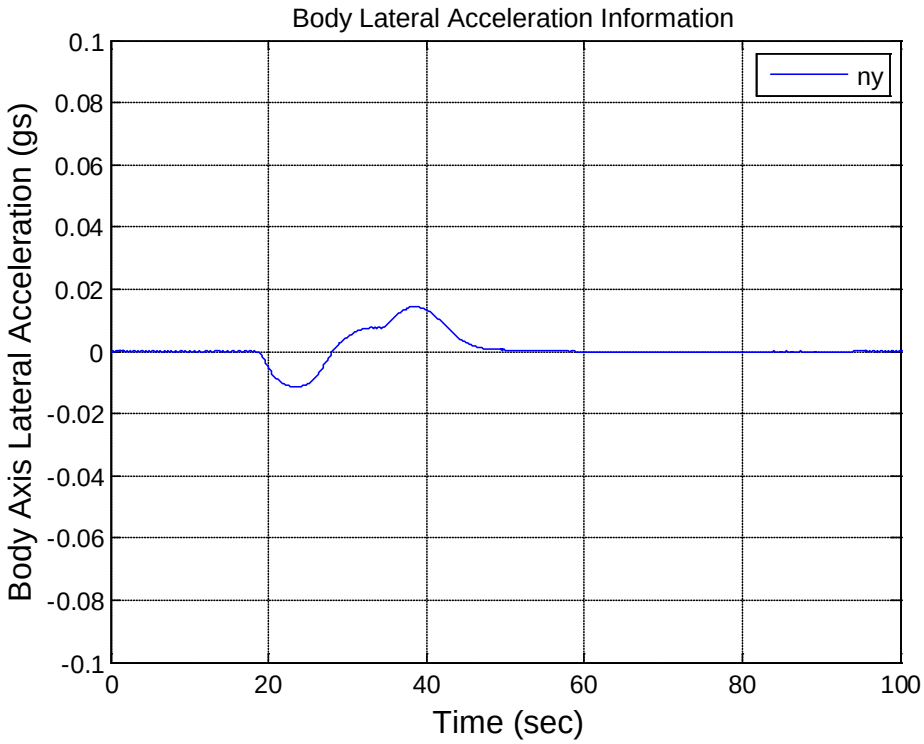

Figure C-86. Lateral Acceleration

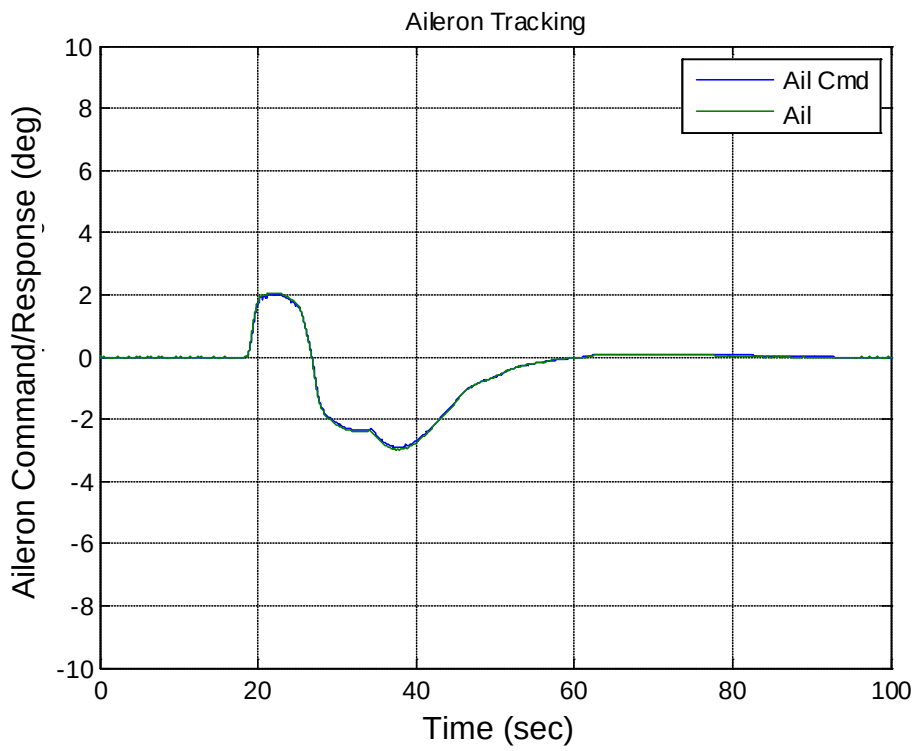

Figure C-87. Aileron Command and Aileron

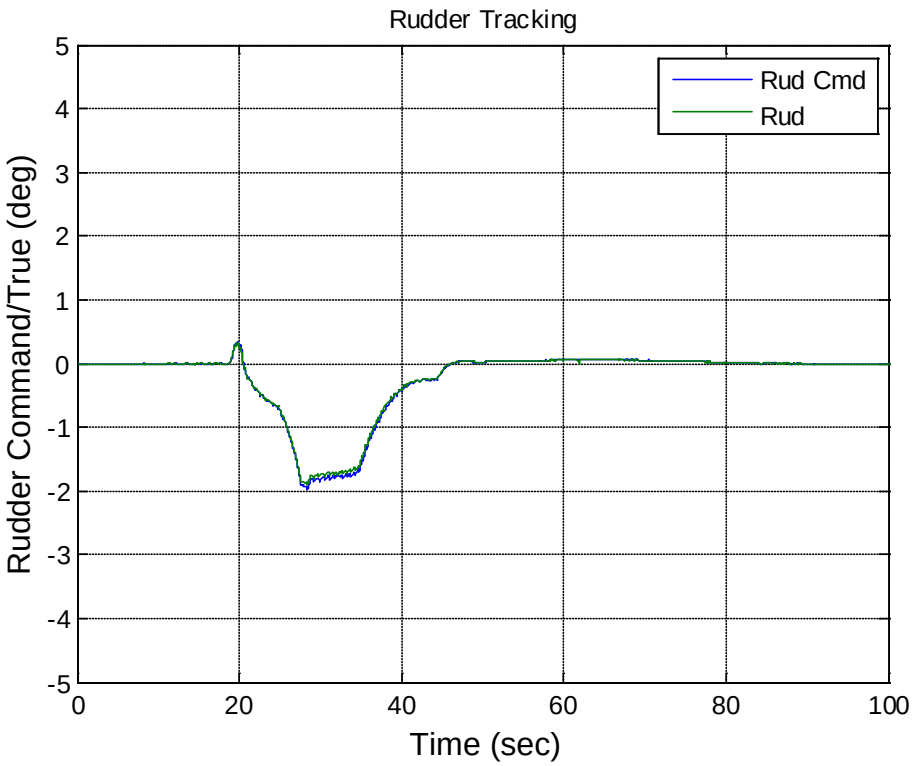

Figure C-88. Rudder Command and Rudder

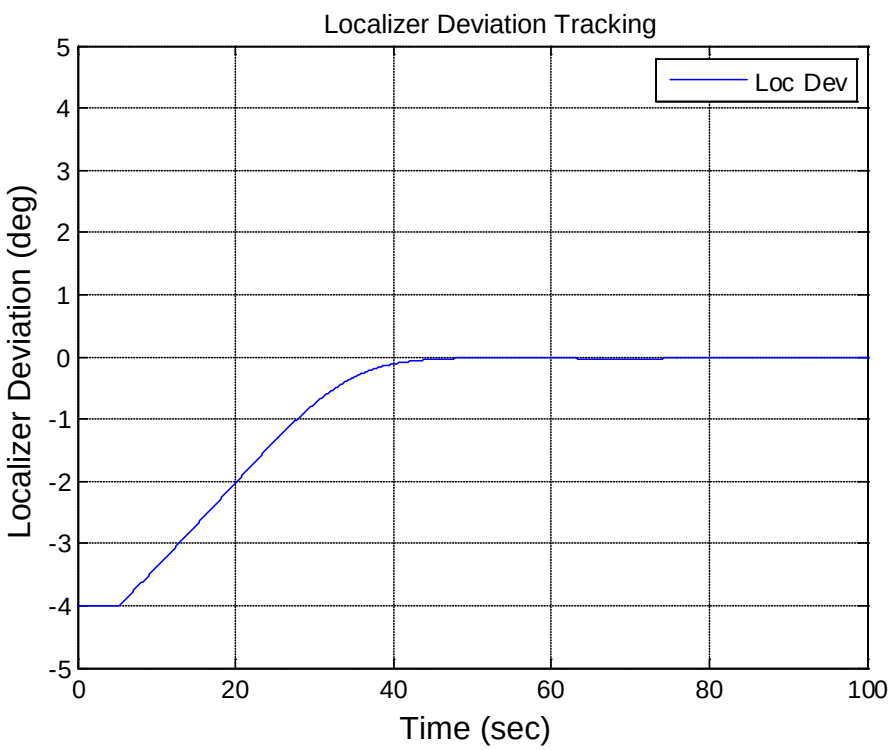

Figure C-89. Localizer Deviation

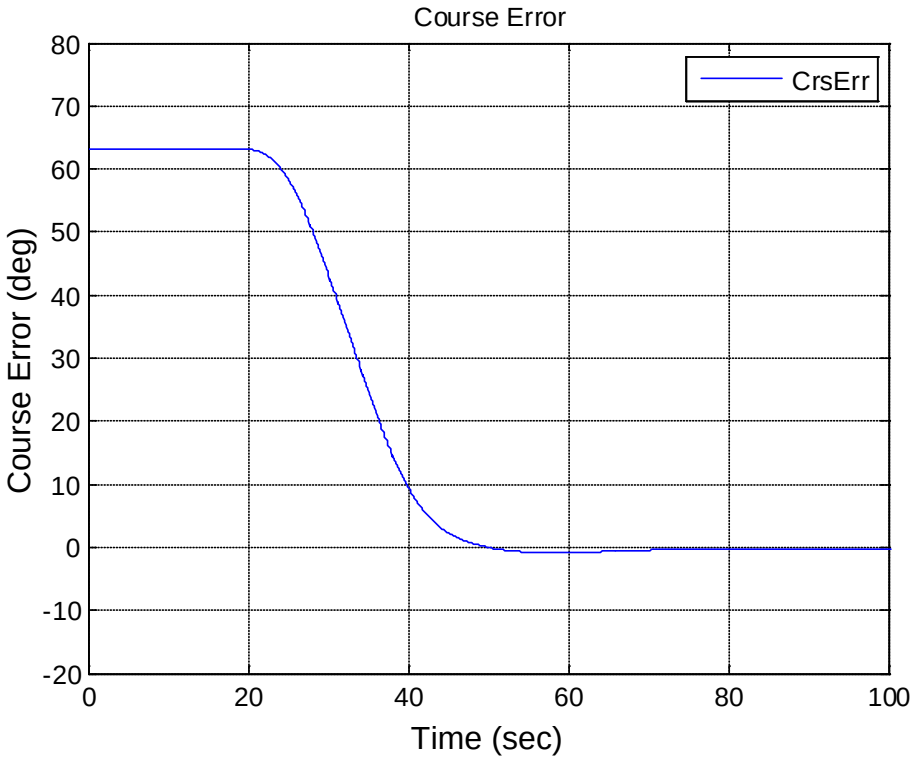

Figure C-90. Course Error